

PCT

WORLD INTELLECTUAL PROPERTY ORGANIZATION  
International Bureau



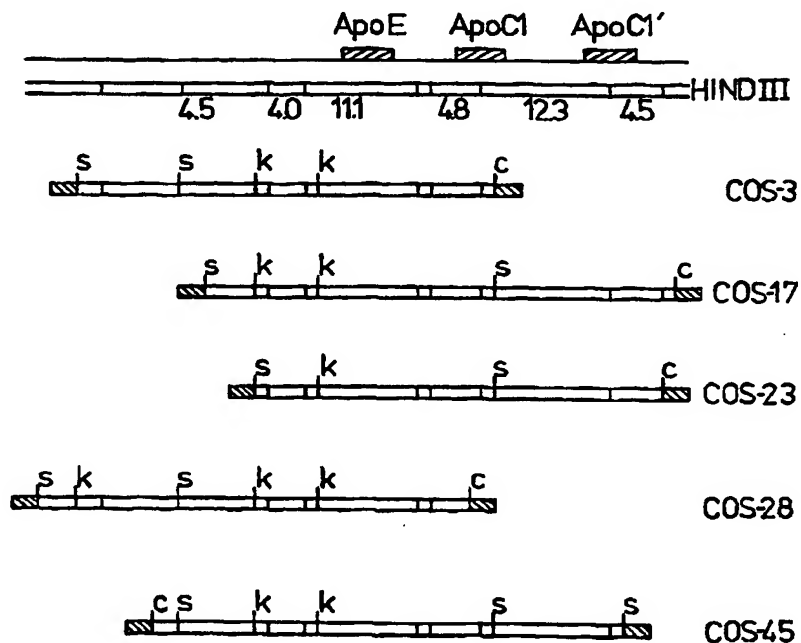
INTERNATIONAL APPLICATION PUBLISHED UNDER THE PATENT COOPERATION TREATY (PCT)

(51) International Patent Classification 6 : C12N 15/00, A01K 67/027, C07K 14/775, C12Q 1/68		A1	(11) International Publication Number: <b>WO 97/05247</b> (43) International Publication Date: 13 February 1997 (13.02.97)
(21) International Application Number: PCT/US96/11394 (22) International Filing Date: 10 July 1996 (10.07.96) (30) Priority Data: 08/509,521 31 July 1995 (31.07.95) US (71) Applicant: DUKE UNIVERSITY [US/US]; Erwin Road, Durham, NC 27706 (US). (72) Inventors: ROSES, Allen, D.; 10 Streamley Court, Durham, NC 27705 (US). GILBERT, John, R.; 3903 Inwood Drive, Durham, NC 27705 (US). XU, Pu-Ting; 4102 Cottonwood Drive, Durham, NC 27705 (US). SCHMECHEL, Donald, E.; 2965 Friendship Road, Durham, NC 27705 (US). (74) Agents: SIBLEY, Kenneth, D. et al.; Bell, Seltzer, Park & Gibson, P.O. Drawer 34009, Charlotte, NC 28234 (US).			(81) Designated States: AU, CA, JP, European patent (AT, BE, CH, DE, DK, ES, FI, FR, GB, GR, IE, IT, LU, MC, NL, PT, SE).  Published With international search report.

(54) Title: TRANSGENIC "KNOCK OUT" MICE EXPRESSING A HUMAN APOLIPOPROTEIN E

(57) Abstract

A transgenic nonhuman animal that expresses the human Apo E isoform Apo E2, Apo E3 or Apo E4 but is essentially incapable of expressing endogenous Apo E. Additionally, animals that express more than one of these isoforms are produced by selectively breeding the transgenic animals expressing the different Apo E isoforms disclosed herein. Thus, the present invention allows, among other things, the study of the effects of different combinations of human Apo E isoform expression on normal brain biology, development, function, ageing and injury.



SCHEMATICS OF Apo E ISOFORM SPECIFIC COSMID CLONES SELECTED TO ISOLATE THE Apo E GENOMIC DNA FOR MICROINJECTION. k, Kpn I; c, Cla I; s, Sca I. Apo E3 CLONES, COS-3 AND COS-17; Apo E4 CLONES, COS-23 AND COS-28; AND Apo E2 CLONE, COS-45.

**FOR THE PURPOSES OF INFORMATION ONLY**

Codes used to identify States party to the PCT on the front pages of pamphlets publishing international applications under the PCT.

AM	Armenia	GB	United Kingdom	MW	Malawi
AT	Austria	GE	Georgia	MX	Mexico
AU	Australia	GN	Guinea	NE	Niger
BB	Barbados	GR	Greece	NL	Netherlands
BE	Belgium	HU	Hungary	NO	Norway
BF	Burkina Faso	IE	Ireland	NZ	New Zealand
BG	Bulgaria	IT	Italy	PL	Poland
BJ	Benin	JP	Japan	PT	Portugal
BR	Brazil	KE	Kenya	RO	Romania
BY	Belarus	KG	Kyrgyzstan	RU	Russian Federation
CA	Canada	KP	Democratic People's Republic of Korea	SD	Sudan
CF	Central African Republic	KR	Republic of Korea	SE	Sweden
CG	Congo	KZ	Kazakhstan	SG	Singapore
CH	Switzerland	LI	Liechtenstein	SI	Slovenia
CI	Côte d'Ivoire	LK	Sri Lanka	SK	Slovakia
CM	Cameroon	LR	Liberia	SN	Senegal
CN	China	LT	Lithuania	SZ	Swaziland
CS	Czechoslovakia	LU	Luxembourg	TD	Chad
CZ	Czech Republic	LV	Latvia	TG	Togo
DE	Germany	MC	Monaco	TJ	Tajikistan
DK	Denmark	MD	Republic of Moldova	TT	Trinidad and Tobago
EE	Estonia	MG	Madagascar	UA	Ukraine
ES	Spain	ML	Mali	UG	Uganda
FI	Finland	MN	Mongolia	US	United States of America
FR	France	MR	Mauritania	UZ	Uzbekistan
GA	Gabon			VN	Viet Nam

## Transgenic "knock out" mice expressing a human apolipoprotein E

This invention was made with Government support under NIH award AG-07922. The Government has certain rights in this invention.

### Field of the Invention

5           The present invention concerns transgenic nonhuman animals containing human DNA coding for human apolipoprotein E isoforms Apo E4, Apo E3 or Apo E2 and which express these human proteins in vivo, and a method for screening a compound for the ability to effect Apo E  
10 activity in these animals

### Background of the Invention

Transgenic animals are characterized by the presence of exogenous DNA integrated in their genetic information. These animals express the genetic  
15 characteristic encoded by the foreign DNA. While the mechanism of integration of exogenous DNA has not been completely elucidated, several methods for the production of transgenic animals exist and include microinjection of exogenous DNA directly into embryos or introduction of  
20 foreign DNA into cells by the technique of calcium phosphate precipitation. For a review of the literature in this area, see PCT Application No. WO90/06992 of Lo et al.

Human apolipoprotein E (Apo E) is a lipid  
25 transport protein that exists in three common isoforms:

-2-

Apo E2, Apo E3 and Apo E4. The absence of a functional Apo E gene in mice is associated with hypercholesterolemia. (See J. Piedrahita et al., *Proc. Natl. Acad. Sci.* **89**, 4471 (1992)). Apo E is also associated with Alzheimer's Disease; the possession of an Apo E4 allele has been shown to be a risk factor for the development of Alzheimer's Disease while possession of an allele of the isoform Apo E2 has been shown to have a protective or delaying effect on the onset of this disease. (See PCT Application No. 5405-75B-1 of Roses et al.). These isoforms exist at a frequency of about 8%, 76% and 16% respectively, in the population of the United States. (See, e.g., J. Poirier et al., *Lancet* **342**, 697 (1993)).

### 15                    Summary of the Invention

The present invention is a transgenic nonhuman animal that expresses the human Apo E isoforms Apo E2, Apo E3 or Apo E4. The animals are essentially incapable of expressing the endogenous Apo E. Additionally, animals that express more than one of these isoforms can be produced by selectively breeding the transgenic animals expressing the different Apo E isoforms disclosed herein. Thus, the present invention allows, among other things, the study of the effects of different combinations of human Apo E isoform expression on normal brain biology, development, function, aging and injury.

A second aspect of the present invention is a method of screening a compound for the ability to effect the activity of Apo E isoforms in transgenic animals comprising treating transgenic animals with the compound, assaying for effects of the compound on animal physiology and evaluating it for possible therapeutic potential.

A third aspect of the present invention is a transgenic animal, created by breeding different isoform specific transgenic animals to each other, that will allow the study and characterization of the biological

-3-

effects of the different combinations of Apo E isoforms that are found in the human population.

The foregoing and other objects and aspects of the present invention are explained in detail in the drawings herein and the specification set forth below.

### Brief Description of the Drawings

Figure 1 illustrates Apo E specific cosmid clones selected to isolate the Apo E genomic DNA for microinjection. The letters k, c and s are abbreviations for the restriction enzymes Kpn I, Cla I and Sca I, respectively. Apo E3 clones are labeled COS-3 and COS-17; Apo E4 clones are labeled COS-23 and COS-28; and the Apo E2 clone is labeled COS-45.

### Detailed Description of the Invention

Nucleotide sequences are presented herein by single strand only, in the 5' to 3' direction, from left to right.

Animals suitable for carrying out the present invention are, in general, nonhuman mammals, such as monkeys, dogs, cats, rats, and mice. Rodent species such as rat and mouse are preferred, and the mouse is the most preferred species. Animals in every stage of development, including juvenile, adolescent, and adult, are included in this description. The progeny of interbreeding the transgenic animals described in the present invention refers to transgenic animals expressing human Apo E isoforms in any and all various combinations, whether heterozygous or homozygous for a particular isoform (e.g., Apo E2/Apo E2; Apo E3/Apo E3; Apo E4/Apo E4; Apo E2/Apo E3; Apo E2/Apo E4; Apo E3/Apo E4).

Apo E "knockout" animals utilized in the present invention refers to mice whose endogenous Apo E gene has been disrupted by homologous recombination and which produce no functional Apo E of their own. ApoE knockout mice are known and have been bred by Dr. N.

-4-

Maeda of the University of North Carolina at Chapel Hill in order to study the role of Apo E in lipid disorders. (See, e.g., Piedrahita et al., *Proc. Natl. Acad. Sci.* 83, 4471 (1992)). Apo E knockout animals of  
5 species other than mice can be produced by variation of the procedures carried to produce Apo E knockout mice that will be apparent to those skilled in the art.

ApoE knockout animals can be modified to contain and express DNA encoding a human DNA for an Apo  
10 E isoform by any suitable technique. The DNA encoding the human ApoE isoform is under the control of any suitable regulatory element for expressing the DNA, but is preferably operably associated with a mammalian ApoE promoter, and is most preferably operably associated with  
15 the human ApoE promoter. In one embodiment, the human DNA for Apo E isoforms employed to carry out the present invention is a 30,000 base pair (bp) sequence extending approximately 5,000 bp proximal (5') to the Apo E gene and to the Apo C1' pseudogene, which is approximately  
20 15,000 bp distal (3') to the Apo E gene. The sequence contains all gene regulatory elements necessary for the normal transcription of the gene in mouse brain. (See, e.g., W. Simonet, *J. Biol. Chem.* 268, 8221 (1993)). In one embodiment of the instant invention, the gene  
25 utilized is was isolated from lymphoblasts of humans homozygous for the Apo E4, Apo E3 or Apo E2 allele.

Supercos1 and pWE 15 cosmid vectors (commercially available from Stratagene) may be used to carry out the present invention.

30 Human DNA for the Apo E isoforms cloned into the Supercos1 vector may be used to create Apo E isoform specific cosmid libraries which are screened with Apo E cDNA for cosmids expressing the human Apo E isoforms. Apo E genomic DNA is then isolated from selected cosmid  
35 clones and purified for microinjection into the pronucleus of mouse oocytes fertilized by "knockout"

-5-

mice. The resulting mouse pups are referred to as founders (F0).

Colonies of transgenic mice are subsequently established by breeding F0 mice to "knockout" mice.

5 Progeny of this mating (F1) contain the human Apo E gene but no functional mouse Apo E gene. F1 mice are then bred to "knockout" mice to create mice heterozygous for the human Apo E gene and which lack the functional mouse Apo E gene.

10 Once colonies of transgenic mice are established, several mice are sacrificed and analyzed for human Apo E gene integration efficiency and transcript expression. Those transgenic founder lines expressing a functional human Apo E gene are expanded and the progeny  
15 of the expansion used to study the effects of the human Apo E gene on animal physiology. Animals of the present invention preferably express the human ApoE at least in brain tissue and/or blood serum, and also express the human ApoE in heart, kidney, spleen, muscle, intestine,  
20 and liver tissue cells.

Animals of the present invention may be used as a source of human ApoE3, ApoE3, or ApoE4, which can be collected from the serum of the animal in accordance with standard techniques. Human ApoE3, ApoE3, or ApoE4, can  
25 in turn be administered to animal subjects as immunogens to raise anti-human ApoE antibodies therein, which antibodies are useful in human ApoE diagnostic assays.

In addition, the animals may be used to characterize the role of Apo E isoform specific  
30 differences in brain development, biology, function, aging and injury. The animals may be used for the study of the role of Apo E isoforms in the regulation of lipid metabolism. The role of Apo E and the importance of the various isoforms in the etiology of neural diseases such  
35 as Alzheimer's Disease may be determined by using animals of the present invention. Interbreeding transgenic mice expressing different Apo E isoforms may also generate a

-6-

transgenic mouse model exhibiting full-blown Alzheimer's Disease symptomatology which would be extremely useful for the study of the pathology of this disease.

Also disclosed herein is a method to study the effects of therapeutic intervention on the activity of Apo E isoforms in transgenic mice expressing these isoforms. Such a method comprises treating the transgenic animal with a compound and assaying or detecting the effect of the compound on animal physiology (e.g., progression of dementia, progression of amyloid plaque formation, etc.).

The animals are useful as a model that allows in vivo studies of the molecular and cellular biochemistry of Apo E isoforms and of interactions between Apo E isoforms and other proteins of interest. The animals are useful as a model that will allow the identification of potential activities of Apo E isoforms in nonneural tissue in animals in vivo. The animals are useful for studying the biological effects of the different combinations of Apo E isoforms that are found in the human population by breeding different isoform specific transgenic mice to each other and characterizing the biological effects of the resulting isoform combinations in the progeny.

Those skilled in the art will appreciate numerous variations which may be made to the foregoing in carrying out the instant invention, which will be readily apparent from the literature concerning transgenic animals. See, e.g., H. Chen et al., PCT Application WO 95/03397; H. Chen et al., PCT Application WO 95/03402; C. Wood et al., PCT Application WO 91/00906; C. Lo et al., PCT Application WO 90/06992; P. Leder et al., U.S. Patent No. 4,736,866; and T. Wagner et al., U.S. Patent Application No. 4,873,191.

The present invention is explained in greater detail by the following Examples. These examples are

-7-

illustrative of the present invention, and are not to be construed as limiting thereof.

### EXAMPLE 1

#### Construction of Apo E Isoform Specific Cosmid Libraries

##### 5        Isolation of high-molecular weight genomic DNA:

Human genomic DNAs used for construction of cosmid libraries were isolated and purified from lymphoblasts of individuals who were verified homozygous carriers for Apo E 2/2, 3/3 and 4/4 alleles. Lymphoblasts were propagated  
10 in DMEM (GIBCO-BRL) supplemented with 10% fetal calf serum (FCS) using standard procedures known in the art. 5x10<sup>7</sup> cultured lymphoblasts were harvested and washed once with cold phosphate-buffered saline (PBS) and resuspended in 15 ml of 20 mM Tris.HCl, pH 8.0, 10 mM NaCl, 1 mM  
15 ethylenediaminetetraacetic acid (EDTA), and digested with 100 mg/ml of proteinase K (Boehringer Mannheim, BMB) including 0.5% sodium dodecyl sulfate (SDS) at 50° C for 6 hours or overnight. The DNA were extracted by gentle inversion with an equal volume of Tris.HCl (pH 8.0)  
20 saturated phenol/chloroform for 10 minutes at room temperature. The mixture was separated by centrifugation at 5000 rpm for 15 minutes at room temperature. The viscous aqueous phase was carefully collected and extracted once with an equal volume of chloroform. The  
25 clear aqueous phase was dialyzed at 4° C four times against 4 liters of a solution of 50 mM Tris.HCl (pH 8.0), 10 mM EDTA. The concentration of the purified DNA was calculated by measuring the absorbance at wavelength of 260 and 280 nm and employing a mathematical formula  
30 known to those skilled in the art.

Preparation of 35-50 kilobase (kb) genomic DNA fragments: In order to clone the genomic DNA fragment into a Bam HI site of the Supercos1 vector (Stratagene), the 150~200 kb high-molecular weight genomic DNA was  
35 partially digested with restriction endonuclease Mbo I (GIBCO-BRL) to produce 35~50 kb fragments. The optical

-8-

time interval and quantity of Mbo I enzyme used for digestion were determined by a series test of partial digests. A sample digest of 10 ug of genomic DNA in a 100 ul reaction was cut by adding one unit of Mbo I enzyme. 15 ul aliquots were removed from the digestion at 0, 5, 10, 15, 20, 25 and 30 minute time points. 3 ul of 6x DNA gel loading buffer (0.25% bromophenol blue, 0.25% xylene cyanol FF and 30% glycerol prepared in water) was added immediately to stop reaction and the digested DNA were checked by electrophoresis on a 0.5% agarose gel. 100 ug of the genomic DNA was partially digested with Mbo I in a total volume of 1.0 ml at the conditions best mimicking the test digestion. After digestion, 18 ul of 0.5 mM EDTA (pH 8.0) was added to stop the reaction. The sample was extracted once with an equal volume of phenol/chloroform. The upper aqueous phase was adjusted to 0.3 M NaOAc, pH 5.2 and precipitated with 2 volumes of ethanol. After centrifugation, the pellet was washed once with 70% ethanol, lyophilized and resuspended in water. The Mbo I-digested DNA was then dephosphorylated with 5 units of calf intestinal alkaline phosphatase (CIAP) (BMB) at 37° C for 60 minutes. The reaction was stopped by adding 3 ul of 0.5 M EDTA and incubated at 56° C for 15 minutes. The sample was extracted once with phenol/chloroform and the aqueous phase was adjusted to 0.3 M NaOAc and precipitated with 2 volumes of ethanol. The dried pellet was resuspended in water at a concentration of 1 mg/ml.

Preparation of Supercos 1 vector: 10 ug of Supercos1 vector DNA was digested with 50 units of XbaI enzyme (GIBCO-BRL) in a total volume of 200 ml in the standard buffer for 2 hours at 37° C. The digested vector DNA was extracted once with phenol/chloroform, precipitated with ethanol, lyophilized and resuspended in 50 ml of water. The XbaI-digested DNA was dephosphorylated with 5 units of CIAP and purified as described above. The Xba I/CIAP-treated vector DNA was

-9-

then digested with 50 units of Bam HI enzyme in a total volume of 200 ul for 2 hours at 37° C. The DNA was purified by phenol/chloroform and precipitated with ethanol as described above.

5        Ligation and Packaging of DNA: 2.5 ug of the Mbo I digested genomic DNA was ligated with 1 ug of Xba I/CIAP/Bam HI-treated Supercos1 vector DNA using 2 units of T4 DNA ligase (BMB) in a total volume of 20 ul at 16° C for 24 hours. The ligated DNA was packaged into  
10 cosmids using high efficient Gigapack II Packaging extract (Stratagene). 4 ml of the ligated DNA was added to each quickly thawed Freeze/Thaw extract, placed on ice and 15 ml Sonic extract was quickly added to the extract. After incubation at room temperature for 2 hours, 500 ml  
15 of SM buffer (100 mM NaCl, 10 mM MgSO<sub>4</sub>, 50 mM Tris.HCl, pH 7.5 and 0.01% gelatin) and 20 ml of chloroform were added to each packaging reaction. The solution was mixed gently and spun briefly to sediment debris and the supernatant was ready to be titered and screened.

20

## EXAMPLE 2

### Isolation of Isoform Specific Apo E Genomic DNA

Screening of cosmid libraries: To isolate the isoform specific Apo E gene, the Apo E2, E3 and E4 isoform specific cosmid libraries were initially screened  
25 with Apo E cDNA and the positive clones were rescreened with an Apo C1 cDNA, this gene being located about 5.3 kb downstream of the Apo E gene. The DH5a-MCR (GIBCO-BRL) cell line was used as host cells. All the packaged cosmid libraries were screened according to Stratagene  
30 protocols. One to two million packaged recombinants from each of the cosmid libraries were spread on 137 mm Colony/PlaqueScreen discs (DU PONT). Each disc contained 40-50,000 cosmid clones. The discs were incubated on 150 mm LB/kanamycin plates (1.0% Bacto-tryptone, 0.5% Bacto-  
35 yeast extract, 150 mM NaCl, 1.5% Difco-agar and 50 mg/ml kanamycin) overnight at 37° C. Two replica filters were

-10-

then made from the master filters and incubated overnight on LB/kanamycin plates at 37° C. The duplicated filters were denatured twice with 0.5 N NaOH solution and neutralized twice with 1 M Tris.HCl pH 7.5 for 5 minutes each at room temperature. The filters were blotted dry on paper towels and baked in a vacuum oven for 2 hours at 80° C. Prehybridization was carried out in 2x SSC (150 mM NaCl, 15 mM Sodium Citrate), 1.0% SDS, 10% dextran sulphate and 50% deionized formamide for one hour to overnight. Following prehybridization,  $5 \times 10^6$  cpm of the Apo E cDNA probe prepared using Multiprimer DNA labelling system (Amersham) were added to the prehybridization solution and incubated overnight at 42° C. The filters were then washed in 0.1 x SSC, 0.1% SDS at 55-60° C with 3 or 4 changes over 2-4 hours, blotted on paper towel and exposed to X-ray film overnight. Autoradiograms were aligned to master filters. A 1-5 mm region surrounding the hybridization signal was scraped with a sterile toothpick and put in 100 ml of LB medium containing 50 mg ampicillin. The bacteria were diluted and replated on 137 mm filters on 150 mm LB/kanamycin plates to give 500-1000 clones per plate. The replica filters were rehybridized with  $^{32}\text{P}$ -labeled Apo C1 probe. Single positive clones were isolated and inoculated in 3.0 ml culture.

Preparation of cosmid DNA from mini-lysates:

The bacterial cells were collected from 1.5 ml culture by centrifugation for 2 minutes in a microcentrifuge. The pellet was resuspended in 300 ul of STET (8% Sucrose, 0.5% Triton X-100, 50 mM Tris.HCl pH 8.0, 50 mM EDTA). 20 ul of fresh lysozyme (10 mg/ml) was added to the suspension and incubated in a boiling water bath for 1 minute, then centrifuged for 10 minutes at 4° C. The gelatinous pellet was removed and discarded. The remaining supernatant was precipitated with 300 ml of isopropanol. The pellet was washed with 70% ethanol, lyophilized and resuspended in 50 ml of water.

-11-

**EXAMPLE 3****Generation of Transgenic Mice**

Mice used for microinjection: An Apo E "knockout" mouse line provided by Dr. N. Maeda of The University of North Carolina at Chapel Hill was used to generate human Apo E transgenic mice. The "knockout" mice carry an inactivated endogenous Apo E gene created by gene targeting in the embryonic stem cells. (See Piedrahita et al., *Proc. Natl. Acad. Sci.* **83**, 4471 (1992)). Briefly, the normal mouse Apo E gene was disrupted by removing an Xho I/Bam HI fragment containing part of exon 3 and part of intron 3 and replacing it by the neomycin resistance gene. After homologous recombination between the endogenous Apo E locus and the targeting plasmid, the size of the Hind III-digested genomic DNA fragment hybridized to the Apo E probe increased from 6.5 to 7.5 kb. Thus, Southern blotting of Hind III-digested DNA from the targeting mice showed 6.5 and/or 7.5 kb bands indicating inheritance of normal and the modified allele, respectively, when probed with a mouse Apo E exon 4 DNA fragment amplified from mouse genomic DNA.

Purification of Apo E genomic DNA fragment for microinjection: 28~30 kb Apo E genomic DNA fragments were purified from the selected cosmid clones by digestion with the appropriate restriction enzyme(s) (KpnI, ClaI, ScaI, as will follow from the foregoing). 20 ug of cosmid DNA was digested with 50~100 units of selected enzymes in a total volume of 300 ul for 2 hours at 37° C. The digested DNA was mixed with 6x DNA loading buffer and separated on 0.7% agarose gel. The specific DNA band was cut from the gel, excess agarose trimmed away and the DNA was electro-eluted into a dialysis bag at 300 V for 30 min. The DNA was washed and collected from the dialysis bag and purified by extracting with an equal volume of phenol, phenol/chloroform and chloroform respectively,

-12-

and then precipitated and resuspended in 50 ul of injection buffer (10 mM Tris.HCl, pH 7.5, 0.1 mM EDTA).

Microinjection of Apo E genomic DNA: The generation of transgenic animals through the  
5 microinjection of single-celled embryos involved four well-recognized steps: the isolation of fertilized eggs from pregnant animals; the injection of the transgene into the pronuclei of the single-celled fertilized embryos; the implantation of the injected embryos into  
10 the oviduct of a pseudo-pregnant female; and lastly, the analysis of the animals generated.

The female mice that acted as egg donors were hormonally stimulated to produce a greater yield of embryos by injection intraperitoneally with 5  
15 international units (IU) of pregnant mare's serum (PMS) which stimulated follicular growth. This injection was followed 48 hours later by a second intraperitoneal injection of 5 IU of human chorionic gonadotropin (hCG) which potentiated the resumption of oocyte meiosis and  
20 ovulation. Even in strains that do not respond well to hormonal stimulation, a higher percentage of hormonally stimulated females plug than females in natural matings. Additionally, although hormonally stimulated matings result in a larger number of abnormal eggs than normal  
25 matings, this is more than compensated for by the greatly increased number of injectable eggs produced per female (an average of 15-40 for stimulated donors versus 8-12 for unstimulated donors).

Mice were maintained on a daily cycle of 12  
30 hours of light followed by 12 hours of darkness. The dark period was maintained between 4 p.m. and 4 a.m., thus, fertilization occurred around midnight and the embryos were isolated the next morning. The oviduct was dissected away and placed in M2 culture medium in  
35 accordance with known techniques. Eggs were recovered using a dissecting microscope at 10-20X magnification and pipetted into a solution of 0.1% hyaluronidase to remove

-13-

cumulus cells. Eggs were then washed in M2 medium and placed in droplets of M16 medium under paraffin oil in accordance with known techniques and incubated at 37° C in 5% CO<sub>2</sub> until injection.

5           The DNA used must be extensively purified prior to microinjection to remove impurities that might be harmful to the eggs or clog the injection needles. DNA used for these experiments was prepared in two ways. The first involved restriction digestion with Kpn I and Cla  
10 I followed by separation of the fragments on agarose gels. Apo E containing transgenes were isolated by electro-elution, dialyzed, extensively extracted with butanol and precipitated. The second procedure involved using the elutrap system (Schleicher & Schuell, S&S) for  
15 DNA fragment isolation.

Microinjection utilized an inverted Olympus microscope with Nomarski differential interference contrast optics. The injection into the pronuclei was carried out using 1 picoliter of DNA solution and  
20 micromanipulators at 200X magnification on a vibration-free table. After injection, the eggs were returned to M16 medium under oil and incubated at 37° C in 5% CO<sub>2</sub> overnight. Embryos that had divided into the two-cell stage by the next day were transferred to the oviduct of  
25 a pseudo-pregnant female. Although eggs may be transferred immediately to the oviduct, allowing the embryos to incubate overnight insured that only viable two-celled embryos were transferred.

Embryos that survived injection were  
30 transferred to the ampulla of the oviduct of a pseudo-pregnant female through the infundibulum. Pseudo-pregnant females were generated by mating vasectomized males to the females the night before transfers were to take place. About 15-20 eggs were transferred to one  
35 oviduct per female. The eggs also migrated into the opposite uterine horn and thus were implanted on both sides.

-14-

## EXAMPLE 4

Characterization and Analysis of Transgenes

Screen of the transgenic mice by polymerase chain reaction: Polymerase chain reaction (PCR) was performed to detect the presence of the human Apo E gene in the transgenic mouse pups and to identify their genotypes. Human Apo E exon 3 specific primers were derived from intronic sequences flanking exon 3 of the human Apo gene. The sequence of the forward primer used was 5'-GGTAGCTAGATGCCTGGACGG-3' (SEQ ID NO:1) and the reverse primer used was 5'-GCTAGAACCAGCAGAGACCC-3' (SEQ ID NO:2). Mouse knockout primers were synthesized from the mouse DNA sequence spanning the disrupted (knockout) region. The forward sequence of the knockout primer used was 5'-GTCTCGGCTCTGAACTACTATG-3' (SEQ ID NO:3) and the reverse primer used was 5'-GCAAGAGGTGATGGTACTCG-3' (SEQ ID NO:4). Each PCR reaction contained 250-500 ng of mouse tail DNA, 100 ng of each primer, 200 mM each dNTP, 0.5 units of Taq DNA polymerase (GIBCO-BRL), in a final volume of 50 ul. An initial denaturation at 94° C for 5 minutes was followed by 35 cycles of annealing at 65° C for 0.5 minutes, extension at 70° C for 1.5 minutes, denaturation at 94° C for 0.5 minutes, and a final extension at 70° C for 10 minutes.

Southern blot analysis: The presence, the mode of integration and the copy numbers of transgenes in the transgenic mice were further confirmed by Southern blot analysis. 20 ug of mouse genomic DNA and 16 ug of human genomic DNA were digested with 100 units of appropriate enzyme in a total volume of 300 ul solution at 37° C overnight. The digested DNA was precipitated with 2 volumes of ethanol and the pellet was washed with 70% ethanol, lyophilized and redigested with 20 units of the enzyme in a total volume of 30 ul at 37° C for 2 hours. The DNA was separated on 0.7% agarose gel and blotted onto GeneScreen membrane (DU PONT) using Posiblot30-30 (Stratagene) following the manufacturer's protocol.

-15-

Results: Results from PCR and Southern blotting analyses indicated that five transgenic founder animals were generated comprising the human Apo E4 gene. Three founder animals were generated concerning the human Apo E3 gene, and five were generated concerning the human Apo E3 gene. Southern blotting and human specific transgene PCR analysis of transgenic mouse genomic DNA that had been cut with the Hind III restriction enzyme and probed with human Apo E and Apo C1 cDNA, showed the presence of the human 11.1 kb Hind III band associated with the presence of cosmid 28 (Apo E4) and cosmid 45 (Apo E2) in the Apo E4 and Apo E2 transgenic animals, respectively. (Data not shown). Data also indicated that, while a founder line labeled E2-267 had the 11.1 kb Hind III fragment (indicating that the Sca I-Sca I fragment from Cos-45 had integrated), an Apo E2 founder line labeled E2-222 lacked the 11.1 kb fragment but possessed a larger hybridizing fragment. Probing the same blots with the human Apo C1 probe demonstrated the human specific 12.3 and 4.8 kb bands associated with the presence of the Kpn I-Cla I fragment derived from the Apo E4 cosmid numbered cosmid 23. The Apo E2 transgenic animal derived from the 267 line, however, lacked both the 12.3 and 4.8 kb fragments. This demonstrated that only the Sca I-Sca I genomic fragment from cosmid 45 (which had the characteristic Apo E 11.1 kb fragment, but lacked the 12.3 and 4.8 kb fragments) was integrated in the 267 line. The Apo E2-222 line, therefore, contained both the Apo E and the Apo C1 gene while the 267 line did not. PCR analysis utilized human specific primers and produced a characteristic 377 bp PCR product specific for the presence of the human transgene in mouse. A routine assay of Apo E4 offspring for the presence of the human Apo E4 gene indicated that animals numbered 42, 43, 44, and 45 possessed the human 377 bp PCR product while Animals 40 and 41 did not inherit the human transgene.

-16-

Northern blot analysis of human Apo E transcription: Total RNA was isolated from mouse brain, liver and kidney using TRIzol reagent (GIBCO-BRL). 50-100 mg of tissues were homogenized in 1 ml of TRIzol reagent and after incubation for 5 minutes at room temperature, 0.2 ml of chloroform was added and mixed well by vigorous shaking. The mixture was separated by centrifugation for 15 minutes at 4° C and the upper aqueous phase was collected and 0.5 ml of isopropanol was added to precipitate the RNA. The RNA pellet was then washed once with 75% ethanol, lyophilized briefly and resuspended in 50 ul of water. The mRNA was purified from the total RNA using an olig-dT cellulose type 7 column (Pharmacia). The mRNA was fractionated by electrophoresis on a 1.0% formaldehyde-agarose gel and then transferred to GeneScreen membranes. The membrane was probed with Apo E cDNA in 50% formamide/6xSSC at 42° C and washed at 0.1 x SSC at 50° C.

Results: Northern analysis of RNA isolated from transgenic mouse brain showed the presence of a human Apo E transcript of 1163 bp transcribed in the brain of an Apo E4 transgenic mouse numbered Apo E4-20 but was not present in the brain of a control "knockout" mouse.

Western immunoblot analysis of human Apo E protein: Mouse proteins were prepared by Dounce homogenization of mouse tissues in TMN buffer (25 mM Tris.HCl [pH 7.6], 3 mM MgCl<sub>2</sub>, 100 mM NaCl) containing 1 mM phenolmethanolsulfonylfluoride (PMSF). 20 ug of the homogenate was mixed with an equal volume of 2x Laemmli loading buffer (100 mM Tris.HCl [pH 6.8], 4% SDS, 10% 2-mercaptoethanol [2-ME], 25% glycerol, and 0.02% bromophenol blue) and heated at 100° C for 3 minutes. The proteins in the lysate were resolved by electrophoresis in discontinuous polyacrylamide gels (10% polyacrylamide with 3% stacking layer) containing 0.1% SDS (SDS-PAGE). The proteins separated by SDS-PAGE were transferred onto Immobilon membranes (Millipore) using a

-17-

semi-dry Trans-blot (Bio-Rad) transfer cell following the manufacturer's protocol. The membrane was blocked in 1.0% bovine serum album (BSA) prepared in 100 mM Tris.HCl pH 7.5, 150 mM NaCl, 0.1% Tween-20 (TBS-T) overnight at 4° C and then probed with polyvalent goat antiserum against human Apo E (Calbiochem) at 1:5000 dilution for 30 minutes at room temperature. After washing three times with TBS-T, the membrane was exposed to horse antigoat second antibody conjugated with horseradish peroxidase (Calbiochem) at 1:10,000 dilution for 30 minutes at room temperature, and then washed 5-7 times in TBS-T at room temperature. Horseradish peroxidase was visualized with an enhanced chemiluminescence detection kit (Amersham) and exposed to ECL hyperfilm.

Results: Western blot analysis indicated Apo E4 and Apo E2 transgenic mice expressed the Apo E protein which was not present in the control "knockout" mice.

Measurement of cholesterol: After an overnight fasting, approximate 250 ul of blood was obtained through tail bleeding or from sacrificed mouse heart. Cholesterol was measured enzymatically using Sigma's Cholesterin detecting kit according to the manufacturer's protocol. The reliability of cholesterol test results was monitored by routine use of control sera with known higher, normal and lower cholesterol concentration (Sigma). 5 ul of mouse serum was mixed with 500 ul of prewarmed cholesterol reagent and incubated at 37° C for 5 minutes. The cholesterol concentration was calculated by measuring the absorbance at wavelength of 500 nm and using a mathematical formula known in the art.

Results: Background sera from a mouse tail bleed was assayed for blood cholesterol levels. In the "knockout" mouse, which lacked an Apo E gene to transport cholesterol, blood levels of cholesterol normally averaged five times the level found in normal mice, 400-600 mg/dl versus approximately 100 mg/dl, respectively, on a normal diet of mouse chow. If the human gene had

-18-

been integrated into the mouse genome and was being expressed, the high cholesterol level of the "knockout" mouse would be corrected or at least substantially reduced due to the ability of the human gene to transport cholesterol in the mouse. The results for the Apo E4 transgene can be seen in Table 1. The human Apo E4 transgenic animals had substantially lower cholesterol levels. The Apo E2 transgenic animal's cholesterol levels were highly variable, however, even between siblings. Since it had been demonstrated that the human gene was present and was being expressed, this variability is believed to reflect how recently the animal had eaten. Homozygous Apo E2 is known to clear cholesterol more slowly than other Apo E isoforms and has been shown, for reasons that are not entirely clear, to be associated with high levels of cholesterol in humans. Thus, the Apo E2 transgenic animals with their highly variable cholesterol levels, in addition to serving as models for the study of the Apo E2 gene in brain, may also be extremely useful for studying the effects of high and low dietary cholesterol levels on lipid transport and metabolism.

TABLE 1. EFFECT OF HUMAN APOLIPOPROTEIN E4 EXPRESSION ON SERUM CHOLESTEROL IN TRANSGENIC MICE.

Mice	Genotypes	Cholesterol (mg/dl)
Knockout	K/K	629.3 $\pm$ 70.9
Normal	N/N	81.6 $\pm$ 14.6
Transgenic	E4(K/K)	112.0 $\pm$ 25.9

#### EXAMPLE 5

##### Screening Assay

The animals of the present invention are used to screen compounds for the ability to effect the activity of Apo E isoforms. A transgenic mouse produced as described above (e.g., an Apo E4/Apo E4 animal) is

-19-

administered a test compound (e.g., orally, or by subcutaneous injection) and the effects of the compound on Apo E activity and animal physiology (e.g., life span, brain atrophy, amyloid plaque formation, are compared to  
5 such activity and physiology in a control animals (e.g., Apo E2/Apo E2 animals given the same treatment, or the same animals administered a placebo treatment).

The foregoing examples are illustrative of the present invention, and are not to be construed as  
10 limiting thereof. The invention is defined by the following claims, with equivalents of the claims to be included therein.

-20-

## SEQUENCE LISTING

## (1) GENERAL INFORMATION:

- (i) APPLICANT: Roses, Allen D.  
Gilbert, John R.  
Xu, Du-Ting  
Schmechel, Donald
- (ii) TITLE OF INVENTION: Creation of Human Apolipoprotein E  
Isoform Specific Transgenic Mice in Apolipoprotein E  
Deficient "Knockout" Mice
- (iii) NUMBER OF SEQUENCES: 4
- (iv) CORRESPONDENCE ADDRESS:
  - (A) ADDRESSEE: Kenneth D. Sibley
  - (B) STREET: P.O. Box 31107
  - (C) CITY: Raleigh
  - (D) STATE: North Carolina
  - (E) COUNTRY: USA
  - (F) ZIP: 27622
- (v) COMPUTER READABLE FORM:
  - (A) MEDIUM TYPE: Floppy disk
  - (B) COMPUTER: IBM PC compatible
  - (C) OPERATING SYSTEM: PC-DOS/MS-DOS
  - (D) SOFTWARE: PatentIn Release #1.0, Version #1.30
- (vi) CURRENT APPLICATION DATA:
  - (A) APPLICATION NUMBER:
  - (B) FILING DATE:
  - (C) CLASSIFICATION:
- (viii) ATTORNEY/AGENT INFORMATION:
  - (A) NAME: Sibley, Kenneth D.
  - (B) REGISTRATION NUMBER: 31,665
  - (C) REFERENCE/DOCKET NUMBER: 5405-111
- (ix) TELECOMMUNICATION INFORMATION:
  - (A) TELEPHONE: (919) 420-2200
  - (B) TELEFAX: (919) 881-3175

## (2) INFORMATION FOR SEQ ID NO:1:

- (i) SEQUENCE CHARACTERISTICS:
  - (A) LENGTH: 21 base pairs
  - (B) TYPE: nucleic acid
  - (C) STRANDEDNESS: single
  - (D) TOPOLOGY: linear
- (ii) MOLECULE TYPE: cDNA
- (xi) SEQUENCE DESCRIPTION: SEQ ID NO:1:

- 21 -

GGTAGCTAGA TGCCTGGACG G

21

## (2) INFORMATION FOR SEQ ID NO:2:

- (i) SEQUENCE CHARACTERISTICS:
  - (A) LENGTH: 20 base pairs
  - (B) TYPE: nucleic acid
  - (C) STRANDEDNESS: single
  - (D) TOPOLOGY: linear

(ii) MOLECULE TYPE: cDNA

(xi) SEQUENCE DESCRIPTION: SEQ ID NO:2:

GCTAGAACCA GCAGAGACCC

20

## (2) INFORMATION FOR SEQ ID NO:3:

- (i) SEQUENCE CHARACTERISTICS:
  - (A) LENGTH: 22 base pairs
  - (B) TYPE: nucleic acid
  - (C) STRANDEDNESS: single
  - (D) TOPOLOGY: linear

(ii) MOLECULE TYPE: cDNA

(xi) SEQUENCE DESCRIPTION: SEQ ID NO:3:

GTCTCGGCTC TGAATACTA TG

22

## (2) INFORMATION FOR SEQ ID NO:4:

- (i) SEQUENCE CHARACTERISTICS:
  - (A) LENGTH: 20 base pairs
  - (B) TYPE: nucleic acid
  - (C) STRANDEDNESS: single
  - (D) TOPOLOGY: linear

(ii) MOLECULE TYPE: cDNA

(xi) SEQUENCE DESCRIPTION: SEQ ID NO:4:

GCAAGAGGTG ATGGTACTCG

20

-22-

## THAT WHICH IS CLAIMED IS:

1. A transgenic nonhuman mammal comprising cells containing and expressing a transgene encoding a human apolipoprotein E (Apo E), said cells essentially incapable of expressing endogenous Apo E.

5                   2. A mammal of claim 1, wherein said mammal is a rodent.

3. A mammal of claim 1, wherein said mammal is a mouse.

4. A mammal of claim 1, wherein said human  
10 Apo E is Apo E4.

5. A mammal of claim 1, wherein said human Apo E is Apo E3.

6. A mammal of claim 1, wherein said human Apo E is Apo E2.

15                   7. A mammal of claim 1, wherein said cells include brain tissue cells.

8. A mammal of claim 1, wherein said cells include brain, heart, kidney, spleen, muscle, intestine and liver tissue cells.

20                   9. A mammal of claim 1 wherein said transgene is positioned downstream of the human Apo E promoter and operatively associated therewith.

10. The animal of claim 9 which is a mouse.

11. The mouse of claim 9 wherein the transgene  
25 is Apo E2.

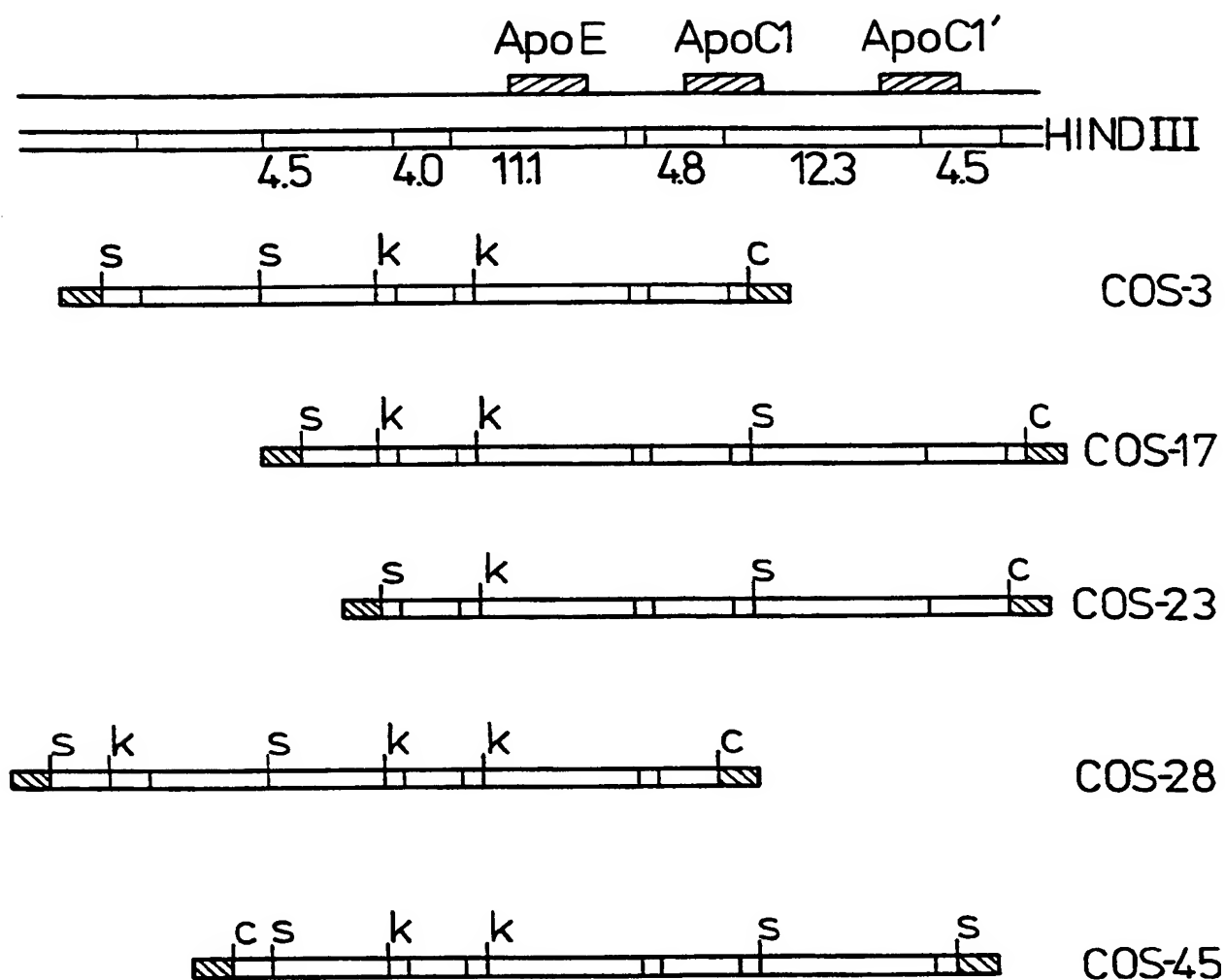
-23-

12. The mouse of claim 9 wherein the transgene is Apo E3.

13. The mouse of claim 9 wherein the transgene is Apo E4.

- 5           14. A method for screening a compound for the ability to effect the activity of Apo E isoforms in transgenic animal expressing human Apo E isoforms, comprising:
- 10               (a) administering the transgenic animal a test compound; and then
- (b) detecting the effect of the test compound on said animal.

1/1



SCHEMATICS OF Apo E ISOFORM SPECIFIC COSMID CLONES SELECTED TO ISOLATE THE Apo E GENOMIC DNA FOR MICROINJECTION. k, Kpn I; c, Cla I; s, Sca I. Apo E3 CLONES, COS-3 AND COS -17; Apo E4 CLONES, COS-23 AND COS-28; AND Apo E2 CLONE, COS-45.

Fig. 1.

# INTERNATIONAL SEARCH REPORT

International Application No  
PCT/US 96/11394

A. CLASSIFICATION OF SUBJECT MATTER  
IPC 6 C12N15/00 A01K67/027 C07K14/775 C12Q1/68

According to International Patent Classification (IPC) or to both national classification and IPC

## B. FIELDS SEARCHED

Minimum documentation searched (classification system followed by classification symbols)

IPC 6 A01K C07K

Documentation searched other than minimum documentation to the extent that such documents are included in the fields searched

Electronic data base consulted during the international search (name of data base and, where practical, search terms used)

## C. DOCUMENTS CONSIDERED TO BE RELEVANT

Category *	Citation of document, with indication, where appropriate, of the relevant passages	Relevant to claim No.
Y	JOURNAL OF BIOLOGICAL CHEMISTRY (MICROFILMS), vol. 265, no. 25, 5 September 1990, MD US, pages 14709-14712, XP000142449 SMITH, J.D. ET AL.: "Accumulation of human apolipoprotein E in the plasma of the transgenic mice" see the whole document --- -/-	1-8, 14

☒ Further documents are listed in the continuation of box C.

☒ Patent family members are listed in annex.

### \* Special categories of cited documents:

- \*A\* document defining the general state of the art which is not considered to be of particular relevance
- \*E\* earlier document but published on or after the international filing date
- \*L\* document which may throw doubts on priority claim(s) or which is cited to establish the publication date of another citation or other special reason (as specified)
- \*O\* document referring to an oral disclosure, use, exhibition or other means
- \*P\* document published prior to the international filing date but later than the priority date claimed

\*T\* later document published after the international filing date or priority date and not in conflict with the application but cited to understand the principle or theory underlying the invention

\*X\* document of particular relevance; the claimed invention cannot be considered novel or cannot be considered to involve an inventive step when the document is taken alone

\*Y\* document of particular relevance; the claimed invention cannot be considered to involve an inventive step when the document is combined with one or more other such documents, such combination being obvious to a person skilled in the art.

\*&\* document member of the same patent family

Date of the actual completion of the international search

3 October 1996

Date of mailing of the international search report

28. 10. 96

Name and mailing address of the ISA

European Patent Office, P.B. 5818 Patentlaan 2  
NL - 2280 HV Rijswijk  
Tel. (+31-70) 340-2040, Tx. 31 651 epo nl,  
Fax (+31-70) 340-3016

Authorized officer

Chambonnet, F

# INTERNATIONAL SEARCH REPORT

Intern      d Application No  
PCT/US 96/11394

C.(Continuation) DOCUMENTS CONSIDERED TO BE RELEVANT

Category *	Citation of document, with indication, where appropriate, of the relevant passages	Relevant to claim No.
Y	JOURNAL OF BIOLOGICAL CHEMISTRY (MICROFILMS), vol. 266, no. 14, 15 May 1991, MD US, pages 8651-8654, XP000604832 SIMONET, W.S. ET AL.: "Multiple tissue-specific elements control the apolipoprotein E7C-I gene locus in transgenic mice" see the whole document ---	1-14
Y	WO,A,93 19166 (UNIV NORTH CAROLINA) 30 September 1993 see claims 1,2,7-10,17,18,23,24,29 ---	1-14
Y	WO,A,94 09155 (UNIV DUKE ;ROSES ALLEN D (US); STRITTMATTER WARREN J (US); SALVESE) 28 April 1994 see the whole document ---	1-4, 7-10,13, 14
Y	WO,A,95 16791 (UNIV MCGILL ;POIRIER JUDES (CA)) 22 June 1995 see claims ---	1-14
P,X	AMERICAN JOURNAL OF HUMAN GENETICS, vol. 57, no. 4 sup, October 1995, page a254 XP000603672 XU, P.T. ET AL.: "Expression of human isoform specific apolipoprotein E2 and E4 in transgenic mice" see abstract & 45th annual Meeting of the American Society of Human Genetics, Minneapolis, USA, October 24-28 1995 ---	1-4, 6-11,13, 14
P,X	JOURNAL OF CLINICAL INVESTIGATION, vol. 96, no. 5, November 1995, pages 2170-2179, XP000603631 BELLOSTA, S. ET AL.: "Macrophage-specific expression of human apolipoprotein E reduces atherosclerosis in hypercholesterolemic apolipoprotein E-null mice" see the whole document ---	1-3,14
Y,P	WO,A,95 29257 (MARTINEX R & D INC ;POIRIER JUDES (CA)) 2 November 1995 see claims ---	1-3,5-8, 14
	--- -/--	

1

# INTERNATIONAL SEARCH REPORT

Inter: al Application No  
PCT/US 96/11394

C.(Continuation) DOCUMENTS CONSIDERED TO BE RELEVANT		
Category	Citation of document, with indication, where appropriate, of the relevant passages	Relevant to claim No.
P,Y	<p>PROCEEDINGS OF THE NATIONAL ACADEMY OF SCIENCES OF USA, vol. 92, no. 26, December 1995, WASHINGTON US, pages 12115-12119, XP000604864 BOWMAN, B. H. ET AL.: "Discovery of a brain promoter from the human transferrin gene and its utilization for development of transgenic mice that express human apolipoprotein E alleles" see the whole document -----</p>	1-8,14

# INTERNATIONAL SEARCH REPORT

Information on patent family members

International Application No

PCT/US 96/11394

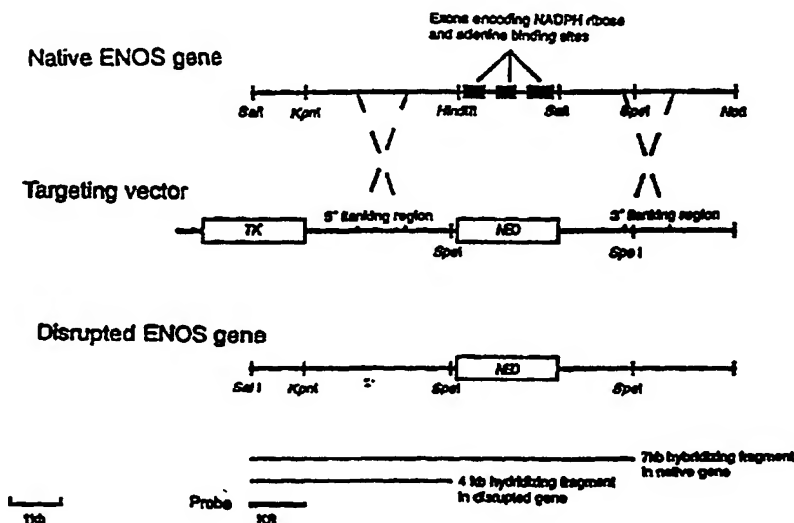
Patent document cited in search report	Publication date	Patent family member(s)	Publication date
WO-A-9319166	30-09-93	AU-A- 3814393	21-10-93
WO-A-9409155	28-04-94	AU-A- 5350094	09-05-94
		CA-A- 2142300	28-04-94
		CN-A- 1092525	21-09-94
		EP-A- 0625212	23-11-94
		FI-A- 951701	10-04-95
		JP-T- 7502418	16-03-95
		NO-A- 951383	07-04-95
		US-A- 5508167	16-04-96
		ZA-A- 9307536	03-05-94
WO-A-9516791	22-06-95	CA-A- 2111503	16-06-95
		AU-A- 1189395	03-07-95
WO-A-9529257	02-11-95	AU-A- 2300695	16-11-95



## INTERNATIONAL APPLICATION PUBLISHED UNDER THE PATENT COOPERATION TREATY (PCT)

<b>(51) International Patent Classification:</b> <b>C12N 15/00, A01K 67/027, C12N 9/02, 15/53</b>	<b>A1</b>	<b>(11) International Publication Number:</b> <b>WO 97/33989</b> <b>(43) International Publication Date:</b> 18 September 1997 (18.09.97)
<b>(21) International Application Number:</b> PCT/US97/04184 <b>(22) International Filing Date:</b> 14 March 1997 (14.03.97)  <b>(30) Priority Data:</b> 60/013,525           15 March 1996 (15.03.96)   US 60/027,362           18 September 1996 (18.09.96)   US  <b>(71) Applicant:</b> THE GENERAL HOSPITAL CORPORATION [US/US]; Fruit Street, Boston, MA 02114 (US).  <b>(72) Inventors:</b> HUANG, Paul, L.; 18 Temple Street, Boston, MA 02114 (US). FISHMAN, Mark, C.; 43 Kenwood Avenue, Newton Center, MA 02159 (US). MOSKOWITZ, Michael, A.; 275 Prospect Street, Belmont, MA 02178 (US).  <b>(74) Agents:</b> GOLDSTEIN, Jorge, A. et al.; Sterne, Kessler, Goldstein & Fox P.L.L.C., Suite 600, 1100 New York Avenue, N.W., Washington, DC 20005-3934 (US).		<b>(81) Designated States:</b> CA, JP, MX, European patent (AT, BE, CH, DE, DK, ES, FI, FR, GB, GR, IE, IT, LU, MC, NL, PT, SE).  <b>Published</b> <i>With international search report.</i> <i>Before the expiration of the time limit for amending the claims and to be republished in the event of the receipt of amendments.</i>

**(54) Title:** TRANSGENIC ANIMALS HAVING A DISRUPTED eNOS GENE AND USE THEREOF



**(57) Abstract**

This invention relates to transgenic non-human animals comprising a disrupted endothelial nitric oxide synthase gene. These animals exhibit abnormal wound-healing properties and hypertension. This invention also relates to methods of using the transgenic animals to screen for compounds having a potential therapeutic utility for vascular endothelial disorders, such as hypertension, cerebral ischemia or stroke, atherosclerosis and wound-healing activities. Moreover, this invention also relates to methods of treating a patient suffering from hypertension and wound-healing abnormalities with the compounds identified using the transgenic animals, and methods of making the transgenic animals. A method of treating a wound using nitroglycerin is also provided.

**FOR THE PURPOSES OF INFORMATION ONLY**

Codes used to identify States party to the PCT on the front pages of pamphlets publishing international applications under the PCT.

AM	Armenia	GB	United Kingdom	MW	Malawi
AT	Austria	GE	Georgia	MX	Mexico
AU	Australia	GN	Guinea	NE	Niger
BB	Barbados	GR	Greece	NL	Netherlands
BE	Belgium	HU	Hungary	NO	Norway
BF	Burkina Faso	IE	Ireland	NZ	New Zealand
BG	Bulgaria	IT	Italy	PL	Poland
BJ	Benin	JP	Japan	PT	Portugal
BR	Brazil	KE	Kenya	RO	Romania
BY	Belarus	KG	Kyrgyzstan	RU	Russian Federation
CA	Canada	KP	Democratic People's Republic of Korea	SD	Sudan
CF	Central African Republic	KR	Republic of Korea	SE	Sweden
CG	Congo	KZ	Kazakhstan	SG	Singapore
CH	Switzerland	LJ	Liechtenstein	SI	Slovenia
CI	Côte d'Ivoire	LK	Sri Lanka	SK	Slovakia
CM	Cameroon	LR	Liberia	SN	Senegal
CN	China	LT	Lithuania	SZ	Swaziland
CS	Czechoslovakia	LU	Luxembourg	TD	Chad
CZ	Czech Republic	LV	Latvia	TG	Togo
DE	Germany	MC	Monaco	TJ	Tajikistan
DK	Denmark	MD	Republic of Moldova	TT	Trinidad and Tobago
EE	Estonia	MG	Madagascar	UA	Ukraine
ES	Spain	ML	Mali	UG	Uganda
FI	Finland	MN	Mongolia	US	United States of America
FR	France	MR	Mauritania	UZ	Uzbekistan
GA	Gabon			VN	Viet Nam

Transgenic animals having a disrupted eNOS gene and use there f

## ***Background of the Invention***

### ***Statement as to Rights to Inventions Made Under Federally-Sponsored Research and Development***

Part of the work performed during the development of this invention was supported by U.S. Government funds. The U.S. Government may have certain rights in this invention.

### ***Field of the Invention***

This invention relates to transgenic non-human animals comprising a disrupted endothelial nitric oxide synthase gene. This invention also relates to methods of using these transgenic animals to screen compounds for activity against vascular endothelial disorders such as hypertension, stroke, and atherosclerosis, as well as for wound healing activity; methods of treating a patient suffering from a vascular endothelial disorder; methods of making the transgenic animals; and cell lines comprising a disrupted eNOS gene.

### ***Related Art***

In 1980, Furchgott and Zawadzki first proposed the existence of endothelium derived relaxing factor or EDRF, later identified as nitric oxide. Furchgott (1980); Furchgott (1988); Ignarro (1988); Palmer (1987). Nitric oxide is an important messenger molecule produced by endothelial cells, neurons, macrophages, and other tissues. Marletta (1989); Moncada (1991); Nathan (1992); Snyder (1992); and Dawson *et al.* (1992). Since nitric oxide is a gas with no known storage mechanism, it diffuses freely across membranes and is extremely labile. Nitric oxide has a biological half-life on the order of seconds.

-2-

Nitric oxide exhibits several biochemical activities. This compound can bind to and activate soluble guanyl cyclase, resulting in increased cGMP levels. Nitric oxide also modifies a cysteine residue in glyceraldehyde-3-phosphate dehydrogenase by adenosine diphosphate ribosylation, Zhang & Snyder (1992), Katz *et al.* (1992), and Dimmeler *et al.* (1992), or S-nitrosylation via NAD interactions, McDonald & Moss (1993). Nitric oxide also binds to a variety of iron- and sulphur-containing proteins, Marletta (1993), and may have other modes of action as well.

Nitric oxide formation is catalyzed by the nitric oxide synthase enzymes (NOS). These enzymes act by producing nitric oxide from the terminal guanidino nitrogen of arginine, with the stoichiometric production of citrulline. There are several NOS isoforms encoded by separate genes. Marletta (1993), and Lowenstein & Snyder (1992). The various NOS isoforms are about 50-60% homologous overall. Some forms of NOS are found in most tissues. The different NOS isoforms: neuronal NOS (nNOS), macrophage NOS (iNOS), and endothelial NOS (eNOS), are now known as type I NOS, type II NOS and type III NOS, respectively. The properties of these NOS isoforms are summarized in the following Table:

Property	Type I NOS	Type II NOS	Type III NOS
Common name	nNOS	iNOS	eNOS
Typical cell	neurons	macrophages	endothelium
Other sites of expression	smooth muscle	endothelium smooth muscle	smooth muscle neurons
Expression	constitutive	inducible	constitutive
Regulation	Ca/CaM	transcription	Ca/CaM
Output	moderate (nM to $\mu$ M)	high ( $\mu$ M)	low (pM to nM)
Function	signalling	toxin	signalling

The ubiquitous presence of blood vessels and nerves means that the endothelial and neuronal isoforms may be present in most tissues. The expression of the endothelial and neuronal isoforms can also be induced in cells that normally do not express them. The sequence of these isoforms have been published or are available in Genbank under the following accession numbers:

Gene:	Species:			
	Man	Rat	Mouse	Cow
<b>Neuronal (type I)</b>	U17327	X59949	D14552	
	D16408			
	L02881			
<b>Macrophage (type II)</b>	L09210	D14051	M87039	U18331
	X85759-81	D83661	U43428	U14640
	U18334	U26686	L23806	
	U31511	U16359	L09126	
	U20141	D44591	M92649	
	U05810	X76881	M84373	
	X73029	U02534		
	L24553	L12562		
<b>Endothelial (type III)</b>	X76303-16	U18336		M89952
	L26914	U28933		L27056
	L23210			M95674
	L10693			M99057
	M95296			M89952
	M93718			

Each of these sequences are expressly incorporated herein by reference.

In blood vessels, the endothelial NOS isoform mediates endothelium-dependent vasodilation in response to acetylcholine, bradykinin, and other mediators. Nitric oxide also maintains basal vascular tone and regulates regional

blood flow. Nitric oxide levels increase in response to shear stress, i.e., forces on the blood vessels in the direction of blood flow, and to mediators of inflammation. Furchgott & van Houtte (1989); Ignarro (1989).

5 In the immune system, the macrophage isoform is produced by activated macrophages and neutrophils as a cytotoxic agent. Nitric oxide produced in these cells targets tumor cells and pathogens. Hibbs *et al.* (1988); Nathan (1992); and Marletta (1989).

10 In the nervous system, the neuronal NOS isoform is localized to discrete populations of neurons in the cerebellum, olfactory bulb, hippocampus, cortex, striatum, basal forebrain, and brain stem. Bredt *et al.* (1990). NOS is also concentrated in the posterior pituitary gland, in the superoptic and paraventricular hypothalamic nuclei, and in discrete ganglion cells of the adrenal medulla. *Id.* The widespread cellular localization of neuronal NOS and the short half-life and diffusion properties of nitric oxide suggest that it plays a role in nervous system morphogenesis and synaptic plasticity.

15 During development, NO may influence activity-dependent synaptic pruning, apoptosis, and the establishment of the columnar organization of the cortex. Gally *et al.* (1990), Edelman & Gally (1992). Two forms of long-term synaptic modulation, long-term depression of the cerebellum, Shibuki & Okada (1991), and long-term potentiation (LTP) in the hippocampus, are sensitive to inhibitors of NOS. Bohme *et al.* (1991); Haley *et al.* (1992); O'Dell *et al.* (1991); Schuman & Madison (1991). Thus, nitric oxide may serve as a retrograde neurotransmitter to enhance synaptic function due to correlated firing of pre-and postsynaptic cells.

25 In the peripheral nervous system, nitric oxide mediates relaxation of smooth muscle. Smooth muscle relaxation in the gut, important to adaptation to a bolus of food and peristalsis, depends upon inhibitory non adrenergic, noncholinergic nerves that mediate their effects via nitric oxide. Boeckvstaens *et al.* (1991); Bult *et al.* (1990); Desai *et al.* (1991); Gillespie *et al.* (1989); Gibson *et al.* (1990); Ramagopal & Leighton (1989); Tottrup *et al.* (1991). NOS-

30

containing neurons also innervate the corpus carvornosa of the penis, Burnett *et al.* (1992); Rajfer *et al.* (1992), and the adventitial layer of cerebral blood vessels. Nozaki *et al.* (1993); Toda & Okamura (1990). Stimulation of these nerves can lead to penile erection and dilation of cerebral arteries, respectively. These effects are blocked by inhibition of NOS.

Various biological roles of NO are described by Schmidt & Walter (1994); Nathan & Xie (1994); and Snyder (1995). The major roles of nitric oxide include:

- (1) vasodilation or vasoconstriction with resulting change in blood pressure and blood flow;
- (2) neurotransmission in the central and peripheral nervous system, including mediation of signals for normal gastrointestinal motility; and
- (3) defense against pathogens like bacteria, fungus, and parasites due to the toxicity of high levels of NO to pathogenic organisms.

Recently, a role for NO has been proposed in the pathophysiology of cerebral ischemia, one form of vascular endothelial disorder. Iadecola *et al.* (1994); Dalkara and Moskowitz (1994). Since NO is diffusible, short-lived, and reactive free radical gas that is difficult to measure *in vivo*, Archer (1993), most studies examining ischemic outcomes have based their conclusions on results following NOS inhibition by arginine analogues such as nitro-L-arginine or nitro-L-arginine methyl ester. These inhibitors, however, lack enzyme selectivity and block multiple isoforms. Rees *et al.* (1990). This nonselectivity might account in part for the discrepant outcomes after administration of NOS inhibitors following middle cerebral artery (MCA) occlusion.

Atherosclerosis is another form of a vascular endothelial disorder. This disease, a major cause of morbidity and mortality, is progressive beginning many years before the onset of overt symptoms. During the development of atherosclerosis, biochemical, cellular, and hemodynamic forces drive change in blood vessel walls, which ultimately leads to endothelial dysfunction, cellular proliferation, recruitment of endothelial cells, and accumulation of oxidized LDL.

Ross (1995). The cellular and molecular mechanisms that underlie these processes are complex. Rodent models offer the ability to study the contribution of individual genes, alone or in combination, to the molecular events in atherosclerosis. Breslow (1996); Ross (1996).

5           Cells within atherosclerotic plaques are monoclonal or oligoclonal in origin, indicating that intimal proliferation plays an important role in the development of lesions. Benditt (1973). Intimal proliferation also occurs as a common response to arterial injury of many kinds, regardless of whether the injury is luminal or adventitial. Schwartz (1995). Thus, models of vessel injury  
10           are relevant to atherosclerosis. For example, in a cuff model of adventitial injury, Booth *et al.* (1989); Kockx *et al.* (1993), signals from the adventitia stimulate formation of a neointimal layer in a predictable manner. This model leaves the endothelium intact, so that the role of endothelial gene products can be studied. In a filament model of endothelial injury, Lindner (1993), the endothelium is  
15           physically removed, resulting in proliferation of medial smooth muscle cells. The rate at which endothelial cells resurface the injured areas can be quantitated.

          In another type of atherosclerosis model, defined genetic mutations are used to increase the propensity of mice to atherosclerosis. Breslow (1996); Ross (1996). For example, mutant mice that form atherosclerotic lesions include apoE  
20           gene knockout mice, Plumb (1992); Zhang (1992); apoE Leiden mutation, van der Maagdenberg (1993); LDL receptor gene knockout mice, Ishibayashi (1993); and transgenic mice expressing the human apoB gene, Purcell-Huynh (1995). Of these, apoE knockout mice are an attractive atherosclerosis model, since they develop lesions on a low cholesterol, low-fat diet, and do not require the addition  
25           of cholic acid. These knockout mice develop fatty streaks that progress to fibrous plaques at branchpoints of major vessels, similar to human lesions. The rate and extent of lesion formation and its pathological severity can be quantitated. For example, a Western diet results in faster progression of the disease and formation of larger plaques than a low-cholesterol diet. Thus, the apoE knockout mice  
30           exhibit many aspects of human atherosclerosis.

Nitric oxide has physiological effects in blood vessels that may prevent atherosclerosis, such as suppression of smooth muscle proliferation, Mooradian (1995), inhibition of platelet aggregation and adhesion, Radomski (1991), and inhibition of leukocyte activation and adhesion, Bath (1993); Lefer (1993). It has also been recently reported that arginine inhibits atherosclerosis in LDL receptor mutant mice. Aji (1997).

While certain physiological effects of nitric oxide may prevent atherosclerosis, other studies suggest that excessive nitric oxide production may contribute to the development of atherosclerosis. Busse (1976); Leitinger (1995); Radomski (1995). Evidence for a pro-atherogenic role for nitric oxide includes several different findings. First, expression of iNOS and nNOS isoforms can be induced in atherosclerotic vessels. Aji (1997); Sobey (1995); Topors (1995); Wilcox (1994). Second, human atherosclerotic lesions contain nitrotyrosine, suggesting that peroxynitrite is formed in atherosclerotic lesions. See Beckman (1994b). Peroxynitrite is formed by the reaction of nitric oxide with superoxide in biological systems, Beckman (1994a), and is an extremely potent oxidant that can initiate lipid peroxidation of human LDL. Darley-Usmar (1992). Third, nitric oxide affects redox-sensitive transcription of genes involved in endothelial cell activation such as VCAM-1. This implicates nitric oxide in atherosclerosis.

However, prior to this invention, it was not clear which NOS isoforms were involved in stimulating atherosclerosis. Malinski (1993). Moreover, it was also not clear how important is peroxynitrite formation to the molecular events of atherosclerosis. Peroxynitrite ( $\text{ONOO}^\cdot$ ) is a strong oxidant capable of lipid and protein oxidation. Beckman (1994a). Superoxide reacts with nitric oxide to form peroxynitrite faster, rate constant of  $6.7 \times 10^9$  M/sec, than superoxide is scavenged by superoxide dismutase, rate constant of  $2.0 \times 10^9$  M/sec. Endothelial cells are sensitive to the redox state and may respond with a program of endothelial cell activation, including expression of VCAM-1, ICAM-1, E-selectin, and MCP-1.

Many studies depend on pharmacological agents that block NOS enzymes, such as L-nitroarginine (L-NA) and L-N-arginine methyl ester (L-NAME). Inhibition of a process by these NOS inhibitors, and reversal of inhibition by excess L-arginine, but not D-arginine, provides evidence for the involvement of NO. However, these NOS inhibitors affect all three isoforms, so that the effect on different isoforms cannot be distinguished. Distinguishing between various NOS isoforms is particularly important since NOS isoforms have multiple roles and divergent effects.

Targeted gene disruption of the endothelial or neuronal NOS isoforms offers a new approach to dissect the relevance of NO in brain ischemia and the development of treatments for brain ischemia and stroke. For example, mice deficient in neuronal NOS gene expression were relatively resistant to brain injury after permanent focal cerebral ischemia. Huang *et al.* (1994).

Over the last several years, transgenic animals have been made containing specific genetic defects, e.g., resulting in the development of, or predisposition to, various disease states. These transgenic animals can be useful in characterizing the effect of such a defect on the organism as a whole, and developing pharmacological treatments for these defects.

The relevant techniques whereby foreign DNA sequences can be introduced into the mammalian germ line have been developed in mice. See *Manipulating the Mouse Embryo* (Hogan *et al.*, eds., 2d ed., Cold Spring Harbor Press, 1994) (ISBN 0-87969-384-3). At present, one route of introducing foreign DNA into a germ line entails the direct microinjection of a few hundred linear DNA molecules into a pronucleus of a fertilized one-cell egg. Microinjected eggs may then subsequently be transferred into the oviducts of pseudo-pregnant foster mothers and allowed to develop. It has been reported by Brinster *et al.* (1985), that about 25% of the mice that develop inherit one or more copies of the micro-injected DNA.

In addition to transgenic mice, other transgenic animals have been made. For example, transgenic domestic livestock have also been made, such as pigs, sheep, and cattle.

Once integrated into the germ line, the foreign DNA may be expressed in the tissue of choice at high levels to produce a functional protein. The resulting animal exhibits the desired phenotypic property resulting from the production of the functional protein.

In light of the various biological functions of nitric oxide, there exists a need in the art to develop transgenic animals, e.g., transgenic mice, wherein the endothelial nitric oxide synthase gene has been modified. There also exists a need in the art to develop methods to test compounds for activity against various pathological states associated with the absence of eNOS, such as hypertension, atherosclerosis, and stroke, using these transgenic animals. A further need in the art is to develop treatments for various pathological states using nitric oxide or nitric oxide prodrugs.

### *Summary of the Invention*

This invention satisfies these needs in the art by providing a transgenic non-human animal comprising a disrupted endothelial nitric oxide synthase gene. In embodiments of this invention, the transgenic non-human animal exhibits hypertension or wound-healing abnormalities. In a specific embodiment of the invention, the transgenic non-human animal is a mouse. Moreover, in specific embodiments of this invention, the endothelial nitric oxide synthase gene is disrupted at exons encoding the NADPH ribose and adenine binding sites.

In other embodiments, this invention provides a method of testing compounds for activity against a vascular endothelial disorder by providing a transgenic non-human animal having a disrupted endothelial nitric oxide synthase gene, wherein the animal exhibits either a vascular endothelial disorder or is at increased risk of developing the vascular endothelial disorder, administering a

-10-

compound to be tested to the transgenic animal, and determining the effect of the compound on the vascular endothelial disorder in the animal. In specific embodiments of this invention, the vascular endothelial disorder is hypertension or atherosclerosis.

5           This invention also provides a method for treating vascular endothelial disorders comprising: selectively increasing the expression of eNOS in blood vessels without increasing the expression of iNOS or nNOS. In specific embodiments, gene therapy approaches are used.

10           In a further embodiment, this invention provides a method of testing compounds for wound-healing activity by providing a transgenic non-human animal having a disrupted endothelial nitric oxide synthase gene, administering a compound to be tested to the transgenic animal, and determining the effect of the compound on the wound-healing capabilities of the animal.

15           In another embodiment, this invention provides a method of treating wounds by applying nitric oxide or a prodrug thereof. In a specific embodiment thereof, compounds which release nitric oxide into wounds to improve or speed up wound healing.

20           In an additional embodiment, this invention provides a method of making a transgenic non-human animal of the invention comprising providing an embryonic stem cell comprising an intact eNOS gene; providing a targeting vector capable of disrupting said eNOS gene upon homologous recombination; introducing said targeting vector into said cells under conditions where the intact eNOS gene of said cell and said targeting vector undergo homologous recombination to produce a disrupted eNOS gene; introducing said cells into a  
25           blastocyst; implanting the blastocyst into the uterus of a pseudopregnant female; and delivering transgenic animals of the invention from said pseudopregnant female. In order to obtain homozygous mutant mice of the invention, the resulting animals can be bred, and homozygous mutant mice selected.

30           In another embodiment, this invention provides a method of testing compounds for utility in the treatment of cerebral ischemia or stroke by providing

-11-

a transgenic non-human animal having a disrupted endothelial nitric oxide synthase gene, administering a compound to be tested to the transgenic animal, determining the effect of the compound on infarct size or regional cerebral blood flow (rCBF) following induction of focal cerebral ischemia in the brain of said animal, and correlating the effect of said compound on infarct size or rCBF with a utility for the treatment of cerebral ischemia or stroke. In a preferred embodiment, the eNOS mutant animal has been rendered normotensive.

In a further embodiment, the invention also provides a method for testing compounds for utility in the treatment of atherosclerosis by providing a transgenic non-human animal having a disrupted endothelial nitric oxide synthase gene, administering a compound to be tested for atherosclerosis activity to the transgenic animal, determining the effect of the compound on atherosclerosis, and correlating the effect of said compound on atherosclerosis with a utility for the treatment of atherosclerosis. In specific embodiments, the effect of the compound on atherosclerosis is determined using the vessel or the cuff vessel injury model.

### ***Brief Description of the Figures***

Figure 1 depicts the targeted disruption of the endothelial NOS gene. This Figure shows restriction maps of the native mouse endothelial NOS gene, the targeting vector, and the disrupted eNOS gene. The targeted vector contains 5' and 3' flanking regions of homology and it is designed to replace the *HindIII-SalI* fragment of the eNOS gene containing exons encoding the NADPH ribose and adenine binding sites (amino acids 1010-1144). NEO refers to the neomycin antibiotic resistance gene. The location of the KS probe, used for Southern blot analysis, is also shown.

Figure 2 shows the results of a Southern blot analysis of genomic DNA isolated from mutant mouse tails, digested with *SpeI* and hybridized to the KS probe, shown in Figure 1. Lanes 1, 2, and 3 show wild-type, heterozygous, and homozygous eNOS mutant mice, respectively. The positions of fragments

-12-

hybridizing to the wild-type and the disrupted eNOS gene, as depicted in Figure 1, are indicated.

Figure 3 depicts a Western blot analysis of eNOS mutant mice. Brain, heart, lung and aorta samples of wild-type (wt) and mutant (m) mice were tested for immunological reactivity against a mouse monoclonal antibody directed against eNOS. The position of eNOS is shown.

Figure 4 depicts the endothelium-dependent relaxation of aortic rings in response to acetylcholine. Panel a shows the effect on wild-type aortic segments. Panel b depicts treatment of wild-type vessel rings with L-nitroarginine (L-NA), a NOS inhibitor. Panel c depicts the endothelium-dependent relaxation of eNOS mutant aortic segments.

Figure 5 depicts blood pressure responses to L-NA. Urethane-anesthetized wild-type (solid line) and eNOS mutant mice (dotted line) were measured before and after L-NA administration at time 0.

Figure 6 depicts wound healing in eNOS mutant mice. Figure 6A is a micrograph of a 24 hr. wound in a wild-type mouse. Figure 6B is a micrograph of a 5 day wound in a wild-type mouse. Figure 6C is a 24 hr. wound of an eNOS mutant mouse. Figure 6D is a 5 day wound of an eNOS mutant mouse. (ep) refers to the epidermis, while (d) refers to the dermis. Capillaries are indicated by (cap).

Figure 7 depicts infarct size in wild-type and eNOS mutant mice. In Figure 7A infarct volumes were measured in SV-129 mice (A), C57 Black/6 mice (B), eNOS mutant mice without hydralazine treatment (C), and eNOS mutant mice following hydralazine treatment (D). Infarct size was detected 24 hrs after permanent filament MCA occlusion by TTC staining. A statistically significant increase ( $p < 0.05$ ) in infarct size was noted for eNOS mutant animals. Each dot represents the value from an individual animal, and data are expressed as mean  $\pm$  SD.

Figure 7B depicts infarct areas in five coronal sections from rostral to caudal (2 to 10 mm) of the above groups. Open circles, filled circles, and

triangles represent wild-type SV-129 mice, wild-type C57 Black 6 mice, and eNOS mutant mice, respectively. Data shown are means  $\pm$  SD. \* indicates  $p < 0.05$  as compared to both wild-type SV-129 and wild-type C57 Black/6 mice. # indicates  $p < 0.05$  as compared to SV-129 mice alone.

Figure 8 depicts regional cerebral blood flow (rCBF) as measured by laser Doppler flowmetry after MCA occlusion in the periinfarct area of eNOS mutant mice (dotted line,  $n=11$ ) as compared to wild-type SV-129 animals (continuous line,  $n=10$ ,  $p < 0.05$ ). A greater rCBF reduction was noted in eNOS mutant mice as compared to wild-type mice. A flexible optic probe tip (diameter = 0.5 mm) was secured 2 mm posterior and 3 mm lateral to bregma on the ipsilateral hemisphere. Steady-state rCBF values prior to occlusion were taken as a baseline (100%) and the subsequent changes after the onset of ischemia were shown as a percentage relative to baseline. Time zero represents the point of MCA occlusion. There were no significant differences in rCBF blood flow between SV-129 and C57 Black/6 wild-type mice.

Figure 9 depicts the effect of hemorrhagic hypotension on rCBF in urethane-anesthetized (dotted line) and wild-type animals (continuous line). Hypotension was induced by gradually withdrawing arterial blood as described *infra*, and rCBF was measured by laser Doppler flowmetry. The initial rCBF values were taken as 100% and the corresponding changes thereafter calculated as percentage relative to the initial value. The baseline MABF in wild-type and mutants were  $104 \pm 12$  ( $n=7$ ) and  $117 \pm 13$  mm Hg ( $n=7$ ), respectively. There was a greater tendency toward hypoperfusion at higher levels of MABP in the mutant animals. Data are expressed as mean  $\pm$  SD. \* signifies  $p < 0.05$  as compared to wild-type animals.

Figure 10 shows that the diameter of pial arterioles was increased in eNOS mutant mice (circle,  $n=7$ ), but not in wild-type (square,  $n=8$ ) mice after nitro-L-arginine superfusion in a closed cranial window. Nitro-L-arginine (1 mM) was topically superfused for 40 minutes. Superfusion of nitro-D-arginine (1 mM,  $n=3$ ) did not affect the diameter of pial arterioles in eNOS mutant mice

-14-

(data not shown). The data are calculated as percent from baseline and expressed as mean  $\pm$  SD. \* indicates  $p < 0.05$  and \*\* indicates  $p < 0.01$  vs. wild-type.

Figure 11 depicts the autoradiographic distribution of [ $^3$ H]L-NA binding in sagittal brain sections of wild-type and mutant mice. Figure 11A is the distribution in SV-129 wild-type mice. Figure 11B is the distribution in C57 Black/6 wild-type mice. Figure 11C is the distribution in eNOS mutant mice. Figure 11D is the distribution in nNOS mutant mice. In Figures 11A-D, OB: olfactory bulb; Str: striatum; HP: hippocampus; DG: dentate gyrus; AM: amygdala; CB: cerebellum. Scale bar=300  $\mu$ m.

Figure 12 depicts the autoradiographic distribution of [ $^3$ H]L-NA binding in coronal sections of SV-129 wild-type mouse brain. Figures 12A -G show total binding. Figure 12H shows binding remaining in the presence of 10  $\mu$ M L-NA. In Figure 12, OB: olfactory bulb; TT: tenia tecta; Str: striatum; RF: rhinal fissure; HP: hippocampus; DG: dentate gyrus; MAN: medial amygdaloid nuclei; CAN: anterior cortical amygdaloid nuclei; VMH: ventromedial hypothalamic nuclei; PC: posteromedial cortical amygdaloid nuclei; PT: piriform transition; LM: lateral mammillary nucleus; SG: superficial grey layer superior colliculus; CB: cerebellum; PR: pontine reticular nucleus. Scale bar=300  $\mu$ m.

Figure 13 depicts the correlation between [ $^3$ H]L-NA binding in mouse and rat brain. 1: granular layer of olfactory bulb, 2: amygdaloid nuclei-posteromedial cortical, 3: amygdaloid piriform transition, 4: amygdaloid nuclei-medial, 5: taenia tecta, 6: rhinal fissure, 7: lateral mammillary nucleus, 8: hippocampal CA3 subfield, 9: amygdaloid nuclei-basomedial, 10: superficial grey layer of superior colliculus, 11: molecular layer of cerebellum, 12: amygdaloid nuclei-anterior cortical, 13: dentate gyrus, 14: amygdaloid nuclei-central, 15: I and II layers of occipital cortex, 16: hippocampal CA1, 17: dorsal tegmental nucleus, 18: plexiform layer of olfactory bulb, 19: I and II layers of frontal cortex, 20: ventromedial hypothalamic nuclei, 21: granule layer of cerebellum, 22: dorsomedial hypothalamic nuclei, 23: medial mammillary nucleus, 24: III to VI layers of occipital cortex, 25: III to VI layers of frontal cortex, 26: striatum, 27:

pontine reticular nucleus, 28: posterior thalamus nuclei, 29: ventral posteromedial thalamus nuclei. Values in mouse and rat brain represent the mean of five SV-129 mice and three rats, respectively.

Figure 14 depicts [ $^3\text{H}$ ]L-NA binding in sagittal sections of SV-129 mouse brain. Figure 14A shows total binding. Figures 14B and 14C, respectively, show binding in the presence of 10  $\mu\text{M}$  D-NA, and 100  $\mu\text{M}$  7-NI, a potent and selective type 1 inhibitor. Figure 14D shows the binding in the presence of excess L-NA (10  $\mu\text{M}$ ). Scale bar=300  $\mu\text{m}$ .

Figure 15 is a schematic showing the effects of nitric oxide produced from various NOS isoforms in normal and atherosclerotic arteries. In Figure 15A, nitric oxide produced by normal endothelium prevents proliferative response to injury and suppresses development of atherosclerosis. In Figure 15B, nitric oxide production in atherosclerotic plaques may lead to peroxynitrite formation, lipid oxidation, and endothelial cell inactivation.

Figure 16 is a schematic showing the cuff model of vessel injury.

Figure 17 depicts micrographs of hematoxylin and eosin stained sections of cuff injured vessels. Injured vessels contain neointima seen inside of the internal elastic lamina (shown with arrows). Control vessels do not contain the neointima. Vessels from eNOS mutant mice show significantly increased neointimal formation, which is shown with an asterisk.

Figure 18 depicts histology and immunochemical staining of injured and control vessels from eNOS mutant mice. Control vessels have no intima.

Figure 19 depicts quantitative RT-PCR of eNOS mRNA from mouse aorta.

Figure 20 depicts atherosclerotic lesions from apoE mutant mice at 6 months. Figure 20A shows the aortic arch and carotid arteries; Figure 20B shows the thoracic aorta; Figure 20C shows the descending thoracic aorta; and Figure 20D shows oil red O stain of an aortic lesion.

### *Detailed Description of Preferred Embodiments*

In the description that follows, a variety of various technical terms are used. Unless the context indicates otherwise, these terms shall have their ordinary well-recognized meaning in the art. In order to provide a clearer and more consistent understanding of the specification and claims, the following definitions are provided.

**Transgenic.** As used herein, a "transgenic organism" is an organism containing a defined change to its germ line, wherein the change is not ordinarily found in wild-type organisms. This change can be passed on to the organism's progeny. The change to the organism's germ line can be an insertion, a substitution, or a deletion. Thus, the term "transgenic" encompasses organisms where a gene has been eliminated or disrupted so as to result in the elimination of a phenotype associated with the disrupted gene ("knock-out animals"). The term "transgenic" also encompasses organisms containing modifications to their existing genes and organisms modified to contain exogenous genes introduced into their germ line.

**Nitric oxide synthase (NOS).** As used herein, nitric oxide synthase is an enzyme able to catalyze the formation of nitric oxide. For example, NOS can catalyze the formation of nitric oxide from the terminal guanidino nitrogen of arginine, with the stoichiometric production of citrulline.

**Disrupted gene.** As used herein, "disrupted gene" refers to a gene containing an insertion, substitution, or deletion resulting in the loss of substantially all of the biological activity associated with the gene. For example, a disrupted NOS gene would be unable to express a protein having substantial NOS enzymatic activity.

**Vector.** As used herein, a "vector" is a plasmid, phage, or other DNA sequence, which provides an appropriate nucleic acid environment for a transfer of a gene of interest into a host cell. The cloning vectors of this invention will ordinarily replicate autonomously in eukaryotic hosts. The cloning vector may

be further characterized in terms of endonuclease restriction sites where the vector may be cut in a determinable fashion. The vector may also comprise a marker suitable for use in identifying cells transformed with the cloning vector. For example, markers can be antibiotic resistance genes.

5           **Expression vector.** As used herein, an "expression vector" is a vector comprising a structural gene operably linked to an expression control sequence so that the structural gene can be expressed when the expression vector is transformed into an appropriate host cell.

10           **Targeting vector.** As used herein "a targeting vector" is a vector comprising sequences that can be inserted into a gene to be disrupted, e.g., by homologous recombination. Therefore, a targeting vector may contain sequences homologous to the gene to be disrupted.

This invention relates to non-human transgenic animals comprising a disrupted endothelial NOS gene.

15           In order to obtain a transgenic animal comprising a disrupted eNOS gene, a targeting vector is used. The targeting vector will generally have a 5' flanking region and a 3' flanking region homologous to segments of the eNOS gene surrounding an unrelated DNA sequence to be inserted into the eNOS gene. For example, the unrelated DNA sequence can encode a selectable marker, such as  
20           an antibiotic resistance gene. Specific examples of a suitable selectable marker include the neomycin resistance gene (NEO) and the hygromycin  $\beta$ -phosphotransferase. The 5' flanking region and the 3' flanking region are homologous to regions within the eNOS gene surrounding the portion of the gene to be replaced with the unrelated DNA sequence. DNA comprising the targeting  
25           vector and the native eNOS gene are brought together under conditions where homologous recombination is favored. For example, the targeting vector and native eNOS gene sequence can be used to transform embryonic stem (ES) cells, where they can subsequently undergo homologous recombination. For example, J1 embryonic stem cells obtained from Dr. En Li of the Cardiovascular Research  
30           Center of the Massachusetts General Hospital and Dr. Rudolph Jaenisch of the

-18-

Whitehead Institute of MIT. The targeting vector, pPNT-ENOS, has been deposited with the American Type Culture Collection (A.T.C.C.), 12301 Parklawn Drive, Rockville, Maryland 20852 USA, under the terms of the Budapest Treaty under accession number A.T.C.C. 97469 on March 13, 1996.

5           Proper homologous recombination can be tested by Southern blot analysis of restriction endonuclease digested DNA using a probe to a non-disrupted region of the eNOS gene. For example, the KS probe, identified in Figure 1, can be used. Since the native eNOS gene will exhibit a different restriction pattern from the disrupted eNOS gene, the presence of a disrupted eNOS gene can be  
10           determined from the size of the restriction fragments that hybridize to the probe.

          In one method of producing the transgenic animals, transformed ES cells containing a disrupted eNOS gene having undergone homologous recombination, are introduced into a normal blastocyst. The blastocyst is then transferred into the uterus of a pseudo-pregnant foster mother. Pseudo-pregnant foster mothers had  
15           been mated with vasectomized males, so that they are in the proper stage of their estrus cycle and their uterus is hormonally primed to accept an embryo. The foster mother delivers a transgenic animal containing a disrupted eNOS gene. Homozygous mutant animals are normally obtained by breeding the transgenic animals.

20           The extent of the contribution of the ES cells, containing the disrupted eNOS gene, to the somatic tissues of the transgenic mouse can be determined visually by choosing strains of mice for the source of the ES cells and blastocyst that have different coat colors.

          The resulting homozygous eNOS mutant animals generated by  
25           homologous recombination are viable, fertile, and indistinguishable from wild-type and heterozygous littermates in overall appearance (except for the presence of a selectable marker) or routine behavior. However, the mutant animals can also be sterilized using methods well known in the art, e.g. vasectomy or tubal ligation. *See Manipulating the Mouse Embryo, supra.* The mutant animals can  
30           be mated to obtain homozygous or heterozygous progeny. These mutant animals

contain substantially less immunoreactive eNOS than wild-type animals. Most preferably, these mutant mice contain no immunoreactive eNOS protein as measured by western blot analysis of brain, heart, lung, or aorta tissue.

5 A targeting vector such as pPNT-ENOS can be used to create cell lines or primary cell cultures that do not express NOS. The endogenous eNOS gene can be disrupted by introducing the targeting vector into cells containing the eNOS gene to be disrupted and allowing the targeting vector and the endogenous gene to undergo homologous recombination. For example, the targeting vector can be introduced into the cells by electroporation. If both copies of the eNOS  
10 gene are to be disrupted, higher concentrations of the selection agent, e.g., neomycin or its analog G418 are used. Suitable cell lines and cultures include tumor cells, endothelial cells, epithelial cells, leukocytes, neural cells, glial cells, and muscle cells.

15 The eNOS mutant animals of the invention can be any non-human mammal. In embodiments of this invention, the animal are mice, rats, guinea pigs, rabbits, or dogs. In an especially preferred embodiment of the invention, the eNOS mutant animal is a mouse.

20 These homozygous eNOS mutant animals also exhibit significantly reduced calcium-dependent membrane-associated NOS enzymatic activity. In preferred embodiments of this invention the enzymatic activity in aorta samples is less than  $1.0 \text{ pmol mg}^{-1} \text{ min}^{-1}$   $^3\text{H}$ -arginine to citrulline conversion. In most preferred embodiments of this invention the enzymatic activity in aorta samples is less than  $0.5 \text{ pmol mg}^{-1} \text{ min}^{-1}$   $^3\text{H}$ -arginine to citrulline conversion. Any residual NOS activity may be due to the presence of neuronal NOS (nNOS) in neurons in  
25 the perivascular plexus, and not to the expression of any residual nondisrupted eNOS genes.

30 Endothelium-derived relaxing factor is absent or significantly reduced in eNOS mutant animals. However, vascular smooth-muscle responses are intact. For example, the aortic rings of mutant mice show no relaxation to acetylcholine, while aortic rings from wild-type mice manifest a dose-dependent relaxation to

acetylcholine. *See* Figure 4. Moreover, treatment of wild-type aortic rings with  $10^{-4}$ M L-nitroarginine has no effect on vascular tone by itself, but blocks the relaxation in response to acetylcholine. *Id.* Treatment of the eNOS mutant aortic rings with  $10^{-4}$ M L-nitroarginine also has little or no effect on vessel tone either by itself or on the response to acetylcholine. The maximum dilation of norepinephrine pre-contracted rings from eNOS mutant mice to sodium nitroprusside is similar to wild-type mice. This indicates that vascular smooth-muscle responses in eNOS mutant animals are intact.

The eNOS mutant animals of the invention exhibit various vascular endothelial disorders. These disorders include hypertension and an increased propensity for cerebral ischemia, stroke or atherosclerosis. In addition, the eNOS mutant animals exhibit abnormal wound healing properties. Other vascular endothelial disorders include clotting disorders, other cerebrovascular disorders, coronary artery disease, and peripheral vascular disease. The eNOS mutant animals of the invention exhibit these disorders or an increased propensity of developing these disorders.

Consequently, the eNOS mutant animals are useful as a model to study these and other vascular endothelial disorders. For example, various compounds could be tested for a therapeutic effect on a vascular endothelial disorder by providing a transgenic non-human animal having a disrupted eNOS gene and exhibiting a vascular endothelial disorder; determining the effect of a compound on symptoms of the vascular endothelial disorder; and correlating the effect of the compound on the treatment of the vascular endothelial disorder.

The compounds to be tested are typically not NOS inhibitors. Determining whether a compound exhibits NOS inhibitor activity can be tested based on the information provided herein and in the technical literature. Hevel *et al.* (1994). In preferred embodiments of the invention, compounds that induce NO production are tested; and in more preferred embodiments, compounds that induce NO production in the endothelium are tested. The compounds to be tested can be derived from a variety of sources including, but not limited to, rationally

designed and synthetic molecules, plant extracts, animal extracts, inorganic compounds, mixtures, solutions, and homogeneous molecular or elemental samples.

5 The eNOS mutant animals exhibit a significantly higher blood pressure than the wild-type animals. In specific embodiments of this invention eNOS mutant mice exhibit a mean blood pressure significantly higher than 81 mm Hg. In a preferred embodiment of this invention, eNOS mutant mice exhibit a mean blood pressure greater than about 100 mm Hg. In a most preferred embodiment of this invention, eNOS mutant mice exhibit a mean blood pressure of about 110  
10 mm Hg. Analogous increases in mean blood pressure are expected in other non-murine eNOS mutant (knock-out) animals.

L-NA and other NOS inhibitors cause a rise in blood pressure in many species including humans, rats, guinea pigs, rabbits, dogs, and mice. This effect is consistent with a role of basal nitric oxide production in vasodilation, because  
15 inhibition of eNOS would lead to less basal vasodilation and result in hypertension. However, eNOS mutant mice show a decrease in blood pressure in response to L-NA. See Figure 5. This hypotensive effect is blocked by L-arginine and is not observed with D-nitroarginine. This suggests that pharmacological blockers may have effects in addition to NOS inhibitors, or that  
20 non-endothelial NOS isoforms are involved in the maintenance of blood pressure. For example, nNOS is present both in vasomotor centers of the central nervous system and in perivascular nerves. However, effects of its blockade suggest that it plays a vasodilatory role. Mutant neuronal NOS mice have blood pressures similar to wild-type mice, but they have a tendency towards hypotension when  
25 exposed to anaesthesia, which is consistent with a possible role for nNOS in maintaining, not reducing, blood pressure. Multiple roles for endothelial and non-endothelial NOS isoforms in vasodilation and vasoconstriction may explain the observed variability in maximal pressor effects of various NOS inhibitors.

30 There is evidence that in hypertension the amount of NO produced by the endothelium decreases in humans. The eNOS knockout mice mimic this effect,

-22-

since their endothelium also does not produce any NO. Consequently, these mice serve as a useful model for hypertension. Thus, establishing an anti-hypertensive effect in eNOS mutant animals of the invention for a compound other than an NOS inhibitor, such as a compound that induces the production of NO, would be predictive that this compound would have anti-hypertensive properties in other animals, including humans. However, the opposite result would be expected for a compound that inhibits NOS.

An inhibitor of NOS would be expected to raise blood pressure in wild-type animals, but stabilize or reduce blood pressure in eNOS mutant animals. In eNOS mutant animals, an NOS inhibitor would inhibit the residual NOS, mostly nNOS. nNOS mutant animals may have a tendency toward hypotension. Thus, the preferential inhibition of nNOS in the mutant animals should result in the same or lower blood pressure. However, in normal animals, the role of eNOS on blood pressure regulation is much more pronounced than the role of nNOS. Therefore, the predominant effect of an NOS inhibitor in normal animals would be to inhibit eNOS, which raises blood pressure. This is demonstrated in Example 5, *infra*.

In addition, there is also evidence that in atherosclerosis, diabetes and normal aging, the amount of NO produced by the endothelium decreases in humans. Thus, these mice would serve as a useful model not just for hypertension, but also for vascular responses in atherosclerosis, diabetes and normal aging.

The eNOS mutant animals of this invention are useful as an animal model to study hypertension. For example, various compounds could be tested for an anti-hypertensive effect in the eNOS mutant animals. Specifically, compounds that are not NOS inhibitors can be tested. In more preferred embodiments, compounds that are not eNOS inhibitors are tested. In other preferred embodiments compounds that induce NO production are tested. In additional preferred embodiments, compounds that induce NO production in the endothelium are tested. Therefore, the invention provides methods for screening

compounds using the eNOS mutant animals as an animal model to identify compounds useful in treating hypertension. This aspect of the invention is useful to screen compounds from a variety of sources. Examples of compounds that can be screened using the method of the invention include but are not limited to

5      rationally designed and synthetic molecules, plant extracts, animal extracts, inorganic compounds, mixtures, and solutions, as well as homogeneous molecular or elemental samples.

The invention, therefore, provides a method of screening compounds, comprising: providing a transgenic non-human animal having a disrupted eNOS

10      gene and exhibiting hypertension, administering a compound to be tested to the transgenic animal; determining the effect of the compound on the blood pressure of said animal; and correlating the effect of the compound on the blood pressure of the animal with an anti-hypertensive effect of said compound.

The compounds to be tested can be administered to the transgenic non-

15      human animal having a disrupted eNOS gene in a variety of ways well known to one of ordinary skill in the art. For example, the compound can be administered by parenteral injection, such as subcutaneous, intramuscular, or intra-abdominal injection, infusion, ingestion, suppository administration, and skin-patch application. Moreover, the compound can be provided in a pharmaceutically acceptable carrier. *See* Remington's Pharmaceutical Sciences (1990). The effect

20      of the compound on blood pressure can be determined using methods well known to one of ordinary skill in the art.

In addition, the eNOS mutant animals of this invention unexpectedly exhibit abnormal wound-healing properties. For example, these animals often

25      develop spontaneous wounds that do not heal. In contrast to normal mice, who healed their wounds within 5 days, the eNOS mutant mice exhibit significantly different wound healing properties. First, the eNOS mutant mice exhibit spontaneous wounds that never heal. Second, in experiments where wounds were created, the eNOS mutant mice heal more slowly than normal animals. Healing

30      of eNOS mutant mice typically takes 2-3 times as long as normal mice. The

exact healing time will depend on the type of wound inflicted. Moreover, two specific features of normal wound healing are abnormal in the eNOS mutant mice:

- 1) growth of the epithelial layer of skin across the wound to bridge the gap and close the wound; and
- 2) neovascularization in the granulation tissue that fills the wound.

In the eNOS mutant mice, migration of epithelial cells to the site of the wound is delayed, with epithelial cells remaining at the edge of the wound after five days. The connective tissue is also markedly abnormal, containing few or no new blood vessels. The results demonstrate an important role for eNOS in angiogenesis and epithelial cell migration during wound healing.

The eNOS mutant animals of this invention are useful as an animal model to study wound healing. For example, various compounds could be tested for a wound healing effect in the eNOS mutant animals. Therefore, the invention provides methods for screening compounds using the eNOS mutant animals as an animal model to identify compounds useful in enhancing wound healing. This aspect of the invention is useful to screen compounds from a variety of sources. Examples of compounds that can be screened using the method of the invention include but are not limited to rationally designed and synthetic molecules, plant extracts, animal extracts, inorganic compounds, mixtures, and solutions, as well as homogeneous molecular or elemental samples. For example, various compounds designed to improve wound healing can be tested. For example, compounds that deliver NO to the healing wound can be used. Establishing an enhancement of wound healing by a compound in eNOS mutant animals is predictive that this compound would enhance wound healing in other animals, including humans.

The invention, therefore, provides a method of screening compounds, comprising: providing a transgenic non-human animal having a disrupted eNOS gene and exhibiting abnormal wound healing properties, administering a

compound to be tested to the transgenic animal; determining the effect of the compound on the wound healing properties of said animal; and correlating the effect of the compound on the wound healing properties of the animal with a wound healing effect of said compound.

5           Thus, the eNOS mutant animals of this invention are also useful as animal models to study wound healing.

          Moreover, since the synthesis of nitric oxide appears to enhance wound healing, prodrugs that release nitric oxide *in situ* may improve or speed up healing. Examples of suitable compounds that release nitric oxide include  
10       nitroglycerin, sodium nitroprusside, and SIN-1. The extent to which these and other similar compounds improve or speed up wound healing can be determined experimentally. For example, the compound could be applied at the wound to a patient in need of treatment and its effect on wound healing can be quantified.

          The eNOS mutant animals of this invention are also useful as an animal  
15       model to study cerebral ischemia resulting from stroke. Since endothelial NO production may protect brain tissue by increasing ischemic rCBF, compounds can be tested for the ability to increase rCBF as well as the ability to reduce ischemic infarct size. rCBF and infarct size can be measured as described in the Examples. Compounds that increase rCBF or decrease infarct size would be expected to be  
20       useful as therapeutics for the treatment of stroke or cerebral ischemia from other sources.

          It has been reported that nNOS enzymatic activity may contribute to the development of ischemic brain necrosis. In eNOS mutant animals, any non-specific NOS inhibitor would predominantly inhibit the nNOS isoform.  
25       However, in wild-type animals, both eNOS and nNOS would be inhibited. Since eNOS and nNOS have opposite effects under ischemic conditions, with eNOS activity being protective and nNOS activity being detrimental, compounds that are non-specific NOS inhibitors should not be tested for anti-stroke activity. Therefore, in preferred embodiments compounds that are not NOS inhibitors are  
30       tested. In more preferred embodiments, compounds that induce NO production

can be tested for use as a treatment for stroke or cerebral ischemia. In particularly preferred embodiments, compounds that induce production of NO in the endothelium are tested.

Compounds that can be screened for use in treating stroke or cerebral ischemia can be obtained from a variety of sources. Examples of compounds that can be screened using the method of the invention include but are not limited to rationally designed and synthetic molecules, plant extracts, animal extracts, inorganic compounds, mixtures, and solutions, as well as homogeneous molecular or elemental samples.

The compounds to be tested can be administered to the transgenic non-human animal having a disrupted eNOS gene in a variety of ways well known to one of ordinary skill in the art. For example, the compound can be administered by parenteral injection, such as subcutaneous, intramuscular, or intra-abdominal injection, infusion, ingestion, suppository administration, and skin-patch application. Moreover, the compound can be provided in a pharmaceutically acceptable carrier. *See* Remington's Pharmaceutical Sciences (1990).

The eNOS animals are additionally useful as an animal model to study atherosclerosis. The physiological production of nitric oxide by eNOS suppresses atherosclerosis, whereas the pathologic production of nitric oxide by iNOS and nNOS contributes to atherosclerosis. To test the effect of various compounds on atherosclerosis, various animal models involving eNOS mutant mice are used. Two vessel injury models, the cuff model and the filament model, provide useful data relevant to atherosclerosis. In the cuff model the neointima formation is stimulated by adventitial injury. In the filament model, the endothelium is physically removed, and the rate at which endothelial cells resurface the injured areas is measured. Alternatively, double mutant animals exhibiting aspects of atherosclerosis can be used. For example, double mutant apoE, eNOS mice can be used. Other potential double mutant animals for use in this aspect of the invention include apoE Leiden/eNOS and LDL-receptor eNOS mutants.

By way of example, compounds can be provided to eNOS mutant mice, and the effect of the compound on neointima formation following vessel injury using the cuff model can be determined. The extent of neointima formation can be determined as described in the Examples. Compounds that reduce the extent of neointima formation relative to control eNOS mutant mice not receiving the compound would be expected to be useful as therapeutics for the treatment of atherosclerosis.

In another example, compounds can be provided to eNOS mutant mice and the effect of the compound on the rate at which endothelial cells resurface injured areas of vessels following vessel injury using the filament model can be determined. Compounds that increase the rate of endothelial cell resurfacing relative to control eNOS mutant mice not receiving the compound would be expected to be useful as therapeutics for the treatment of atherosclerosis.

In a further example, compounds can be provided to double mutant animals, which exhibit features of human atherosclerosis. Compounds that reduce symptoms of atherosclerosis in these animals would also be expected to be useful as therapeutics for the treatment of atherosclerosis. A preferred example of a double mutant animal is an apoE/eNOS double mutant.

Since nNOS and iNOS may contribute to atherosclerosis, compounds that are non-specific NOS inhibitors should not be tested for activity against atherosclerosis. Compounds to be tested can be obtained from various sources and administered in various ways as described for other endothelial vascular disorders, *supra*.

Another example of a double mutant animal is eNOS/nNOS mutant mice. These double mutant animals can be obtained by mating eNOS mutant mice to nNOS mutant mice of the same genetic background. Double heterozygous eNOS/nNOS mutant mice are obtained, mating pairs of the double heterozygous mice are obtained, and eNOS/nNOS mutant mice are obtained.

## *Examples*

### *Example 1*

#### *Targeted Disruption of the Endothelial NOS Gene*

The endothelial NOS gene was cloned by screening a mouse genomic library, obtained from Stratagene, using a human eNOS cDNA clone, obtained from Kenneth D. Bloch, as described in Janssens *et al.* (1992), Genbank accession number M93718. Plasmid hNOS3C, containing the endothelial nitric oxide synthase gene, was deposited at the American Type Culture Collection on July 17, 1996. The targeting vector was derived from the pPNT vector, which contains thymidine kinase gene and the neomycin resistance gene. *See Figure 1.* Tybulewicz *et al.* (1991). The targeting vector contains 5' and 3' flanking regions of homology to the eNOS gene, and is designed to replace the *HindIII-SalI* fragment that contains exons encoding the NADPH ribose and adenine binding sites of the eNOS protein (amino acids 1010-1144) following homologous recombination.

J1 ES cells were grown as described in Li *et al.* (1992) on irradiated embryonic fibroblast feeder cells in media containing 200 units/ml leukocyte inhibitory factor. For electroporation,  $10^7$  cells were mixed with targeting vector DNA at 150  $\mu\text{g/ml}$ . A Bio-Rad gene pulsar was used to electroporate the DNA into the cells at a setting of 960  $\mu\text{F}$  capacitance, 250 mV. The targeting vector and the native eNOS gene were then able to undergo homologous recombination. The cells were plated on neomycin-resistant irradiated fibroblast feeder cells, and selection with 150  $\mu\text{g/ml}$  G418 and 2  $\mu\text{M}$  FIAU was started 48 hours later. Doubly resistant colonies were picked seven days after electroporation and grown in 24-well plates.

## ***Example 2***

### ***Generation of Chimeric Mice with Germline Transmission***

Blastocysts were isolated from C57 BL/6 mice on day 3.5 of pregnancy and 20-25 ES cells, following homologous recombination and selection, were  
5 injected into the uterine horn of pseudo-pregnant (C57 BL/6 x DBA/2) F1 mice. Chimeric mice were identified by the agouti contribution of the ES cells to the coat color, and were back-crossed to C57 BL/6 mice. Germline transmission was determined by the presence of agouti mice in the offspring.

Proper recombination was demonstrated by Southern blot analysis of *SpeI*  
10 digested genomic DNA using the KS probe shown in Figure 1. Back-crossed mice were screened by Southern blot, and heterologous mice were selected. In Figure 1, lanes 1, 2 and 3 show wild-type, heterozygous, and homozygous mutant mice, respectively. The positions of the hybridizing fragments for the wild-type and the disrupted eNOS gene are shown. The results demonstrate that the  
15 targeted disruption of the eNOS gene is present in the germline of the transgenic mice.

Western blot analysis of tissue samples from eNOS mutant mice was also performed. 10  $\mu$ g protein extracts from the brain, heart, lung, and aorta/vena cava of wild-type and eNOS mutant animals were electrophoresed through a 10%  
20 SDS-polyacrylamide gel and transferred to nitrocellulose. The blot was incubated with mouse monoclonal antibodies directed against endothelial NOS (Transduction Research Laboratories), and specific hybridization was localized using chemiluminescent alkaline phosphatase conjugated with anti-mouse antibody (ECL, Amersham). Hybridization of endothelial NOS is observed for  
25 the wild-type samples, but not in the eNOS mutant samples. The heart, lung, and aorta samples show a band at relative molecular mass of 50 kDa in both wild-type and eNOS mutant samples, which represents mouse immunoglobulin heavy chains present in the tissue samples. The antibody used was directed against a

-30-

peptide corresponding to amino acids 1030-1209, a region which overlaps with the region deleted in the eNOS mutant mice. See Figure 3. This demonstrates that the eNOS mutant mice (homozygous) produce no immunoreactive undisrupted eNOS, further demonstrating successful transmission of the disruption to the germline of the transgenic mice.

Aorta samples from eNOS mutant mice were tested for calcium-dependent membrane-associated NOS enzymatic activity. This enzymatic activity was reduced to about  $0.5 \text{ pmol mg}^{-1} \text{ min}^{-1}$ . The residual activity is likely due to neuronal NOS in neurons in the perivascular plexus.

### Example 3

#### *Determination of blood pressure of eNOS mutant and wild-type mice*

Mice were kept at normal temperature ( $37^{\circ}\text{C}$ ), anesthetized with urethane (1.5 mg/kg, intraperitoneal injection) or halothane inhalation, and ventilated using an SAR-830 mouse ventilator (CWE Instruments). Depth of anesthesia was adjusted to keep the blood pressure of animals unresponsive to tail-pinch with forceps. End-tidal  $\text{CO}_2$  was monitored with a microcapnometer and kept constant by adjustment of respiratory parameters. The right femoral artery was cannulated using stretched PE-10 polyethylene tubing (Clay Adams) for mean arterial blood pressure recordings using an ETH-400 transducer and a MacLab data acquisition system (ADI Instruments). For awake measurements, the femoral artery catheter was placed under halothane anesthesia and the wound was covered with 1% xylocane ointment to diminish discomfort. Recordings were made within one hour of the procedure. Data are expressed as means with standard deviation. Statistical evaluation was performed by t-test.

**Table 1. Blood pressure of eNOS mutant and wild-type mice**

	Wild-type mice			eNOS mutant mice		
	Urethane	Halothane	Awake	Urethane	Halothane	Awake
Mean BP (mmHG)	81	90	97	110*	109*	117*
s.d.	9	12	8	8	11	10
<i>n</i>	16	15	14	17	18	17

\*P<0.01 for eNOS mutant animals vs. wild-type mice.

There is no statistically significant difference between the blood pressure of nNOS mutant mice and wild-type mice using this procedure.

Similar results are obtained with different methods of anesthesia and in the awake state. Blood pressure is the same for the wild-type SV129 strain, wild-type C57 B16 strain, and litter mates of the eNOS mutant animals that are wild-type at the eNOS locus.

#### ***Example 4***

##### ***Endothelium-dependent Relaxation of Aortic Rings in Response to Acetylcholine from eNOS Mutant and Wild-type Mice***

The thoracic aorta was dissected from wild-type and eNOS mutant mice and placed in physiological saline aerated with 95% O<sub>2</sub>/5% CO<sub>2</sub>. 4 mm segments of the aorta were mounted on tungsten wires in conventional myographs and maintained at optimal tension in physiological saline for 1 hour at 37°C. The rings were pre-contracted with 10<sup>-7</sup> M norepinephrine and exposed to increasing concentrations of acetylcholine (ACh) from 10<sup>-8</sup> M to 3 x 10<sup>-5</sup> M. 2-3 segments were collected from each mouse, and five mice were used from the wild-type and eNOS mutant groups. Mean data from each animal were used. Respective tracings are shown. Acetylcholine concentrations are expressed in logM.

-32-

Figure 4A depicts wild-type aortic segments responding to acetylcholine with dose-dependent relaxation. At  $3 \times 10^{-5}$  M,  $60.3 \pm 14.6\%$  of pre-addition tone was present. Figure 4B depicts treatment of the wild-type vessel rings with  $10^{-4}$  M L-NA for 1 hour and shows abolished acetylcholine-induced relaxation. Figure 4C shows that eNOS mutant aortic segments do not relax to acetylcholine, demonstrating that EDRF activity is absent from eNOS mutant mice. L-NA has no additional affect on eNOS vessel segments.

Thus, aortic rings from wild-type mice manifest a dose-dependent relaxation to acetylcholine, while aortic rings from eNOS mutant animals show no relaxation to acetylcholine. Treatment of wild-type aortic rings with  $10^{-4}$  M L-NA has no effect on vascular tone by itself, but blocks the relaxation in response to acetylcholine. Treatment of the eNOS mutant aortic rings with  $10^{-4}$  M L-NA has no effect on vessel tone, either by itself or in response to acetylcholine. The maximum dilation of norepinephrine pre-contracted rings from eNOS mutant mice to sodium nitroprusside is no different from wild-type mice, indicating that vascular smooth-muscle responses are intact.

### ***Example 5***

#### ***Blood Pressure Responses to L-NA for Wild-type and eNOS Mutant Mice***

Mean arterial blood pressure (MABP) of urethane-anesthetized wild-type (solid line in Figure 5) and eNOS mutant mice (dotted line in Figure 5) were measured by femoral artery catheterization and recorded for 30 minutes of baseline before L-NA administration (arrows in Figure 5). At time 0, 12 mg/kg of L-NA was given intraperitoneally. Monitoring for 1 hour shows that the blood pressure of wild-type mice rose from a baseline of 78 mm Hg to 109 mm Hg ( $n = 11$ ). The blood pressure of eNOS mutant mice dropped from a baseline of 98 mm Hg to 66 mm Hg ( $n = 5$ ). Each mouse in the wild-type group responded to L-NA with a rise in blood pressure, and each mouse in the eNOS mutant group

responded with a drop in pressure. Mean arterial blood pressure differences between wild-type and eNOS mutant animals are statistically significant by the t-test (#,  $p < 0.01$ ). Differences between baseline blood pressures and following L-NA treatment were also statistically significant (\*,  $P < 0.05$  by ANOVA followed by Dunnett). These effects were prevented by L-arginine (200 mg/kg, intraperitoneal), and were not seen with D-nitroarginine (12 mg/kg). The heart rate of eNOS mutant mice and wild-type mice did not differ, and L-NA had no effect on heart rate.

These results support the conclusion that eNOS in the endothelium regulates blood pressure. The major NOS isoform in the endothelium is eNOS. However, a small amount of nNOS is also present. Disruption of the eNOS gene raises blood pressure, while disruption of the nNOS gene stabilizes or lowers blood pressure. Thus, inhibition of NOS in wild-type animals by L-NA, which would predominantly inhibit eNOS, would be expected to raise blood pressure. This is shown in Figure 5. However, inhibition of NOS in eNOS mutant mice would not be expected to raise blood pressure since the effect of L-NA inhibition in the mutants would be to inhibit nNOS and not eNOS. Since nNOS maintains or raises blood pressure levels, *see supra*, inhibition of nNOS would be expected to lower blood pressure levels. This is also seen in Figure 5.

### ***Example 6***

#### ***Screening of Compounds for Anti-hypertensive Effects using eNOS Mutant Mice***

The eNOS mutant mice exhibit hypertension. Compounds that are associated with NO production in the endothelium, thereby replacing eNOS enzymatic activity, are screened for anti-hypertension activity in eNOS mutant mice. These compounds can be administered to the eNOS mutant mice using pharmaceutically acceptable methods. *See Remington's Pharmaceutical Sciences*

(1990). For example, the compound to be screened can be administered at various concentrations by parenteral injection, infusion, ingestion, and other suitable methods in admixture with a pharmaceutically acceptable carrier. The effect of various concentrations of the screened compound on blood pressure is measured relative to control eNOS mutant animals that have not been administered the compound.

A significant decrease in blood pressure of the eNOS mutant mice by a screened compound is indicative that this compound would exhibit beneficial anti-hypertensive properties in other animals and in humans.

### *Example 7*

#### *Wound Healing in eNOS Mutant Mice*

It was observed that eNOS mutant mice, but not wild-type or nNOS mutant mice, tend to develop chronic wounds. Therefore, eNOS mutant mice were tested in a model of wound healing involving a full thickness transverse incision overlying the lumbar area. The incisions penetrated the deep dermis down to the skeletal muscle. In Figure 6, the histological appearance of these wounds at 24 hours and at 5 days following incision, for wild-type and eNOS mutant mice, are shown. At 24 hours, the wounds are very similar. The epidermis (ep) and the deep dermis (d) are transected. Inflammatory cells are seen in both wild-type and eNOS mutant mice.

By five days, wild-type mice have healed. The epithelial layer is reconstituted, and granulation tissue with newly sprouted capillaries fills in the scar. The dermis, which has been cut, remains absent in the healed wound. Thus, normal healing involves two quantifiable features: rapid epithelial migration from the wound edges, and the development of new capillaries, neovasculation, in the connective tissue matrix.

-35-

In these eNOS mutant animals, little or no healing has been observed at 5 days. The migration of epithelial cells is delayed, and the epithelial cells remain at the edge of the wound (ep). The connective tissue is markedly abnormal, and contains few or no new vessels. These results demonstrate an important role for eNOS in angiogenesis and epithelial cell migration during wound healing.

### ***Example 8***

#### ***Screening of Compounds for Wound Healing Effects using eNOS Mutant Mice***

The eNOS mutant mice exhibit spontaneous wounds. Compounds to be screened for wound healing activity can be administered to the eNOS mutant mice in a pharmaceutically acceptable excipient. For example, the compound can be administered at various concentrations to the wound directly as an ointment or salve. Alternatively, other pharmaceutically acceptable modes of administration can be used. For example, a pharmaceutical composition comprising the compound can be administered by parenteral injection, infusion, ingestion, skin-patch application, and other suitable methods. The effect of the compound is measured relative to control eNOS animals that have not been administered the compound.

A significant enhancement of wound healing on the spontaneous wounds of eNOS mutant mice by a screened compound would indicate that this compound exhibits beneficial wound healing properties in other animals and in humans.

Particularly preferred compounds for screening are compounds known to release NO, such as nitroglycerin, sodium nitroprusside, and SIN-1.

Similarly, eNOS mutant mice having artificially inflicted wounds can also be used in such a screening assay. For example, the effect of various compounds

on a full thickness transverse incision, as described in the preceding example, can be used as a screening assay.

### ***Example 9***

#### ***Determination of Cerebral Infarct Sizes after Middle Cerebral Artery (MCA) Occlusion in Wild-type and eNOS Mutant Mice***

Male and female wild-type (SV-129 and C57 Black/6, Taconic Farms, Germantown, NY) and eNOS mutant mice weighing 20 to 26 g were housed under diurnal lighting conditions and allowed free access to food and water *ad libitum*. Nitro-L-arginine, nitro-D-arginine, hydralazine hydrochloride and 2,3,5-triphenyltetrazolium chloride (TTC) were purchased from Sigma.

Mice were anesthetized with 2% halothane for induction and maintained on 1% halothane in 70/30% nitrous oxide/oxygen by mask. The right femoral artery was cannulated with PE-10 polyethylene tubing for arterial blood pressure measurement (Gould, Oxnard, CA) and blood gas determination (Corning 178, Ciba Corning Diag., Medford, MA). Rectal temperature was maintained between 36.5 - 37.5°C with a homeothermic blanket system (YSI, Yellow Springs, OH).

Focal cerebral ischemia was induced by occlusion of middle cerebral artery (MCA) using the intraluminal filament technique. Zea-Longa *et al.* (1989); Huang *et al.* (1994). Through a ventral midline incision, the right common and external arteries were isolated and ligated. A microvascular clip (Zen temporary clip, Ohwa Tsusho, Tokyo, Japan) was temporarily placed on the internal artery and the pterygopalatine artery. An 8-0 nylon monofilament (Ethicon, Somerville, NJ) coated with silicone was introduced through a small incision in the common carotid artery and advanced 10 mm distal to the carotid bifurcation so as to occlude the MCA and posterior communicating artery. The wound was sutured and the animal returned to its cage and allowed free access to water and food.

Twenty-four hours later, animals were sacrificed with an overdoses of pentobarbital and the brains removed and sectioned coronally into five 2-mm slices in a mouse brain matrix. Slices were placed in 2% TTC solution, followed by 10% formalin overnight. Morikawa *et al.* (1994a). The infarction area, outlined in white, was measured (Bioquant IV image analysis system) on the posterior surface of each section, and the infarction volume was calculated by summing the infarct volumes of sequential 2 mm thick sections.

In protocol 1, MCA occlusion was produced in SV-129 (n=12), C57 Black/6 (n=11), eNOS mutant mice (n=14), and eNOS mutant mice injected with hydralazine (1 mg/kg, ip, 1 hr before and 5, 17 hrs after MCA occlusion) to match the arterial blood pressure of wild-type mice (n=10).

In protocol 2, eNOS mutant and wild-type animals were injected with nitro-L-arginine (6 mg/kg, ip, 5 min, 3 and 6 hrs after ischemia) or an equivalent volume of saline vehicle in order to test the hypothesis that inhibition of nNOS activity alleviated ischemic brain injury. The investigator was blinded to the treatment group in this protocol.

As discussed *supra*, the mean arterial blood pressures in eNOS mutant mice were higher ( $115 \pm 8$  mmHg) than wild-type animals ( $98 \pm 7$  mmHg and  $94 \pm 7$  mmHg in SV-129 and C57 B/6, respectively). After hydralazine administration however, mean arterial blood pressures (MABP) did not differ between groups (Table 2).

In this and in Examples 10-11, data are expressed as means  $\pm$  SD. Statistical evaluation was performed by analysis of variance (ANOVA) followed by *t*-test to compare the data among groups in protocol 1. Unpaired Student's *t*-test was used to test the significance between two groups in protocol 2 and rCBF measurement. ANOVA with repeated measures and ANOVA followed by *t*-test were used to evaluate significance within group differences and individual points between groups in the autoregulation experiment. *Probability* values less than 0.05 were considered of statistical significance.

-38-

In protocol 1, wild-type SV-129 and C57 Black/6 developed infarcts that were  $37 \pm 7\%$  (n=12) and  $38 \pm 15\%$  (n=11) of their respective hemispheres. Larger infarct volumes ( $46 \pm 9\%$  of hemisphere, n=14,  $p < 0.05$  as compared to wild-type SV-129 and C57 Black/6) were measured in eNOS mutant mice. Larger infarct volumes were also recorded in eNOS mutant mice made normotensive by hydralazine treatment ( $48 \pm 7\%$  of hemisphere, n=10,  $p < 0.05$  vs wild-type SV-129 or C57 Black/6) (Fig. 7A,B). There were no significant group differences in physiology or blood gases before and 24 hrs after MCA occlusion to explain these differences (Table 2).

In protocol 2, administration of nitro-L-arginine decreased infarct volume in the eNOS mutant mice by 24% and injury volumes became equivalent to wild type. Nitro-L-arginine treatment, however, did not change lesion size after MCA occlusion in wild-type mice (Table 3).

-39-

Table 2. Physiological data 10 min before MCA occlusion and 24 hrs after ischemia

	pH		pCO <sub>2</sub> (mmHg)		pO <sub>2</sub> (mmHg)		MABP (mmHg)	
	before	after	before	after	before	after	before	after
<b>Protocol 1</b>								
Wt SV-129	7.33±0.04	7.29±0.06	42.2±4.5	43.8±6.6	153±20	146±29	98±7	95±6
Wt C57 B/6	7.34±0.05	7.35±0.06	49.5±3.1	51.1±4.7	148±30	137±38	94±7	96±4
eNOS mutant <sup>a</sup>	7.33±0.07	7.32±0.08	47.2±4.8	49.6±7.3	139±37	128±35	115±8	117±9
eNOS mutant <sup>b</sup>	7.35±0.04	7.30±0.05	43.8±5.9	47.3±2.9	148±16	139±28	102±6	102±
<b>Protocol 2</b>								
<b>eNOS mutant</b>								
nitro-L-arginine	7.36±0.07	7.33±0.05	47.6±4.3	51.0±2.9	120±38	134±35	110±10	107±9
Vehicle	7.32±0.07	7.32±0.07	44.6±4.2	43.6±6.3	129±32	138±32	113±8	118±8
<b>Wt SV-129</b>								
nitro-L-arginine	7.36±0.04	7.35±0.03	47.8±3.5	49.3±6.3	142±17	158±22	92±4	97±14
Vehicle	7.37±0.04	7.36±0.03	46.8±4.4	45.6±2.0	134±35	146±28	94±5	98±13

5

10

-40-

Data are expressed as means  $\pm$  SD. n=5-7 in each group.

<sup>a</sup>: Hypertensive group; <sup>b</sup>: normotensive group treated with hydralazine.

Table 3. Effects of nitro-L-arginine on infarct size 24 hrs after middle cerebral artery occlusion in mice.

	Infarct Volume (mm <sup>3</sup> )	
	Wild-type	eNOS mutant
Vehicle	94 ± 27	116 ± 13
Nitro-L-arginine	97 ± 13	88 ± 23*

Data are expressed as mean ± SD. n=8-12 in each group. \*p<0.05 vs vehicle.

### ***Example 10***

#### ***Measurement of rCBF in Wild-type and eNOS Mutant Mice Following MCA Occlusion***

In randomly selected mice, rCBF was determined by laser-Doppler  
5 flowmetry (Perimed, PF2B, Stockholm, Sweden) and recorded on a MacLab/8  
data acquisition system (AD Instruments, Milford, MA). Two fiberoptic probe  
tips (Perimed PF 319:2, diameter = 0.5 mm) were fixed 2 mm posterior, 3 mm  
lateral to bregma and 2 mm posterior, 6 mm lateral to bregma on the ipsilateral  
10 hemisphere. These two coordinates identify sites on the convex brain surface  
within the vascular territory supplied by distal and proximal segments of the  
middle cerebral artery, respectively, and they correspond to peri-infarct zone and  
deeply ischemic territory, respectively. Yang *et al.* (1994); Huang *et al.* (1994).  
Steady-state baseline values were recorded before MCA occlusion. rCBF was  
15 recorded continuously during and after ischemia and expressed as percentage  
relative to the baseline value.

As depicted in Figure 8, rCBF reduction was greater in the zone  
corresponding to the per infarct area ( $30 \pm 16\%$  of baseline,  $n=11$ ), in eNOS  
mutant mice ( $p<0.05$ ) as compared to SV-129 ( $40 \pm 13\%$  of baseline,  $n=10$ ),  
20 although there was no significant difference in the MCA core territory (data not  
shown).

#### ***Autoregulation Study***

Mice were anesthetized with urethane (1.5 g/kg, ip) and ventilated (SAR-  
830 ventilator, CWE Inc., Ardmore, PA) with 70/30% nitrous oxide/oxygen after  
tracheostomy. Both femoral arteries were cannulated for arterial blood pressure  
25 measurement, blood gas determination and for blood withdrawal. Respiratory  
parameters were adjusted to keep the  $P_aCO_2$  in normal ranges (30-40 mmHg).

The core temperature was kept normothermic as above. The level of rCBF was monitored by laser Doppler flowmetry. Dalkara *et al.* (1995).

Following reflection of the skin and subcutaneous tissue, an rCBF probe tip was secured directly over the parietal skull with glue (Borden Inc, Columbus, OH), away from pial vessels. An initial rCBF recording was taken as 100% and subsequent flow changes were expressed relative to this value. After heparin (10 units, iv) administration, arterial blood pressure was lowered -10 mmHg every 5 min by withdrawing femoral artery blood (0.05-0.15 ml). Corresponding rCBF readings were averaged for each 10 mm Hg stepwise reduction. The duration of total experiment was approximately 2 - 2.5 hrs. The upper limit of autoregulation was not tested in these mice.

When arterial blood pressure was lowered step-wise by controlled hemorrhagic hypotension in wild-type mice, cerebral blood flow stayed relatively constant until <40 mmHg. However, as depicted in Figure 9, at low blood pressures, the autoregulation curve was shifted slightly to the right in eNOS mutant animals, suggesting higher cerebrovascular resistance than wild type at lower perfusion pressures.

The data in Examples 9-10 demonstrate that deletion of the mouse eNOS gene is associated with larger brain infarcts and more pronounced rCBF reductions in corresponding brain regions after MCA occlusion. *See* Figure 8. eNOS mutants also exhibit proportionally lower rCBFs at reduced perfusion pressures during controlled hemorrhagic hypotension. *See* Figure 9. While the reduction in rCBF at reduced perfusion pressure may be due to hypertension in the eNOS mutant animal, no hypertensive changes were noted in the vessel wall or heart on preliminary histopathological analyses. The contribution of high blood pressure to infarct enlargement in eNOS animals was probably minor since infarct size did not change in eNOS mutants made normotensive by hydralazine administration.

Nitro-L-arginine decreased infarct volumes in eNOS mutant mice but not in wild-type animals. Since nNOS is the only constitutively expressed isoform

in eNOS mutant mice, this decrease was likely caused by nNOS inhibition. However, the reductions after nitro-L-arginine treatment were not as large as expected (24% decrease) based on the observation in nNOS mutant, suggesting that either the degree of nNOS inhibition was small using the employed protocol or that undocumented factors such as systemic hypotension induced by nitro-L-arginine, may have attenuated an even greater reduction in infarct size.

### ***Example 11***

#### ***Increase in Blood Vessel Diameter after Nitro-L-arginine Superfusion in Wild-type and eNOS Mutant Mice***

The mouse head was fixed in a stereotaxic frame and the skull exposed by a longitudinal skin incision. A stainless steel cranial window ring (8.0 mm in inner diameter, 2.0 mm in height) containing three ports was imbedded into a loop of bone wax over the skull. Dental acrylic was then applied. A craniotomy (2 x 1.5 mm) was made in the left parietal bone within the ring of the window. After dura was opened and the brain surface superfused with artificial cerebrospinal fluid (aCSF), a cover glass was placed to close the window. The volume under the window was approximately 0.1 ml. The composition of aCSF was as follows (in mMol/L): Na<sup>+</sup> 156.5, K<sup>+</sup> 2.95, Ca<sup>++</sup> 1.25, Mg<sup>++</sup> 0.67, Cl<sup>-</sup> 138.7, HCO<sub>3</sub><sup>-</sup> 24.6, dextrose 3.7 and urea 0.67. The pH value of aCSF was kept at 7.35-7.45, and monitored continuously with a pH meter (Corning Inc., Corning, NY). The aCSF was superfused by an infusion pump (0.4 ml/min) via a PE-100 tubing connected to a window port. Intracranial pressure was maintained at 5-8 mm Hg. The temperature of aCSF within the windows was maintained at 36.5-37.0°C.

Pial vessels were visualized through a cranial window by an intravital microscope (Leitz, Germany) equipped with a video camera (C2400, Hamamatsu Photonics, Hamamatsu, Japan). The diameter of a single pial arteriole (20-30 µm) was continuously measured by a video width analyzer (C3161, Hamamatsu,

Japan) and recorded using the MacLab data acquisition and analysis system. After baseline stabilization, nitro-L-arginine or nitro-D-arginine solution (1 mM) was superfused into the window and the diameter of pial arteriole measured continuously 40 min thereafter.

5 As depicted in Figure 10, unlike wild-type mice, nitro-L-arginine superfusion alone increased vessel diameter in eNOS mutant animals, reaching maximum at 30 min ( $p < 0.05$  vs wild-type). Similar changes in rCBF were recorded in preliminary experiments by laser Doppler flowmetry using the closed cranial window technique (data not shown). There was no change in MABP during nitro-L-arginine superfusion. No change was found in pial diameter after nitro-D-arginine superfusion in eNOS mutant mice (data not shown).

10 In the eNOS mutant, nitro-L-arginine superfusion inhibits nNOS within subjacent brain parenchyma, and there is published evidence for a contribution from parenchymally-derived NO to cerebrovascular tone. Iadecola *et al.*, 1994. This example provides evidence that nitro-L-arginine may directly decrease tone in resistance vessels or surrounding tissues of eNOS mutants by showing that nitro-L-arginine superfusion dilates pial arterioles in these mutants. However, the mechanism remains unknown.

15 NO is a potent vasodilator and it, or a closely related chemical, is proposed as EDRF or endothelium-derived relaxing factor. Ignarro *et al.* (1987); Palmer *et al.* (1988). This is evidence to support the hypothesis that endothelium-derived NO or reaction product may be beneficial to stroke by augmenting rCBF in ischemic territory. Infusion of L-arginine, a substrate for NOS, caused NO-dependent vasodilation and increased rCBF distal to MCA occlusion in rats. Morikawa *et al.* (1994a). Dynamic susceptibility contrast magnetic resonance imaging also suggests that L-arginine infusion cerebral blood flow and blood volume. Hamberg *et al.* (1993). Zhang *et al.* (1994) reported that NO donors improved rCBF in the ischemic area and reduced infarct size as well. In addition, sectioning of NOS-containing parasympathetic cerebrovascular fibers in sphenopalatine ganglia, Nozaki *et al.* (1993), increased infarct size after focal

20

25

30

ischemia, Kano *et al.* (1991), and reduced cerebral perfusion during hemorrhagic hypotension. Koketsu *et al.* (1992). The above evidence coupled with our observation that arterial blood pressures are less stable in eNOS mutant animals, e.g., during hypercapnic challenge, shows the importance of eNOS regulation of vascular hemodynamics and its potential importance to stroke outcome.

eNOS mutant mice maybe more susceptible to ischemic injury because NO modulates the microcirculation. NO may also block leukocyte adhesion and decrease microvascular stasis often seen following MCA occlusion. Garcia *et al.* (1993). Kubes *et al.* (1991) reported that superfusing mesenteric vessels with NOS inhibitors increased leukocyte adhesion. Kurose *et al.* (1994) found that L-arginine attenuated ischemia-induced platelet-leukocyte aggregation, mast cell degranulation and albumin extravasation. We also found that rCBF was more severely reduced in homologous brain areas after MCA occlusion in eNOS but not nNOS mutant mice. Huang *et al.* (1994). These findings confirm that NO plays a role in the modulation of the microcirculation which may contribute to the outcome of ischemia.

eNOS inhibition may account for the increases in infarct size in some studies after nitro-L-arginine, particularly after large doses. Yamamoto *et al.* (1992); Zhang and Iadecola (1993); Morikawa *et al.* (1994b). By contrast, neuroprotection was reported after selective nNOS inhibition with 7-nitroindazole, Yoshida *et al.* (1994), or FPL17477, Zhang *et al.* (1995). Consistent with present findings, infarction size increased when nitro-L-arginine was administered to mutant mice expressing only the eNOS isoform (i.e., nNOS knockout mouse). Importantly, iNOS enzyme activity is not measurable in mouse (SV-129 strain) brain for at least 4 days after permanent MCA occlusion. Yoshida *et al.* (1995).

We conclude that NO possesses a dual role in focal cerebral ischemia. Depending upon its source, NO may be toxic or protective to brain under ischemic conditions. Parenchymal NO overproduction may lead to neurotoxicity whereas endothelial NO may protect brain tissue by increasing rCBF or some

other hemodynamic mechanism. These results emphasize the importance of knockout mice to dissect the role of individual proteins in these pathophysiological events.

## ***Example 12***

### 5                    ***Brain Distribution of NOS in Wild-type and Mutant Mice***

#### ***Experimental Procedures***

##### ***Animals***

Adult male wild-type, SV-129 and C57black/6 (Taconic Farms, Germantown, NY, U.S.A.), and adult male and female nNOS mutant, Huang *et al.*, Cell 75:1273-1286 (1993), and eNOS mutant mice weighing 22 to 29 g and adult male Wistar rats (Charles River, MA, U.S.A.) weighing 250 to 300 g were allowed free access to food and water.

##### ***Tissue preparation***

Mice and rats were sacrificed by decapitation under 2% halothane anesthesia (30% O<sub>2</sub> + 70% N<sub>2</sub>O). The brains were rapidly removed, immediately frozen in powdered dry ice, and stored at -70°C. Twelve µm sagittal or coronal sections were cut in a cryostat-microtome at -18°C (Leitz 1720, Leica, Deerfield, IL, U.S.A.) and thaw-mounted onto gelatin-coated slides (1% gelatin and 0.1% KCr<sub>2</sub>O<sub>7</sub>). Adjacent sections were stained with cresyl violet and hematoxylin eosin, and stored at -70°C.

##### ***[<sup>3</sup>H]L-NG-Nitro-arginine autoradiographic binding assay***

The method for the autoradiographic visualization of NOS binding using [<sup>3</sup>H]L-NG-Nitro-arginine ([<sup>3</sup>H]L-NA) has been described previously. Rutherford

*et al.*, (1995). Prior to experiments, sections were brought to -20°C and then to room temperature. Sections were preincubated for 15 min at room temperature in 50 mM Tris-HCl (pH 7.3) to remove the endogenous ligands and/or modulators, then incubated for 30 min at room temperature in 50 mM Tris-HCl buffer containing 10 µM CaCl<sub>2</sub> and 25 nM N<sup>G</sup>-nitro-L-[2,3,4,5-<sup>3</sup>H]arginine hydrochloride ([<sup>3</sup>H]L-NA, specific activity: 48-57 Ci/mmol, Amersham, Arlington Heights, IL, U.S.A.). Unlabelled L-N<sup>G</sup>-nitro-arginine (L-NA, Sigma, St. Louis, MO, U.S.A.), D-N<sup>G</sup>-nitro-arginine (D-NA, RBI, Natick, MA, U.S.A.) and 7-nitroindazole (7-NI, Cookson Chemicals Ltd., England) was added at concentrations of 10, 10, and 100 µM, respectively. The sections were then washed twice for 5 min in ice-cold buffer and rinsed for 10 sec in ice-cold distilled water to eliminate residual buffer. After drying with cold air, the slides were tightly apposed to <sup>3</sup>H-Hyperfilm (Amersham) together with tritiated polymer standards (Amersham) and exposed at -4°C for 6 weeks.

#### ***Densitometric analysis***

Films were developed in Kodak D-19 and fixed in Kodak Rapid Fixer, according to the manufacturer's instructions. The optical density of the regions of interest was measured by a computer-assisted image analysis (System M4, Imaging Research, St. Catharines, Ontario, Canada). The relationship between optical density and radioactivity was examined with reference to the tritium standards (Amersham, [<sup>3</sup>H]microscale) co-exposed with the tissue sections. The optical density of the brain regions measured in the present study was in a range in which the optical density and the radioactivity of the <sup>3</sup>H-microscale showed a near linear relationship. The densities of NOS binding sites are expressed in fmol bound [<sup>3</sup>H]L-NA/mg tissue using the [<sup>3</sup>H]L-NA concentration of 25 nM.

### *NOS catalytic activity*

NOS activity was measured by the conversion of [<sup>3</sup>H]arginine to [<sup>3</sup>H]citrulline according to the method described by Bredt *et al.* (1990b) with minor modifications. Samples were homogenized in 500 µl cold 50 mM HEPES buffer (Research Organics Inc., OH, U.S.A.) containing 1 mM EDTA (pH 7.4, Sigma). Homogenates were centrifuged at 500 x g for 5 min. at 4°C and the supernatant used for assay. The incubation mixture contained 100 µl HEPES (50 mM, pH 7.4), EDTA (1 mM), reduced β-nicotinamide adenine dinucleotide phosphate (β-NADPH, 1 mM, Sigma), dithiothreitol (1 mM, Sigma), calmodulin (10 µg/ml, Calbiochem, CA, U.S.A.) and CaCl<sub>2</sub> (1 mM) and 25 µl of 100 mM L-[<sup>3</sup>H]arginine (1 mCi, Dupont NEN, MA, U.S.A.). The reaction was started by adding the supernatant (25 µl) and stopped after 20 min incubation at 37°C by adding HEPES buffer (20 mM, pH 5.5) containing EDTA (2 mM), pH 5.5. The mixture was then applied to cation-exchange columns containing Dowex AG50WX-8 (Na<sup>+</sup> form; Bio-Rad, Richmond, VA, U.S.A.) and eluted with 2 ml of distilled water. [<sup>3</sup>H]Citrulline was measured within eluates by a scintillation spectrometry (Packbeta 1209, LKB, Gaithersburg, MD, U.S.A.).

### *Statistical analysis*

Data are presented as mean ± SE. Statistical comparisons were made by one-way ANOVA and Tukey's multiple-range test or Student's *t*-test using the software super ANOVA (Abacus Concepts, Berkeley, CA, U.S.A.).

### *Results*

#### *Regional distribution of [<sup>3</sup>H]L-N<sup>G</sup>-nitro-arginine binding in the 4 mouse strains (Figs. 11-13, Table 4)*

[<sup>3</sup>H]L-NA binding was heterogeneously distributed in wild-type (SV-129 and C57Black/6) mouse brain, with highest densities (>90 fmol/mg tissue) associated with the granular layer of the olfactory bulb, the medial amygdaloid nuclei, posteromedial cortical amygdaloid nuclei and amygdaloid piriform

transition. Also, the islands of Calleja, tenia tecta, rhinal fissure, hippocampal CA3 subfield, dentate gyrus, anterior cortical and basomedial amygdaloid nuclei, lateral mammillary nucleus, superficial grey layer of the superior colliculus and cerebellar molecular layer contained high densities of [<sup>3</sup>H]L-NA (50-90 fmol/mg tissue). Other area of prominent binding (30-50 fmol/mg tissue) were the plexiform layer of the olfactory bulb, cortical layers I-II, hippocampal CA1 subfield, dorsomedial and ventromedial hypothalamic nuclei, central amygdaloid nuclei and granule layer of cerebellum. The striatum and pontine reticular nucleus showed relatively poor binding (<20 fmol/mg tissue) (Figs 11A, 11B and 12, Table 4). Binding was not significantly different from background in cortical layers III-VI, posterior and ventral posteromedial thalamus nuclei and medial mammillary nucleus (Figs 11A, 11B and 12).

The density of [<sup>3</sup>H]L-NA binding in nNOS mutant mice was significantly decreased in all regions (Fig. 11D). [<sup>3</sup>H]L-NA in eNOS mutant mice was similar to wild-type mice (Fig. 11C, Table 4).

The distribution of [<sup>3</sup>H]L-NA binding was similar in mouse and rat brain as shown in Fig. 13. Although the binding was relatively higher in mouse brain.

***Effects of 7-NI on [<sup>3</sup>H]L-N<sup>G</sup>-nitro-arginine binding (Fig. 14 and Table 5)***

In the presence of 7-NI (100 μM), [<sup>3</sup>H]L-NA binding was significantly decreased in all regions measured in wild-type (Fig. 14) and eNOS mutant mice, but not in nNOS mutant mice. In the presence of 7-NI, the densities of [<sup>3</sup>H]L-NA binding did not show significant differences between wild-type, eNOS mutant and nNOS mutant mice (Table 5).

***Effects of L-NA and D-NA on [<sup>3</sup>H]L-N<sup>G</sup>-nitro-arginine binding (Figs. 11, 14 and Table 6)***

In the presence of L-NA (10 μM), the density of [<sup>3</sup>H]L-NA binding sites was very low in all brain regions of all mouse strains (Figs. 11D, 12H). In the presence of D-NA (10 μM), the density of [<sup>3</sup>H]L-NA binding sites was decreased

by approximately 20 to 30% in SV-129 mice (Figs. 14A, 14B, Table 6). Both L-NA and D-NA decreased slightly the binding to the gelatinized slide itself (Fig. 14C, 14D). Binding in brain of the nNOS mutant mice was not significantly higher than background in any regions (Fig. 11D).

5      ***NOS catalytic activity (Table 7)***

The highest NOS catalytic activities in SV-129 mice were found in the cerebellum, thalamus/hypothalamus and cerebral cortex/amygdala. Moderate activities were observed in the brain stem, hippocampus, olfactory bulb and striatum. The activities in eNOS mutant mouse brain were similar to those found  
10      in SV-129. In nNOS mutant mice NOS activity was dramatically reduced in all regions investigated. Very low levels of residual NOS catalytic activity were measured in type 1 mutant mice (0-1.7% of SV-129) (Table 7).

***Discussion***

In this Example, the distribution and density of [<sup>3</sup>H]L-NA NOS binding  
15      sites in the brains of wild-type, eNOS mutant mice, and nNOS mutant mice was examined using quantitative *in vitro* autoradiography. Previous studies showed that [<sup>3</sup>H]L-NA binds specifically and stereospecifically to the nNOS isoform in the rat brain. Kidd *et al.* (1995); Michel *et al.* (1993). Specific binding of [<sup>3</sup>H]L-NA to the endothelium of placental blood vessels was recently established by  
20      Rutherford *et al.* (1996) using *in vitro* autoradiography. Using similar techniques, we recently observed specific [<sup>3</sup>H]L-NA binding to pig aortic endothelium, which is displaceable by unlabelled L-NA. Hence, this ligand can detect the presence of both eNOS and nNOS by *in vitro* autoradiography.

The highest density of [<sup>3</sup>H]L-NA binding was observed in the olfactory  
25      bulb, the amygdaloid complex, the islands of Calleja, and the cerebellum (Fig. 12). In general, these regions exhibit the highest NADPH-diaphorase activity and brain NOS positive immunostaining in the mouse, Huang *et al.* (1993), and in the rat, Schmidt *et al.* (1992); Vincent *et al.* (1992). Thus, the density and

distribution of [ $^3\text{H}$ ]L-NA binding presumably reflects the density and distribution of nNOS, the predominant isoform in brain which comprises more than 95% of NOS activity in the brain.

While the density and distribution of binding was similar in the two wild-type strains, it was relatively higher in mouse than rat brain (Fig. 13). In particular, higher binding was detected in the hippocampus of the mouse which may correspond to the greater NADPH-diaphorase activity reported in mouse CA1 pyramidal cells. Wallace *et al.* (1992). Because activity of the inducible isoform, type 2 NOS (iNOS), is undetectable in normal mouse brain, Yoshida *et al.* (1995), it is unlikely to be a major source for [ $^3\text{H}$ ]L-NA binding in our studies. The values of [ $^3\text{H}$ ]L-NA binding in our rat study were higher than those of Kidd *et al.* (1995), although the rank order of binding activity in rat brain regions was similar in both studies. *Id.* These discrepancies may be due to strain differences or different concentrations of added [ $^3\text{H}$ ]L-NA.

[ $^3\text{H}$ ]L-NA binding in nNOS mutant mice was remarkably lower than wild-type or eNOS mutant mice and the L-NA displaceable [ $^3\text{H}$ ]L-NA binding was distributed diffusely throughout the brain (Table 4). Thus, it is presumed that the loss of [ $^3\text{H}$ ]L-NA binding reflected the absence of nNOS. The residual binding probably did not reflect the labeling of eNOS, since the binding in nNOS mutant brain was not stereoselective and could be displaced by both L- and D-NA.

D-NA displaceable binding, detectable in brain of both wild-type strains, may represent an additional binding site for L-arginine unrelated to NOS protein. The fact that both L-NA and D-NA were able to decrease [ $^3\text{H}$ ]L-NA binding to the gelatinized glass slide (see Fig. 14) suggests that the D-NA-displaceable component of [ $^3\text{H}$ ]L-NA binding is non-specific. Therefore, "specific" binding should not be equated with "displaceable" binding, especially when the displacer is the unlabelled tracer, or closely related to the tracer.

Michel *et al.* (1993) reported that L-NA and D-NA displaced [ $^3\text{H}$ ]L-NA binding with  $\text{pI}_{50}$  values, i.e., the logarithm of the concentration of competing compound causing 50% inhibition of [ $^3\text{H}$ ]L-NA binding, of 7.1 and 3.1 (log

molar concentration), respectively. Hence 10  $\mu$ M D-NA is unlikely to affect the [ $^3$ H]L-NA labelling of specific NOS binding sites and could be used to mask part of the non-specific component of [ $^3$ H]L-NA binding.

There was no significant difference between [ $^3$ H]L-NA binding in eNOS mutant and wild-type mice (Fig. 11, Table 4). Furthermore, NOS enzymatic activity in eNOS mutant mice was almost the same as that in wild-type mice (Table 7). Therefore, these results indicate that the expression of eNOS is low in the mouse brain. However, Dinerman *et al.* (1994) reported the presence of eNOS in the hippocampal pyramidal cells, the cerebellum and olfactory bulb by immunohistochemistry in the rat brain. This discrepancy may reflect species differences and/or the technical differences between quantitative autoradiography and immunohistochemistry.

[ $^3$ H]L-NA binding was inhibited by 7-NI in wild-type and eNOS mutant mice, but not in nNOS mutant mice (Table 5). Hence, the results indicate that binding site of 7-NI in the mouse brain is mainly to nNOS. 7-NI and related substituted indazoles are potent and competitive nNOS inhibitors, Babbedge *et al.* (1993); Moore *et al.* (1993a); Moore *et al.* (1993b), and have been useful for treatment of focal ischemia damage *in vivo*, Yoshida *et al.* (1994), MPTP neurotoxicity *in vivo*, Schulz *et al.* (1995a) and NMDA-induced excitotoxicity *in vivo*, Schulz *et al.* (1995b). 7-NI may also compete with L-arginine for binding to the prosthetic heme group, and affect the pteridine site of the enzyme. Mayer *et al.* (1994). The mechanism of selective nNOS inhibition remains unclear. However, 7-NI at 10 mg/kg i.p., decreases NOS catalytic activity by approximately 30 to 40% within the mouse cerebellum, cerebral cortex and hippocampus. Moore *et al.* (1993); Moore *et al.* (1993). 7-NI does not increase blood pressure, like other NOS inhibitors. Babbedge *et al.* (1993). Moreover, the similarity in [ $^3$ H]L-NA binding in eNOS mutant mice and wild-type mice further supports the use of eNOS mutant mice to screen compounds for use in the treatment or prevention of cerebral ischemia or stroke.

***Conclusion***

This regional distribution of [<sup>3</sup>H]L-NA binding was similar to that seen with the NADPH-diaphorase method. The density of [<sup>3</sup>H]L-NA binding in nNOS mutant mice was dramatically reduced in all regions, compared with wild-type mice, but not eNOS mutant mice. nNOS in mouse brain may represent the majority of [<sup>3</sup>H]L-NA binding sites. [<sup>3</sup>H]L-NA autoradiography may provide a useful method for estimating the distribution of NOS, effects of drugs and pathogenesis of NO-related diseases such as stroke, Alzheimer's disease and tumor. For example, it should be useful for estimating regional changes in NOS binding after cerebral ischemia.

**Table 4.** Regional distribution of L-NA displaceable ( $^3\text{H}$ )L-N<sup>G</sup>-nitro-arginine binding in wild-type (SV-129 and C57black/6) and mutant (eNOS and nNOS mutant) mice.

Brain regions		Wild-type		Mutant	
		SV-129	C57black/6	eNOS	nNOS
5	Olfactory bulb-granular layer	106 ± 2.5	101 ± 12.1	108 ± 3.8	13 ± 1.6*,#,+
	Olfactory bulb-plexiform layer	43 ± 3.1	32 ± 3.1	33 ± 1.6	18 ± 0.6*,#,+
	Islands of Calleja	71 ± 7.9	70 ± 13.7	51 ± 3.5	5 ± 0.6*,#,+
	Tenia tecta	85 ± 6.7	106 ± 8.0	94 ± 6.1	13 ± 0.6*,#,+
	Rhinal fissure	84 ± 5.2	80 ± 5.8	70 ± 3.9	17 ± 2.0*,#,+
10	Striatum	18 ± 1.4	16 ± 1.7	12 ± 0.7	9 ± 0.7*,#
	Frontal cortex I-II	40 ± 1.4	40 ± 3.0	32 ± 2.6	19 ± 1.5*,#,+
	Occipital cortex I-II	47 ± 4.6	42 ± 5.9	36 ± 3.9	16 ± 0.9*,#
	Hippocampal CA1 subfield	44 ± 2.4	42 ± 5.1	43 ± 2.3	13 ± 1.3*,#,+
	Hippocampal CA3 subfield	70 ± 2.5	63 ± 4.0	63 ± 2.2	13 ± 1.1*,#,+
15	Dentate gyrus	57 ± 4.6	56 ± 4.0	52 ± 1.1	14 ± 1.2*,#,+
	Dorsomedial hypothalamic nuclei	34 ± 2.6	25 ± 4.2	29 ± 6.0	12 ± 1.4*
	Ventromedial hypothalamic nuclei	42 ± 5.8	47 ± 7.4	45 ± 5.9	13 ± 1.8*,#
	Amygdaloid complex				
	Amygdaloid nuclei-medial	90 ± 5.6	96 ± 8.8	89 ± 4.2	14 ± 2.2*,#,+
20	Amygdaloid nuclei-anterior cortical	57 ± 7.9	73 ± 8.6	69 ± 5.7	15 ± 2.9*,#,+
	Amygdaloid nuclei-basomedial	70 ± 5.7	53 ± 7.7	63 ± 8.2	13 ± 1.9*,#,+
	Amygdaloid nuclei-central	48 ± 6.5	41 ± 2.4	33 ± 4.4	14 ± 2.1*,#
	Amygdaloid nuclei-posteromedial cortical				
	Amygdaloid piriform transition	101 ± 5.0	98 ± 5.7	98 ± 3.5	15 ± 1.5*,#,+
25	Lateral mammillary nucleus	91 ± 6.3	93 ± 5.9	87 ± 5.1	13 ± 0.7*,#,+
	Superficial grey layer superior colliculus	71 ± 6.3	52 ± 5.4	52 ± 3.7	13 ± 1.6*,#,+
	Cerebellum	67 ± 4.4	54 ± 4.4	61 ± 5.4	16 ± 3.3*,#,+
	Molecular layer	64 ± 4.2	70 ± 4.9	67 ± 7.0	14 ± 3.0*,#,+
	Granule layer	40 ± 2.2	42 ± 4.6	42 ± 3.6	13 ± 2.7*,#,+
	Pontine reticular nucleus	14 ± 1.3	10 ± 1.9	10 ± 0.4	6 ± 1.4*

30 Values (fmol/mg tissue) represent mean ± S.E. of five mice per group and were determined by subtracting binding remaining in the presence of 10  $\mu\text{M}$  L-NA from the total binding in serial sections. \*:  $p < 0.01$  vs. SV-129, #:  $p < 0.01$  vs. C57black, +:  $p < 0.01$  vs. type 3 mutant (Turkey's multiple range test).

**Table 5.** Effects of 7-NI on the regional distribution of [ $^3$ H]L-NA binding in wild-type (SV-129 and C57black/6) and mutant (type 3 and type 1) mice.

Brain regions	Wild-type		Mutant	
	SV-129	C57black/6	eNOS	nNOS
Olfactory bulb (granular layer)				
5 L-NA displaceable <sup>1)</sup>	109 $\pm$ 1.9	113 $\pm$ 9.9	106 <sup>3)</sup>	33 $\pm$ 1.9
	7-NI <sup>2)</sup> 17 $\pm$ 0.7	28 $\pm$ 4.1*	N.T.	30 $\pm$ 2.7
Hippocampal CA3 subfield				
10 L-NA displaceable	60 $\pm$ 3.1	53 $\pm$ 2.3	50 $\pm$ 6.2	25 $\pm$ 0.9
	7-NI 18 $\pm$ 1.8*	22 $\pm$ 4.7*	21 $\pm$ 1.8*	23 $\pm$ 2.3
Dentate gyrus				
10 L-NA displaceable	48 $\pm$ 2.6	58 $\pm$ 5.6	58 $\pm$ 5.4	28 $\pm$ 2.2
	7-NI 18 $\pm$ 0.7*	22 $\pm$ 4.6*	20 $\pm$ 2.7*	22 $\pm$ 1.7
Amygdaloid complex				
15 L-NA displaceable	90 $\pm$ 4.9	89 $\pm$ 11.3	88 $\pm$ 2.9	29 $\pm$ 1.4
	7-NI 21 $\pm$ 2.1*	21 $\pm$ 4.8*	21 $\pm$ 2.9*	23 $\pm$ 2.5
Cerebellum (molecular layer)				
L-NA displaceable	67 $\pm$ 1.7	78 $\pm$ 6.8	67 $\pm$ 5.8	30 $\pm$ 0.8
	7-NI 18 $\pm$ 1.3*	23 $\pm$ 5.4*	20 $\pm$ 2.2*	24 $\pm$ 1.0

Values (fmol/mg tissue) represent mean  $\pm$  S.E. of three mice per group.

20 <sup>1)</sup>: L-NA displaceable = (total -binding in the presence of 10 $\mu$ M L-NA) binding

<sup>2)</sup>: 7-NI = L-NA displaceable binding in the presence of 100  $\mu$ M 7-NI,

<sup>3)</sup>: n=1, N.T.: not tested,

\*: p<0.01 vs. L-NA displaceable. There are no significant differences between L-NA displaceable and 7-NI groups in type 1 mice.

**Table 6.** Effects of D-nitro-arginine (D-NA) on the regional distribution of [<sup>3</sup>H]L-NA binding in wild-type (SV-129) and nNOS mutant mice.

Brain Regions	Binding	SV-129	nNOS mutant
Olfactory bulb (granular layer)			
	L-NA displaceable <sup>1)</sup>	121 ± 12.4	32 ± 2.3 <sup>#</sup>
	D-NA <sup>2)</sup>	92 ± 10.8	5 ± 3.0 <sup>*,#</sup>
Hippocampal CA3 subfield			
	L-NA displaceable	83 ± 2.4	33 ± 4.2 <sup>#</sup>
	D-NA	66 ± 5.9	3 ± 1.9 <sup>*,#</sup>
Dentate gyrus			
	L-NA displaceable	67 ± 3.7	33 ± 5.5 <sup>#</sup>
	D-NA	43 ± 4.8	2 ± 1.9 <sup>*,#</sup>
Amygdaloid complex			
	L-NA displaceable	96 ± 12.6	32 ± 5.9 <sup>#</sup>
	D-NA	64 ± 7.6	3 ± 1.7 <sup>*,#</sup>
Cerebellum (molecular layer)			
	L-NA displaceable	86 ± 4.5	32 ± 6.2 <sup>#</sup>
	D-NA	59 ± 6.7	0 ± 3.6 <sup>*,#</sup>

10 Values (fmol/mg tissue) represent mean ± S.E. of four to five mice per group.

<sup>1)</sup>: L-NA displaceable = (total - binding remaining in the presence of 10 µM L-NA) binding;

<sup>2)</sup>: D-NA = L-NA displaceable binding in the presence of 10 µM D-NA,

\*: p<0.01 vs. L-NA displaceable, #: p<0.01 vs. SV-129

**Table 7.** NOS catalytic activity in SV-129, eNOS mutant and nNOS mutant mice.

Brain regions	NOS catalytic activity (fmol/mg wet weight/min)		
	SV-129	eNOS mutant	nNOS mutant
Olfactory bulb	3.1 ± 0.9	4.0 ± 1.2	0 ± 0 <sup>#</sup>
Striatum	2.4 ± 0.3	2.4 ± 0.8	0.04 ± 0.04 <sup>*,#</sup>
5 Thalamus/Hypothalamus	6.2 ± 1.8	5.8 ± 1.2	0.07 ± 0.04 <sup>*,#</sup>
Hippocampus	3.1 ± 0.9	3.2 ± 0.5	0.03 ± 0.03 <sup>*,#</sup>
Cerebral cortex/Amygdala	4.0 ± 1.0	4.0 ± 0.7	0.07 ± 0.02 <sup>*,#</sup>
Cerebellum	9.0 ± 2.0	7.3 ± 1.7	0.04 ± 0.04 <sup>*,#</sup>
Brain stem	3.3 ± 0.7	3.5 ± .09	0.05 ± 0.05 <sup>*,#</sup>

- 10 \*: p<0.05 vs. SV-129, #: p<0.05 vs. type 3 mutant mice (Turkey's multiple range test).  
NOS catalytic activity was measured by calcium-dependent [<sup>3</sup>H]arginine to [<sup>3</sup>H]citrulline conversion. The experiment was performed three times in duplicate.

### Example 13

#### *Use of the Vessel Injury Models of Atherosclerosis in eNOS Mutant Mice*

- 15 Both the cuff model and the filament model of vessel injury can be used  
as an animal model for atherosclerosis. Major features of these two vessel injury  
models can be seen in the following Table:

**Table 8.** Comparison of Vessel Injury Models

Feature	Cuff Model	Filament Model
20 Exemplary Location	femoral artery	carotid artery
Method of Injury	placement of non-occlusive cuff around vessel	insertion of filament to denude endothelial layer
Manipulated Area	adventitia	endothelium

Response	adventitial inflammation; medial cellular proliferation	removal of endothelium, medial cellular proliferation
Time to response	14-28 days	14-28 days
Measurements	quantitative morphometry; immunohistochemistry; expression studies (RT-PCR); indices of cellular proliferation	quantitative morphometry; immunohistochemistry; expression studies (RT-PCR); indices of cellular proliferation

### *The Cuff Model:*

5                   Mice aged 7-8 weeks were anesthetized with pentobarbital (50 mg/kg ip). Femoral arteries were surgically exposed and dissected from the surrounding tissue. A nonocclusive polyethylene cuff (2 mm in length, 0.58 mm inner diameter, made of PE-50 tubing split longitudinally) was placed around the left femoral artery and tied snugly with a silk thread. The right femoral artery served as a sham control. The wounds were then closed and the animals allowed to awaken from anesthesia. Animals were euthanized at 3, 14, 21, and 28 days after cuff placement. The femoral arteries were fixed under perfusion in 10% formalin, and embedded in paraffin.

10                   The cuffed vessel segment and the corresponding sham operated vessel were cut into 200 serial 10 µm sections, and were placed in order on five series of slides, as shown in Figure 16. One series was stained with hematoxylin-eosin, another with elastin, and the others were saved for immunohistochemistry. The slides were scanned into Adobe Photoshop, and the quantitative morphometry was performed using the public domain program *NIH Image*.

20                   We performed two types of measurements. First, for area/volume measurements, the areas within the lumen, internal elastic lamina, and external elastic lamina were measured. The intimal area was calculated as the difference between the area within the internal elastic lamina and the lumen. The medial area was calculated as the difference between the areas within the external and

internal elastic laminae. The areas were integrated over the length of the vessel segment to calculate the volume of intima and media. Second, for thickness measurements, the thickness of the intima and the media at four points located 90° to each other, and averages over the length of the vessel segment.

5 Table 9 shows the representative data from individual wild-type and eNOS mutant male mice, to indicate the types of measurements and their variance.

(wild-type male mice)

No.	Genotype	Sex	Age	Wt. g.	Linear measurements, $\mu\text{m}$								
					Volume measurements			Injured side			Control side		
					Intima	Media	I/M ratio	Lum diam	Intima	Media	Lum diam	Intima	Media
70	Wild-type	M	8	24.0	5.9	25.1	0.23	111.4	7.9	27.7	110.9	0	28.8
71	Wild-type	M	8	23.0	7.5	23.1	0.32	210.1	5.5	15.6	166.2	0	23.5
72	Wild-type	M	8	24.0	6.5	22.8	0.28	172.8	5.8	17.9	154.9	0	22.4
73	Wild-type	M	8	25.9	8.9	31.5	0.28	160.4	8.3	23.4	119.7	0	29.8
74	Wild-type	M	8	26.1	6.4	23.6	0.23	198.5	4.9	17.1	211.6	0	20.0
75	Wild-type	M	8	24.3	6.7	24.5	0.27	227.3	3.2	15.6	162.6	0	27.3
76	Wild-type	M	8	23.9	9.3	32.7	0.28	212.5	6.8	21.1	153.8	0	20.3
77	Wild-type	M	8	25.0	6.3	26.9	0.23	142.7	6.7	23.1	183.7	0	25.8
78	Wild-type	M	8	23.0	10.7	39.5	0.27	172.5	9.3	28.6	159.2	0	32.5
79	Wild-type	M	8	28.3	10.9	41.8	0.26	198.1	6.1	21.4	183.3	0	27.6
132	Wild-type	M	8	26.1	11.3	35.6	0.32	182.4	6.5	18.7	176.6	0	26.9
133	Wild-type	M	8	25.2	8.1	32.8	0.25	142.7	6.7	29.9	183.7	0	30.8
134	Wild-type	M	8	23.8	10.7	39.5	0.27	172.5	9.3	28.6	159.2	0	31.9
135	Wild-type	M	8	25.9	8.7	25.9	0.33	150.6	8.3	24.5	180.3	0	22.3
136	Wild-type	M	8	24.8	7.6	26.4	0.29	162.6	5.1	26.6	156.1	0	18.6
137	Wild-type	M	8	22.9	11.2	31.2	0.36	180.0	5.9	21.6	180.1	0	20.7
138	Wild-type	M	8	26.8	7.5	28.6	0.26	195.2	6.3	19.6	196.5	0	23.9
139	Wild-type	M	8	26.3	10.2	29.2	0.35	186.3	7.0	25.4	198.5	0	22.6
140	Wild-type	M	8	25.9	9.1	29.8	0.30	210.1	4.9	28.0	168.2	0	23.6
141	Wild-type	M	8	22.9	8.5	23.6	0.36	175.4	8.6	24.6	145.3	0	29.0
Mean					8.5	29.7	0.29	178.2	6.6	22.9	167.5	0	25.4
Std. dev.					1.9	5.8	0.04	28.3	1.6	4.5	24.7	0	4.2

(eNOS mutant male mice)

No.	Genotype	Sex	Age	Wt. g.	Linear measurements, $\mu\text{m}$								
					Volume measurements			Injured side			Control side		
					Intima	Media	I/M ratio	Lum diam	Intima	Media	Lum diam	Intima	Media
98	eNOS -/-	M	8	28.0	20.8	32.1	0.65	122.5	22.8	26.3	116.4	0	27.7
99	eNOS -/-	M	8	25.2	23.5	36.6	0.64	165.5	20.1	25.3	131.9	0	27.3
100	eNOS -/-	M	8	23.5	33.2	36.4	0.91	203.6	29.4	20.5	133.3	0	25.7
101	eNOS -/-	M	8	20.5	19.7	27.9	0.71	136.9	20.0	22.3	151.3	0	31.1
102	eNOS -/-	M	8	22.7	22.5	33.4	0.67	144.9	21.5	25.0	138.1	0	33.6
103	eNOS -/-	M	8	25.8	21.5	30.6	0.70	157.4	21.5	23.9	134.1	0	30.5
104	eNOS -/-	M	8	23.6	19.8	31.2	0.63	146.6	19.0	23.8	168.4	0	29.6
105	eNOS -/-	M	8	28.1	21.4	36.0	0.59	177.6	15.2	24.6	159.4	0	28.1
106	eNOS -/-	M	8	21.0	16.3	23.4	0.70	157.6	13.2	19.3	162.7	0	26.3
147	eNOS -/-	M	8	26.6	21.7	30.5	0.71	160.2	20.3	23.4	181.2	0	24.5
148	eNOS -/-	M	8	25.8	23.1	36.2	0.64	180.9	24.1	24.3	167.4	0	22.8
149	eNOS -/-	M	8	24.2	26.2	29.9	0.88	149.2	25.9	23.8	162.4	0	23.1
150	eNOS -/-	M	8	20.6	25.2	31.5	0.80	150.2	24.6	23.1	155.2	0	23.8
151	eNOS -/-	M	8	26.6	27.0	34.3	0.79	150.9	28.9	23.8	153.7	0	24.6
152	NOS -/-	M	8	26.4	22.2	32.2	0.69	188.6	19.2	24.6	180.4	0	24.8
153	eNOS -/-	M	8	27.5	26.5	26.8	0.99	139.5	23.5	24.1	138.5	0	28.3
154	eNOS -/-	M	8	29.7	21.7	29.1	0.75	154.2	19.8	22.5	168.0	0	21.6
155	eNOS -/-	M	8	25.4	23.3	31.1	0.75	132.0	22.5	23.1	151.8	0	25.4
156	NOS -/-	M	8	24.3	24.6	32.6	0.75	168.5	26.5	21.3	160.2	0	22.5
157	eNOS -/-	M	8	24.0	21.3	30.3	0.70	156.4	16.7	22.5	165.3	0	27.0
Mean					23.1	31.6	0.73	157.2	21.7	23.4	154.0	0.00	26.4
Std. dev.					3.5	3.4	0.10	19.6	4.2	1.7	17.2	0.00	3.2

These results are summarized in Table 10. Wild-type mice, which have no detectable intima at baseline, develop neointima within 14 days of cuff injury, with an intima to media (I/M) volume ratio of 0.29 for males and 0.18 for females. The eNOS mutant animals developed substantially more neointima, with an I/M volume ratio of 0.73 for males and 0.43 for females. Thus, animals with a disrupted eNOS gene exhibit greater neointimal formation in response to cuff injury. Figure 17 shows representative section of vessels stained with hematoxylin-eosin. The internal elastic lamina is indicated by arrows, and the degree of neointima formation can be easily seen.

**Table 10. Neointima Formation Measured 14 Days After Cuff Placement**

Mouse strain	Intima volume	Media volume	I/M ratio	Intima ( $\mu\text{m}$ )
Wild-type, males (n=20)	0.0085 $\pm$ 0.0019	0.0297 $\pm$ 0.0058	0.29 $\pm$ 0.04	6.6 $\pm$ 1.6
Wild-type, females (n=20)	0.0059 $\pm$ 0.0018	0.0321 $\pm$ 0.0087	0.18 $\pm$ 0.06	4.9 $\pm$ 1.8
eNOS mutant, males (n=20)	0.0231 $\pm$ 0.0035	0.0316 $\pm$ 0.0034	0.73 $\pm$ 0.10	21.7 $\pm$ 4.2
eNOS mutant, females (n=20)	0.0123 $\pm$ 0.0028	0.0286 $\pm$ 0.0062	0.43 $\pm$ 0.09	11.7 $\pm$ 2.7

In Table 10, all measurements are expressed as mean  $\pm$  standard deviation. Volumes are expressed in  $\text{mm}^3$ , and are calculated as outlined in the text from area measurements. The last column shows thickness measurements of intima on the injured side. There was no detectable intima on the control side.  $p < 0.05$  was obtained for each gender, eNOS mutant mice vs. wild-type mice by ANOVA followed by Dunnett statistical analysis.

Figure 18 shows the histology and immunochemical staining of the cuff-injured and control vessels from eNOS mutant mice. Hematoxylin-eosin and elastin stains outline the intima clearly on the injured side; the control has no intima. Cells throughout the neointimal layer stain strongly for actin (E). This staining is also seen in the media of injured and control vessels (E, F), consistent

with smooth muscle staining. In contrast, only the luminal cells stain for von Willebrand factor, a marker of endothelial cells, as shown in panels G and H.

***The Filament Model:***

A comparison of the eNOS mutant mice and wild-type mice using the filament model of vessel injury is performed. As a first step, the size of the carotid arteries of eNOS mutant mice, nNOS mutant mice, and wild-type mice have been quantitated. Carotid arteries were fixed by perfusion at a pressure of 100 mm Hg. The luminal diameter was calculated by dividing the luminal circumference by  $\pi$  to account for differences in luminal shape. As shown in Table 11, the diameters of the carotid artery of wild-type mice do not differ substantially from those of the NOS mutant mice (n=20 in each group). Thus, the filament model can be used with a comparable degree of injury between different mouse strains.

**Table 11. Luminal diameters of perfusions fixed carotid arteries**

	Wild-type	eNOS mutant	nNOS mutant
Mean (mm)	0.42	0.45	0.41
Std. dev. (mm)	0.06	0.08	0.05

The filament model addresses eNOS expression by non-endothelial cells, since it removes the endothelial layer of cells. The filament injury model is performed in eNOS mutant mice and C57BL/6 wild-type mice, and morphometry, immunohistochemistry, and BrdU staining is performed as outlined. Briefly, the external carotid artery is identified, and two ligatures are placed around it. The artery is tied distally and a filament is inserted through an incision and advanced down the common carotid artery. The filament is rotated and passed three times. The external carotid artery is tied off proximally, and the right carotid artery serves as a sham operated control.

The process of endothelial resurfacing, which occurs by migration from uninjured areas such as the aortic arch, is also studied. It is expected that the rate of resurfacing of the endothelial layer following denudation will be much slower in eNOS mutant mice.

5 In order to examine endothelial regeneration, animals are injected with Evan's blue solution (150  $\mu$ l of 5% solution in PBS, iv) 10 minutes before euthanasia to identify de-endothelialized segments. Vessel segments are cut open longitudinally and pinned onto Teflon cards with the lumen facing up. For determination of smooth muscle cell proliferation, mice are injected  
10 intraperitoneally with 5'-bromo-2'-deoxyuridine (BrdU, 25 mg/kg, Boehringer Mannheim) one hour prior to euthanasia. Immunostaining with antibody to BrdU is carried out.

This result would demonstrate that eNOS expression in both endothelial and non-endothelial cells affect the response to injury. However, if no  
15 differences between mutant and wild-type mice are observed, these results would suggest that local production of eNOS by the endothelium and not other cells, is the overriding factor determining vessel response to filament injury.

Two independent methods are used to characterize vessel morphometry: area/volume calculations and thickness measurements of the intima and the  
20 media. Intimal, medial, and luminal volumes are calculated by integrating areas along the injured region to ensure that inhomogeneities in neointimal formation along the length of the injured region do not give spurious results. Absolute volumes and intima/media (I/M) ratios are compared. The I/M ratio is a standardized measure that accounts for differences in vessel size, even within the  
25 same group of animals.

The effect of hypertension in vascular injury responses (both filament and cuff models) is measured by repeating the experiments after treating eNOS mutant mice with hydralazine to reduce their blood pressure to normotensive levels. The addition of hydralazine to drinking water at 250  $\mu$ g/ml gives a daily  
30 dose of about 750  $\mu$ g, and results in a stable decrease in mean arterial pressure

-64-

from 102 mm Hg to 72 mm Hg, which is equivalent to the blood pressure of untreated wild-type C57BL/6 mice. This will control hypertension during the duration of the experiment (3 to 28 days). Alternatively, local gene therapy to express eNOS in the femoral artery of the eNOS mutant mice could be used, leaving systemic eNOS deficiency and hypertension unaltered.

### ***Example 14***

#### ***Quantitative RT-PCR to Study Expression of NOS Isoforms***

Primers for RT-PCR detection of NOS isoforms in small amounts of tissue from mice have been devised, and are shown below:

The nNOS (type I) primers are as follows:

B1 primer: 5' CCT TAG AGA GTA AGG AAG GGG GCG GG 3' (26-mer)

B2 primer: 5' GGG CCG ATC ATT GAC GGC GAG AAT GAT G 3' (28-mer)

These primers amplify a 404 bp fragment from nNOS cDNA.

The eNOS (type III) NOS primers are as follows:

E1 primer: 5' GGG CTC CCT CCT TCC GGC TGC CAC C 3' (25-mer)

E2 primer: 5' GGA TCC CTG GAA AAG GCG GTG AGG 3' (24-mer)

These primers amplify a 254 bp fragment from eNOS cDNA, and an 800 bp fragment from the eNOS gene.

The iNOS (type II) NOS primers are as follows:

I1 primer: 5' ATC AGG AAC CTG AAG CCC CAG GAC 3' (24-mer)

I2 primer: 5' TGT TGC CAG ATT TCT CTG CAC GGT 3' (24-mer)

These primers amplify a 338 bp fragment from iNOS cDNA.

These primers are specific, and do not prime cDNA corresponding to the other NOS isoforms.

The quantitative nature of this technique was validated by using fixed amounts of aorta RNA (5µg) as starting material for reverse transcription. Vessels are frozen in liquid nitrogen and homogenized in the presence of phenol and guanidine isothiocyanate (RNAzol B). Total cellular RNA is prepared by extration of the homogenate with chloroform and isopropanol. The proportion of eNOS mutant mRNA to wild-type mRNA varied 100% eNOS mutant (no

wild-type mRNA) to 0% eNOS mutant (100% wild-type RNA). Using these mixtures, first strand cDNA was synthesized and used as a template for PCR using the eNOS specific primers. As seen in Figure 19, the amount of PCR product varied according to the amount of eNOS RNA present in the initial RNA sample, validating the quantitative nature of the reaction. Additional controls for expression of actin and GAPDH were performed as well.

### ***Example 15***

#### ***ApoE/NOS Mutant Mice***

ApoE mutant mice of a C57BL/6 genetic background were obtained from Jackson Labs. These mice were mated to eNOS mutant mice and nNOS mutant mice of the same genetic background. Double heterozygous apoE/eNOS and apoE/nNOS mice have been obtained. Mating pairs of each double heterozygous mice were bred, and the genotype of the offspring is determined using Southern blot analysis. For example, the ApoE mutation is genotyped by digesting genomic DNA with *HindIII* and using a 0.6 kb *SacI/HindIII* fragment. A ubiquitous endogenous *HindIII* band is 7.5 kb, the wild-type band is about 9 kb, and the disrupted band is 3 kb. See Huang (1994); Huang (1995).

The development of atherosclerotic lesions in the aorta of apoE mutant mice have been observed over time. Figure 20 shows a 6 month old apoE mutant mice with macroscopically visible lesions within the aortic arch, the origins of the carotid arteries, and the thoracic and abdominal aorta. Lipid in an aortic lesion stains with oil red O. The apoE mutant mice develop fatty streak lesions by 10 weeks of age, and evolve foam cells and fibrous plaque lesions by 15-20 weeks. The lesions typically occur in regions of shear stress, at the origins of the carotid arteries, intercostal arteries, renal arteries, and aortic bifurcation.

Since the apoE single or double mutant mice develop predictable, spontaneous atherosclerotic lesions, they provide a genetic background on which to study the effect of mutations in other genes, e.g., eNOS. The development of

-66-

atherosclerotic lesions in mice homozygous for apoE and eNOS mutations is compared vs. apoE mutant mice that are wild-type for eNOS.

The animals will be fed a typical high-cholesterol, high-fat Western-type diet to mimic the human atherosclerotic process. This diet contains 16% crude fat, 1.25% cholesterol (Harlan Teklad Diets, Madison, WI). The mice have elevated VLDL and chylomicron levels. The lipid profiles of these mice will also be measured to ensure that eNOS gene disruption does not independently affect the lipid profile.

ApoE and ApoE/eNOS mutant mice are sacrificed at age 5, 10, 20, and 30 weeks. The lungs, liver, stomach, and intestines are removed so that the thoracic and abdominal aorta can be dissected. The tissue is stained with Oil Red O to quantitate the total area of atherosclerotic lesions compared with the area of aorta, from the aortic valve down to 1 cm past the aortic bifurcation. The time points are selected to determine if there is a difference in the rate of lesion development versus the severity of the lesions. The dependence of apoE atherosclerosis on diet demonstrates that these variables can be modulated, and that their quantitation is feasible.

Serial sections are taken for histologic analysis and to quantitate intimal proliferation. The volume of intima is calculated by integrating their affected areas over the length of the affected segment, as described above in the injury models. The cell types involved in these lesions, e.g., smooth muscle, endothelium, and foam cells, are identified by immunohistochemical staining with antibodies for alpha actin, vimentin, factor VIII related antigen, and CD31. The expression of remaining NOS isoforms will be examined by immunocytochemistry, and quantitated by RT-PCR, as described *supra*.

In other experiments, a low-fat, low-cholesterol diet can be used if the effect of the apoE mutation masks the effect of the eNOS mutation. Alternatively, cholic acid can be added to the diet to increase the atherosclerotic stimulus.

5 In these experiments, statistical differences in lipid levels among groups are tested by one-way ANOVA, and post hoc tests of individual means are performed with Tukey's test. Differences in atherosclerotic lesion area between groups will be statistically analyzed with the non-parametric Kruskal-Wallis procedure.

### ***Example 16***

#### ***iNOS and nNOS Isoforms Contribute to the Development of Atherosclerosis***

10 In this Example, iNOS and nNOS mutant mice are used to determine if the loss of these pro-atherogenic isoforms show less response to injury and less atherogenesis. The cuff model of vessel injury is used in iNOS and nNOS mutant mice. These mice have normal vascular anatomy, so their response can be compared with those of wild-type C57BL/6 mice. Quantitative morphometry, immunohistochemistry, indices of cellular proliferation, and NOS isoform studies are performed as part of the filament or cuff injury models as described *supra*.

15 Double mutant apoE/iNOS and apoE/nNOS mice are bred to compare the development of atherosclerotic lesions in these animals with apoE mice. A typical high-cholesterol, high-fat Western type diet without cholic acid is used to mimic the human atherosclerotic process. The lipid profiles of these animals are measured, to ensure that the disruption of iNOS or nNOS do not have independent effects on the lipid profile.

20 The mice are sacrificed at age 5, 10, 20, 25, and 30 weeks. The thoracic and abdominal aorta is stained with Oil Red O, to quantitate the total area of atherosclerotic lesions compared with the area of the aorta. Serial sections are taken for histological analysis and to quantitate intimal proliferation. the volume of intima is calculated by integrating the affected areas over the length of the affected segment. The cell types involved in these lesions are identified by immunohistochemical staining, and expression of the remaining NOS isoforms will be examined by immunohistochemistry, and quantitated by RT-PCR.

-68-

This experiment extends the results from injury models to the development of atherosclerotic lesions. The development of lesions involves not only cellular differentiation, but also the recruitment of inflammatory cells, lipid oxidation and phagocytosis, and endothelial cell activation. Due to the participation of iNOS or nNOS isoforms in the pathophysiology of atherosclerosis, the disruption of these genes would be expected to result in a less severe phenotype than apoE mutant mice alone.

### ***Example 17***

#### ***The Effect of NOS Isoform Expression Patterns on Lipid Oxidation and Endothelial Cell Activation***

Peroxynitrite is formed in biological systems only by the reaction of nitric oxide with superoxide. Since human atherosclerotic lesions contain nitrotyrosine, it is known that at least one isoform of NOS generates nitric oxide and peroxynitrite in atherosclerotic lesions. iNOS and nNOS, but not eNOS, are believed to be involved in the generation of peroxynitrite. If so, iNOS and nNOS mutant mice will exhibit decreased amounts of nitrotyrosine. Therefore, atherosclerotic lesions in animals that lack apoE and each isoform (eNOS/apoE, iNOS/apoE, nNOS/apoE) are examined for the presence of nitrotyrosine.

Two independent methods to detect 3-nitrotyrosine are used: immunohistochemical detection and HPLC. For immunohistochemistry, a rabbit antiserum specific for nitrotyrosine, obtainable from Upstate Biotechnology is used. Alternatively, the level of nitrotyrosine is independently assessed by 16 electrode HPLC. Schultz (1996).

Briefly, tissue from a 50  $\mu$ m section of brain, comparable to the amount of tissue in atherosclerotic plaques, is used for this analysis. Atherosclerotic plaques from apoE and apoE/NOS double mutant mice are dissected and frozen. The level of 3-nitrotyrosine will be measured by HPLC with 16 electrode electrochemical detection. Reaction of standards and tissue extracts with 1M

sodium hydrosulfite should abolish the peaks by converting 3-nitrotyrosine to aminotyrosine. The levels of 3-nitrotyrosine are expressed as a ratio of 3-nitrotyrosine to total tyrosine, to normalize for the varying arterial concentrations of tyrosine. This method is more quantitative than immunohistochemical detection and offers an independent measure of nitrotyrosine formation.

Under physiological conditions, eNOS suppresses the expression of endothelial activation genes by inducing and stabilizing I $\kappa$ B. Peng (1995). In atherosclerotic lesions, NOS expression patterns change, and iNOS and/or nNOS expression increases, while eNOS levels drop. Wilcox (1994). These changes are believed to contribute to increased oxidant stress in the vessel wall, and endothelial cell activation. To test for endothelial cell activation, the expression of VCAM-1 can be used as a preferred marker, since its expression is longer lived than other markers. However, ICAM-1, E-selectin and MCP-1 can be used. eNOS mutant mice will exhibit greater expression of VCAM-1 (more endothelial activation) in atherosclerotic lesions, while iNOS and nNOS would be expected to show diminished VCAM-1 expression (less endothelial activation).

VCAM-1 expression is examined by two methods: immunohistochemistry and RT-PCR quantitation of mRNA expression. For immunohistochemistry, a rat monoclonal anti-VCAM-1 antibody obtained from Southern Biotechnology Associates, Inc., Birmingham, AL, is used as the primary antibody, and biotinylated goat anti-rat antibody as a secondary antibody. For RT-PCR primers that amplify VCAM-1 cDNA, conditions are used that ensure that the amount of amplified PCR product is proportional to the level of mRNA. Actin mRNA will be used to standardize the amount of total mRNA, and internal quantitative standards will be employed as described *supra*.

Lipid peroxidation results in many changes, including altered electrophoretic mobility and modification of apolipoprotein B. Many of these can be assessed in purified LDL that has been subject to oxidation, but are more difficult to study *in vivo*. The protein modification epitopes malondialdehyde-

-70-

lysine (MDA-lysine) and 4-hydroxynonenal-lysine (4HNE-lysine) as markers for lipid oxidation events. Palinski *et al.* (1989); Palinski *et al.* (1994); Itabe *et al.* (1994); Yla-Herttuala (1989). These epitopes are found in atherosclerotic lesions in apoE-deficient mice and humans. A panel of antibodies against MDA-lysine and 4-HNE epitopes is used to study whether the absence of any one of the NOS isoforms results in a reduction in staining, implicating that NOS isoform in lipid oxidation. These results are correlated with a histologic assessment of lesion extent, severity, and the presence of foam cells, macrophages, and other inflammatory cells. Independent methods to measure the same process are used, e.g., HPLC for nitrotyrosine or RT-PCR for VCAM-1 expression to improve our ability to detect differences due to NOS isoform deletion.

*Literature Cited*<sup>1</sup>

- Aji *et al.* (1997), *Circulation* 95:430-437.
- Archer, S., (1993), *FASEB J.* 7:349-360.
- Babbedge *et al.* (1993), *Br. J. Pharmacol.* 110:225-228.
- 5 Bath (1993), *Eur. J. Clin. Pharmacol.*, 45:53-58.
- Beckman *et al.* (1994a), *Methods Enzymol.* 233:229-240.
- Beckman *et al.* (1994b), *Biol. Chem. Hoppe-Seyler* 375:81-88.
- Benditt *et al.* (1973), *Proc. Natl. Acad. Sci. (USA)* 70:1753-1756.
- Boeckstaens *et al.* (1991), *Br. J. Pharmacol.* 102:434-438.
- 10 Bohme *et al.* (1991), *Eur. J. Pharmacol.* 199:379-381.
- Booth *et al.* (1989), *Atherosclerosis* 76:257-268.
- Bredt *et al.* (1994), *Ann Rev. Biochem.* 63:175-195.
- Bredt *et al.* (1992), *Neuron* 8:3-11.
- Bredt *et al.* (1990a), *Nature* 347:768-770.
- 15 Bredt *et al.* (1990b), *Proc. Natl. Acad. Sci. USA.* 87:682-685 (1990) - 129/130
- Breslow (1996), *Science* 272:685-688.
- Brinster *et al.* (1985), *Cell* 27: 4438-4442.
- Bult *et al.* (1990) *Nature* 345: 346-347.
- Burnett *et al.* (1992), *Science* 257: 401-403.
- 20 Busse *et al.* (1996), *J. Vasc. Res.* 33: 181-194.
- Curran *et al.* (1989), *J. Exp. Med.* 170:1769-1774.
- Dalkara *et al.* (1994), *Brain Pathol.* 4:49-57.
- Dalkara *et al.*, (1995), *J Cereb Blood Flow Metab.* 15:631-638.
- Darley-Ussmar *et al.* (1992), *Free Rad. Res. Commun.* 17:19-20.
- 25 Dawson *et al.*, (1991) *Proc Natl Acad Sci USA.* 88:6368-6371.
- Dawson *et al.* (1992), *Ann. Neurol.* 32: 297-311.
- Desai *et al.* (1991), *Nature* 351:477-479.
- Dimmeler *et al.* (1992), *J. Biol. Chem.* 267: 16771-16774.
- Dinerman *et al.* (1994), *Proc. Natl. Acad. Sci. (USA)* 91:4214-4218.
- 30 Edelman & Gally (1992), *Proc. Nat'l Acad. Sci. (USA)* 89:11651-11652.
- Furchgott *et al.* (1980), *Nature* 288:373-376.
- Furchgott (1988), Studies on the relaxation of the rabbit aorta by sodium nitrate: basis for the proposal that the acid-activatable component of the inhibitory factor from retractor penis is inorganic nitrate and the endothelium-derived relaxing factor is nitric oxide, *In: Mechanisms of Vasodilation*, P.M. Vanhoutte ed.
- 35 Furchgott & Vanhoutte (1989), *FASEB J.* 3: 2007-2018.
- Gally *et al.* (1990), *Proc. Nat'l Acad. Sci. (USA)* 87:3547-3551.
- Garcia *et al.* (1993), *Am J Pathol.* 142:623-635.

---

<sup>1</sup> All of the literature cited in this application is expressly incorporated herein by reference.

- Gibson *et al.* (1990), *Br. J. Pharmacol.* 99: 602-606.  
Gillespie *et al.* (1989), *Br. J. Pharmacol.* 98: 1080-1082.  
Haley *et al.* (1992), *Neuron* 8: 211-216.  
5 Hamberg *et al.* (1993) In: *Proceedings of the Society of Magnetic Resonance in Medicine, 12th Annual Scientific Meeting*, Society of Magnetic Resonance in Medicine NY. 1:397.  
Hevel *et al.* (1994), *Methods Enzymol.* 233:250-258 (1994).  
Hibbs *et al.* (1988), *Biochem. Biophys. Res. Comm.* 157: 87-94.  
Huang *et al.* (1993), *Cell* 75:1273-1286.  
10 Huang *et al.* (1994), *Science* 265:1883-1885.  
Huang *et al.* (1995), *Nature* 377:239-242.  
Iadecola *et al.* (1994), *J Cereb Blood Flow Metab.* 14:175-192.  
Ignarro *et al.* (1988), *Proc. Natl. Acad. Sci. USA.* 84:9265-9269.  
Ignarro (1989), *FASEB J.* 3: 31-36.  
15 Ishibashi *et al.*, *J. Clin. Invest.* 92: 883-893.  
Itabe *et al.* (1994), *J. Biol. Chem.* 269:15274-15279 (1994).  
Jannsens *et al.* (1992), *J. Biol. Chem.* 267:14519-14522, and erratum published in *J. Biol. Chem.* 267:22694.  
Kano *et al.* (1991), *J Cereb Blood Flow Metab.* 11:628-637.  
20 Kaufman *et al.* (1995), *Handbook of Molec. and Cell. Methods in Biol. and Medicine*, pp. 329-366.  
Kidd *et al.* (1995), *Neuropharmacol.* 34:63-73.  
Knowles *et al.* (1992), *Trends Biochem Sci.* 17:399-402.  
Kockx *et al.* (1993), *Arterioscl. Thromb.* 13: 1874-1884.  
25 Koketsu *et al.* (1992), *J Cereb Blood Flow Metab.* 12:613-620.  
Kots *et al.* (1992), *FEBS Lett.* 300: 9-12.  
Kubes *et al.* (1991), *Proc. Natl. Acad. Sci. USA.* 88:4651-4655.  
Kurose *et al.* (1994), *Circ Res.* 74:376-382.  
Lamas *et al.* (1992), *Proc. Natl. Acad. Sci. (USA)* 89:6348-6352.  
30 Lefer *et al.* (1993), *Arterioscler. Thromb.* 13:1874-1884.  
Leitinger *et al.* (1995), *J. Physiol. Pharmacol.* 46: 385-408.  
Li *et al.* (1992), *Cell* 69: 915-926.  
Linder *et al.* (1993), *Circ. Res.* 73:792-796.  
Lowenstein & Snyder (1992), *Cell* 70: 705-707.  
35 Malinski *et al.*, *J. Cereb. Blood Flow Metab.* 13: 355-358.  
Marletta (1989), *Trends Biochem. Sci.* 14: 488-492.  
Marletta (1993), *J. Biol. Chem.* 268: 12231-12234.  
Mayer *et al.* (1994), *Neuropharmacol.* 33:1253-1259.  
McDonald & Moss (1993), *Proc. Nat'l Acad. Sci (USA)* 90: 6238-6241.  
40 Michel *et al.* (1993), *Br. J. Pharmacol.* 109:287-288.  
Moncada (1992), *Acta Physiol. Scand.* 145:201-227.  
Moncada *et al.* (1991), *Pharmacol. Rev.* 43: 109-142.  
Moore *et al.* (1993a), *Br. J. Pharmacol.* 108:296-297.  
Moore *et al.* (1993b), *Br. J. Pharmacol.* 110:219-224.  
45 Mooradian *et al.* (1995), *J. Cardiovasc. Pharmacol.* 25: 674-678.

- Morikawa *et al.* (1994a), *Stroke*. 25:429-435.
- Morikawa *et al.* (1994b), In: *The human brain circulation (J Bevens, eds.)*, Harbor Basin Conference, Vermont. 373-387.
- Murphy *et al.* (1993), *Trends Neurosci.* 16:323-328.
- 5 Nathan (1992), *FASEB J.* 6: 3051-3064.
- Nathan & Xie (1994), *Cell* 278:915-918.
- Nozaki *et al.* (1993), *J. Cereb. Blood Flow Metab.* 13: 70-79.
- O'Dell *et al.* (1991), *Proc. Nat'l Acad. Sci. (USA)* 88: 11285-11289.
- O'Dell *et al.* (1994), *Science*. 265:542-546.
- 10 Palinski *et al.*, *Proc. Natl. Acad. Sci (USA)* 86:1372-1376 (1989).
- Palinski *et al.*, *Arterioscler. Thromb.* 14:605-616 (1994).
- Palmer *et al.* (1987), *Nature* 327: 524-526.
- Palmer *et al.* (1988), *Nature*. 333:664-666.
- Peng *et al.* (1995), *J. Biol. Chem.* 270: 14214-14219.
- 15 Plump *et al.* (1992), *Cell* 71:343-353.
- Purcell-Huynh *et al.* (1995), *J. Clin. Invest.* 95: 2246-2257.
- Radomski *et al.* (1991), *Trends in Pharm. Sci.* 12:87-88.
- Radomski *et al.* (1995), *Atherosclerosis* 18: S69-80.
- Rajfer *et al.* (1992), *N. Engl. J. Med.* 326: 90-94.
- 20 Ramagopal & Leighton (1989), *Eur. J. Pharmacol.* 174: 297-299.
- Ramdomsky *et al.* (1990), *Proc Natl Acad Sci USA.* 87:5193-5197.
- Rees *et al.* (1990), *Br J Pharmacol.* 101: 746-752.
- Remington's Pharmaceutical Sciences, Mack Publishing Co., Easton, PA (1990).
- Ross (1996), *Nature Medicine* 2:527-528.
- 25 Ross (1995), *Ann. Rev. Physiol.* 57:791-804.
- Rutherford *et al.* (1995), *Br. J. Pharmacol.* 116:3099-3109.
- Schmidt & Walter (1994), *Cell* 78:919-925.
- Schmidt *et al.* (1992), *J. Histchem. Cytochem.* 40:1439-1456.
- Schultz *et al.* (1996), *J. Neurochem.* 67:430-433.
- 30 Schulz *et al.* (1995a), *J. Neurochem.* 64:936-939.
- Schulz *et al.* (1995b), *J. Neurosci.* 15: 8419-8429.
- Schuman & Madison (1991), *Science* 254: 1503-1506.
- Schwartz *et al.* (1995), *Circulation Res.* 77: 445-465.
- Shibuki & Okada (1991), *Nature* 349: 326-328.
- 35 Snyder *et al.* (1991), *Trends Pharmacol Sci.* 12:125-128.
- Snyder (1992), *Science* 257: 494-496.
- Snyder (1995), *Nature* 377:196-197.
- Sobey *et al.* (1995), *Circ. Res.* 77: 536-543.
- Toda & Okamura (1990), *Biochem. Biophys. Res. Comm.* 170: 308-313.
- 40 Topors *et al.* (1995), *Circulation* 92:I-564.
- Tottrup *et al.* (1991), *Am. J. Physiol.* 260:G385-G387.
- Tybulewicz *et al.* (1991), *Cell* 65: 1153-1163.
- van den Maagdenberg *et al.* (1993), *J. Biol. Chem.* 268: 10540-10545.
- Vincent *et al.* (1992), *Neurosci* 46:755-784.
- 45 Wallace *et al.* (1992), *NeuroReport* 3:953-956.

-74-

- Wilcox *et al.* (1994), *Circulation* 90 (supp I):I-298.  
Yamamoto *et al.* (1992), *J Cereb Blood Flow Metab.* 12:717-726.  
Yang *et al.* (1994), *Stroke* 25:165-170.  
Yla-Herttuala *et al.*, *J. Clin. Invest.* 84:1086-1095 (1989).  
5 Yoshida *et al.* (1994), *J Cereb Blood Flow Metab.* 14:924-929.  
Yoshida *et al.* (1995), *Neuroscience Letter.* 194:214-218.  
Zea-Longa *et al.* (1989), *Stroke.* 20:84-91.  
Zhang *et al.* (1992), *Science* 258:468-471.  
Zhang *et al.* (1993), *NeuroReport.* 4:559-562.  
10 Zhang *et al.* (1994), *J Cereb Blood Flow Metab.* 14:217-226.  
Zhang *et al.* (1995), *J Cereb Blood Flow Metab.* 15(Suppl.):S90.  
Zhang & Snyder (1992), *Proc. Nat'l Acad. Sci (USA)* 89: 9387-9385.

***What Is Claimed Is:***

1. A method of screening compounds for potential utility to treat cerebral ischemia or stroke, comprising:

5 (a) providing a transgenic non-human animal having a disrupted endothelial nitric oxide synthase gene;

(b) administering a compound to be tested to said transgenic animal;

(c) determining the effect of said compound on infarct size following induction of focal cerebral ischemia in the brain of said animal; and

10 (d) correlating the effect of said compound on infarct size with a potential therapeutic utility to treat cerebral ischemia or stroke;

wherein said compound is not a NOS inhibitor.

2. The method of screening compounds as claimed in claim 1, wherein said transgenic non-human animal is a mouse.

15 3. The method of screening compounds as claimed in claim 1, wherein the blood pressure of said transgenic non-human animal has been rendered normotensive.

4. The method of screening compounds as claimed in claim 2, wherein said compound induces nitric oxide synthesis in the endothelia.

-76-

5. The method of screening compounds as claimed in claim 4, wherein said compound does not induce neuronal nitric oxide overproduction.

6. The method of screening compounds as claimed in claim 4, wherein focal ischemia is induced by occluding the middle cerebral artery.

5 7. A method of screening compounds for potential utility to treat atherosclerosis, comprising:

(a) providing a transgenic non-human animal having a disrupted endothelial nitric oxide synthase gene;

(b) administering a compound to be tested to said transgenic animal;

10 (c) determining the effect of said compound on atherosclerosis in said animal; and

(d) correlating the effect of said compound on atherosclerosis in said animal with a potential utility to treat atherosclerosis;

wherein said compound is not a NOS inhibitor.

15 8. The method of screening compounds as claimed in claim 6, wherein determining the effect of said compound on atherosclerosis is determined by measuring neointima formation following vascular injury.

-77-

9. The method of screening compounds as claimed in claim 6, wherein determining the effect of said compound on atherosclerosis is determined by measuring the rate of endothelial regeneration following vascular injury.

5 10. The method of screening compounds as claimed in claim 6, wherein said transgenic non-human animal has a disrupted apoE gene.

11. A method of screening compounds for potential utility to treat a vascular endothelial disorder comprising:

(a) providing a transgenic non-human animal having a disrupted endothelial nitric oxide synthase gene;

10 (b) administering a compound to be tested to said transgenic animal;

(c) determining the effect of said compound on said vascular endothelial disorder in said animal; and

(d) correlating the effect of said compound on said vascular endothelial disorder in said animal with a potential utility to treat said vascular  
15 endothelial disorder;

wherein said compound is not a NOS inhibitor.

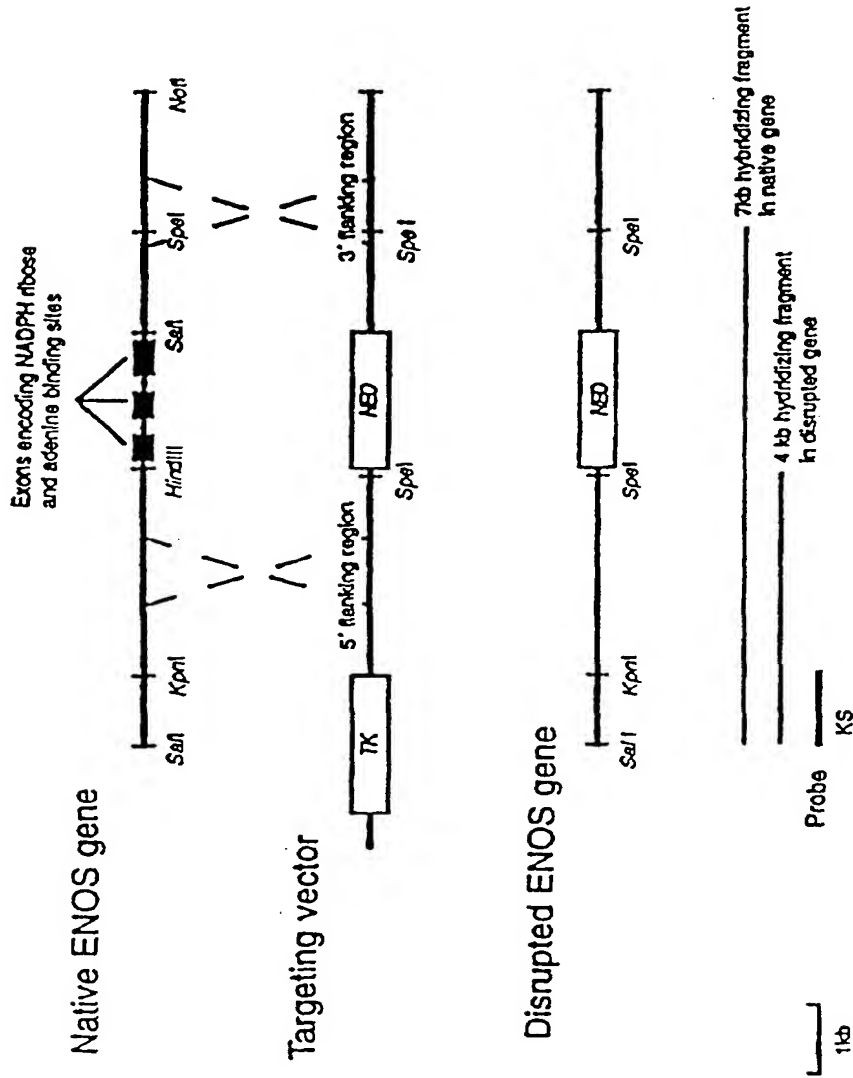
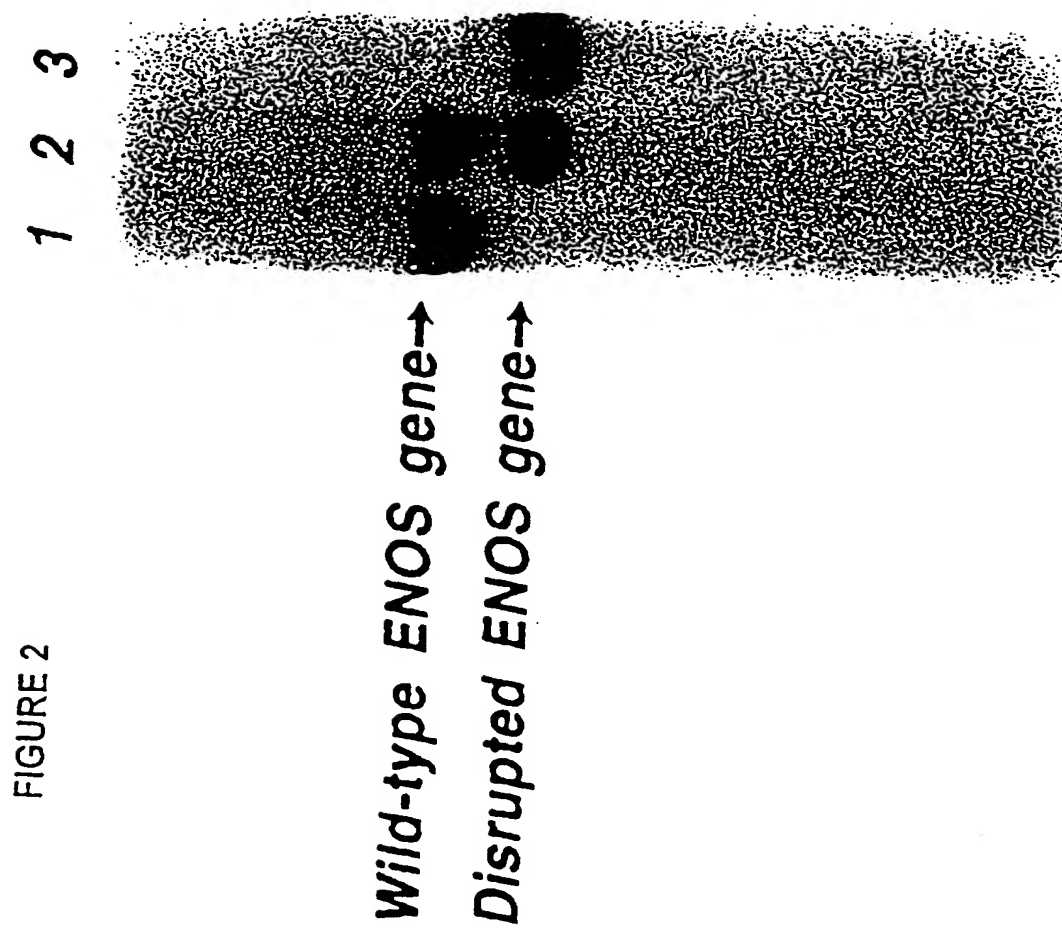


FIGURE 1



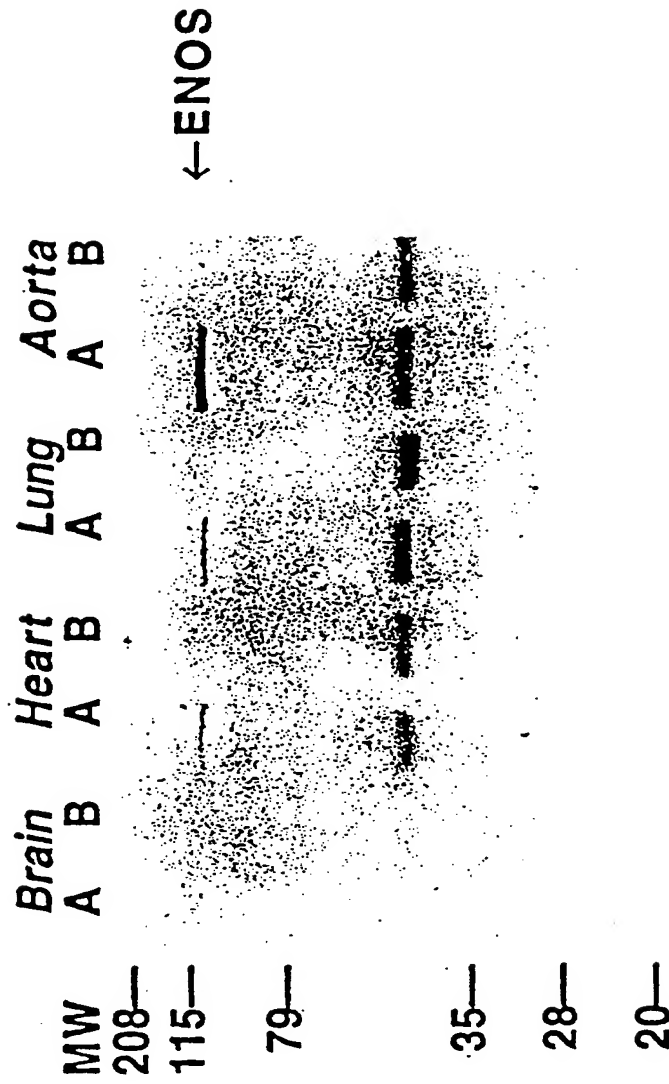


FIGURE 3

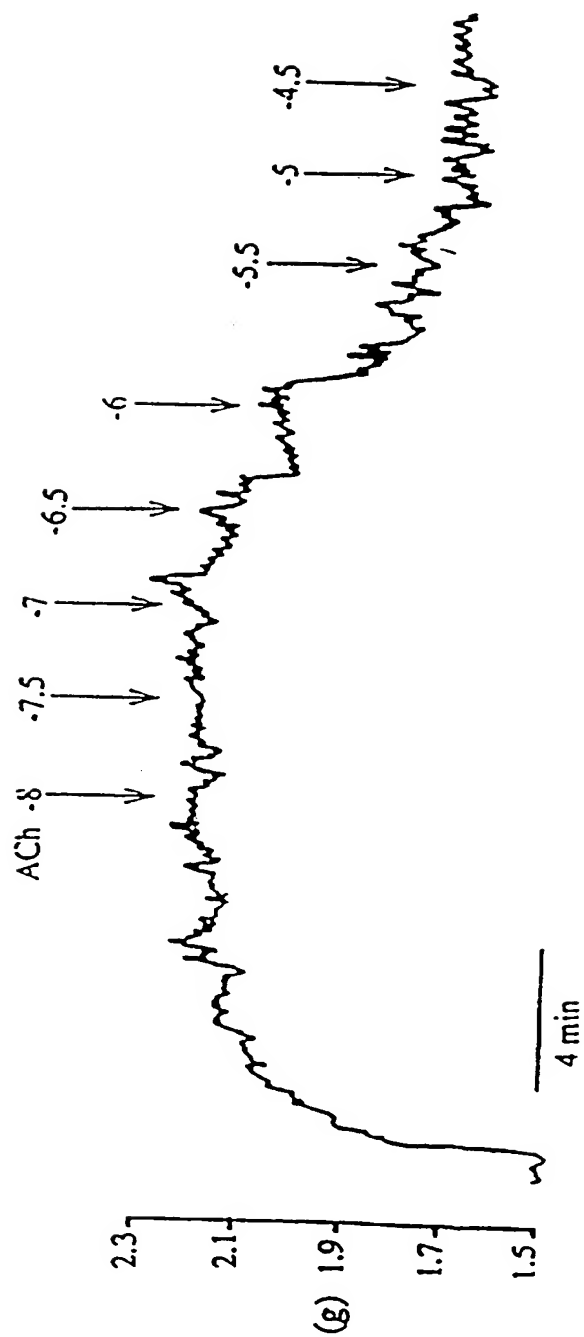


FIGURE 4A

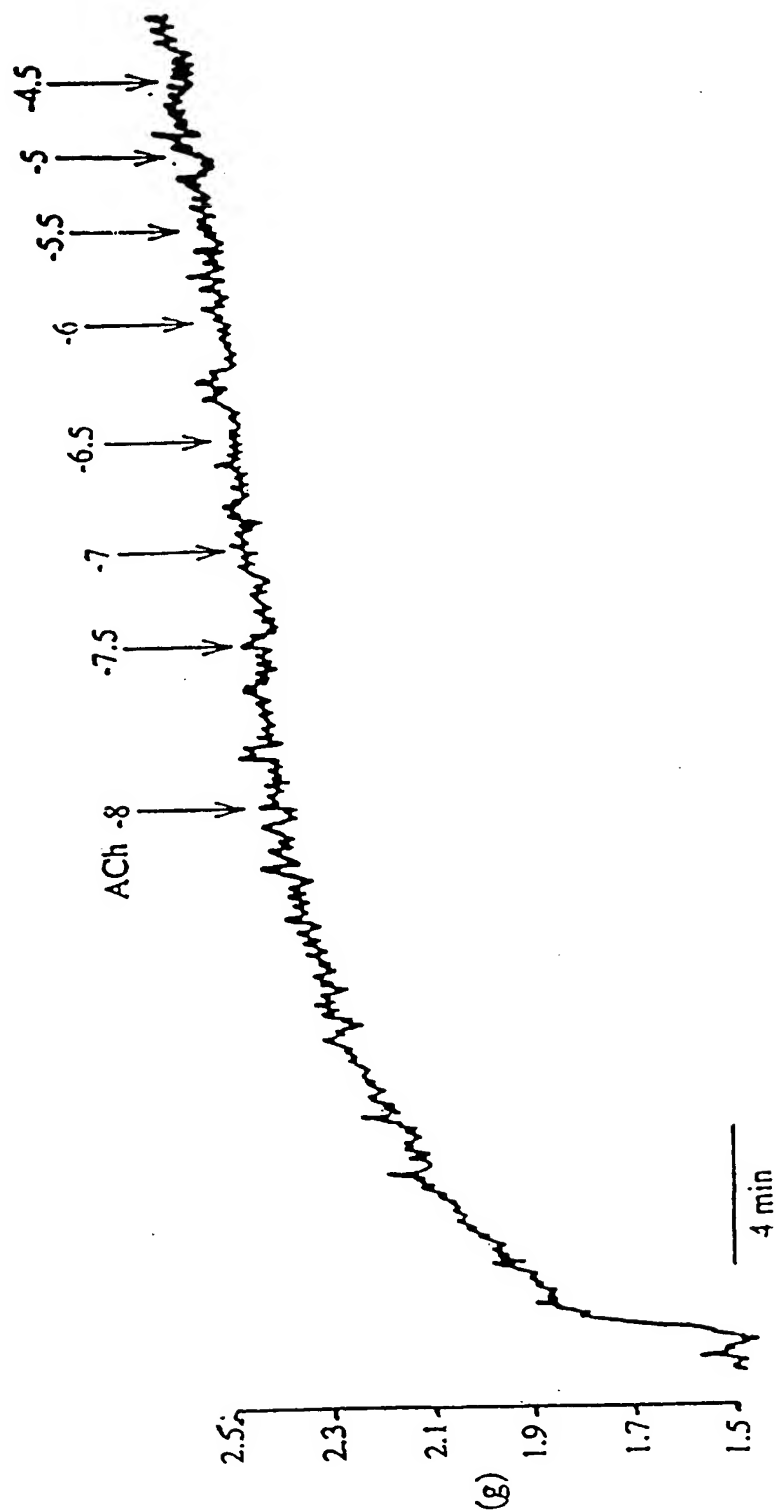


FIGURE 4B

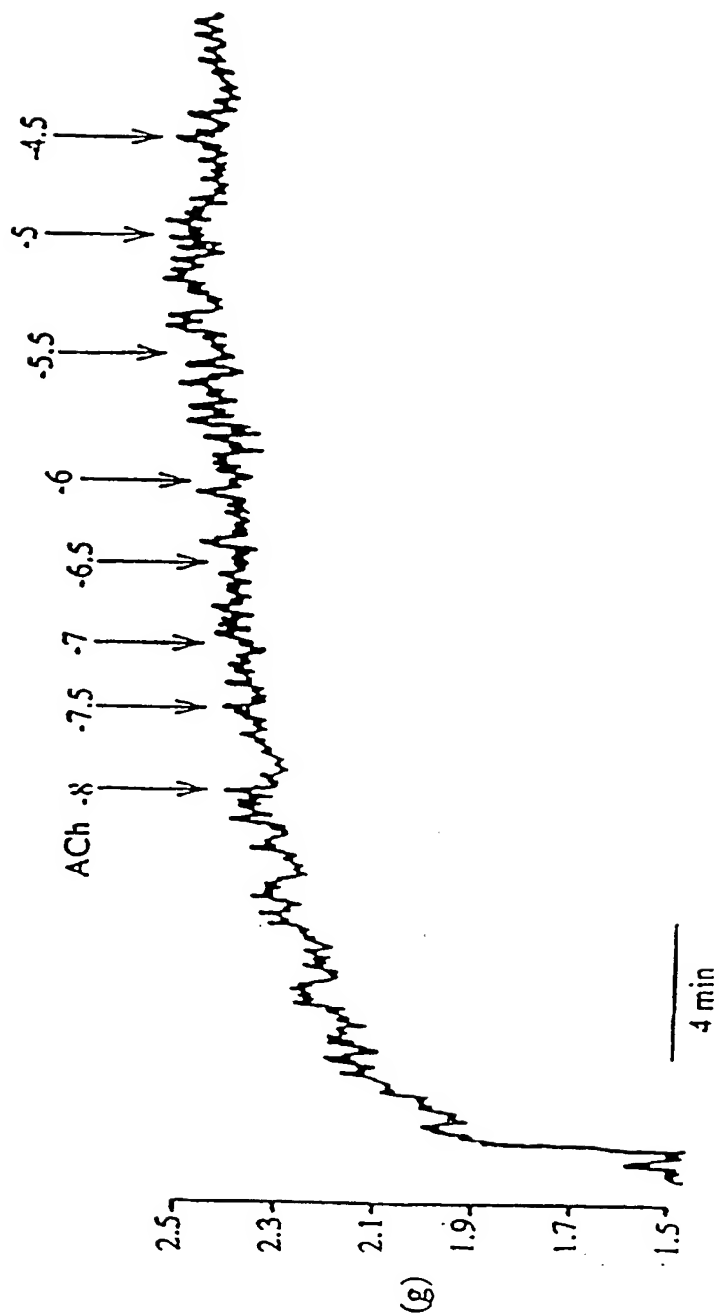


FIGURE 4C

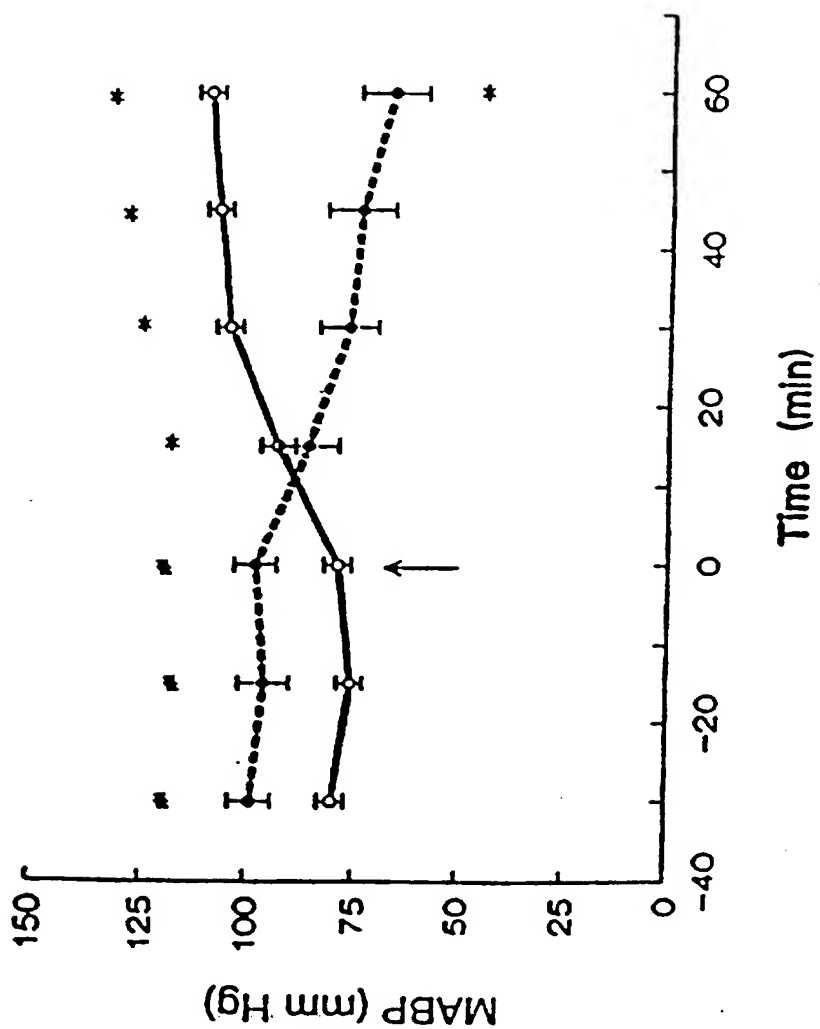
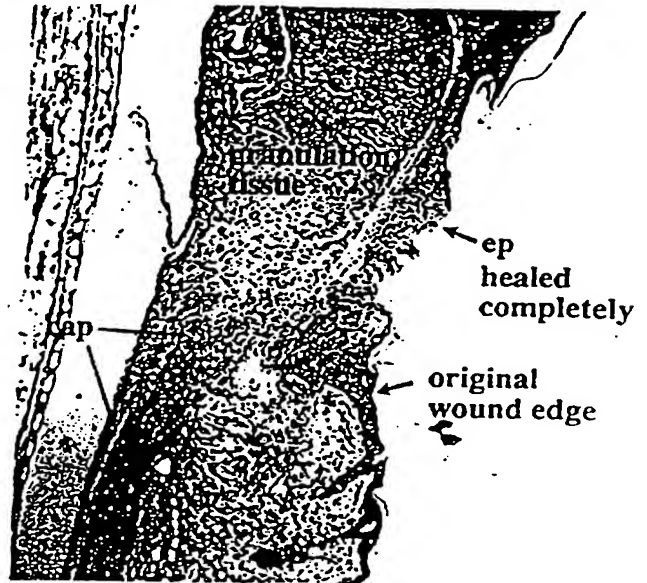


FIGURE 5

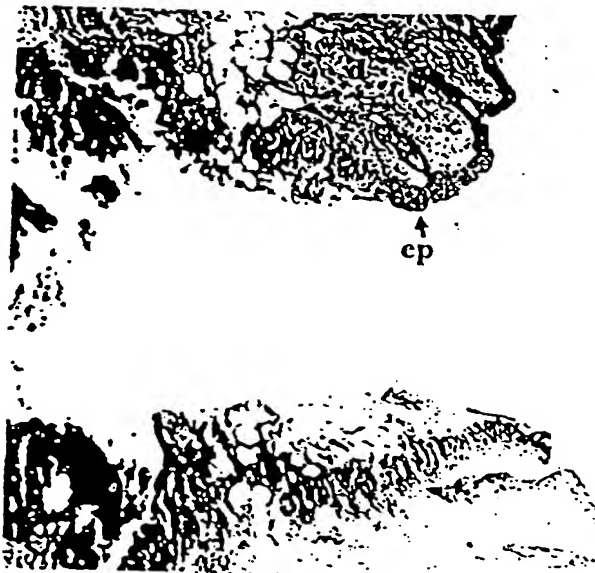
**FIGURE 6. WOUND HEALING IS ABNORMAL IN eNOS MUTANT MICE**



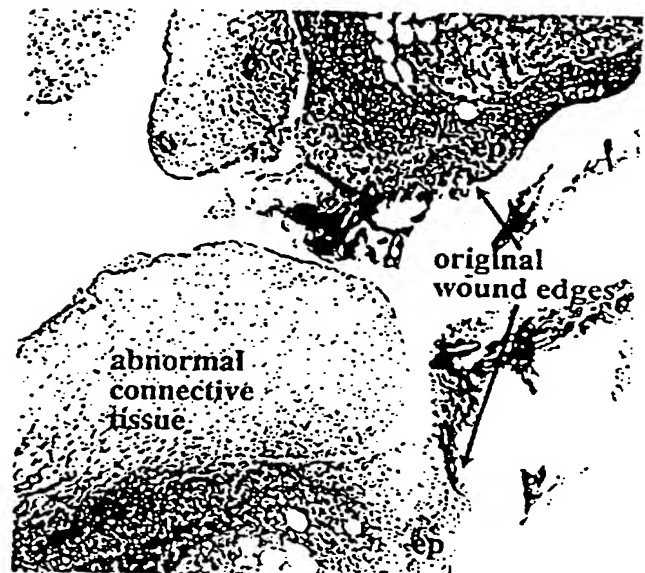
**A. Wild-type mouse, 24 hour wound**



**B. Wild-type mouse, 5 day wound**



**C. eNOS mutant mouse, 24 hour wound**

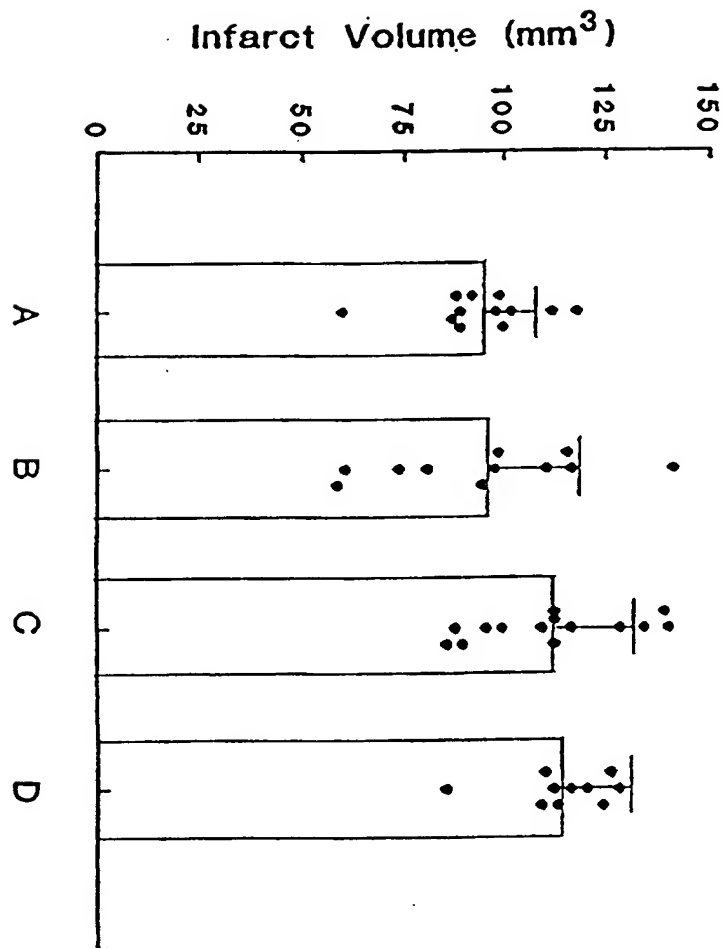


**D. eNOS mutant mouse, 5 day wound**

**Wound healing in eNOS mutant mice**

Wounds taken at 24 hours and 5 days. Wild-type wound has healed by 5 days. eNOS mutant wound does not heal, and demonstrates defective neovascularization. Details are described in the text.

FIGURE 7A



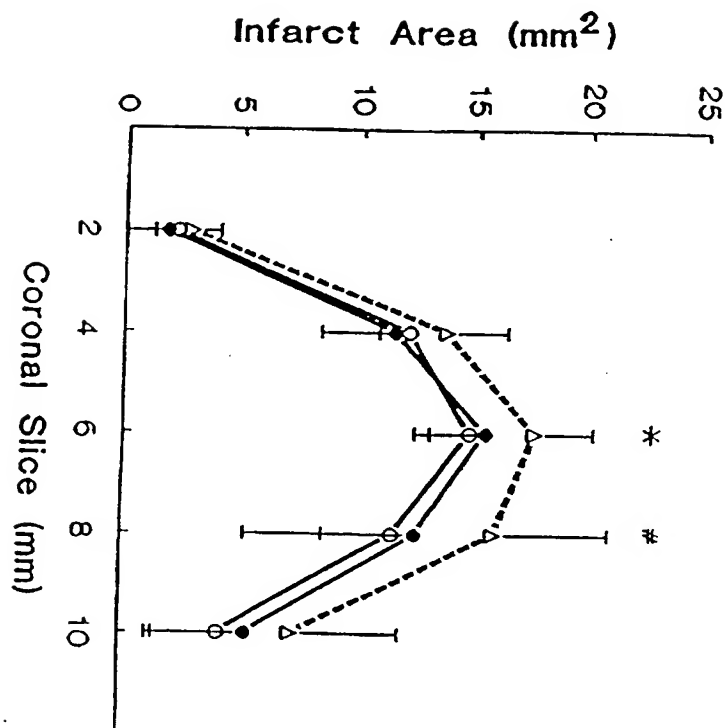
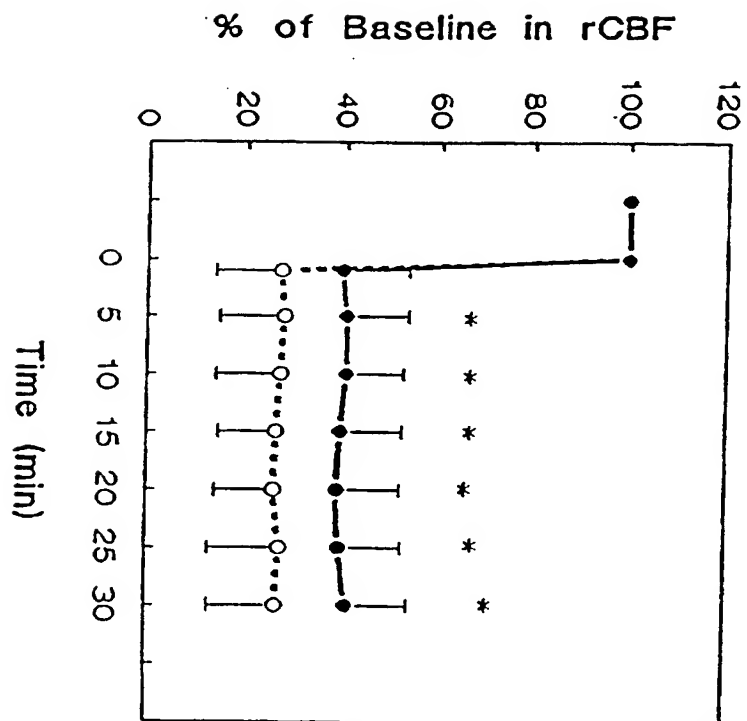
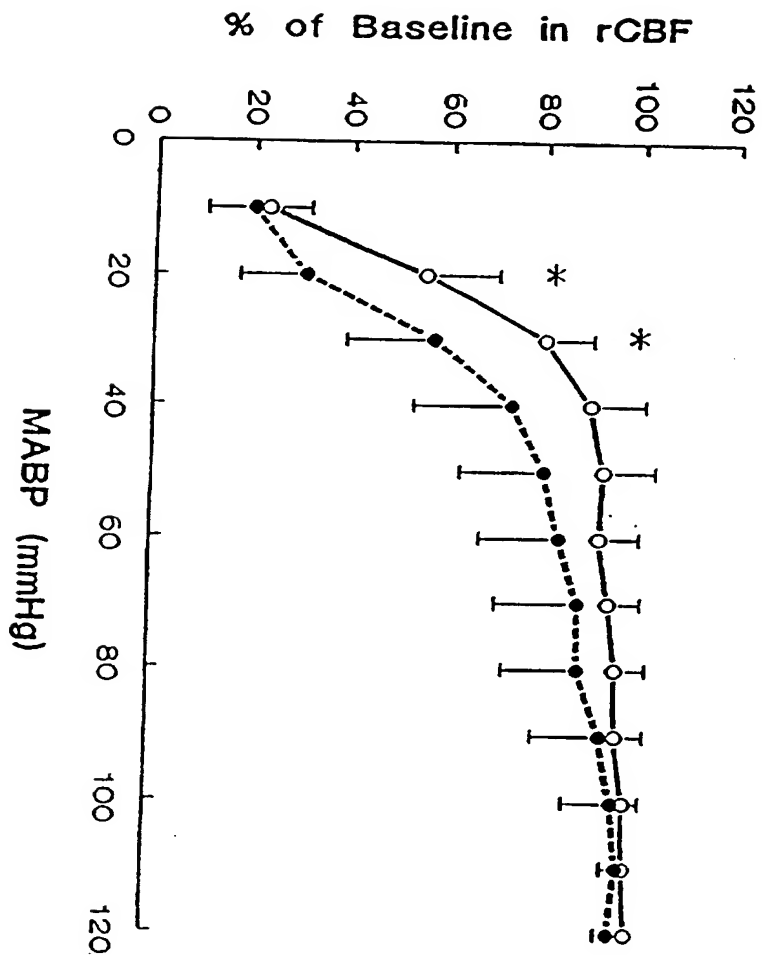


FIGURE 8



12/23  
FIGURE 9

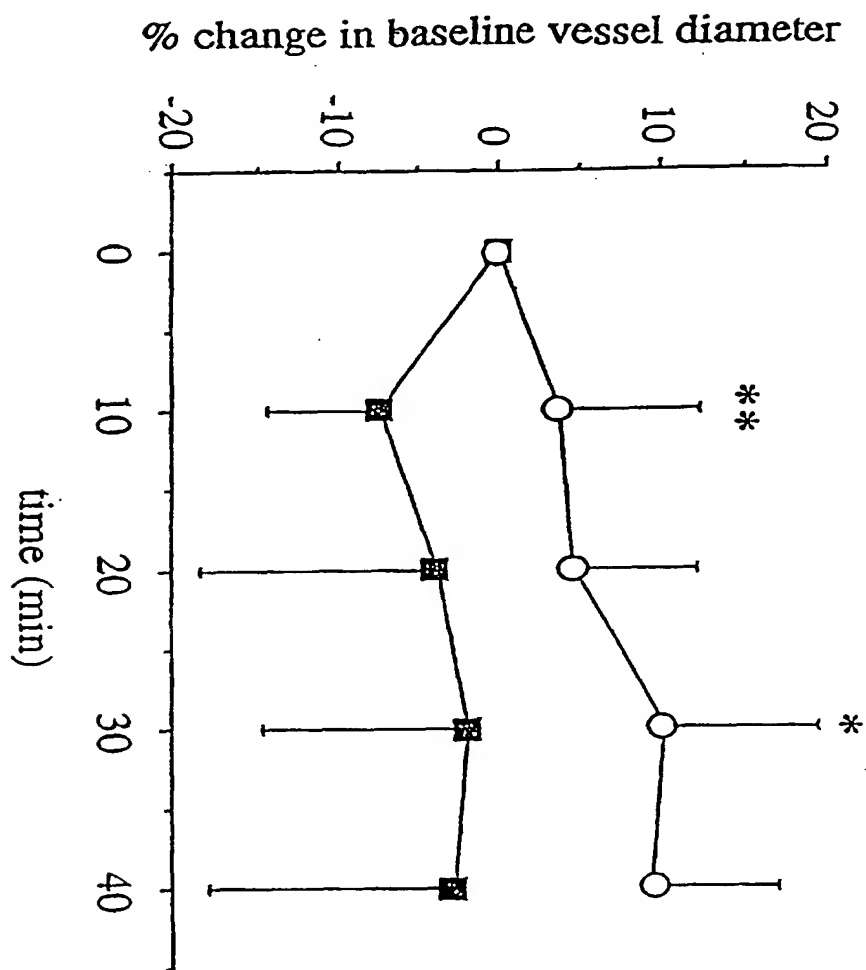
**FIGURE 10**

FIGURE 11



FIGURE 12

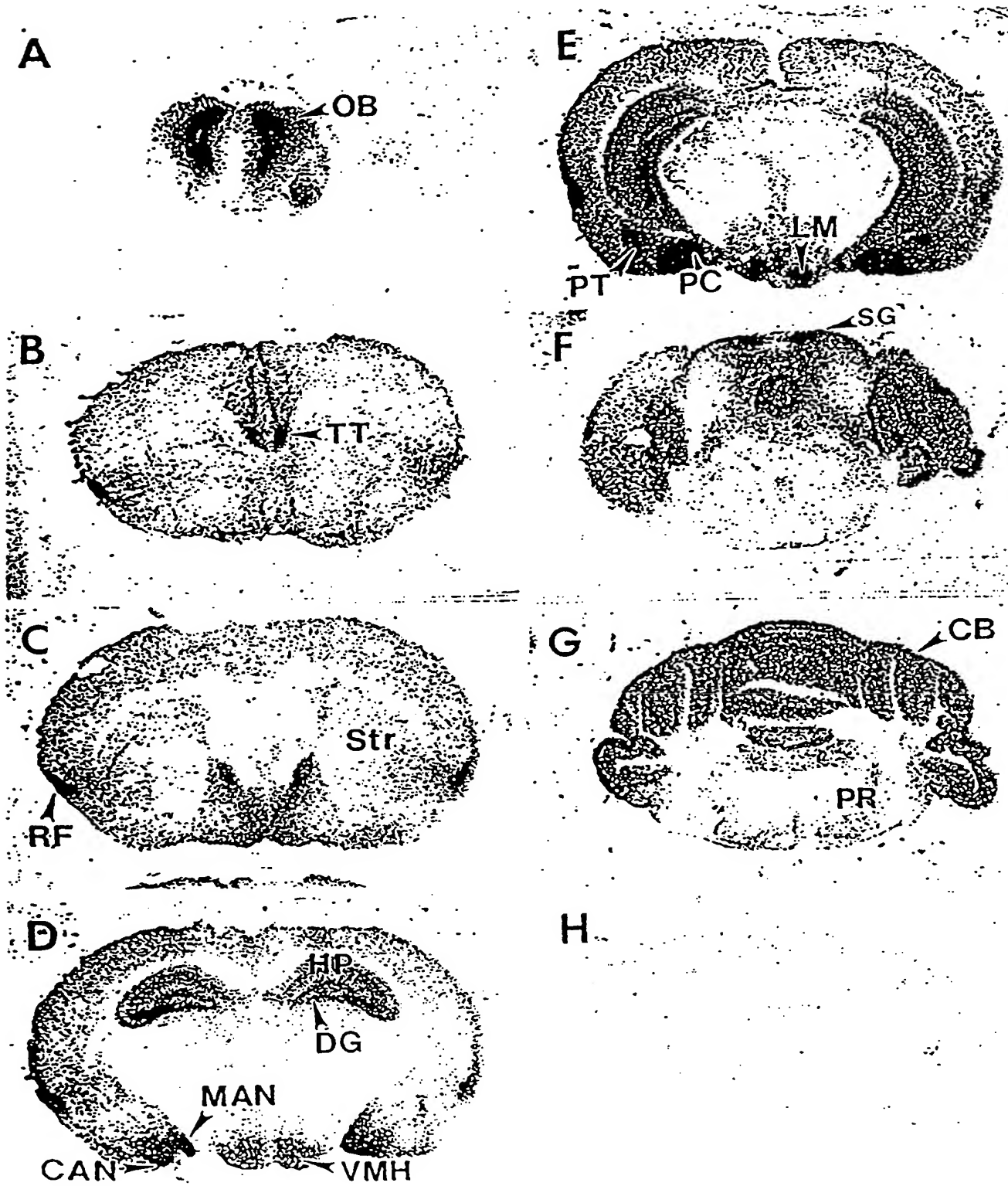


FIGURE 13

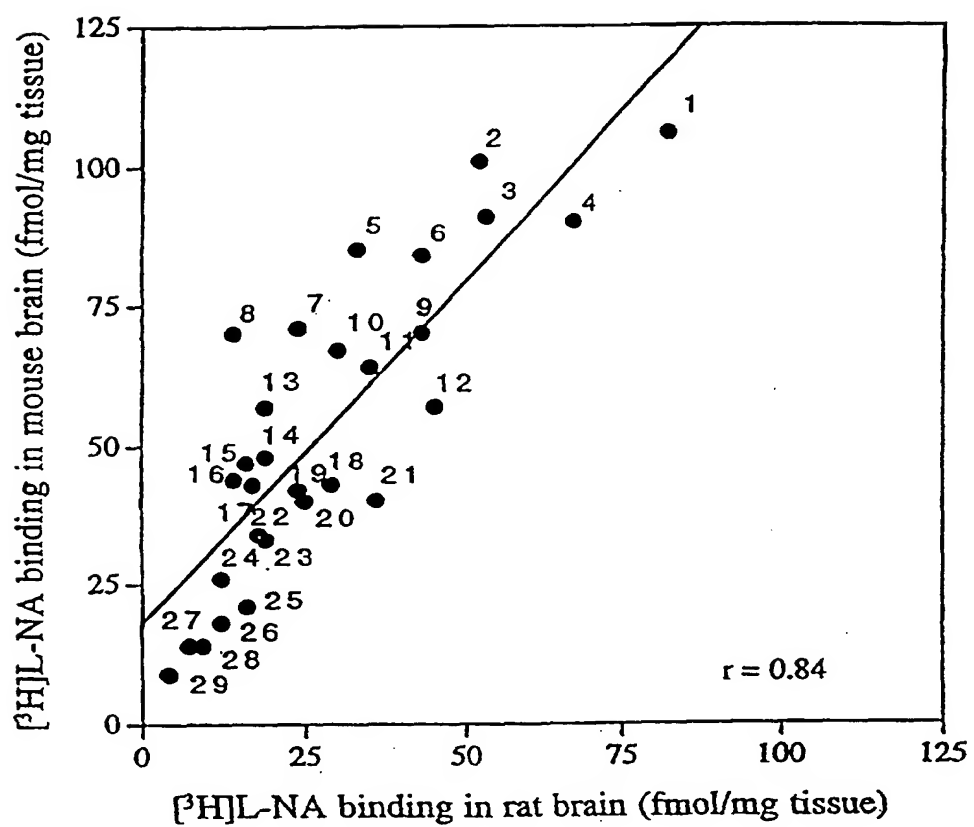
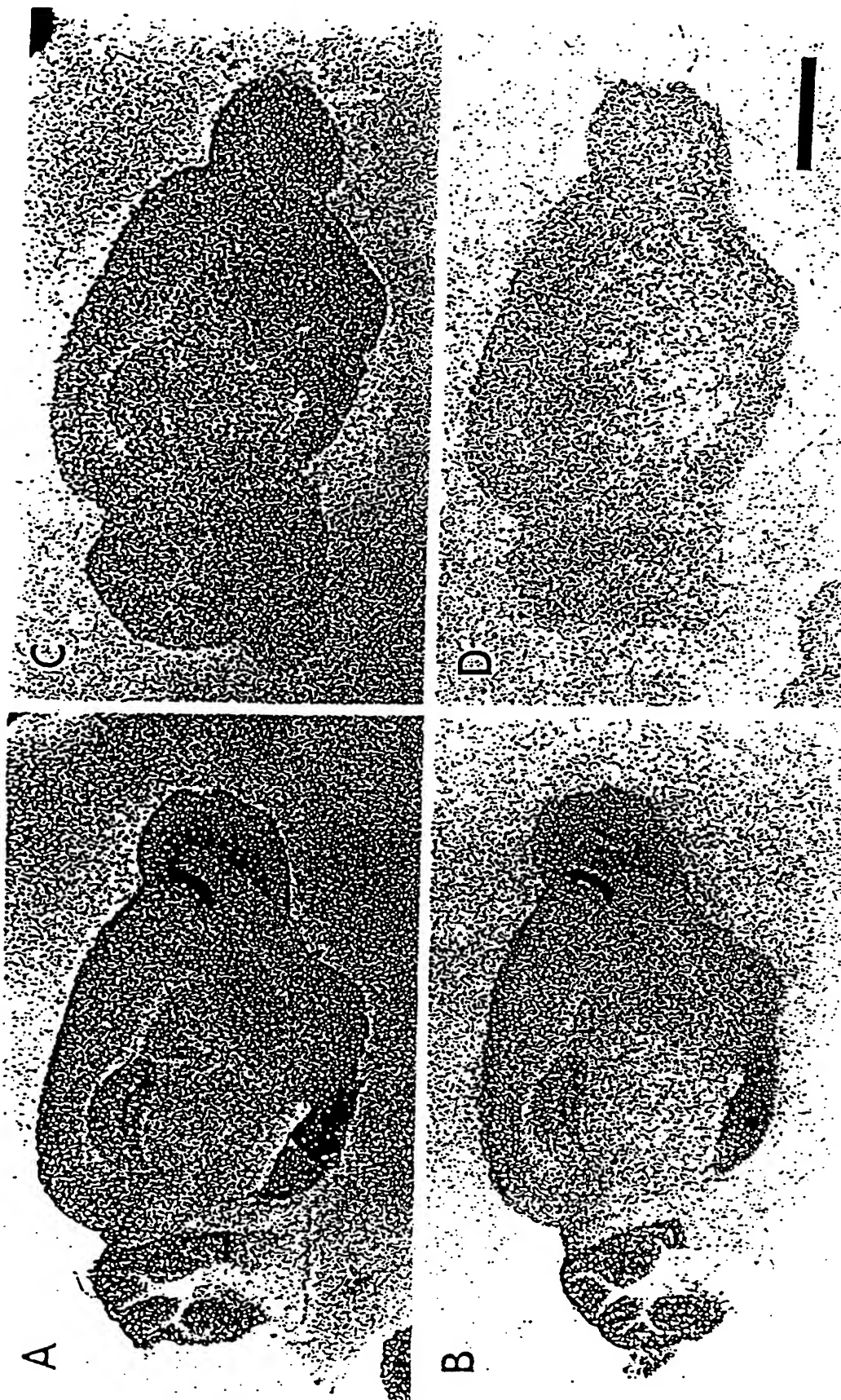
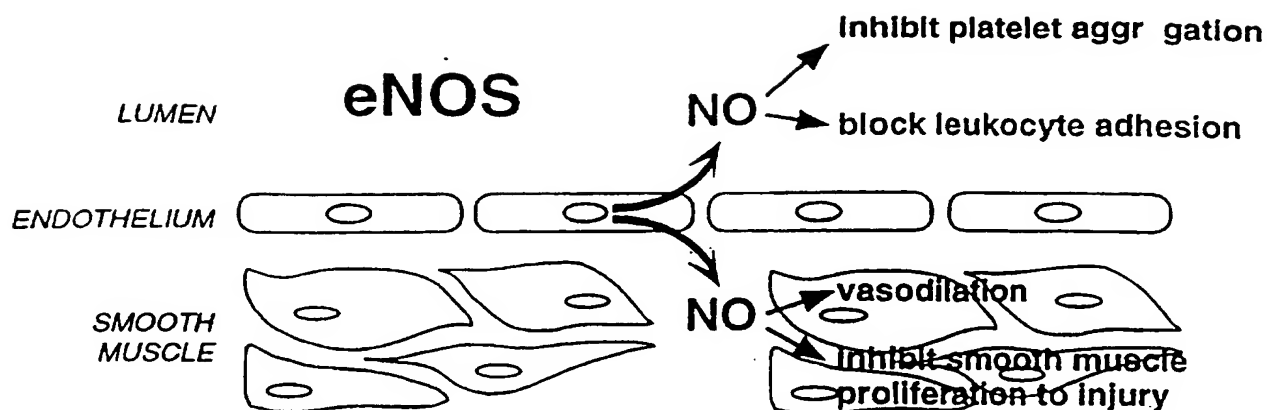
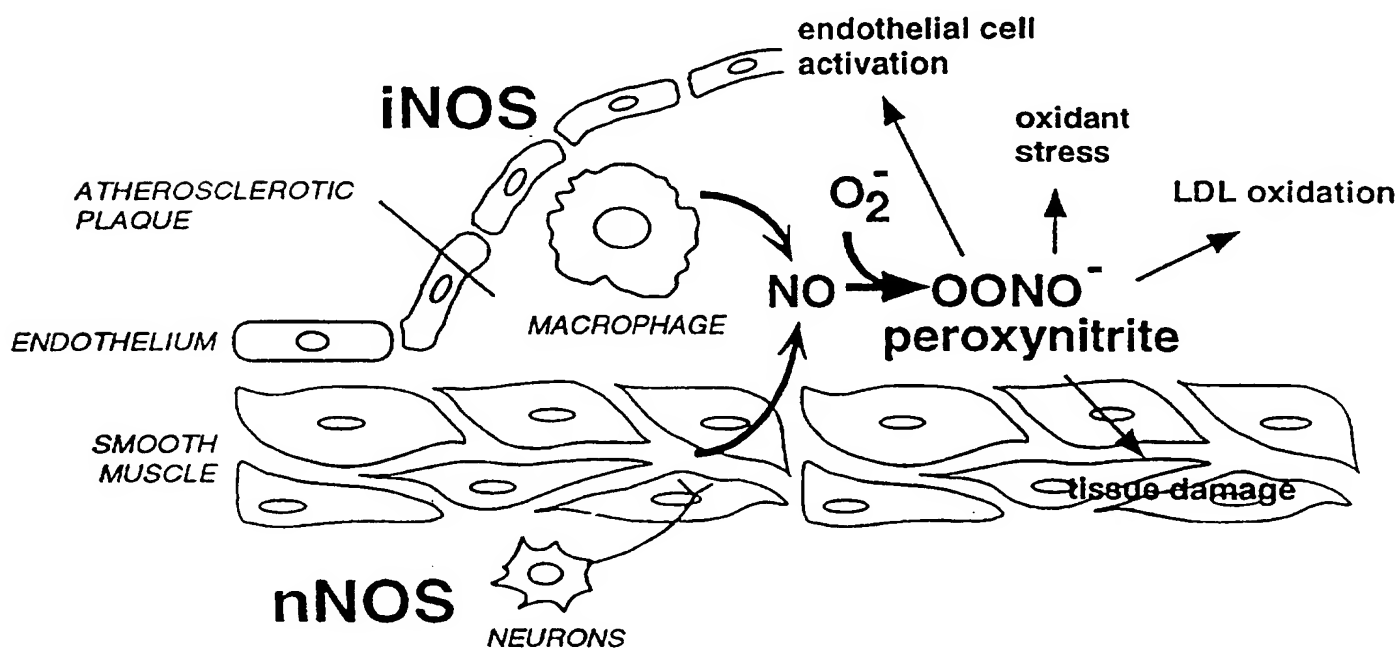


FIGURE 14





A. NO produced by normal vessels prevents proliferative response to injury and suppresses development of atherosclerosis



B. NO production in atherosclerotic plaques may lead to peroxynitrite formation, lipid oxidation, and endothelial cell activation

Figure 15 Effects of NO in normal and atherosclerotic arteries.

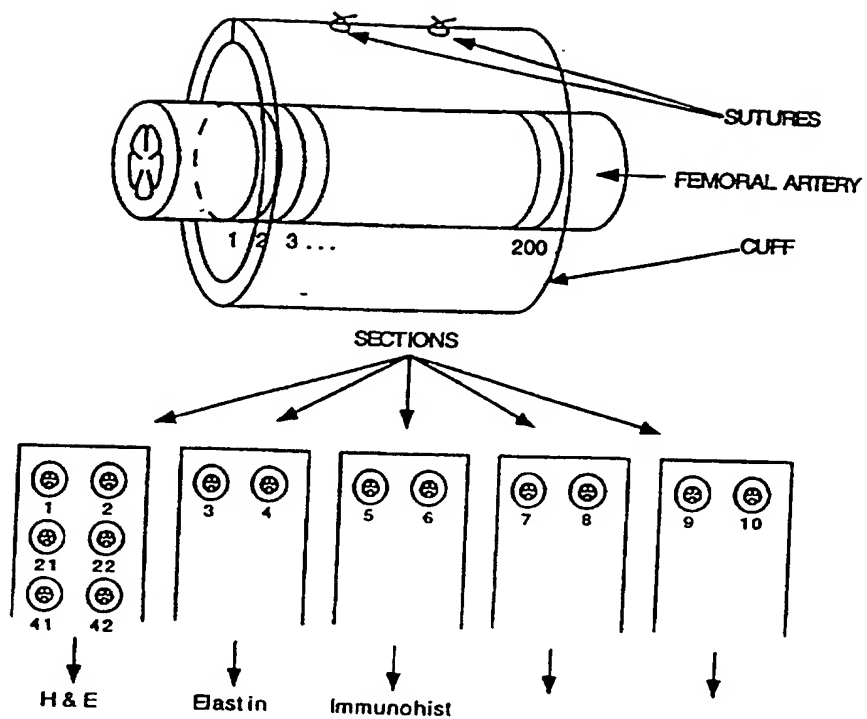
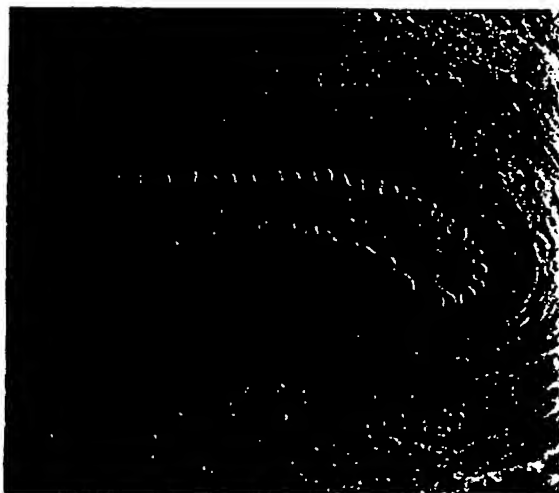


Figure 16

## H &amp; E stained sections of cuff-injured vessels



A. Wild-type vessel, injured



B. Wild-type vessel, control



C. eNOS mutant vessel, injured



D. eNOS mutant vessel, control

*Figure 17* Hematoxylin and eosin stained sections of cuff-injured vessels. Injured vessels contain neointima seen inside of the internal elastic lamina (shown with arrows). Control vessels do not. eNOS mutant mice show significantly increased neointimal formation, shown with asterisk (\*).



Figure 18 Histology and immunochemical staining of injured and control vessels from eNOS mutant mice. Note the position of the internal elastic lamina in each section. Control vessels have no intima.

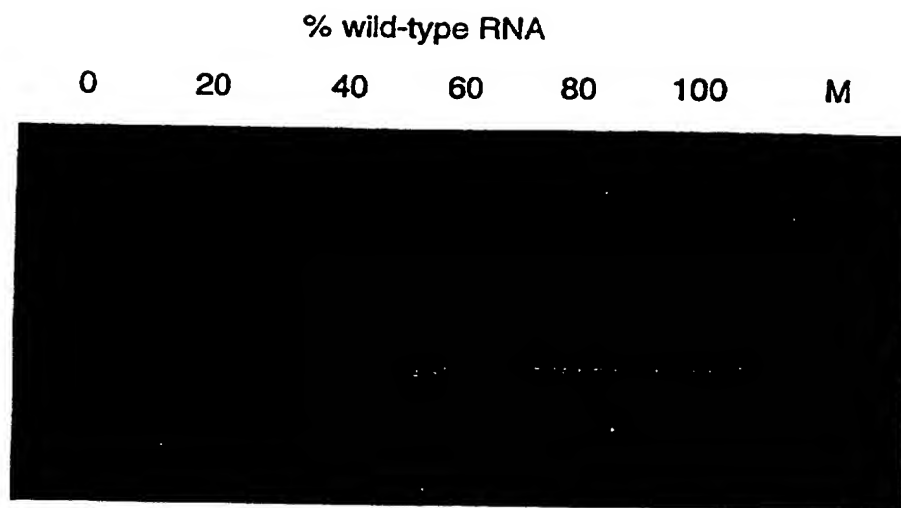
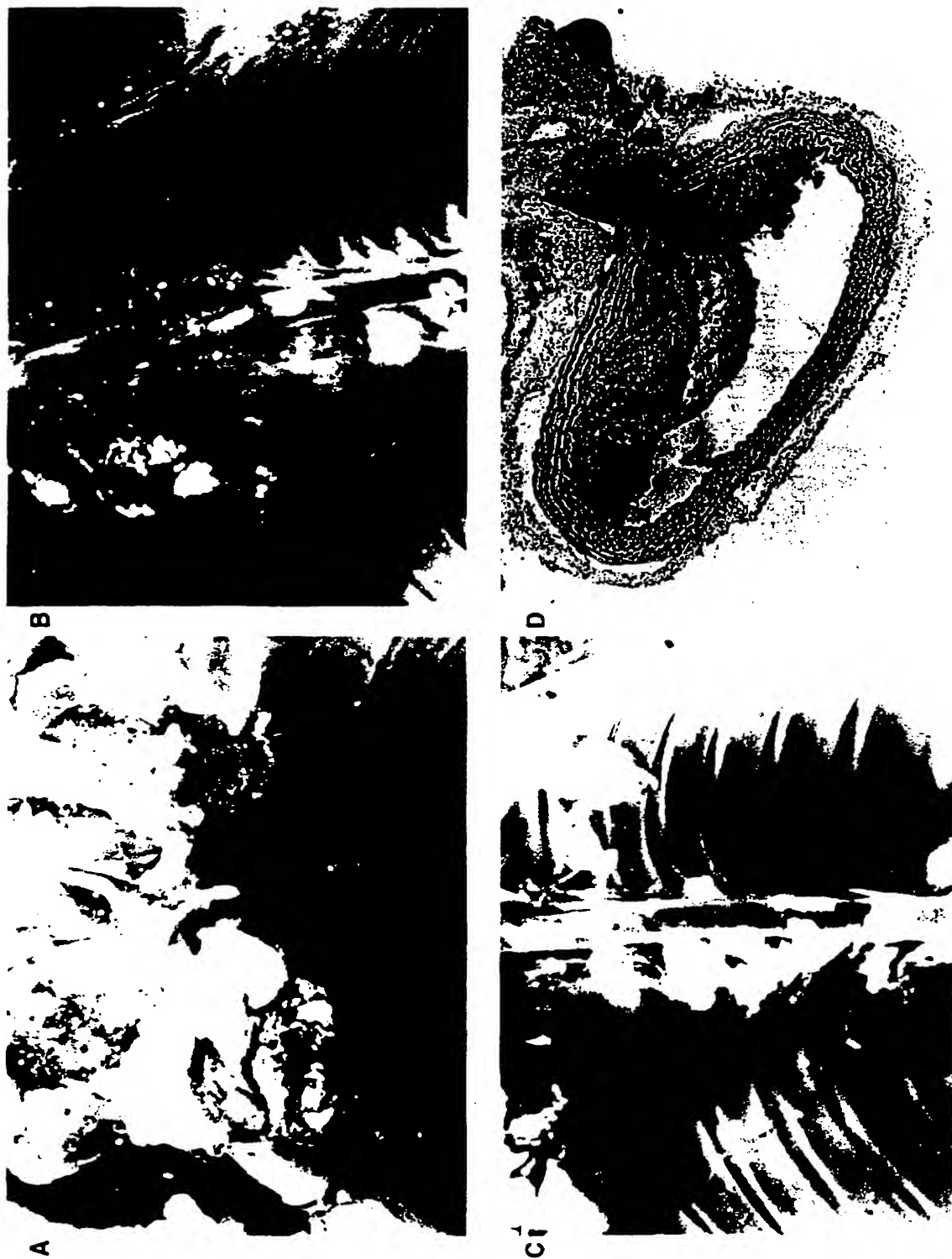


Figure 19. Quantitative RT-PCR of eNOS mRNA from mouse aorta



*Figure 20* Atherosclerotic lesions from apoE mutant mice at 6 months.  
A. Aortic arch and carotid arteries. B. Thoracic aorta. C. Descending  
thoracic aorta. D. Oil red O stain of an aortic lesion.

## INTERNATIONAL SEARCH REPORT

International Application No

PCT/US 97/04184

## A. CLASSIFICATION OF SUBJECT MATTER

IPC 6 C12N15/00 A01K67/027 C12N9/02 C12N15/53

According to International Patent Classification (IPC) or to both national classification and IPC

## B. FIELDS SEARCHED

Minimum documentation searched (classification system followed by classification symbols)

IPC 6 A01K C12N

Documentation searched other than minimum documentation to the extent that such documents are included in the fields searched

Electronic data base consulted during the international search (name of data base and, where practical, search terms used)

## C. DOCUMENTS CONSIDERED TO BE RELEVANT

Category *	Citation of document, with indication, where appropriate, of the relevant passages	Relevant to claim No.
X	STROKE, vol. 27, no. 1, 25 January 1996, page 173 XP000607805 HUANG Z ET AL: "FOCAL CEREBRAL ISCHEMIA IN MICE DEFICIENT IN EITHER ENDOTHELIAL (ENOS) OR NEURONAL NITRIC OXIDE (NNOS) SYNTHASE" see abstract ---	1-4,6,11
X	NATURE, vol. 377, 21 September 1995, pages 239-242, XP002021109 HUANG P L ET AL: "HYPERTENSION IN MICE LACKING THE GENE FOR ENDOTHELIAL NITRIC OXIDE SYNTHASE" see abstract see page 241, column 1, paragraph 2 --- -/--	7-9,11

☒ Further documents are listed in the continuation of box C.☒ Patent family members are listed in annex.

## \* Special categories of cited documents:

- \*A\* document defining the general state of the art which is not considered to be of particular relevance
- \*E\* earlier document but published on or after the international filing date
- \*L\* document which may throw doubts on priority claim(s) or which is cited to establish the publication date of another citation or other special reason (as specified)
- \*O\* document referring to an oral disclosure, use, exhibition or other means
- \*P\* document published prior to the international filing date but later than the priority date claimed

- \*T\* later document published after the international filing date or priority date and not in conflict with the application but cited to understand the principle or theory underlying the invention
- \*X\* document of particular relevance; the claimed invention cannot be considered novel or cannot be considered to involve an inventive step when the document is taken alone
- \*Y\* document of particular relevance; the claimed invention cannot be considered to involve an inventive step when the document is combined with one or more other such documents, such combination being obvious to a person skilled in the art.
- \*Z\* document member of the same patent family

Date of the actual completion of the international search

26 June 1997

Date of mailing of the international search report

11.07.97.

Name and mailing address of the ISA

European Patent Office, P.B. 5818 Patentlaan 2  
NL - 2280 HV Rijswijk  
Tel. (+31-70) 340-2040, Tx. 31 651 epo nl,  
Fax (+31-70) 340-3016

Authorized officer

Chambonnet, F

# INTERNATIONAL SEARCH REPORT

Patent Application No.

PCT/US 97/04184

C(Continuation) DOCUMENTS CONSIDERED TO BE RELEVANT		
Category	Citation of document, with indication, where appropriate, of the relevant passages	Relevant to claim No.
A	WO 93 19166 A (UNIV NORTH CAROLINA) 30 September 1993 see the whole document ---	10
P,X	CIRCULATION, vol. 94, no. 8 sup, 15 October 1996, page 1154 XP000676824 MOROI, M. ET AL.: "Mice mutant in endothelial Nitric Oxide synthase: vessel growth and response to injury" see abstract ---	8,9,11
P,X	AMERICAN JOURNAL OF PHYSIOLOGY, vol. 272, no. 3 pt 2, March 1997, page h1401 XP000676924 HUANG, Z. ET AL.: "bFGF ameliorates focal ischemic injury by blood flow-independent mechanisms in eNOS mutant mice" see the whole document ---	1
T	JOURNAL OF MOLECULAR MEDICINE, vol. 74, no. 8, 1996, pages 415-421, XP000610408 HUANG P L ET AL: "GENETIC ANALYSIS OF NITRIC OXIDE SYNTHASE ISOFORMS: TARGETED MUTATION IN MICE" see the whole document -----	1

# INTERNATIONAL SEARCH REPORT

information on patent family members

International Application No

PCT/US 97/04184

Patent document cited in search report	Publication date	Patent family member(s)	Publication date
WO 9319166 A	30-09-93	AU 3814393 A	21-10-93
-----			

Form PCT/ISA/210 (patent family annex) (July 1992)

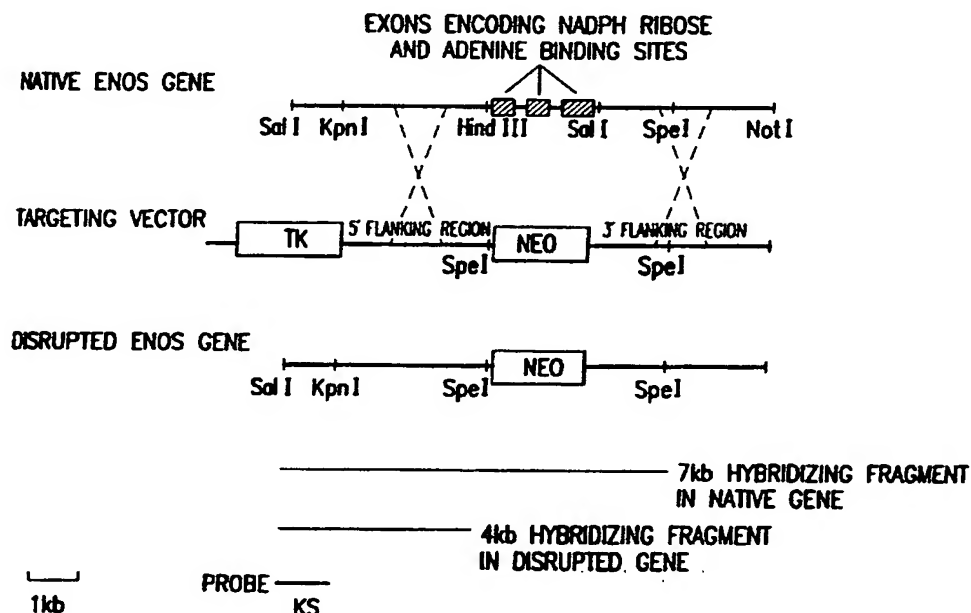




INTERNATIONAL APPLICATION PUBLISHED UNDER THE PATENT COOPERATION TREATY (PCT)

(51) International Patent Classification <sup>6</sup> : <b>C12N 15/00, A01K 67/027, C12N 9/02, 15/53</b>		<b>A1</b>	(11) International Publication Number: <b>WO 97/33989</b>
			(43) International Publication Date: 18 September 1997 (18.09.97)
(21) International Application Number: <b>PCT/US97/04184</b>		(81) Designated States: CA, JP, MX, European patent (AT, BE, CH, DE, DK, ES, FI, FR, GB, GR, IE, IT, LU, MC, NL, PT, SE).	
(22) International Filing Date: 14 March 1997 (14.03.97)		<b>Published</b> <i>With international search report.</i> <i>Before the expiration of the time limit for amending the claims and to be republished in the event of the receipt of amendments.</i>	
(30) Priority Data: 60/013,525                      15 March 1996 (15.03.96)                      US 60/027,362                      18 September 1996 (18.09.96)                      US			
(71) Applicant: THE GENERAL HOSPITAL CORPORATION [US/US]; Fruit Street, Boston, MA 02114 (US).			
(72) Inventors: HUANG, Paul, L.; 18 Temple Street, Boston, MA 02114 (US). FISHMAN, Mark, C.; 43 Kenwood Avenue, Newton Center, MA 02159 (US). MOSKOWITZ, Michael, A.; 275 Prospect Street, Belmont, MA 02178 (US).			
(74) Agents: GOLDSTEIN, Jorge, A. et al.; Sterne, Kessler, Goldstein & Fox P.L.L.C., Suite 600, 1100 New York Avenue, N.W., Washington, DC 20005-3934 (US).			

(54) Title: TRANSGENIC ANIMALS HAVING A DISRUPTED eNOS GENE AND USE THEREOF



(57) Abstract

This invention relates to transgenic non-human animals comprising a disrupted endothelial nitric oxide synthase gene. These animals exhibit abnormal wound-healing properties and hypertension. This invention also relates to methods of using the transgenic animals to screen for compounds having a potential therapeutic utility for vascular endothelial disorders, such as hypertension, cerebral ischemia or stroke, atherosclerosis and wound-healing activities. Moreover, this invention also relates to methods of treating a patient suffering from hypertension and wound-healing abnormalities with the compounds identified using the transgenic animals, and methods of making the transgenic animals. A method of treating a wound using nitroglycerin is also provided.

**FOR THE PURPOSES OF INFORMATION ONLY**

Codes used to identify States party to the PCT on the front pages of pamphlets publishing international applications under the PCT.

AM	Armenia	GB	United Kingdom	MW	Malawi
AT	Austria	GE	Georgia	MX	Mexico
AU	Australia	GN	Guinea	NE	Niger
BB	Barbados	GR	Greece	NL	Netherlands
BE	Belgium	HU	Hungary	NO	Norway
BF	Burkina Faso	IE	Ireland	NZ	New Zealand
BG	Bulgaria	IT	Italy	PL	Poland
BJ	Benin	JP	Japan	PT	Portugal
BR	Brazil	KE	Kenya	RO	Romania
BY	Belarus	KG	Kyrgyzstan	RU	Russian Federation
CA	Canada	KP	Democratic People's Republic of Korea	SD	Sudan
CF	Central African Republic	KR	Republic of Korea	SE	Sweden
CG	Congo	KZ	Kazakhstan	SG	Singapore
CH	Switzerland	LI	Liechtenstein	SI	Slovenia
CI	Côte d'Ivoire	LK	Sri Lanka	SK	Slovakia
CM	Cameroon	LR	Liberia	SN	Senegal
CN	China	LT	Lithuania	SZ	Swaziland
CS	Czechoslovakia	LU	Luxembourg	TD	Chad
CZ	Czech Republic	LV	Latvia	TG	Togo
DE	Germany	MC	Monaco	TJ	Tajikistan
DK	Denmark	MD	Republic of Moldova	TT	Trinidad and Tobago
EE	Estonia	MG	Madagascar	UA	Ukraine
ES	Spain	ML	Mali	UG	Uganda
FI	Finland	MN	Mongolia	US	United States of America
FR	France	MR	Mauritania	UZ	Uzbekistan
GA	Gabon			VN	Viet Nam

**Transgenic animals having a disrupted eNOS gen and use thereof*****Background of the Invention******Statement as to Rights to Inventions Made Under  
Federally-Sponsored Research and Development***

Part of the work performed during the development of this invention was supported by U.S. Government funds. The U.S. Government may have certain rights in this invention.

***Field of the Invention***

This invention relates to transgenic non-human animals comprising a disrupted endothelial nitric oxide synthase gene. This invention also relates to methods of using these transgenic animals to screen compounds for activity against vascular endothelial disorders such as hypertension, stroke, and atherosclerosis, as well as for wound healing activity; methods of treating a patient suffering from a vascular endothelial disorder; methods of making the transgenic animals; and cell lines comprising a disrupted eNOS gene.

***Related Art***

In 1980, Furchgott and Zawadzki first proposed the existence of endothelium derived relaxing factor or EDRF, later identified as nitric oxide. Furchgott (1980); Furchgott (1988); Ignarro (1988); Palmer (1987). Nitric oxide is an important messenger molecule produced by endothelial cells, neurons, macrophages, and other tissues. Marletta (1989); Moncada (1991); Nathan (1992); Snyder (1992); and Dawson *et al.* (1992). Since nitric oxide is a gas with no known storage mechanism, it diffuses freely across membranes and is extremely labile. Nitric oxide has a biological half-life on the order of seconds.

-2-

Nitric oxide exhibits several biochemical activities. This compound can bind to and activate soluble guanyl cyclase, resulting in increased cGMP levels. Nitric oxide also modifies a cysteine residue in glyceraldehyde-3-phosphate dehydrogenase by adenosine diphosphate ribosylation, Zhang & Snyder (1992), Katz *et al.* (1992), and Dimmeler *et al.* (1992), or S-nitrosylation via NAD interactions, McDonald & Moss (1993). Nitric oxide also binds to a variety of iron- and sulphur-containing proteins, Marletta (1993), and may have other modes of action as well.

Nitric oxide formation is catalyzed by the nitric oxide synthase enzymes (NOS). These enzymes act by producing nitric oxide from the terminal guanidino nitrogen of arginine, with the stoichiometric production of citrulline. There are several NOS isoforms encoded by separate genes. Marletta (1993), and Lowenstein & Snyder (1992). The various NOS isoforms are about 50-60% homologous overall. Some forms of NOS are found in most tissues. The different NOS isoforms: neuronal NOS (nNOS), macrophage NOS (iNOS), and endothelial NOS (eNOS), are now known as type I NOS, type II NOS and type III NOS, respectively. The properties of these NOS isoforms are summarized in the following Table:

Property	Type I NOS	Type II NOS	Type III NOS
Common name	nNOS	iNOS	eNOS
Typical cell	neurons	macrophages	endothelium
Other sites of expression	smooth muscle	endothelium smooth muscle	smooth muscle neurons
Expression	constitutive	inducible	constitutive
Regulation	Ca/CaM	transcription	Ca/CaM
Output	moderate (nM to $\mu$ M)	high ( $\mu$ M)	low (pM to nM)
Function	signalling	toxin	signalling

-3-

The ubiquitous presence of blood vessels and nerves means that the endothelial and neuronal isoforms may be present in most tissues. The expression of the endothelial and neuronal isoforms can also be induced in cells that normally do not express them. The sequence of these isoforms have been published or are available in Genbank under the following accession numbers:

Gene:	Species:			
	Man	Rat	Mouse	Cow
<b>Neuronal (type I)</b>	U17327	X59949	D14552	
	D16408			
	L02881			
<b>Macrophage (type II)</b>	L09210	D14051	M87039	U18331
	X85759-81	D83661	U43428	U14640
	U18334	U26686	L23806	
	U31511	U16359	L09126	
	U20141	D44591	M92649	
	U05810	X76881	M84373	
	X73029	U02534		
	L24553	L12562		
<b>Endothelial (type III)</b>	X76303-16	U18336		M89952
	L26914	U28933		L27056
	L23210			M95674
	L10693			M99057
	M95296			M89952
	M93718			

Each of these sequences are expressly incorporated herein by reference.

In blood vessels, the endothelial NOS isoform mediates endothelium-dependent vasodilation in response to acetylcholine, bradykinin, and other mediators. Nitric oxide also maintains basal vascular tone and regulates regional

blood flow. Nitric oxide levels increase in response to shear stress, i.e., forces on the blood vessels in the direction of blood flow, and to mediators of inflammation. Furchgott & van Houtte (1989); Ignarro (1989).

5 In the immune system, the macrophage isoform is produced by activated macrophages and neutrophils as a cytotoxic agent. Nitric oxide produced in these cells targets tumor cells and pathogens. Hibbs *et al.* (1988); Nathan (1992); and Marletta (1989).

10 In the nervous system, the neuronal NOS isoform is localized to discrete populations of neurons in the cerebellum, olfactory bulb, hippocampus, cortex, striatum, basal forebrain, and brain stem. Bredt *et al.* (1990). NOS is also concentrated in the posterior pituitary gland, in the superoptic and paraventricular hypothalamic nuclei, and in discrete ganglion cells of the adrenal medulla. *Id.* The widespread cellular localization of neuronal NOS and the short half-life and diffusion properties of nitric oxide suggest that it plays a role in nervous system morphogenesis and synaptic plasticity.

15 During development, NO may influence activity-dependent synaptic pruning, apoptosis, and the establishment of the columnar organization of the cortex. Gally *et al.* (1990), Edelman & Gally (1992). Two forms of long-term synaptic modulation, long-term depression of the cerebellum, Shibuki & Okada (1991), and long-term potentiation (LTP) in the hippocampus, are sensitive to inhibitors of NOS. Bohme *et al.* (1991); Haley *et al.* (1992); O'Dell *et al.* (1991); Schuman & Madison (1991). Thus, nitric oxide may serve as a retrograde neurotransmitter to enhance synaptic function due to correlated firing of pre-and postsynaptic cells.

25 In the peripheral nervous system, nitric oxide mediates relaxation of smooth muscle. Smooth muscle relaxation in the gut, important to adaptation to a bolus of food and peristalsis, depends upon inhibitory non adrenergic, noncholinergic nerves that mediate their effects via nitric oxide. Boeckvstaens *et al.* (1991); Bult *et al.* (1990); Desai *et al.* (1991); Gillespie *et al.* (1989); Gibson *et al.* (1990); Ramagopal & Leighton (1989); Tottrup *et al.* (1991). NOS-

containing neurons also innervate the corpus carvornosa of the penis, Burnett *et al.* (1992); Rajfer *et al.* (1992), and the adventitial layer of cerebral blood vessels. Nozaki *et al.* (1993); Toda & Okamura (1990). Stimulation of these nerves can lead to penile erection and dilation of cerebral arteries, respectively. These effects are blocked by inhibition of NOS.

Various biological roles of NO are described by Schmidt & Walter (1994); Nathan & Xie (1994); and Snyder (1995). The major roles of nitric oxide include:

- (1) vasodilation or vasoconstriction with resulting change in blood pressure and blood flow;
- (2) neurotransmission in the central and peripheral nervous system, including mediation of signals for normal gastrointestinal motility; and
- (3) defense against pathogens like bacteria, fungus, and parasites due to the toxicity of high levels of NO to pathogenic organisms.

Recently, a role for NO has been proposed in the pathophysiology of cerebral ischemia, one form of vascular endothelial disorder. Iadecola *et al.* (1994); Dalkara and Moskowitz (1994). Since NO is diffusible, short-lived, and reactive free radical gas that is difficult to measure *in vivo*, Archer (1993), most studies examining ischemic outcomes have based their conclusions on results following NOS inhibition by arginine analogues such as nitro-L-arginine or nitro-L-arginine methyl ester. These inhibitors, however, lack enzyme selectivity and block multiple isoforms. Rees *et al.* (1990). This nonselectivity might account in part for the discrepant outcomes after administration of NOS inhibitors following middle cerebral artery (MCA) occlusion.

Atherosclerosis is another form of a vascular endothelial disorder. This disease, a major cause of morbidity and mortality, is progressive beginning many years before the onset of overt symptoms. During the development of atherosclerosis, biochemical, cellular, and hemodynamic forces drive change in blood vessel walls, which ultimately leads to endothelial dysfunction, cellular proliferation, recruitment of endothelial cells, and accumulation of oxidized LDL.

Ross (1995). The cellular and molecular mechanisms that underlie these processes are complex. Rodent models offer the ability to study the contribution of individual genes, alone or in combination, to the molecular events in atherosclerosis. Breslow (1996); Ross (1996).

5           Cells within atherosclerotic plaques are monoclonal or oligoclonal in origin, indicating that intimal proliferation plays an important role in the development of lesions. Benditt (1973). Intimal proliferation also occurs as a common response to arterial injury of many kinds, regardless of whether the injury is luminal or adventitial. Schwartz (1995). Thus, models of vessel injury  
10           are relevant to atherosclerosis. For example, in a cuff model of adventitial injury, Booth *et al.* (1989); Kockx *et al.* (1993), signals from the adventitia stimulate formation of a neointimal layer in a predictable manner. This model leaves the endothelium intact, so that the role of endothelial gene products can be studied. In a filament model of endothelial injury, Lindner (1993), the endothelium is  
15           physically removed, resulting in proliferation of medial smooth muscle cells. The rate at which endothelial cells resurface the injured areas can be quantitated.

          In another type of atherosclerosis model, defined genetic mutations are used to increase the propensity of mice to atherosclerosis. Breslow (1996); Ross (1996). For example, mutant mice that form atherosclerotic lesions include apoE  
20           gene knockout mice, Plumb (1992); Zhang (1992); apoE Leiden mutation, van der Maagdenberg (1993); LDL receptor gene knockout mice, Ishibayashi (1993); and transgenic mice expressing the human apoB gene, Purcell-Huynh (1995). Of these, apoE knockout mice are an attractive atherosclerosis model, since they develop lesions on a low cholesterol, low-fat diet, and do not require the addition  
25           of cholic acid. These knockout mice develop fatty streaks that progress to fibrous plaques at branchpoints of major vessels, similar to human lesions. The rate and extent of lesion formation and its pathological severity can be quantitated. For example, a Western diet results in faster progression of the disease and formation of larger plaques than a low-cholesterol diet. Thus, the apoE knockout mice  
30           exhibit many aspects of human atherosclerosis.

Nitric oxide has physiological effects in blood vessels that may prevent atherosclerosis, such as suppression of smooth muscle proliferation, Mooradian (1995), inhibition of platelet aggregation and adhesion, Radomski (1991), and inhibition of leukocyte activation and adhesion, Bath (1993); Lefer (1993). It has also been recently reported that arginine inhibits atherosclerosis in LDL receptor mutant mice. Aji (1997).

While certain physiological effects of nitric oxide may prevent atherosclerosis, other studies suggest that excessive nitric oxide production may contribute to the development of atherosclerosis. Busse (1976); Leitinger (1995); Radomski (1995). Evidence for a pro-atherogenic role for nitric oxide includes several different findings. First, expression of iNOS and nNOS isoforms can be induced in atherosclerotic vessels. Aji (1997); Sobey (1995); Topors (1995); Wilcox (1994). Second, human atherosclerotic lesions contain nitrotyrosine, suggesting that peroxynitrite is formed in atherosclerotic lesions. See Beckman (1994b). Peroxynitrite is formed by the reaction of nitric oxide with superoxide in biological systems, Beckman (1994a), and is an extremely potent oxidant that can initiate lipid peroxidation of human LDL. Darley-Usmar (1992). Third, nitric oxide affects redox-sensitive transcription of genes involved in endothelial cell activation such as VCAM-1. This implicates nitric oxide in atherosclerosis.

However, prior to this invention, it was not clear which NOS isoforms were involved in stimulating atherosclerosis. Malinski (1993). Moreover, it was also not clear how important is peroxynitrite formation to the molecular events of atherosclerosis. Peroxynitrite ( $\text{ONOO}^-$ ) is a strong oxidant capable of lipid and protein oxidation. Beckman (1994a). Superoxide reacts with nitric oxide to form peroxynitrite faster, rate constant of  $6.7 \times 10^{-9}$  M/sec, than superoxide is scavenged by superoxide dismutase, rate constant of  $2.0 \times 10^{-9}$  M/sec. Endothelial cells are sensitive to the redox state and may respond with a program of endothelial cell activation, including expression of VCAM-1, ICAM-1, E-selectin, and MCP-1.

Many studies depend on pharmacological agents that block NOS enzymes, such as L-nitroarginine (L-NA) and L-N-arginine methyl ester (L-NAME). Inhibition of a process by these NOS inhibitors, and reversal of inhibition by excess L-arginine, but not D-arginine, provides evidence for the involvement of NO. However, these NOS inhibitors affect all three isoforms, so that the effect on different isoforms cannot be distinguished. Distinguishing between various NOS isoforms is particularly important since NOS isoforms have multiple roles and divergent effects.

Targeted gene disruption of the endothelial or neuronal NOS isoforms offers a new approach to dissect the relevance of NO in brain ischemia and the development of treatments for brain ischemia and stroke. For example, mice deficient in neuronal NOS gene expression were relatively resistant to brain injury after permanent focal cerebral ischemia. Huang *et al.* (1994).

Over the last several years, transgenic animals have been made containing specific genetic defects, e.g., resulting in the development of, or predisposition to, various disease states. These transgenic animals can be useful in characterizing the effect of such a defect on the organism as a whole, and developing pharmacological treatments for these defects.

The relevant techniques whereby foreign DNA sequences can be introduced into the mammalian germ line have been developed in mice. See *Manipulating the Mouse Embryo* (Hogan *et al.*, eds., 2d ed., Cold Spring Harbor Press, 1994) (ISBN 0-87969-384-3). At present, one route of introducing foreign DNA into a germ line entails the direct microinjection of a few hundred linear DNA molecules into a pronucleus of a fertilized one-cell egg. Microinjected eggs may then subsequently be transferred into the oviducts of pseudo-pregnant foster mothers and allowed to develop. It has been reported by Brinster *et al.* (1985), that about 25% of the mice that develop inherit one or more copies of the micro-injected DNA.

In addition to transgenic mice, other transgenic animals have been made. For example, transgenic domestic livestock have also been made, such as pigs, sheep, and cattle.

Once integrated into the germ line, the foreign DNA may be expressed in the tissue of choice at high levels to produce a functional protein. The resulting animal exhibits the desired phenotypic property resulting from the production of the functional protein.

In light of the various biological functions of nitric oxide, there exists a need in the art to develop transgenic animals, e.g., transgenic mice, wherein the endothelial nitric oxide synthase gene has been modified. There also exists a need in the art to develop methods to test compounds for activity against various pathological states associated with the absence of eNOS, such as hypertension, atherosclerosis, and stroke, using these transgenic animals. A further need in the art is to develop treatments for various pathological states using nitric oxide or nitric oxide prodrugs.

### *Summary of the Invention*

This invention satisfies these needs in the art by providing a transgenic non-human animal comprising a disrupted endothelial nitric oxide synthase gene. In embodiments of this invention, the transgenic non-human animal exhibits hypertension or wound-healing abnormalities. In a specific embodiment of the invention, the transgenic non-human animal is a mouse. Moreover, in specific embodiments of this invention, the endothelial nitric oxide synthase gene is disrupted at exons encoding the NADPH ribose and adenine binding sites.

In other embodiments, this invention provides a method of testing compounds for activity against a vascular endothelial disorder by providing a transgenic non-human animal having a disrupted endothelial nitric oxide synthase gene, wherein the animal exhibits either a vascular endothelial disorder or is at increased risk of developing the vascular endothelial disorder, administering a

-10-

compound to be tested to the transgenic animal, and determining the effect of the compound on the vascular endothelial disorder in the animal. In specific embodiments of this invention, the vascular endothelial disorder is hypertension or atherosclerosis.

5 This invention also provides a method for treating vascular endothelial disorders comprising: selectively increasing the expression of eNOS in blood vessels without increasing the expression of iNOS or nNOS. In specific embodiments, gene therapy approaches are used.

10 In a further embodiment, this invention provides a method of testing compounds for wound-healing activity by providing a transgenic non-human animal having a disrupted endothelial nitric oxide synthase gene, administering a compound to be tested to the transgenic animal, and determining the effect of the compound on the wound-healing capabilities of the animal.

15 In another embodiment, this invention provides a method of treating wounds by applying nitric oxide or a prodrug thereof. In a specific embodiment thereof, compounds which release nitric oxide into wounds to improve or speed up wound healing.

20 In an additional embodiment, this invention provides a method of making a transgenic non-human animal of the invention comprising providing an embryonic stem cell comprising an intact eNOS gene; providing a targeting vector capable of disrupting said eNOS gene upon homologous recombination; introducing said targeting vector into said cells under conditions where the intact eNOS gene of said cell and said targeting vector undergo homologous recombination to produce a disrupted eNOS gene; introducing said cells into a  
25 blastocyst; implanting the blastocyst into the uterus of a pseudopregnant female; and delivering transgenic animals of the invention from said pseudopregnant female. In order to obtain homozygous mutant mice of the invention, the resulting animals can be bred, and homozygous mutant mice selected.

30 In another embodiment, this invention provides a method of testing compounds for utility in the treatment of cerebral ischemia or stroke by providing

-11-

a transgenic non-human animal having a disrupted endothelial nitric oxide synthase gene, administering a compound to be tested to the transgenic animal, determining the effect of the compound on infarct size or regional cerebral blood flow (rCBF) following induction of focal cerebral ischemia in the brain of said animal, and correlating the effect of said compound on infarct size or rCBF with a utility for the treatment of cerebral ischemia or stroke. In a preferred embodiment, the eNOS mutant animal has been rendered normotensive.

In a further embodiment, the invention also provides a method for testing compounds for utility in the treatment of atherosclerosis by providing a transgenic non-human animal having a disrupted endothelial nitric oxide synthase gene, administering a compound to be tested for atherosclerosis activity to the transgenic animal, determining the effect of the compound on atherosclerosis, and correlating the effect of said compound on atherosclerosis with a utility for the treatment of atherosclerosis. In specific embodiments, the effect of the compound on atherosclerosis is determined using the vessel or the cuff vessel injury model.

### ***Brief Description of the Figures***

Figure 1 depicts the targeted disruption of the endothelial NOS gene. This Figure shows restriction maps of the native mouse endothelial NOS gene, the targeting vector, and the disrupted eNOS gene. The targeted vector contains 5' and 3' flanking regions of homology and it is designed to replace the *HindIII-SaII* fragment of the eNOS gene containing exons encoding the NADPH ribose and adenine binding sites (amino acids 1010-1144). NEO refers to the neomycin antibiotic resistance gene. The location of the KS probe, used for Southern blot analysis, is also shown.

Figure 2 shows the results of a Southern blot analysis of genomic DNA isolated from mutant mouse tails, digested with *SpeI* and hybridized to the KS probe, shown in Figure 1. Lanes 1, 2, and 3 show wild-type, heterozygous, and homozygous eNOS mutant mice, respectively. The positions of fragments

-12-

hybridizing to the wild-type and the disrupted eNOS gene, as depicted in Figure 1, are indicated.

Figure 3 depicts a Western blot analysis of eNOS mutant mice. Brain, heart, lung and aorta samples of wild-type (wt) and mutant (m) mice were tested for immunological reactivity against a mouse monoclonal antibody directed against eNOS. The position of eNOS is shown.

Figure 4 depicts the endothelium-dependent relaxation of aortic rings in response to acetylcholine. Panel a shows the effect on wild-type aortic segments. Panel b depicts treatment of wild-type vessel rings with L-nitroarginine (L-NA), a NOS inhibitor. Panel c depicts the endothelium-dependent relaxation of eNOS mutant aortic segments.

Figure 5 depicts blood pressure responses to L-NA. Urethane-anesthetized wild-type (solid line) and eNOS mutant mice (dotted line) were measured before and after L-NA administration at time 0.

Figure 6 depicts wound healing in eNOS mutant mice. Figure 6A is a micrograph of a 24 hr. wound in a wild-type mouse. Figure 6B is a micrograph of a 5 day wound in a wild-type mouse. Figure 6C is a 24 hr. wound of an eNOS mutant mouse. Figure 6D is a 5 day wound of an eNOS mutant mouse. (ep) refers to the epidermis, while (d) refers to the dermis. Capillaries are indicated by (cap).

Figure 7 depicts infarct size in wild-type and eNOS mutant mice. In Figure 7A infarct volumes were measured in SV-129 mice (A), C57 Black/6 mice (B), eNOS mutant mice without hydralazine treatment (C), and eNOS mutant mice following hydralazine treatment (D). Infarct size was detected 24 hrs after permanent filament MCA occlusion by TTC staining. A statistically significant increase ( $p < 0.05$ ) in infarct size was noted for eNOS mutant animals. Each dot represents the value from an individual animal, and data are expressed as mean  $\pm$  SD.

Figure 7B depicts infarct areas in five coronal sections from rostral to caudal (2 to 10 mm) of the above groups. Open circles, filled circles, and

triangles represent wild-type SV-129 mice, wild-type C57 Black 6 mice, and eNOS mutant mice, respectively. Data shown are means  $\pm$  SD. \* indicates  $p < 0.05$  as compared to both wild-type SV-129 and wild-type C57 Black/6 mice. # indicates  $p < 0.05$  as compared to SV-129 mice alone.

Figure 8 depicts regional cerebral blood flow (rCBF) as measured by laser Doppler flowmetry after MCA occlusion in the periinfarct area of eNOS mutant mice (dotted line,  $n=11$ ) as compared to wild-type SV-129 animals (continuous line,  $n=10$ ,  $p < 0.05$ ). A greater rCBF reduction was noted in eNOS mutant mice as compared to wild-type mice. A flexible optic probe tip (diameter = 0.5 mm) was secured 2 mm posterior and 3 mm lateral to bregma on the ipsilateral hemisphere. Steady-state rCBF values prior to occlusion were taken as a baseline (100%) and the subsequent changes after the onset of ischemia were shown as a percentage relative to baseline. Time zero represents the point of MCA occlusion. There were no significant differences in rCBF blood flow between SV-129 and C57 Black/6 wild-type mice.

Figure 9 depicts the effect of hemorrhagic hypotension on rCBF in urethane-anesthetized (dotted line) and wild-type animals (continuous line). Hypotension was induced by gradually withdrawing arterial blood as described *infra*, and rCBF was measured by laser Doppler flowmetry. The initial rCBF values were taken as 100% and the corresponding changes thereafter calculated as percentage relative to the initial value. The baseline MABP in wild-type and mutants were  $104 \pm 12$  ( $n=7$ ) and  $117 \pm 13$  mm Hg ( $n=7$ ), respectively. There was a greater tendency toward hypoperfusion at higher levels of MABP in the mutant animals. Data are expressed as mean  $\pm$  SD. \* signifies  $p < 0.05$  as compared to wild-type animals.

Figure 10 shows that the diameter of pial arterioles was increased in eNOS mutant mice (circle,  $n=7$ ), but not in wild-type (square,  $n=8$ ) mice after nitro-L-arginine superfusion in a closed cranial window. Nitro-L-arginine (1 mM) was topically superfused for 40 minutes. Superfusion of nitro-D-arginine (1 mM,  $n=3$ ) did not affect the diameter of pial arterioles in eNOS mutant mice

(data not shown). The data are calculated as percent from baseline and expressed as mean  $\pm$  SD. \* indicates  $p < 0.05$  and \*\* indicates  $p < 0.01$  vs. wild-type.

Figure 11 depicts the autoradiographic distribution of [ $^3\text{H}$ ]L-NA binding in sagittal brain sections of wild-type and mutant mice. Figure 11A is the distribution in SV-129 wild-type mice. Figure 11B is the distribution in C57 Black/6 wild-type mice. Figure 11C is the distribution in eNOS mutant mice. Figure 11D is the distribution in nNOS mutant mice. In Figures 11A-D, OB: olfactory bulb; Str: striatum; HP: hippocampus; DG: dentate gyrus; AM: amygdala; CB: cerebellum. Scale bar=300  $\mu\text{m}$ .

Figure 12 depicts the autoradiographic distribution of [ $^3\text{H}$ ]L-NA binding in coronal sections of SV-129 wild-type mouse brain. Figures 12A -G show total binding. Figure 12H shows binding remaining in the presence of 10  $\mu\text{M}$  L-NA. In Figure 12, OB: olfactory bulb; TT: tenia tecta; Str: striatum; RF: rhinal fissure; HP: hippocampus; DG: dentate gyrus; MAN: medial amygdaloid nuclei; CAN: anterior cortical amygdaloid nuclei; VMH: ventromedial hypothalamic nuclei; PC: posteromedial cortical amygdaloid nuclei; PT: piriform transition; LM: lateral mammillary nucleus; SG: superficial grey layer superior colliculus; CB: cerebellum; PR: pontine reticular nucleus. Scale bar=300  $\mu\text{m}$ .

Figure 13 depicts the correlation between [ $^3\text{H}$ ]L-NA binding in mouse and rat brain. 1: granular layer of olfactory bulb, 2: amygdaloid nuclei-posteromedial cortical, 3: amygdaloid piriform transition, 4: amygdaloid nuclei-medial, 5: taenia tecta, 6: rhinal fissure, 7: lateral mammillary nucleus, 8: hippocampal CA3 subfield, 9: amygdaloid nuclei-basomedial, 10: superficial grey layer of superior colliculus, 11: molecular layer of cerebellum, 12: amygdaloid nuclei-anterior cortical, 13: dentate gyrus, 14: amygdaloid nuclei-central, 15: I and II layers of occipital cortex, 16: hippocampal CA1, 17: dorsal tegmental nucleus, 18: plexiform layer of olfactory bulb, 19: I and II layers of frontal cortex, 20: ventromedial hypothalamic nuclei, 21: granule layer of cerebellum, 22: dorsomedial hypothalamic nuclei, 23: medial mammillary nucleus, 24: III to VI layers of occipital cortex, 25: III to VI layers of frontal cortex, 26: striatum, 27:

pontine reticular nucleus, 28: posterior thalamus nuclei, 29: ventral posteromedial thalamus nuclei. Values in mouse and rat brain represent the mean of five SV-129 mice and three rats, respectively.

Figure 14 depicts [ $^3\text{H}$ ]L-NA binding in sagittal sections of SV-129 mouse brain. Figure 14A shows total binding. Figures 14B and 14C, respectively, show binding in the presence of 10  $\mu\text{M}$  D-NA, and 100  $\mu\text{M}$  7-NI, a potent and selective type 1 inhibitor. Figure 14D shows the binding in the presence of excess L-NA (10  $\mu\text{M}$ ). Scale bar=300  $\mu\text{m}$ .

Figure 15 is a schematic showing the effects of nitric oxide produced from various NOS isoforms in normal and atherosclerotic arteries. In Figure 15A, nitric oxide produced by normal endothelium prevents proliferative response to injury and suppresses development of atherosclerosis. In Figure 15B, nitric oxide production in atherosclerotic plaques may lead to peroxynitrite formation, lipid oxidation, and endothelial cell inactivation.

Figure 16 is a schematic showing the cuff model of vessel injury.

Figure 17 depicts micrographs of hematoxylin and eosin stained sections of cuff injured vessels. Injured vessels contain neointima seen inside of the internal elastic lamina (shown with arrows). Control vessels do not contain the neointima. Vessels from eNOS mutant mice show significantly increased neointimal formation, which is shown with an asterisk.

Figure 18 depicts histology and immunochemical staining of injured and control vessels from eNOS mutant mice. Control vessels have no intima.

Figure 19 depicts quantitative RT-PCR of eNOS mRNA from mouse aorta.

Figure 20 depicts atherosclerotic lesions from apoE mutant mice at 6 months. Figure 20A shows the aortic arch and carotid arteries; Figure 20B shows the thoracic aorta; Figure 20C shows the descending thoracic aorta; and Figure 20D shows oil red O stain of an aortic lesion.

### ***Detailed Description of Preferred Embodiments***

In the description that follows, a variety of various technical terms are used. Unless the context indicates otherwise, these terms shall have their ordinary well-recognized meaning in the art. In order to provide a clearer and more consistent understanding of the specification and claims, the following definitions are provided.

**Transgenic.** As used herein, a "transgenic organism" is an organism containing a defined change to its germ line, wherein the change is not ordinarily found in wild-type organisms. This change can be passed on to the organism's progeny. The change to the organism's germ line can be an insertion, a substitution, or a deletion. Thus, the term "transgenic" encompasses organisms where a gene has been eliminated or disrupted so as to result in the elimination of a phenotype associated with the disrupted gene ("knock-out animals"). The term "transgenic" also encompasses organisms containing modifications to their existing genes and organisms modified to contain exogenous genes introduced into their germ line.

**Nitric oxide synthase (NOS).** As used herein, nitric oxide synthase is an enzyme able to catalyze the formation of nitric oxide. For example, NOS can catalyze the formation of nitric oxide from the terminal guanidino nitrogen of arginine, with the stoichiometric production of citrulline.

**Disrupted gene.** As used herein, "disrupted gene" refers to a gene containing an insertion, substitution, or deletion resulting in the loss of substantially all of the biological activity associated with the gene. For example, a disrupted NOS gene would be unable to express a protein having substantial NOS enzymatic activity.

**Vector.** As used herein, a "vector" is a plasmid, phage, or other DNA sequence, which provides an appropriate nucleic acid environment for a transfer of a gene of interest into a host cell. The cloning vectors of this invention will ordinarily replicate autonomously in eukaryotic hosts. The cloning vector may

be further characterized in terms of endonuclease restriction sites where the vector may be cut in a determinable fashion. The vector may also comprise a marker suitable for use in identifying cells transformed with the cloning vector. For example, markers can be antibiotic resistance genes.

5           **Expression vector.** As used herein, an "expression vector" is a vector comprising a structural gene operably linked to an expression control sequence so that the structural gene can be expressed when the expression vector is transformed into an appropriate host cell.

10           **Targeting vector.** As used herein "a targeting vector" is a vector comprising sequences that can be inserted into a gene to be disrupted, e.g., by homologous recombination. Therefore, a targeting vector may contain sequences homologous to the gene to be disrupted.

This invention relates to non-human transgenic animals comprising a disrupted endothelial NOS gene.

15           In order to obtain a transgenic animal comprising a disrupted eNOS gene, a targeting vector is used. The targeting vector will generally have a 5' flanking region and a 3' flanking region homologous to segments of the eNOS gene surrounding an unrelated DNA sequence to be inserted into the eNOS gene. For example, the unrelated DNA sequence can encode a selectable marker, such as  
20           an antibiotic resistance gene. Specific examples of a suitable selectable marker include the neomycin resistance gene (NEO) and the hygromycin  $\beta$ -phosphotransferase. The 5' flanking region and the 3' flanking region are homologous to regions within the eNOS gene surrounding the portion of the gene to be replaced with the unrelated DNA sequence. DNA comprising the targeting  
25           vector and the native eNOS gene are brought together under conditions where homologous recombination is favored. For example, the targeting vector and native eNOS gene sequence can be used to transform embryonic stem (ES) cells, where they can subsequently undergo homologous recombination. For example,  
30           J1 embryonic stem cells obtained from Dr. En Li of the Cardiovascular Research Center of the Massachusetts General Hospital and Dr. Rudolph Jaenisch of the

-18-

Whitehead Institute of MIT. The targeting vector, pPNT-ENOS, has been deposited with the American Type Culture Collection (A.T.C.C.), 12301 Parklawn Drive, Rockville, Maryland 20852 USA, under the terms of the Budapest Treaty under accession number A.T.C.C. 97469 on March 13, 1996.

5 Proper homologous recombination can be tested by Southern blot analysis of restriction endonuclease digested DNA using a probe to a non-disrupted region of the eNOS gene. For example, the KS probe, identified in Figure 1, can be used. Since the native eNOS gene will exhibit a different restriction pattern from the disrupted eNOS gene, the presence of a disrupted eNOS gene can be  
10 determined from the size of the restriction fragments that hybridize to the probe.

In one method of producing the transgenic animals, transformed ES cells containing a disrupted eNOS gene having undergone homologous recombination, are introduced into a normal blastocyst. The blastocyst is then transferred into the uterus of a pseudo-pregnant foster mother. Pseudo-pregnant foster mothers had  
15 been mated with vasectomized males, so that they are in the proper stage of their estrus cycle and their uterus is hormonally primed to accept an embryo. The foster mother delivers a transgenic animal containing a disrupted eNOS gene. Homozygous mutant animals are normally obtained by breeding the transgenic animals.

20 The extent of the contribution of the ES cells, containing the disrupted eNOS gene, to the somatic tissues of the transgenic mouse can be determined visually by choosing strains of mice for the source of the ES cells and blastocyst that have different coat colors.

The resulting homozygous eNOS mutant animals generated by  
25 homologous recombination are viable, fertile, and indistinguishable from wild-type and heterozygous littermates in overall appearance (except for the presence of a selectable marker) or routine behavior. However, the mutant animals can also be sterilized using methods well known in the art, e.g. vasectomy or tubal ligation. See *Manipulating the Mouse Embryo, supra*. The mutant animals can  
30 be mated to obtain homozygous or heterozygous progeny. These mutant animals

contain substantially less immunoreactive eNOS than wild-type animals. Most preferably, these mutant mice contain no immunoreactive eNOS protein as measured by western blot analysis of brain, heart, lung, or aorta tissue.

5 A targeting vector such as pPNT-ENOS can be used to create cell lines or primary cell cultures that do not express NOS. The endogenous eNOS gene can be disrupted by introducing the targeting vector into cells containing the eNOS gene to be disrupted and allowing the targeting vector and the endogenous gene to undergo homologous recombination. For example, the targeting vector can be introduced into the cells by electroporation. If both copies of the eNOS  
10 gene are to be disrupted, higher concentrations of the selection agent, e.g., neomycin or its analog G418 are used. Suitable cell lines and cultures include tumor cells, endothelial cells, epithelial cells, leukocytes, neural cells, glial cells, and muscle cells.

15 The eNOS mutant animals of the invention can be any non-human mammal. In embodiments of this invention, the animal are mice, rats, guinea pigs, rabbits, or dogs. In an especially preferred embodiment of the invention, the eNOS mutant animal is a mouse.

20 These homozygous eNOS mutant animals also exhibit significantly reduced calcium-dependent membrane-associated NOS enzymatic activity. In preferred embodiments of this invention the enzymatic activity in aorta samples is less than  $1.0 \text{ pmol mg}^{-1} \text{ min}^{-1}$   $^3\text{H}$ -arginine to citrulline conversion. In most preferred embodiments of this invention the enzymatic activity in aorta samples is less than  $0.5 \text{ pmol mg}^{-1} \text{ min}^{-1}$   $^3\text{H}$ -arginine to citrulline conversion. Any residual NOS activity may be due to the presence of neuronal NOS (nNOS) in neurons in  
25 the perivascular plexus, and not to the expression of any residual nondisrupted eNOS genes.

30 Endothelium-derived relaxing factor is absent or significantly reduced in eNOS mutant animals. However, vascular smooth-muscle responses are intact. For example, the aortic rings of mutant mice show no relaxation to acetylcholine, while aortic rings from wild-type mice manifest a dose-dependent relaxation to

acetylcholine. See Figure 4. Moreover, treatment of wild-type aortic rings with  $10^{-4}$ M L-nitroarginine has no effect on vascular tone by itself, but blocks the relaxation in response to acetylcholine. *Id.* Treatment of the eNOS mutant aortic rings with  $10^{-4}$ M L-nitroarginine also has little or no effect on vessel tone either by itself or on the response to acetylcholine. The maximum dilation of norepinephrine pre-contracted rings from eNOS mutant mice to sodium nitroprusside is similar to wild-type mice. This indicates that vascular smooth-muscle responses in eNOS mutant animals are intact.

The eNOS mutant animals of the invention exhibit various vascular endothelial disorders. These disorders include hypertension and an increased propensity for cerebral ischemia, stroke or atherosclerosis. In addition, the eNOS mutant animals exhibit abnormal wound healing properties. Other vascular endothelial disorders include clotting disorders, other cerebrovascular disorders, coronary artery disease, and peripheral vascular disease. The eNOS mutant animals of the invention exhibit these disorders or an increased propensity of developing these disorders.

Consequently, the eNOS mutant animals are useful as a model to study these and other vascular endothelial disorders. For example, various compounds could be tested for a therapeutic effect on a vascular endothelial disorder by providing a transgenic non-human animal having a disrupted eNOS gene and exhibiting a vascular endothelial disorder; determining the effect of a compound on symptoms of the vascular endothelial disorder; and correlating the effect of the compound on the treatment of the vascular endothelial disorder.

The compounds to be tested are typically not NOS inhibitors. Determining whether a compound exhibits NOS inhibitor activity can be tested based on the information provided herein and in the technical literature. Hevel *et al.* (1994). In preferred embodiments of the invention, compounds that induce NO production are tested; and in more preferred embodiments, compounds that induce NO production in the endothelium are tested. The compounds to be tested can be derived from a variety of sources including, but not limited to, rationally

designed and synthetic molecules, plant extracts, animal extracts, inorganic compounds, mixtures, solutions, and homogeneous molecular or elemental samples.

5 The eNOS mutant animals exhibit a significantly higher blood pressure than the wild-type animals. In specific embodiments of this invention eNOS mutant mice exhibit a mean blood pressure significantly higher than 81 mm Hg. In a preferred embodiment of this invention, eNOS mutant mice exhibit a mean blood pressure greater than about 100 mm Hg. In a most preferred embodiment of this invention, eNOS mutant mice exhibit a mean blood pressure of about 110  
10 mm Hg. Analogous increases in mean blood pressure are expected in other non-murine eNOS mutant (knock-out) animals.

L-NA and other NOS inhibitors cause a rise in blood pressure in many species including humans, rats, guinea pigs, rabbits, dogs, and mice. This effect is consistent with a role of basal nitric oxide production in vasodilation, because  
15 inhibition of eNOS would lead to less basal vasodilation and result in hypertension. However, eNOS mutant mice show a decrease in blood pressure in response to L-NA. See Figure 5. This hypotensive effect is blocked by L-arginine and is not observed with D-nitroarginine. This suggests that pharmacological blockers may have effects in addition to NOS inhibitors, or that  
20 non-endothelial NOS isoforms are involved in the maintenance of blood pressure. For example, nNOS is present both in vasomotor centers of the central nervous system and in perivascular nerves. However, effects of its blockade suggest that it plays a vasodilatory role. Mutant neuronal NOS mice have blood pressures similar to wild-type mice, but they have a tendency towards hypotension when  
25 exposed to anaesthesia, which is consistent with a possible role for nNOS in maintaining, not reducing, blood pressure. Multiple roles for endothelial and non-endothelial NOS isoforms in vasodilation and vasoconstriction may explain the observed variability in maximal pressor effects of various NOS inhibitors.

30 There is evidence that in hypertension the amount of NO produced by the endothelium decreases in humans. The eNOS knockout mice mimic this effect,

since their endothelium also does not produce any NO. Consequently, these mice serve as a useful model for hypertension. Thus, establishing an anti-hypertensive effect in eNOS mutant animals of the invention for a compound other than an NOS inhibitor, such as a compound that induces the production of NO, would be predictive that this compound would have anti-hypertensive properties in other animals, including humans. However, the opposite result would be expected for a compound that inhibits NOS.

An inhibitor of NOS would be expected to raise blood pressure in wild-type animals, but stabilize or reduce blood pressure in eNOS mutant animals. In eNOS mutant animals, an NOS inhibitor would inhibit the residual NOS, mostly nNOS. nNOS mutant animals may have a tendency toward hypotension. Thus, the preferential inhibition of nNOS in the mutant animals should result in the same or lower blood pressure. However, in normal animals, the role of eNOS on blood pressure regulation is much more pronounced than the role of nNOS. Therefore, the predominant effect of an NOS inhibitor in normal animals would be to inhibit eNOS, which raises blood pressure. This is demonstrated in Example 5, *infra*.

In addition, there is also evidence that in atherosclerosis, diabetes and normal aging, the amount of NO produced by the endothelium decreases in humans. Thus, these mice would serve as a useful model not just for hypertension, but also for vascular responses in atherosclerosis, diabetes and normal aging.

The eNOS mutant animals of this invention are useful as an animal model to study hypertension. For example, various compounds could be tested for an anti-hypertensive effect in the eNOS mutant animals. Specifically, compounds that are not NOS inhibitors can be tested. In more preferred embodiments, compounds that are not eNOS inhibitors are tested. In other preferred embodiments compounds that induce NO production are tested. In additional preferred embodiments, compounds that induce NO production in the endothelium are tested. Therefore, the invention provides methods for screening

-23-

compounds using the eNOS mutant animals as an animal model to identify compounds useful in treating hypertension. This aspect of the invention is useful to screen compounds from a variety of sources. Examples of compounds that can be screened using the method of the invention include but are not limited to

5 rationally designed and synthetic molecules, plant extracts, animal extracts, inorganic compounds, mixtures, and solutions, as well as homogeneous molecular or elemental samples.

The invention, therefore, provides a method of screening compounds, comprising: providing a transgenic non-human animal having a disrupted eNOS

10 gene and exhibiting hypertension, administering a compound to be tested to the transgenic animal; determining the effect of the compound on the blood pressure of said animal; and correlating the effect of the compound on the blood pressure of the animal with an anti-hypertensive effect of said compound.

The compounds to be tested can be administered to the transgenic non-human animal having a disrupted eNOS gene in a variety of ways well known to one of ordinary skill in the art. For example, the compound can be administered

15 by parenteral injection, such as subcutaneous, intramuscular, or intra-abdominal injection, infusion, ingestion, suppository administration, and skin-patch application. Moreover, the compound can be provided in a pharmaceutically acceptable carrier. *See* Remington's Pharmaceutical Sciences (1990). The effect

20 of the compound on blood pressure can be determined using methods well known to one of ordinary skill in the art.

In addition, the eNOS mutant animals of this invention unexpectedly exhibit abnormal wound-healing properties. For example, these animals often

25 develop spontaneous wounds that do not heal. In contrast to normal mice, who healed their wounds within 5 days, the eNOS mutant mice exhibit significantly different wound healing properties. First, the eNOS mutant mice exhibit spontaneous wounds that never heal. Second, in experiments where wounds were created, the eNOS mutant mice heal more slowly than normal animals. Healing

30 of eNOS mutant mice typically takes 2-3 times as long as normal mice. The

-24-

exact healing time will depend on the type of wound inflicted. Moreover, two specific features of normal wound healing are abnormal in the eNOS mutant mice:

- 1) growth of the epithelial layer of skin across the wound to bridge the gap and close the wound; and
- 2) neovascularization in the granulation tissue that fills the wound.

In the eNOS mutant mice, migration of epithelial cells to the site of the wound is delayed, with epithelial cells remaining at the edge of the wound after five days. The connective tissue is also markedly abnormal, containing few or no new blood vessels. The results demonstrate an important role for eNOS in angiogenesis and epithelial cell migration during wound healing.

The eNOS mutant animals of this invention are useful as an animal model to study wound healing. For example, various compounds could be tested for a wound healing effect in the eNOS mutant animals. Therefore, the invention provides methods for screening compounds using the eNOS mutant animals as an animal model to identify compounds useful in enhancing wound healing. This aspect of the invention is useful to screen compounds from a variety of sources. Examples of compounds that can be screened using the method of the invention include but are not limited to rationally designed and synthetic molecules, plant extracts, animal extracts, inorganic compounds, mixtures, and solutions, as well as homogeneous molecular or elemental samples. For example, various compounds designed to improve wound healing can be tested. For example, compounds that deliver NO to the healing wound can be used. Establishing an enhancement of wound healing by a compound in eNOS mutant animals is predictive that this compound would enhance wound healing in other animals, including humans.

The invention, therefore, provides a method of screening compounds, comprising: providing a transgenic non-human animal having a disrupted eNOS gene and exhibiting abnormal wound healing properties, administering a

compound to be tested to the transgenic animal; determining the effect of the compound on the wound healing properties of said animal; and correlating the effect of the compound on the wound healing properties of the animal with a wound healing effect of said compound.

5           Thus, the eNOS mutant animals of this invention are also useful as animal models to study wound healing.

          Moreover, since the synthesis of nitric oxide appears to enhance wound healing, prodrugs that release nitric oxide *in situ* may improve or speed up healing. Examples of suitable compounds that release nitric oxide include  
10           nitroglycerin, sodium nitroprusside, and SIN-1. The extent to which these and other similar compounds improve or speed up wound healing can be determined experimentally. For example, the compound could be applied at the wound to a patient in need of treatment and its effect on wound healing can be quantified.

          The eNOS mutant animals of this invention are also useful as an animal  
15           model to study cerebral ischemia resulting from stroke. Since endothelial NO production may protect brain tissue by increasing ischemic rCBF, compounds can be tested for the ability to increase rCBF as well as the ability to reduce ischemic infarct size. rCBF and infarct size can be measured as described in the Examples. Compounds that increase rCBF or decrease infarct size would be expected to be  
20           useful as therapeutics for the treatment of stroke or cerebral ischemia from other sources.

          It has been reported that nNOS enzymatic activity may contribute to the development of ischemic brain necrosis. In eNOS mutant animals, any non-specific NOS inhibitor would predominantly inhibit the nNOS isoform.  
25           However, in wild-type animals, both eNOS and nNOS would be inhibited. Since eNOS and nNOS have opposite effects under ischemic conditions, with eNOS activity being protective and nNOS activity being detrimental, compounds that are non-specific NOS inhibitors should not be tested for anti-stroke activity. Therefore, in preferred embodiments compounds that are not NOS inhibitors are  
30           tested. In more preferred embodiments, compounds that induce NO production

can be tested for use as a treatment for stroke or cerebral ischemia. In particularly preferred embodiments, compounds that induce production of NO in the endothelium are tested.

Compounds that can be screened for use in treating stroke or cerebral ischemia can be obtained from a variety of sources. Examples of compounds that can be screened using the method of the invention include but are not limited to rationally designed and synthetic molecules, plant extracts, animal extracts, inorganic compounds, mixtures, and solutions, as well as homogeneous molecular or elemental samples.

The compounds to be tested can be administered to the transgenic non-human animal having a disrupted eNOS gene in a variety of ways well known to one of ordinary skill in the art. For example, the compound can be administered by parenteral injection, such as subcutaneous, intramuscular, or intra-abdominal injection, infusion, ingestion, suppository administration, and skin-patch application. Moreover, the compound can be provided in a pharmaceutically acceptable carrier. *See* Remington's Pharmaceutical Sciences (1990).

The eNOS animals are additionally useful as an animal model to study atherosclerosis. The physiological production of nitric oxide by eNOS suppresses atherosclerosis, whereas the pathologic production of nitric oxide by iNOS and nNOS contributes to atherosclerosis. To test the effect of various compounds on atherosclerosis, various animal models involving eNOS mutant mice are used. Two vessel injury models, the cuff model and the filament model, provide useful data relevant to atherosclerosis. In the cuff model the neointima formation is stimulated by adventitial injury. In the filament model, the endothelium is physically removed, and the rate at which endothelial cells resurface the injured areas is measured. Alternatively, double mutant animals exhibiting aspects of atherosclerosis can be used. For example, double mutant apoE, eNOS mice can be used. Other potential double mutant animals for use in this aspect of the invention include apoE Leiden/eNOS and LDL-receptor eNOS mutants.

By way of example, compounds can be provided to eNOS mutant mice, and the effect of the compound on neointima formation following vessel injury using the cuff model can be determined. The extent of neointima formation can be determined as described in the Examples. Compounds that reduce the extent of neointima formation relative to control eNOS mutant mice not receiving the compound would be expected to be useful as therapeutics for the treatment of atherosclerosis.

In another example, compounds can be provided to eNOS mutant mice and the effect of the compound on the rate at which endothelial cells resurface injured areas of vessels following vessel injury using the filament model can be determined. Compounds that increase the rate of endothelial cell resurfacing relative to control eNOS mutant mice not receiving the compound would be expected to be useful as therapeutics for the treatment of atherosclerosis.

In a further example, compounds can be provided to double mutant animals, which exhibit features of human atherosclerosis. Compounds that reduce symptoms of atherosclerosis in these animals would also be expected to be useful as therapeutics for the treatment of atherosclerosis. A preferred example of a double mutant animal is an apoE/eNOS double mutant.

Since nNOS and iNOS may contribute to atherosclerosis, compounds that are non-specific NOS inhibitors should not be tested for activity against atherosclerosis. Compounds to be tested can be obtained from various sources and administered in various ways as described for other endothelial vascular disorders, *supra*.

Another example of a double mutant animal is eNOS/nNOS mutant mice. These double mutant animals can be obtained by mating eNOS mutant mice to nNOS mutant mice of the same genetic background. Double heterozygous eNOS/nNOS mutant mice are obtained, mating pairs of the double heterozygous mice are obtained, and eNOS/nNOS mutant mice are obtained.

## ***Examples***

### ***Example 1***

#### ***Targeted Disruption of the Endothelial NOS Gene***

The endothelial NOS gene was cloned by screening a mouse genomic library, obtained from Stratagene, using a human eNOS cDNA clone, obtained from Kenneth D. Bloch, as described in Janssens *et al.* (1992), Genbank accession number M93718. Plasmid hNOS3C, containing the endothelial nitric oxide synthase gene, was deposited at the American Type Culture Collection on July 17, 1996. The targeting vector was derived from the pPNT vector, which contains thymidine kinase gene and the neomycin resistance gene. See Figure 1. Tybulewicz *et al.* (1991). The targeting vector contains 5' and 3' flanking regions of homology to the eNOS gene, and is designed to replace the *HindIII-SalI* fragment that contains exons encoding the NADPH ribose and adenine binding sites of the eNOS protein (amino acids 1010-1144) following homologous recombination.

J1 ES cells were grown as described in Li *et al.* (1992) on irradiated embryonic fibroblast feeder cells in media containing 200 units/ml leukocyte inhibitory factor. For electroporation,  $10^7$  cells were mixed with targeting vector DNA at 150  $\mu\text{g/ml}$ . A Bio-Rad gene pulsar was used to electroporate the DNA into the cells at a setting of 960  $\mu\text{F}$  capacitance, 250 mV. The targeting vector and the native eNOS gene were then able to undergo homologous recombination. The cells were plated on neomycin-resistant irradiated fibroblast feeder cells, and selection with 150  $\mu\text{g/ml}$  G418 and 2  $\mu\text{M}$  FIAU was started 48 hours later. Doubly resistant colonies were picked seven days after electroporation and grown in 24-well plates.

## Example 2

### *Generation of Chimeric Mice with Germline Transmission*

Blastocysts were isolated from C57 BL/6 mice on day 3.5 of pregnancy and 20-25 ES cells, following homologous recombination and selection, were  
5 injected into the uterine horn of pseudo-pregnant (C57 BL/6 x DBA/2) F1 mice. Chimeric mice were identified by the agouti contribution of the ES cells to the coat color, and were back-crossed to C57 BL/6 mice. Germline transmission was determined by the presence of agouti mice in the offspring.

Proper recombination was demonstrated by Southern blot analysis of *SpeI*  
10 digested genomic DNA using the KS probe shown in Figure 1. Back-crossed mice were screened by Southern blot, and heterologous mice were selected. In Figure 1, lanes 1, 2 and 3 show wild-type, heterozygous, and homozygous mutant mice, respectively. The positions of the hybridizing fragments for the wild-type and the disrupted eNOS gene are shown. The results demonstrate that the  
15 targeted disruption of the eNOS gene is present in the germline of the transgenic mice.

Western blot analysis of tissue samples from eNOS mutant mice was also performed. 10  $\mu$ g protein extracts from the brain, heart, lung, and aorta/vena cava of wild-type and eNOS mutant animals were electrophoresed through a 10%  
20 SDS-polyacrylamide gel and transferred to nitrocellulose. The blot was incubated with mouse monoclonal antibodies directed against endothelial NOS (Transduction Research Laboratories), and specific hybridization was localized using chemiluminescent alkaline phosphatase conjugated with anti-mouse antibody (ECL, Amersham). Hybridization of endothelial NOS is observed for  
25 the wild-type samples, but not in the eNOS mutant samples. The heart, lung, and aorta samples show a band at relative molecular mass of 50 kDa in both wild-type and eNOS mutant samples, which represents mouse immunoglobulin heavy chains present in the tissue samples. The antibody used was directed against a

-30-

peptide corresponding to amino acids 1030-1209, a region which overlaps with the region deleted in the eNOS mutant mice. See Figure 3. This demonstrates that the eNOS mutant mice (homozygous) produce no immunoreactive undisrupted eNOS, further demonstrating successful transmission of the disruption to the germline of the transgenic mice.

Aorta samples from eNOS mutant mice were tested for calcium-dependent membrane-associated NOS enzymatic activity. This enzymatic activity was reduced to about  $0.5 \text{ pmol mg}^{-1} \text{ min}^{-1}$ . The residual activity is likely due to neuronal NOS in neurons in the perivascular plexus.

### *Example 3*

#### *Determination of blood pressure of eNOS mutant and wild-type mice*

Mice were kept at normal temperature ( $37^{\circ}\text{C}$ ), anesthetized with urethane (1.5 mg/kg, intraperitoneal injection) or halothane inhalation, and ventilated using an SAR-830 mouse ventilator (CWE Instruments). Depth of anesthesia was adjusted to keep the blood pressure of animals unresponsive to tail-pinch with forceps. End-tidal  $\text{CO}_2$  was monitored with a microcapnometer and kept constant by adjustment of respiratory parameters. The right femoral artery was cannulated using stretched PE-10 polyethylene tubing (Clay Adams) for mean arterial blood pressure recordings using an ETH-400 transducer and a MacLab data acquisition system (ADI Instruments). For awake measurements, the femoral artery catheter was placed under halothane anesthesia and the wound was covered with 1% xylocane ointment to diminish discomfort. Recordings were made within one hour of the procedure. Data are expressed as means with standard deviation. Statistical evaluation was performed by t-test.

-31-

**Table 1.** Blood pressure of eNOS mutant and wild-type mice

	Wild-type mice			eNOS mutant mice		
	Urethane	Halothane	Awake	Urethane	Halothane	Awake
Mean BP (mmHG)	81	90	97	110*	109*	117*
s.d.	9	12	8	8	11	10
<i>n</i>	16	15	14	17	18	17

\*P<0.01 for eNOS mutant animals vs. wild-type mice.

There is no statistically significant difference between the blood pressure of nNOS mutant mice and wild-type mice using this procedure.

Similar results are obtained with different methods of anesthesia and in the awake state. Blood pressure is the same for the wild-type SV129 strain, wild-type C57 B16 strain, and litter mates of the eNOS mutant animals that are wild-type at the eNOS locus.

### *Example 4*

#### *Endothelium-dependent Relaxation of Aortic Rings in Response to Acetylcholine from eNOS Mutant and Wild-type Mice*

The thoracic aorta was dissected from wild-type and eNOS mutant mice and placed in physiological saline aerated with 95% O<sub>2</sub>/5% CO<sub>2</sub>. 4 mm segments of the aorta were mounted on tungsten wires in conventional myographs and maintained at optimal tension in physiological saline for 1 hour at 37°C. The rings were pre-contracted with 10<sup>-7</sup> M norepinephrine and exposed to increasing concentrations of acetylcholine (ACh) from 10<sup>-8</sup> M to 3 x 10<sup>-5</sup> M. 2-3 segments were collected from each mouse, and five mice were used from the wild-type and eNOS mutant groups. Mean data from each animal were used. Respective tracings are shown. Acetylcholine concentrations are expressed in logM.

Figure 4A depicts wild-type aortic segments responding to acetylcholine with dose-dependent relaxation. At  $3 \times 10^{-5}$  M,  $60.3 \pm 14.6\%$  of pre-addition tone was present. Figure 4B depicts treatment of the wild-type vessel rings with  $10^{-4}$  M L-NA for 1 hour and shows abolished acetylcholine-induced relaxation. Figure 4C shows that eNOS mutant aortic segments do not relax to acetylcholine, demonstrating that EDRF activity is absent from eNOS mutant mice. L-NA has no additional affect on eNOS vessel segments.

Thus, aortic rings from wild-type mice manifest a dose-dependent relaxation to acetylcholine, while aortic rings from eNOS mutant animals show no relaxation to acetylcholine. Treatment of wild-type aortic rings with  $10^{-4}$  M L-NA has no effect on vascular tone by itself, but blocks the relaxation in response to acetylcholine. Treatment of the eNOS mutant aortic rings with  $10^{-4}$  M L-NA has no effect on vessel tone, either by itself or in response to acetylcholine. The maximum dilation of norepinephrine pre-contracted rings from eNOS mutant mice to sodium nitroprusside is no different from wild-type mice, indicating that vascular smooth-muscle responses are intact.

### *Example 5*

#### *Blood Pressure Responses to L-NA for Wild-type and eNOS Mutant Mice*

Mean arterial blood pressure (MABP) of urethane-anesthetized wild-type (solid line in Figure 5) and eNOS mutant mice (dotted line in Figure 5) were measured by femoral artery catheterization and recorded for 30 minutes of baseline before L-NA administration (arrows in Figure 5). At time 0, 12 mg/kg of L-NA was given intraperitoneally. Monitoring for 1 hour shows that the blood pressure of wild-type mice rose from a baseline of 78 mm Hg to 109 mm Hg ( $n = 11$ ). The blood pressure of eNOS mutant mice dropped from a baseline of 98 mm Hg to 66 mm Hg ( $n = 5$ ). Each mouse in the wild-type group responded to L-NA with a rise in blood pressure, and each mouse in the eNOS mutant group

responded with a drop in pressure. Mean arterial blood pressure differences between wild-type and eNOS mutant animals are statistically significant by the t-test (#,  $p < 0.01$ ). Differences between baseline blood pressures and following L-NA treatment were also statistically significant (\*,  $P < 0.05$  by ANOVA followed by Dunnett). These effects were prevented by L-arginine (200 mg/kg, intraperitoneal), and were not seen with D-nitroarginine (12 mg/kg). The heart rate of eNOS mutant mice and wild-type mice did not differ, and L-NA had no effect on heart rate.

These results support the conclusion that eNOS in the endothelium regulates blood pressure. The major NOS isoform in the endothelium is eNOS. However, a small amount of nNOS is also present. Disruption of the eNOS gene raises blood pressure, while disruption of the nNOS gene stabilizes or lowers blood pressure. Thus, inhibition of NOS in wild-type animals by L-NA, which would predominantly inhibit eNOS, would be expected to raise blood pressure. This is shown in Figure 5. However, inhibition of NOS in eNOS mutant mice would not be expected to raise blood pressure since the effect of L-NA inhibition in the mutants would be to inhibit nNOS and not eNOS. Since nNOS maintains or raises blood pressure levels, *see supra*, inhibition of nNOS would be expected to lower blood pressure levels. This is also seen in Figure 5.

### ***Example 6***

#### ***Screening of Compounds for Anti-hypertensive Effects using eNOS Mutant Mice***

The eNOS mutant mice exhibit hypertension. Compounds that are associated with NO production in the endothelium, thereby replacing eNOS enzymatic activity, are screened for anti-hypertension activity in eNOS mutant mice. These compounds can be administered to the eNOS mutant mice using pharmaceutically acceptable methods. *See* Remington's Pharmaceutical Sciences

-34-

(1990). For example, the compound to be screened can be administered at various concentrations by parenteral injection, infusion, ingestion, and other suitable methods in admixture with a pharmaceutically acceptable carrier. The effect of various concentrations of the screened compound on blood pressure is measured relative to control eNOS mutant animals that have not been administered the compound.

A significant decrease in blood pressure of the eNOS mutant mice by a screened compound is indicative that this compound would exhibit beneficial anti-hypertensive properties in other animals and in humans.

### *Example 7*

#### *Wound Healing in eNOS Mutant Mice*

It was observed that eNOS mutant mice, but not wild-type or nNOS mutant mice, tend to develop chronic wounds. Therefore, eNOS mutant mice were tested in a model of wound healing involving a full thickness transverse incision overlying the lumbar area. The incisions penetrated the deep dermis down to the skeletal muscle. In Figure 6, the histological appearance of these wounds at 24 hours and at 5 days following incision, for wild-type and eNOS mutant mice, are shown. At 24 hours, the wounds are very similar. The epidermis (ep) and the deep dermis (d) are transected. Inflammatory cells are seen in both wild-type and eNOS mutant mice.

By five days, wild-type mice have healed. The epithelial layer is reconstituted, and granulation tissue with newly sprouted capillaries fills in the scar. The dermis, which has been cut, remains absent in the healed wound. Thus, normal healing involves two quantifiable features: rapid epithelial migration from the wound edges, and the development of new capillaries, neovasculation, in the connective tissue matrix.

-35-

In these eNOS mutant animals, little or no healing has been observed at 5 days. The migration of epithelial cells is delayed, and the epithelial cells remain at the edge of the wound (ep). The connective tissue is markedly abnormal, and contains few or no new vessels. These results demonstrate an important role for eNOS in angiogenesis and epithelial cell migration during wound healing.

### ***Example 8***

#### ***Screening of Compounds for Wound Healing Effects using eNOS Mutant Mice***

The eNOS mutant mice exhibit spontaneous wounds. Compounds to be screened for wound healing activity can be administered to the eNOS mutant mice in a pharmaceutically acceptable excipient. For example, the compound can be administered at various concentrations to the wound directly as an ointment or salve. Alternatively, other pharmaceutically acceptable modes of administration can be used. For example, a pharmaceutical composition comprising the compound can be administered by parenteral injection, infusion, ingestion, skin-patch application, and other suitable methods. The effect of the compound is measured relative to control eNOS animals that have not been administered the compound.

A significant enhancement of wound healing on the spontaneous wounds of eNOS mutant mice by a screened compound would indicate that this compound exhibits beneficial wound healing properties in other animals and in humans.

Particularly preferred compounds for screening are compounds known to release NO, such as nitroglycerin, sodium nitroprusside, and SIN-1.

Similarly, eNOS mutant mice having artificially inflicted wounds can also be used in such a screening assay. For example, the effect of various compounds

on a full thickness transverse incision, as described in the preceding example, can be used as a screening assay.

### ***Example 9***

#### ***Determination of Cerebral Infarct Sizes after Middle Cerebral Artery (MCA) Occlusion in Wild-type and eNOS Mutant Mice***

Male and female wild-type (SV-129 and C57 Black/6, Taconic Farms, Germantown, NY) and eNOS mutant mice weighing 20 to 26 g were housed under diurnal lighting conditions and allowed free access to food and water *ad libitum*. Nitro-L-arginine, nitro-D-arginine, hydralazine hydrochloride and 2,3,5-triphenyltetrazolium chloride (TTC) were purchased from Sigma.

Mice were anesthetized with 2% halothane for induction and maintained on 1% halothane in 70/30% nitrous oxide/oxygen by mask. The right femoral artery was cannulated with PE-10 polyethylene tubing for arterial blood pressure measurement (Gould, Oxnard, CA) and blood gas determination (Corning 178, Ciba Corning Diag., Medford, MA). Rectal temperature was maintained between 36.5 - 37.5°C with a homeothermic blanket system (YSI, Yellow Springs, OH).

Focal cerebral ischemia was induced by occlusion of middle cerebral artery (MCA) using the intraluminal filament technique. Zea-Longa *et al.* (1989); Huang *et al.* (1994). Through a ventral midline incision, the right common and external arteries were isolated and ligated. A microvascular clip (Zen temporary clip, Ohwa Tsusho, Tokyo, Japan) was temporarily placed on the internal artery and the pterygopalatine artery. An 8-0 nylon monofilament (Ethicon, Somerville, NJ) coated with silicone was introduced through a small incision in the common carotid artery and advanced 10 mm distal to the carotid bifurcation so as to occlude the MCA and posterior communicating artery. The wound was sutured and the animal returned to its cage and allowed free access to water and food.

Twenty-four hours later, animals were sacrificed with an overdoses of pentobarbital and the brains removed and sectioned coronally into five 2-mm slices in a mouse brain matrix. Slices were placed in 2% TTC solution, followed by 10% formalin overnight. Morikawa *et al.* (1994a). The infarction area, outlined in white, was measured (Bioquant IV image analysis system) on the posterior surface of each section, and the infarction volume was calculated by summing the infarct volumes of sequential 2 mm thick sections.

In protocol 1, MCA occlusion was produced in SV-129 (n=12), C57 Black/6 (n=11), eNOS mutant mice (n=14), and eNOS mutant mice injected with hydralazine (1 mg/kg, ip, 1 hr before and 5, 17 hrs after MCA occlusion) to match the arterial blood pressure of wild-type mice (n=10).

In protocol 2, eNOS mutant and wild-type animals were injected with nitro-L-arginine (6 mg/kg, ip, 5 min, 3 and 6 hrs after ischemia) or an equivalent volume of saline vehicle in order to test the hypothesis that inhibition of nNOS activity alleviated ischemic brain injury. The investigator was blinded to the treatment group in this protocol.

As discussed *supra*, the mean arterial blood pressures in eNOS mutant mice were higher ( $115 \pm 8$  mmHg) than wild-type animals ( $98 \pm 7$  mmHg and  $94 \pm 7$  mmHg in SV-129 and C57 B/6, respectively). After hydralazine administration however, mean arterial blood pressures (MABP) did not differ between groups (Table 2).

In this and in Examples 10-11, data are expressed as means  $\pm$  SD. Statistical evaluation was performed by analysis of variance (ANOVA) followed by *t*-test to compare the data among groups in protocol 1. Unpaired Student's *t*-test was used to test the significance between two groups in protocol 2 and rCBF measurement. ANOVA with repeated measures and ANOVA followed by *t*-test were used to evaluate significance within group differences and individual points between groups in the autoregulation experiment. *Probability* values less than 0.05 were considered of statistical significance.

-38-

In protocol 1, wild-type SV-129 and C57 Black/6 developed infarcts that were  $37 \pm 7\%$  (n=12) and  $38 \pm 15\%$  (n=11) of their respective hemispheres. Larger infarct volumes ( $46 \pm 9\%$  of hemisphere, n=14,  $p < 0.05$  as compared to wild-type SV-129 and C57 Black/6) were measured in eNOS mutant mice. Larger infarct volumes were also recorded in eNOS mutant mice made normotensive by hydralazine treatment ( $48 \pm 7\%$  of hemisphere, n=10,  $p < 0.05$  vs wild-type SV-129 or C57 Black/6) (Fig. 7A,B). There were no significant group differences in physiology or blood gases before and 24 hrs after MCA occlusion to explain these differences (Table 2).

In protocol 2, administration of nitro-L-arginine decreased infarct volume in the eNOS mutant mice by 24% and injury volumes became equivalent to wild type. Nitro-L-arginine treatment, however, did not change lesion size after MCA occlusion in wild-type mice (Table 3).

Table 2. Physiological data 10 min before MCA occlusion and 24 hrs after ischemia

	pH		pCO <sub>2</sub> (mmHg)		pO <sub>2</sub> (mmHg)		MABP (mmHg)	
	before	after	before	after	before	after	before	after
<b>Protocol 1</b>								
Wt SV-129	7.33±0.04	7.29±0.06	42.2±4.5	43.8±6.6	153±20	146±29	98±7	95±6
Wt C57 B/6	7.34±0.05	7.35±0.06	49.5±3.1	51.1±4.7	148±30	137±38	94±7	96±4
eNOS mutant <sup>a</sup>	7.33±0.07	7.32±0.08	47.2±4.8	49.6±7.3	139±37	128±35	115±8	117±9
eNOS mutant <sup>b</sup>	7.35±0.04	7.30±0.05	43.8±5.9	47.3±2.9	148±16	139±28	102±6	102±
<b>Protocol 2</b>								
<b>eNOS mutant</b>								
nitro-L-arginine	7.36±0.07	7.33±0.05	47.6±4.3	51.0±2.9	120±38	134±35	110±10	107±9
Vehicle	7.32±0.07	7.32±0.07	44.6±4.2	43.6±6.3	129±32	138±32	113±8	118±8
<b>Wt SV-129</b>								
nitro-L-arginine	7.36±0.04	7.35±0.03	47.8±3.5	49.3±6.3	142±17	158±22	92±4	97±14
Vehicle	7.37±0.04	7.36±0.03	46.8±4.4	45.6±2.0	134±35	146±28	94±5	98±13

Data are expressed as means  $\pm$  SD. n=5-7 in each group.

<sup>a</sup>: Hypertensive group; <sup>b</sup>: normotensive group treated with hydralazine.

-41-

**Table 3.** Effects of nitro-L-arginine on infarct size 24 hrs after middle cerebral artery occlusion in mice.

	Infarct Volume (mm <sup>3</sup> )	
	Wild-type	eNOS mutant
Vehicle	94 ± 27	116 ± 13
Nitro-L-arginine	97 ± 13	88 ± 23*

Data are expressed as mean ± SD. n=8-12 in each group. \*p<0.05 vs vehicle.

-41-

### ***Example 10***

#### ***Measurement of rCBF in Wild-type and eNOS Mutant Mice Following MCA Occlusion***

In randomly selected mice, rCBF was determined by laser-Doppler flowmetry (Perimed, PF2B, Stockholm, Sweden) and recorded on a MacLab/8 data acquisition system (AD Instruments, Milford, MA). Two fiberoptic probe tips (Perimed PF 319:2, diameter = 0.5 mm) were fixed 2 mm posterior, 3 mm lateral to bregma and 2 mm posterior, 6 mm lateral to bregma on the ipsilateral hemisphere. These two coordinates identify sites on the convex brain surface within the vascular territory supplied by distal and proximal segments of the middle cerebral artery, respectively, and they correspond to peri-infarct zone and deeply ischemic territory, respectively. Yang *et al.* (1994); Huang *et al.* (1994). Steady-state baseline values were recorded before MCA occlusion. rCBF was recorded continuously during and after ischemia and expressed as percentage relative to the baseline value.

As depicted in Figure 8, rCBF reduction was greater in the zone corresponding to the per infarct area ( $30 \pm 16\%$  of baseline,  $n=11$ ), in eNOS mutant mice ( $p<0.05$ ) as compared to SV-129 ( $40 \pm 13\%$  of baseline,  $n=10$ ), although there was no significant difference in the MCA core territory (data not shown).

#### ***Autoregulation Study***

Mice were anesthetized with urethane (1.5 g/kg, ip) and ventilated (SAR-830 ventilator, CWE Inc., Ardmore, PA) with 70/30% nitrous oxide/oxygen after tracheostomy. Both femoral arteries were cannulated for arterial blood pressure measurement, blood gas determination and for blood withdrawal. Respiratory parameters were adjusted to keep the  $P_aCO_2$  in normal ranges (30-40 mmHg).

- Gibson *et al.* (1990), *Br. J. Pharmacol.* 99: 602-606.  
Gillespie *et al.* (1989), *Br. J. Pharmacol.* 98: 1080-1082.  
Haley *et al.* (1992), *Neuron* 8: 211-216.  
Hamberg *et al.* (1993) In: *Proceedings of the Society of Magnetic Resonance in Medicine, 12th Annual Scientific Meeting*, Society of Magnetic Resonance in  
5 Medicine NY. 1:397.  
Hevel *et al.* (1994), *Methods Enzymol.* 233:250-258 (1994).  
Hibbs *et al.* (1988), *Biochem. Biophys. Res. Comm.* 157: 87-94.  
Huang *et al.* (1993), *Cell* 75:1273-1286.  
10 Huang *et al.* (1994), *Science* 265:1883-1885.  
Huang *et al.* (1995), *Nature* 377:239-242.  
Iadecola *et al.* (1994), *J Cereb Blood Flow Metab.* 14:175-192.  
Ignarro *et al.* (1988), *Proc. Natl. Acad. Sci. USA.* 84:9265-9269.  
Ignarro (1989), *FASEB J.* 3: 31-36.  
15 Ishibashi *et al.*, *J. Clin. Invest.* 92: 883-893.  
Itabe *et al.* (1994), *J. Biol. Chem.* 269:15274-15279 (1994).  
Jannsens *et al.* (1992), *J. Biol. Chem.* 267:14519-14522, and erratum published  
in *J. Biol. Chem.* 267:22694.  
Kano *et al.* (1991), *J Cereb Blood Flow Metab.* 11:628-637.  
20 Kaufman *et al.* (1995), *Handbook of Molec. and Cell. Methods in Biol. and Medicine*, pp. 329-366.  
Kidd *et al.* (1995), *Neuropharmacol.* 34:63-73.  
Knowles *et al.* (1992), *Trends Biochem Sci.* 17:399-402.  
Kockx *et al.* (1993), *Arterioscl. Thromb.* 13: 1874-1884.  
25 Koketsu *et al.* (1992), *J Cereb Blood Flow Metab.* 12:613-620.  
Kots *et al.* (1992), *FEBS Lett.* 300: 9-12.  
Kubes *et al.* (1991), *Proc. Natl. Acad. Sci. USA.* 88:4651-4655.  
Kurose *et al.* (1994), *Circ Res.* 74:376-382.  
Lamas *et al.* (1992), *Proc. Natl. Acad. Sci. (USA)* 89:6348-6352.  
30 Lefer *et al.* (1993), *Arterioscler. Thromb.* 13:1874-1884.  
Leitinger *et al.* (1995), *J. Physiol. Pharmacol.* 46: 385-408.  
Li *et al.* (1992), *Cell* 69: 915-926.  
Linder *et al.* (1993), *Circ. Res.* 73:792-796.  
Lowenstein & Snyder (1992), *Cell* 70: 705-707.  
35 Malinski *et al.*, *J. Cereb. Blood Flow Metab.* 13: 355-358.  
Marletta (1989), *Trends Biochem. Sci.* 14: 488-492.  
Marletta (1993), *J. Biol. Chem.* 268: 12231-12234.  
Mayer *et al.* (1994), *Neuropharmacol.* 33:1253-1259.  
McDonald & Moss (1993), *Proc. Nat'l Acad. Sci (USA)* 90: 6238-6241.  
40 Michel *et al.* (1993), *Br. J. Pharmacol.* 109:287-288.  
Moncada (1992), *Acta Physiol. Scand.* 145:201-227.  
Moncada *et al.* (1991), *Pharmacol. Rev.* 43: 109-142.  
Moore *et al.* (1993a), *Br. J. Pharmacol.* 108:296-297.  
Moore *et al.* (1993b), *Br. J. Pharmacol.* 110:219-224.  
45 Mooradian *et al.* (1995), *J. Cardiovasc. Pharmacol.* 25: 674-678.

*Literature Cited*<sup>1</sup>

- Aji *et al.* (1997), *Circulation* 95:430-437.  
 Archer, S., (1993), *FASEB J.* 7:349-360.  
 Babbedge *et al.* (1993), *Br. J. Pharmacol.* 110:225-228.  
 5 Bath (1993), *Eur. J. Clin. Pharmacol.*, 45:53-58.  
 Beckman *et al.* (1994a), *Methods Enzymol.* 233:229-240.  
 Beckman *et al.* (1994b), *Biol. Chem. Hoppe-Seyler* 375:81-88.  
 Benditt *et al.* (1973), *Proc. Natl. Acad. Sci. (USA)* 70:1753-1756.  
 Boeckvstaens *et al.* (1991), *Br. J. Pharmacol.* 102:434-438.  
 10 Bohme *et al.* (1991), *Eur. J. Pharmacol.* 199:379-381.  
 Booth *et al.* (1989), *Atherosclerosis* 76:257-268.  
 Bredt *et al.* (1994), *Ann Rev. Biochem.* 63:175-195.  
 Bredt *et al.* (1992), *Neuron* 8:3-11.  
 Bredt *et al.* (1990a), *Nature* 347:768-770.  
 15 Bredt *et al.* (1990b), *Proc. Natl. Acad. Sci. USA.* 87:682-685 (1990) - 129/130  
 Breslow (1996), *Science* 272:685-688.  
 Brinster *et al.* (1985), *Cell* 27: 4438-4442.  
 Bult *et al.* (1990) *Nature* 345: 346-347.  
 Burnett *et al.* (1992), *Science* 257: 401-403.  
 20 Busse *et al.* (1996), *J. Vasc. Res.* 33: 181-194.  
 Curran *et al.* (1989), *J. Exp. Med.* 170:1769-1774.  
 Dalkara *et al.* (1994), *Brain Pathol.* 4:49-57.  
 Dalkara *et al.*, (1995), *J Cereb Blood Flow Metab.* 15:631-638.  
 Darley-USmar *et al.* (1992), *Free Rad. Res. Commun.* 17:19-20.  
 25 Dawson *et al.*, (1991) *Proc Natl Acad Sci USA.* 88:6368-6371.  
 Dawson *et al.* (1992), *Ann. Neurol.* 32: 297-311.  
 Desai *et al.* (1991), *Nature* 351:477-479.  
 Dimmeler *et al.* (1992), *J. Biol. Chem.* 267: 16771-16774.  
 Dinerman *et al.* (1994), *Proc. Natl. Acad. Sci. (USA)* 91:4214-4218.  
 30 Edelman & Gally (1992), *Proc. Nat'l Acad. Sci. (USA)* 89:11651-11652.  
 Furchgott *et al.* (1980), *Nature* 288:373-376.  
 Furchgott (1988), Studies on the relaxation of the rabbit aorta by sodium nitrate: basis for the proposal that the acid-activatable component of the inhibitory factor from retractor penis is inorganic nitrate and the endothelium-derived relaxing factor is nitric oxide, *In: Mechanisms of Vasodilation*, P.M. Vanhoutte ed.  
 35 Furchgott & Vanhoutte (1989), *FASEB J.* 3: 2007-2018.  
 Gally *et al.* (1990), *Proc. Nat'l Acad. Sci. (USA)* 87:3547-3551.  
 Garcia *et al.* (1993), *Am J Pathol.* 142:623-635.

---

<sup>1</sup> All of the literature cited in this application is expressly incorporated herein by reference.

-70-

lysine (MDA-lysine) and 4-hydroxynonenal-lysine (4HNE-lysine) as markers for lipid oxidation events. Palinski *et al.* (1989); Palinski *et al.* (1994); Itabe *et al.* (1994); Yla-Herttuala (1989). These epitopes are found in atherosclerotic lesions in apoE-deficient mice and humans. A panel of antibodies against MDA-lysine and 4-HNE epitopes is used to study whether the absence of any one of the NOS isoforms results in a reduction in staining, implicating that NOS isoform in lipid oxidation. These results are correlated with a histologic assessment of lesion extent, severity, and the presence of foam cells, macrophages, and other inflammatory cells. Independent methods to measure the same process are used, e.g., HPLC for nitrotyrosine or RT-PCR for VCAM-1 expression to improve our ability to detect differences due to NOS isoform deletion.

sodium hydrosulfite should abolish the peaks by converting 3-nitrotyrosine to aminotyrosine. The levels of 3-nitrotyrosine are expressed as a ratio of 3-nitrotyrosine to total tyrosine, to normalize for the varying arterial concentrations of tyrosine. This method is more quantitative than immunohistochemical detection and offers an independent measure of nitrotyrosine formation.

Under physiological conditions, eNOS suppresses the expression of endothelial activation genes by inducing and stabilizing I $\kappa$ B. Peng (1995). In atherosclerotic lesions, NOS expression patterns change, and iNOS and/or nNOS expression increases, while eNOS levels drop. Wilcox (1994). These changes are believed to contribute to increased oxidant stress in the vessel wall, and endothelial cell activation. To test for endothelial cell activation, the expression of VCAM-1 can be used as a preferred marker, since its expression is longer lived than other markers. However, ICAM-1, E-selectin and MCP-1 can be used. eNOS mutant mice will exhibit greater expression of VCAM-1 (more endothelial activation) in atherosclerotic lesions, while iNOS and nNOS would be expected to show diminished VCAM-1 expression (less endothelial activation).

VCAM-1 expression is examined by two methods: immunohistochemistry and RT-PCR quantitation of mRNA expression. For immunohistochemistry, a rat monoclonal anti-VCAM-1 antibody obtained from Southern Biotechnology Associates, Inc., Birmingham, AL, is used as the primary antibody, and biotinylated goat anti-rat antibody as a secondary antibody. For RT-PCR primers that amplify VCAM-1 cDNA, conditions are used that ensure that the amount of amplified PCR product is proportional to the level of mRNA. Actin mRNA will be used to standardize the amount of total mRNA, and internal quantitative standards will be employed as described *supra*.

Lipid peroxidation results in many changes, including altered electrophoretic mobility and modification of apolipoprotein B. Many of these can be assessed in purified LDL that has been subject to oxidation, but are more difficult to study *in vivo*. The protein modification epitopes malondialdehyde-

This experiment extends the results from injury models to the development of atherosclerotic lesions. The development of lesions involves not only cellular differentiation, but also the recruitment of inflammatory cells, lipid oxidation and phagocytosis, and endothelial cell activation. Due to the participation of iNOS or nNOS isoforms in the pathophysiology of atherosclerosis, the disruption of these genes would be expected to result in a less severe phenotype than apoE mutant mice alone.

### ***Example 17***

#### ***The Effect of NOS Isoform Expression Patterns on Lipid Oxidation and Endothelial Cell Activation***

Peroxynitrite is formed in biological systems only by the reaction of nitric oxide with superoxide. Since human atherosclerotic lesions contain nitrotyrosine, it is known that at least one isoform of NOS generates nitric oxide and peroxynitrite in atherosclerotic lesions. iNOS and nNOS, but not eNOS, are believed to be involved in the generation of peroxynitrite. If so, iNOS and nNOS mutant mice will exhibit decreased amounts of nitrotyrosine. Therefore, atherosclerotic lesions in animals that lack apoE and each isoform (eNOS/apoE, iNOS/apoE, nNOS/apoE) are examined for the presence of nitrotyrosine.

Two independent methods to detect 3-nitrotyrosine are used: immunohistochemical detection and HPLC. For immunohistochemistry, a rabbit antiserum specific for nitrotyrosine, obtainable from Upstate Biotechnology is used. Alternatively, the level of nitrotyrosine is independently assessed by 16 electrode HPLC. Schultz (1996).

Briefly, tissue from a 50  $\mu$ m section of brain, comparable to the amount of tissue in atherosclerotic plaques, is used for this analysis. Atherosclerotic plaques from apoE and apoE/NOS double mutant mice are dissected and frozen. The level of 3-nitrotyrosine will be measured by HPLC with 16 electrode electrochemical detection. Reaction of standards and tissue extracts with 1M

In these experiments, statistical differences in lipid levels among groups are tested by one-way ANOVA, and post hoc tests of individual means are performed with Tukey's test. Differences in atherosclerotic lesion area between groups will be statistically analyzed with the non-parametric Kruskal-Wallis procedure.

### ***Example 16***

#### ***iNOS and nNOS Isoforms Contribute to the Development of Atherosclerosis***

In this Example, iNOS and nNOS mutant mice are used to determine if the loss of these pro-atherogenic isoforms show less response to injury and less atherogenesis. The cuff model of vessel injury is used in iNOS and nNOS mutant mice. These mice have normal vascular anatomy, so their response can be compared with those of wild-type C57BL/6 mice. Quantitative morphometry, immunohistochemistry, indices of cellular proliferation, and NOS isoform studies are performed as part of the filament or cuff injury models as described *supra*.

Double mutant apoE/iNOS and apoE/nNOS mice are bred to compare the development of atherosclerotic lesions in these animals with apoE mice. A typical high-cholesterol, high-fat Western type diet without cholic acid is used to mimic the human atherosclerotic process. The lipid profiles of these animals are measured, to ensure that the disruption of iNOS or nNOS do not have independent effects on the lipid profile.

The mice are sacrificed at age 5, 10, 20, 25, and 30 weeks. The thoracic and abdominal aorta is stained with Oil Red O, to quantitate the total area of atherosclerotic lesions compared with the area of the aorta. Serial sections are taken for histological analysis and to quantitate intimal proliferation. the volume of intima is calculated by integrating the affected areas over the length of the affected segment. The cell types involved in these lesions are identified by immunohistochemical staining, and expression of the remaining NOS isoforms will be examined by immunohistochemistry, and quantitated by RT-PCR.

-66-

atherosclerotic lesions in mice homozygous for apoE and eNOS mutations is compared vs. apoE mutant mice that are wild-type for eNOS.

The animals will be fed a typical high-cholesterol, high-fat Western-type diet to mimic the human atherosclerotic process. This diet contains 16% crude fat, 1.25% cholesterol (Harlan Teklad Diets, Madison, WI). The mice have elevated VLDL and chylomicron levels. The lipid profiles of these mice will also be measured to ensure that eNOS gene disruption does not independently affect the lipid profile.

ApoE and ApoE/eNOS mutant mice are sacrificed at age 5, 10, 20, and 30 weeks. The lungs, liver, stomach, and intestines are removed so that the thoracic and abdominal aorta can be dissected. The tissue is stained with Oil Red O to quantitate the total area of atherosclerotic lesions compared with the area of aorta, from the aortic valve down to 1 cm past the aortic bifurcation. The time points are selected to determine if there is a difference in the rate of lesion development versus the severity of the lesions. The dependence of apoE atherosclerosis on diet demonstrates that these variables can be modulated, and that their quantitation is feasible.

Serial sections are taken for histologic analysis and to quantitate intimal proliferation. The volume of intima is calculated by integrating their affected areas over the length of the affected segment, as described above in the injury models. The cell types involved in these lesions, e.g., smooth muscle, endothelium, and foam cells, are identified by immunohistochemical staining with antibodies for alpha actin, vimentin, factor VIII related antigen, and CD31. The expression of remaining NOS isoforms will be examined by immunocytochemistry, and quantitated by RT-PCR, as described *supra*.

In other experiments, a low-fat, low-cholesterol diet can be used if the effect of the apoE mutation masks the effect of the eNOS mutation. Alternatively, cholic acid can be added to the diet to increase the atherosclerotic stimulus.

-65-

wild-type mRNA) to 0% eNOS mutant (100% wild-type RNA). Using these mixtures, first strand cDNA was synthesized and used as a template for PCR using the eNOS specific primers. As seen in Figure 19, the amount of PCR product varied according to the amount of eNOS RNA present in the initial RNA sample, validating the quantitative nature of the reaction. Additional controls for expression of actin and GAPDH were performed as well.

### *Example 15*

#### *ApoE/NOS Mutant Mice*

ApoE mutant mice of a C57BL/6 genetic background were obtained from Jackson Labs. These mice were mated to eNOS mutant mice and nNOS mutant mice of the same genetic background. Double heterozygous apoE/eNOS and apoE/nNOS mice have been obtained. Mating pairs of each double heterozygous mice were bred, and the genotype of the offspring is determined using Southern blot analysis. For example, the ApoE mutation is genotyped by digesting genomic DNA with *HindIII* and using a 0.6 kb *SacI/HindIII* fragment. A ubiquitous endogenous *HindIII* band is 7.5 kb, the wild-type band is about 9 kb, and the disrupted band is 3 kb. See Huang (1994); Huang (1995).

The development of atherosclerotic lesions in the aorta of apoE mutant mice have been observed over time. Figure 20 shows a 6 month old apoE mutant mice with macroscopically visible lesions within the aortic arch, the origins of the carotid arteries, and the thoracic and abdominal aorta. Lipid in an aortic lesion stains with oil red O. The apoE mutant mice develop fatty streak lesions by 10 weeks of age, and evolve foam cells and fibrous plaque lesions by 15-20 weeks. The lesions typically occur in regions of shear stress, at the origins of the carotid arteries, intercostal arteries, renal arteries, and aortic bifurcation.

Since the apoE single or double mutant mice develop predictable, spontaneous atherosclerotic lesions, they provide a genetic background on which to study the effect of mutations in other genes, e.g., eNOS. The development of

-64-

from 102 mm Hg to 72 mm Hg, which is equivalent to the blood pressure of untreated wild-type C57BL/6 mice. This will control hypertension during the duration of the experiment (3 to 28 days). Alternatively, local gene therapy to express eNOS in the femoral artery of the eNOS mutant mice could be used, leaving systemic eNOS deficiency and hypertension unaltered.

### *Example 14*

#### *Quantitative RT-PCR to Study Expression of NOS Isoforms*

Primers for RT-PCR detection of NOS isoforms in small amounts of tissue from mice have been devised, and are shown below:

The nNOS (type I) primers are as follows:

B1 primer: 5' CCT TAG AGA GTA AGG AAG GGG GCG GG 3' (26-mer)

B2 primer: 5' GGG CCG ATC ATT GAC GGC GAG AAT GAT G 3' (28-mer)

These primers amplify a 404 bp fragment from nNOS cDNA.

The eNOS (type III) NOS primers are as follows:

E1 primer: 5' GGG CTC CCT CCT TCC GGC TGC CAC C 3' (25-mer)

E2 primer: 5' GGA TCC CTG GAA AAG GCG GTG AGG 3' (24-mer)

These primers amplify a 254 bp fragment from eNOS cDNA, and an 800 bp fragment from the eNOS gene.

The iNOS (type II) NOS primers are as follows:

I1 primer: 5' ATC AGG AAC CTG AAG CCC CAG GAC 3' (24-mer)

I2 primer: 5' TGT TGC CAG ATT TCT CTG CAC GGT 3' (24-mer)

These primers amplify a 338 bp fragment from iNOS cDNA.

These primers are specific, and do not prime cDNA corresponding to the other NOS isoforms.

The quantitative nature of this technique was validated by using fixed amounts of aorta RNA (5µg) as starting material for reverse transcription. Vessels are frozen in liquid nitrogen and homogenized in the presence of phenol and guanidine isothiocyanate (RNAzol B). Total cellular RNA is prepared by extraction of the homogenate with chloroform and isopropanol. The proportion of eNOS mutant mRNA to wild-type mRNA varied 100% eNOS mutant (no

The process of endothelial resurfacing, which occurs by migration from uninjured areas such as the aortic arch, is also studied. It is expected that the rate of resurfacing of the endothelial layer following denudation will be much slower in eNOS mutant mice.

5 In order to examine endothelial regeneration, animals are injected with Evan's blue solution (150  $\mu$ l of 5% solution in PBS, iv) 10 minutes before euthanasia to identify de-endothelialized segments. Vessel segments are cut open longitudinally and pinned onto Teflon cards with the lumen facing up. For determination of smooth muscle cell proliferation, mice are injected  
10 intraperitoneally with 5'-bromo-2'-deoxyuridine (BrdU, 25 mg/kg, Boehringer Mannheim) one hour prior to euthanasia. Immunostaining with antibody to BrdU is carried out.

This result would demonstrate that eNOS expression in both endothelial and non-endothelial cells affect the response to injury. However, if no  
15 differences between mutant and wild-type mice are observed, these results would suggest that local production of eNOS by the endothelium and not other cells, is the overriding factor determining vessel response to filament injury.

Two independent methods are used to characterize vessel morphometry: area/volume calculations and thickness measurements of the intima and the  
20 media. Intimal, medial, and luminal volumes are calculated by integrating areas along the injured region to ensure that inhomogeneities in neointimal formation along the length of the injured region do not give spurious results. Absolute volumes and intima/media (I/M) ratios are compared. The I/M ratio is a standardized measure that accounts for differences in vessel size, even within the  
25 same group of animals.

The effect of hypertension in vascular injury responses (both filament and cuff models) is measured by repeating the experiments after treating eNOS mutant mice with hydralazine to reduce their blood pressure to normotensive levels. The addition of hydralazine to drinking water at 250  $\mu$ g/ml gives a daily  
30 dose of about 750  $\mu$ g, and results in a stable decrease in mean arterial pressure

with smooth muscle staining. In contrast, only the luminal cells stain for von Willebrand factor, a marker of endothelial cells, as shown in panels G and H.

***The Filament Model:***

A comparison of the eNOS mutant mice and wild-type mice using the filament model of vessel injury is performed. As a first step, the size of the carotid arteries of eNOS mutant mice, nNOS mutant mice, and wild-type mice have been quantitated. Carotid arteries were fixed by perfusion at a pressure of 100 mm Hg. The luminal diameter was calculated by dividing the luminal circumference by  $\pi$  to account for differences in luminal shape. As shown in Table 11, the diameters of the carotid artery of wild-type mice do not differ substantially from those of the NOS mutant mice (n=20 in each group). Thus, the filament model can be used with a comparable degree of injury between different mouse strains.

**Table 11. Luminal diameters of perfusions fixed carotid arteries**

	Wild-type	eNOS mutant	nNOS mutant
Mean (mm)	0.42	0.45	0.41
Std. dev. (mm)	0.06	0.08	0.05

The filament model addresses eNOS expression by non-endothelial cells, since it removes the endothelial layer of cells. The filament injury model is performed in eNOS mutant mice and C57BL/6 wild-type mice, and morphometry, immunohistochemistry, and BrdU staining is performed as outlined. Briefly, the external carotid artery is identified, and two ligatures are placed around it. The artery is tied distally and a filament is inserted through an incision and advanced down the common carotid artery. The filament is rotated and passed three times. The external carotid artery is tied off proximally, and the right carotid artery serves as a sham operated control.

These results are summarized in Table 10. Wild-type mice, which have no detectable intima at baseline, develop neointima within 14 days of cuff injury, with an intima to media (I/M) volume ratio of 0.29 for males and 0.18 for females. The eNOS mutant animals developed substantially more neointima, with an I/M volume ratio of 0.73 for males and 0.43 for females. Thus, animals with a disrupted eNOS gene exhibit greater neointimal formation in response to cuff injury. Figure 17 shows representative section of vessels stained with hematoxylin-eosin. The internal elastic lamina is indicated by arrows, and the degree of neointima formation can be easily seen.

**Table 10. Neointima Formation Measured 14 Days After Cuff Placement**

Mouse strain	Intima volume	Media volume	I/M ratio	Intima ( $\mu\text{m}$ )
Wild-type, males (n=20)	0.0085 $\pm$ 0.0019	0.0297 $\pm$ 0.0058	0.29 $\pm$ 0.04	6.6 $\pm$ 1.6
Wild-type, females (n=20)	0.0059 $\pm$ 0.0018	0.0321 $\pm$ 0.0087	0.18 $\pm$ 0.06	4.9 $\pm$ 1.8
eNOS mutant, males (n=20)	0.0231 $\pm$ 0.0035	0.0316 $\pm$ 0.0034	0.73 $\pm$ 0.10	21.7 $\pm$ 4.2
eNOS mutant, females (n=20)	0.0123 $\pm$ 0.0028	0.0286 $\pm$ 0.0062	0.43 $\pm$ 0.09	11.7 $\pm$ 2.7

In Table 10, all measurements are expressed as mean  $\pm$  standard deviation. Volumes are expressed in  $\text{mm}^3$ , and are calculated as outlined in the text from area measurements. The last column shows thickness measurements of intima on the injured side. There was no detectable intima on the control side.  $p < 0.05$  was obtained for each gender, eNOS mutant mice vs. wild-type mice by ANOVA followed by Dunnett statistical analysis.

Figure 18 shows the histology and immunochemical staining of the cuff-injured and control vessels from eNOS mutant mice. Hematoxylin-eosin and elastin stains outline the intima clearly on the injured side; the control has no intima. Cells throughout the neointimal layer stain strongly for actin (E). This staining is also seen in the media of injured and control vessels (E, F), consistent

internal elastic laminae. The areas were integrated over the length of the vessel segment to calculate the volume of intima and media. Second, for thickness measurements, the thickness of the intima and the media at four points located 90° to each other, and averages over the length of the vessel segment.

5 Table 9 shows the representative data from individual wild-type and eNOS mutant male mice, to indicate the types of measurements and their variance.

(wild-type male mice)

					Linear measurements, $\mu\text{m}$								
					Volume measurements			Injured side			Control side		
No.	Genotype	Sex	Age	Wt. g.	Intima	Media	I/M ratio	Lum diam	Intima	Media	Lum diam	Intima	Media
70	Wild-type	M	8	24.0	5.9	25.1	0.23	111.4	7.9	27.7	110.9	0	28.8
71	Wild-type	M	8	23.0	7.5	23.1	0.32	210.1	5.5	15.6	166.2	0	23.5
72	Wild-type	M	8	24.0	6.5	22.8	0.28	172.8	5.8	17.9	154.9	0	22.4
73	Wild-type	M	8	25.9	8.9	31.5	0.28	160.4	8.3	23.4	119.7	0	29.8
74	Wild-type	M	8	26.1	5.4	23.6	0.23	198.5	4.9	17.1	211.6	0	20.0
75	Wild-type	M	8	24.3	6.7	24.5	0.27	227.3	3.2	15.6	162.6	0	27.3
76	Wild-type	M	8	23.9	9.3	32.7	0.28	212.5	6.8	21.1	153.8	0	20.3
77	Wild-type	M	8	25.0	6.3	26.9	0.23	142.7	6.7	23.1	183.7	0	25.8
78	Wild-type	M	8	23.0	10.7	39.5	0.27	172.5	9.3	28.6	159.2	0	32.5
79	Wild-type	M	8	28.3	10.9	41.8	0.26	198.1	6.1	21.4	183.3	0	27.6
132	Wild-type	M	8	26.1	11.3	35.6	0.32	182.4	6.5	18.7	176.6	0	26.9
133	Wild-type	M	8	25.2	8.1	32.8	0.25	142.7	6.7	28.9	183.7	0	30.8
134	Wild-type	M	8	23.8	10.7	39.5	0.27	172.5	9.3	28.6	159.2	0	31.9
135	Wild-type	M	8	25.9	8.7	25.9	0.33	150.6	8.3	24.5	180.3	0	22.3
136	Wild-type	M	8	24.8	7.6	26.4	0.29	162.6	5.1	26.6	156.1	0	18.6
137	Wild-type	M	8	22.9	11.2	31.2	0.36	180.0	5.9	21.6	180.1	0	20.7
138	Wild-type	M	8	26.8	7.5	28.6	0.26	195.2	6.3	19.6	196.5	0	23.9
139	Wild-type	M	8	26.3	10.2	29.2	0.35	186.3	7.0	25.4	198.5	0	22.6
140	Wild-type	M	8	25.9	9.1	29.8	0.30	210.1	4.9	28.0	168.2	0	23.6
141	Wild-type	M	8	22.9	8.5	23.6	0.36	175.4	8.6	24.6	145.3	0	29.0
Mean					8.5	29.7	0.29	178.2	6.6	22.9	167.5	0	25.4
Std. dev.					1.9	5.8	0.04	28.3	1.6	4.5	24.7	0	4.2

(eNOS mutant male mice)

Linear measurements, $\mu\text{m}$													
					Volume measurements			Injured side			Control side		
No.	Genotype	Sex	Age	Wt. g.	Intima	Media	I/M ratio	Lum diam	Intima	Media	Lum diam	Intima	Media
98	eNOS -/-	M	8	28.0	20.8	32.1	0.65	122.5	22.8	26.3	116.4	0	27.7
99	eNOS -/-	M	8	25.2	23.5	36.6	0.64	165.5	20.1	25.3	131.9	0	27.3
100	eNOS -/-	M	8	23.5	33.2	36.4	0.91	203.6	29.4	20.5	133.3	0	25.7
101	eNOS -/-	M	8	20.5	19.7	27.9	0.71	136.9	20.0	22.3	151.3	0	31.1
102	NOS -/-	M	8	22.7	22.5	33.4	0.67	144.9	21.5	25.0	138.1	0	33.6
103	NOS -/-	M	8	25.8	21.5	30.6	0.70	157.4	21.5	23.9	134.1	0	30.5
104	eNOS -/-	M	8	23.6	19.8	31.2	0.63	146.6	19.0	23.8	168.4	0	29.6
105	eNOS -/-	M	8	28.1	21.4	36.0	0.59	177.6	15.2	24.6	159.4	0	28.1
106	eNOS -/-	M	8	21.0	16.3	23.4	0.70	157.6	13.2	19.3	162.7	0	26.3
147	eNOS -/-	M	8	26.6	21.7	30.5	0.71	160.2	20.3	23.4	181.2	0	24.5
148	eNOS -/-	M	8	25.8	23.1	36.2	0.64	180.9	24.1	24.3	167.4	0	22.8
149	eNOS -/-	M	8	24.2	26.2	29.9	0.88	149.2	25.9	23.8	162.4	0	23.1
150	NOS -/-	M	8	20.6	25.2	31.5	0.80	150.2	24.6	23.1	155.2	0	23.8
151	eNOS -/-	M	8	26.6	27.0	34.3	0.79	150.9	28.9	23.8	153.7	0	24.6
152	eNOS -/-	M	8	28.4	22.2	32.2	0.69	188.6	19.2	24.6	180.4	0	24.8
153	eNOS -/-	M	8	27.5	26.5	26.8	0.99	139.5	23.5	24.1	138.5	0	28.3
154	NOS -/-	M	8	29.7	21.7	29.1	0.75	154.2	19.8	22.5	168.0	0	21.6
155	eNOS -/-	M	8	25.4	23.3	31.1	0.75	132.0	22.5	23.1	151.8	0	25.4
156	eNOS -/-	M	8	24.3	24.6	32.6	0.75	168.5	26.5	21.3	160.2	0	22.5
157	eNOS -/-	M	8	24.0	21.3	30.3	0.70	156.4	16.7	22.5	165.3	0	27.0
Mean					23.1	31.6	0.73	157.2	21.7	23.4	154.0	0.00	26.4
Std. dev.					3.5	3.4	0.10	19.6	4.2	1.7	17.2	0.00	3.2

-59-

Response	adventitial inflammation; medial cellular proliferation	removal of endothelium, medial cellular proliferation
Time to response	14-28 days	14-28 days
Measurements	quantitative morphometry; immunohistochemistry; expression studies (RT-PCR); indices of cellular proliferation	quantitative morphometry; immunohistochemistry; expression studies (RT-PCR); indices of cellular proliferation

### *The Cuff Model:*

5           Mice aged 7-8 weeks were anesthetized with pentobarbital (50 mg/kg ip). Femoral arteries were surgically exposed and dissected from the surrounding tissue. A nonocclusive polyethylene cuff (2 mm in length, 0.58 mm inner diameter, made of PE-50 tubing split longitudinally) was placed around the left femoral artery and tied snugly with a silk thread. The right femoral artery served  
10 as a sham control. The wounds were then closed and the animals allowed to awaken from anesthesia. Animals were euthanized at 3, 14, 21, and 28 days after cuff placement. The femoral arteries were fixed under perfusion in 10% formalin, and embedded in paraffin.

15           The cuffed vessel segment and the corresponding sham operated vessel were cut into 200 serial 10  $\mu$ m sections, and were placed in order on five series of slides, as shown in Figure 16. One series was stained with hematoxylin-eosin, another with elastin, and the others were saved for immunohistochemistry. The slides were scanned into Adobe Photoshop, and the quantitative morphometry was performed using the public domain program *NIH Image*.

20           We performed two types of measurements. First, for area/volume measurements, the areas within the lumen, internal elastic lamina, and external elastic lamina were measured. The intimal area was calculated as the difference between the area within the internal elastic lamina and the lumen. The medial area was calculated as the difference between the areas within the external and

**Table 7.** NOS catalytic activity in SV-129, eNOS mutant and nNOS mutant mice.

Brain regions	NOS catalytic activity (fmol/mg wet weight/min)		
	SV-129	eNOS mutant	nNOS mutant
Olfactory bulb	3.1 ± 0.9	4.0 ± 1.2	0 ± 0 <sup>#</sup>
Striatum	2.4 ± 0.3	2.4 ± 0.8	0.04 ± 0.04 <sup>*,#</sup>
5 Thalamus/Hypothalamus	6.2 ± 1.8	5.8 ± 1.2	0.07 ± 0.04 <sup>*,#</sup>
Hippocampus	3.1 ± 0.9	3.2 ± 0.5	0.03 ± 0.03 <sup>*,#</sup>
Cerebral cortex/Amygdala	4.0 ± 1.0	4.0 ± 0.7	0.07 ± 0.02 <sup>*,#</sup>
Cerebellum	9.0 ± 2.0	7.3 ± 1.7	0.04 ± 0.04 <sup>*,#</sup>
Brain stem	3.3 ± 0.7	3.5 ± .09	0.05 ± 0.05 <sup>*,#</sup>

- 10 \*: p<0.05 vs. SV-129, #: p<0.05 vs. type 3 mutant mice (Turkey's multiple range test).  
NOS catalytic activity was measured by calcium-dependent [<sup>3</sup>H]arginine to [<sup>3</sup>H]citruline conversion. The experiment was performed three times in duplicate.

### Example 13

#### *Use of the Vessel Injury Models of Atherosclerosis in eNOS Mutant Mice*

- 15 Both the cuff model and the filament model of vessel injury can be used  
as an animal model for atherosclerosis. Major features of these two vessel injury  
models can be seen in the following Table:

**Table 8.** Comparison of Vessel Injury Models

Feature	Cuff Model	Filament Model
20 Exemplary Location	femoral artery	carotid artery
Method of Injury	placement of non-occlusive cuff around vessel	insertion of filament to denude endothelial layer
Manipulated Area	adventitia	endothelium

**Table 6.** Effects of D-nitro-arginine (D-NA) on the regional distribution of [<sup>3</sup>H]L-NA binding in wild-type (SV-129) and nNOS mutant mice.

Brain Regions	Binding	SV-129	nNOS mutant
Olfactory bulb (granular layer)			
	L-NA displaceable <sup>1)</sup>	121 ± 12.4	32 ± 2.3 <sup>#</sup>
	D-NA <sup>2)</sup>	92 ± 10.8	5 ± 3.0 <sup>*,#</sup>
Hippocampal CA3 subfield			
	L-NA displaceable	83 ± 2.4	33 ± 4.2 <sup>#</sup>
	D-NA	66 ± 5.9	3 ± 1.9 <sup>*,#</sup>
Dentate gyrus			
	L-NA displaceable	67 ± 3.7	33 ± 5.5 <sup>#</sup>
	D-NA	43 ± 4.8	2 ± 1.9 <sup>*,#</sup>
Amygdaloid complex			
	L-NA displaceable	96 ± 12.6	32 ± 5.9 <sup>#</sup>
	D-NA	64 ± 7.6	3 ± 1.7 <sup>*,#</sup>
Cerebellum (molecular layer)			
	L-NA displaceable	86 ± 4.5	32 ± 6.2 <sup>#</sup>
	D-NA	59 ± 6.7	0 ± 3.6 <sup>*,#</sup>

10 Values (fmol/mg tissue) represent mean ± S.E. of four to five mice per group.

<sup>1)</sup>: L-NA displaceable = (total - binding remaining in the presence of 10 μM L-NA) binding;

<sup>2)</sup>: D-NA = L-NA displaceable binding in the presence of 10 μM D-NA,

\*: p<0.01 vs. L-NA displaceable, #: p<0.01 vs. SV-129

**Table 5.** Effects of 7-NI on the regional distribution of [ $^3$ H]L-NA binding in wild-type (SV-129 and C57black/6) and mutant (type 3 and type 1) mice.

Brain regions	Wild-type		Mutant	
	SV-129	C57black/6	eNOS	nNOS
Olfactory bulb (glanular layer)				
5 L-NA displaceable <sup>1)</sup>	109 $\pm$ 1.9	113 $\pm$ 9.9	106 <sup>3)</sup>	33 $\pm$ 1.9
	7-NI <sup>2)</sup> 17 $\pm$ 0.7	28 $\pm$ 4.1*	N.T.	30 $\pm$ 2.7
Hippocampal CA3 subfield				
10 L-NA displaceable	60 $\pm$ 3.1	53 $\pm$ 2.3	50 $\pm$ 6.2	25 $\pm$ 0.9
	7-NI 18 $\pm$ 1.8*	22 $\pm$ 4.7*	21 $\pm$ 1.8*	23 $\pm$ 2.3
Dentate gyrus				
10 L-NA displaceable	48 $\pm$ 2.6	58 $\pm$ 5.6	58 $\pm$ 5.4	28 $\pm$ 2.2
	7-NI 18 $\pm$ 0.7*	22 $\pm$ 4.6*	20 $\pm$ 2.7*	22 $\pm$ 1.7
Amygdaloid complex				
15 L-NA displaceable	90 $\pm$ 4.9	89 $\pm$ 11.3	88 $\pm$ 2.9	29 $\pm$ 1.4
	7-NI 21 $\pm$ 2.1*	21 $\pm$ 4.8*	21 $\pm$ 2.9*	23 $\pm$ 2.5
Cerebellum (molecular layer)				
L-NA displaceable	67 $\pm$ 1.7	78 $\pm$ 6.8	67 $\pm$ 5.8	30 $\pm$ 0.8
	7-NI 18 $\pm$ 1.3*	23 $\pm$ 5.4*	20 $\pm$ 2.2*	24 $\pm$ 1.0

Values (fmol/mg tissue) represent mean  $\pm$  S.E. of three mice per group.

<sup>1)</sup>: L-NA displaceable = (total -binding in the presence of 10 $\mu$ M L-NA) binding

<sup>2)</sup>: 7-NI = L-NA displaceable binding in the presence of 100  $\mu$ M 7-NI,

<sup>3)</sup>: n=1, N.T.: not tested,

\*: p<0.01 vs. L-NA displaceable. There are no significant differences between L-NA displaceable and 7-NI groups in type 1 mice.

**Table 4.** Regional distribution of L-NA displaceable ( $^3\text{H}$ )L-N<sup>G</sup>-nitro-arginine binding in wild-type (SV-129 and C57black/6) and mutant (eNOS and nNOS mutant) mice.

Brain regions	Wild-type		Mutant	
	SV-129	C57black/6	eNOS	nNOS
5 Olfactory bulb-granular layer	106 ± 2.5	101 ± 12.1	108 ± 3.8	13 ± 1.6 <sup>*,#,+</sup>
Olfactory bulb-plexiform layer	43 ± 3.1	32 ± 3.1	33 ± 1.6	18 ± 0.6 <sup>*,#,+</sup>
Islands of Calleja	71 ± 7.9	70 ± 13.7	51 ± 3.5	5 ± 0.6 <sup>*,#,+</sup>
Tenia tecta	85 ± 6.7	106 ± 8.0	94 ± 6.1	13 ± 0.6 <sup>*,#,+</sup>
Rhinal fissure	84 ± 5.2	80 ± 5.8	70 ± 3.9	17 ± 2.0 <sup>*,#,+</sup>
Striatum	18 ± 1.4	16 ± 1.7	12 ± 0.7	9 ± 0.7 <sup>*,#</sup>
10 Frontal cortex I-II	40 ± 1.4	40 ± 3.0	32 ± 2.6	19 ± 1.5 <sup>*,#,+</sup>
Occipital cortex I-II	47 ± 4.6	42 ± 5.9	36 ± 3.9	16 ± 0.9 <sup>*,#</sup>
Hippocampal CA1 subfield	44 ± 2.4	42 ± 5.1	43 ± 2.3	13 ± 1.3 <sup>*,#,+</sup>
Hippocampal CA3 subfield	70 ± 2.5	63 ± 4.0	63 ± 2.2	13 ± 1.1 <sup>*,#,+</sup>
Dentate gyrus	57 ± 4.6	56 ± 4.0	52 ± 1.1	14 ± 1.2 <sup>*,#,+</sup>
15 Dorsomedial hypothalamic nuclei	34 ± 2.6	25 ± 4.2	29 ± 6.0	12 ± 1.4 <sup>*</sup>
Ventromedial hypothalamic nuclei	42 ± 5.8	47 ± 7.4	45 ± 5.9	13 ± 1.8 <sup>*,#,+</sup>
Amygdaloid complex				
Amygdaloid nuclei-medial	90 ± 5.6	96 ± 8.8	89 ± 4.2	14 ± 2.2 <sup>*,#,+</sup>
Amygdaloid nuclei-anterior cortical	57 ± 7.9	73 ± 8.6	69 ± 5.7	15 ± 2.9 <sup>*,#,+</sup>
20 Amygdaloid nuclei-basomedial	70 ± 5.7	53 ± 7.7	63 ± 8.2	13 ± 1.9 <sup>*,#,+</sup>
Amygdaloid nuclei-central	48 ± 6.5	41 ± 2.4	33 ± 4.4	14 ± 2.1 <sup>*,#</sup>
Amygdaloid nuclei-posteromedial cortical				
Amygdaloid piriform transition	101 ± 5.0	98 ± 5.7	98 ± 3.5	15 ± 1.5 <sup>*,#,+</sup>
Lateral mammillary nucleus	91 ± 6.3	93 ± 5.9	87 ± 5.1	13 ± 0.7 <sup>*,#,+</sup>
25 Superficial grey layer superior colliculus	71 ± 6.3	52 ± 5.4	52 ± 3.7	13 ± 1.6 <sup>*,#,+</sup>
Cerebellum	67 ± 4.4	54 ± 4.4	61 ± 5.4	16 ± 3.3 <sup>*,#,+</sup>
Molecular layer	64 ± 4.2	70 ± 4.9	67 ± 7.0	14 ± 3.0 <sup>*,#,+</sup>
Granule layer	40 ± 2.2	42 ± 4.6	42 ± 3.6	13 ± 2.7 <sup>*,#,+</sup>
Pontine reticular nucleus	14 ± 1.3	10 ± 1.9	10 ± 0.4	6 ± 1.4 <sup>*</sup>

30 Values (fmol/mg tissue) represent mean ± S.E. of five mice per group and were determined by subtracting binding remaining in the presence of 10  $\mu\text{M}$  L-NA from the total binding in serial sections. \*:  $p < 0.01$  vs. SV-129, #:  $p < 0.01$  vs. C57black, +:  $p < 0.01$  vs. type 3 mutant (Turkey's multiple range test).

***Conclusion***

This regional distribution of [ $^3\text{H}$ ]L-NA binding was similar to that seen with the NADPH-diaphorase method. The density of [ $^3\text{H}$ ]L-NA binding in nNOS mutant mice was dramatically reduced in all regions, compared with wild-type mice, but not eNOS mutant mice. nNOS in mouse brain may represent the majority of [ $^3\text{H}$ ]L-NA binding sites. [ $^3\text{H}$ ]L-NA autoradiography may provide a useful method for estimating the distribution of NOS, effects of drugs and pathogenesis of NO-related diseases such as stroke, Alzheimer's disease and tumor. For example, it should be useful for estimating regional changes in NOS binding after cerebral ischemia.

molar concentration), respectively. Hence 10  $\mu$ M D-NA is unlikely to affect the [ $^3$ H]L-NA labelling of specific NOS binding sites and could be used to mask part of the non-specific component of [ $^3$ H]L-NA binding.

There was no significant difference between [ $^3$ H]L-NA binding in eNOS mutant and wild-type mice (Fig. 11, Table 4). Furthermore, NOS enzymatic activity in eNOS mutant mice was almost the same as that in wild-type mice (Table 7). Therefore, these results indicate that the expression of eNOS is low in the mouse brain. However, Dinerman *et al.* (1994) reported the presence of eNOS in the hippocampal pyramidal cells, the cerebellum and olfactory bulb by immunohistochemistry in the rat brain. This discrepancy may reflect species differences and/or the technical differences between quantitative autoradiography and immunohistochemistry.

[ $^3$ H]L-NA binding was inhibited by 7-NI in wild-type and eNOS mutant mice, but not in nNOS mutant mice (Table 5). Hence, the results indicate that binding site of 7-NI in the mouse brain is mainly to nNOS. 7-NI and related substituted indazoles are potent and competitive nNOS inhibitors, Babbedge *et al.* (1993); Moore *et al.* (1993a); Moore *et al.* (1993b), and have been useful for treatment of focal ischemia damage *in vivo*, Yoshida *et al.* (1994), MPTP neurotoxicity *in vivo*, Schulz *et al.* (1995a) and NMDA-induced excitotoxicity *in vivo*, Schulz *et al.* (1995b). 7-NI may also compete with L-arginine for binding to the prosthetic heme group, and affect the pteridine site of the enzyme. Mayer *et al.* (1994). The mechanism of selective nNOS inhibition remains unclear. However, 7-NI at 10 mg/kg i.p., decreases NOS catalytic activity by approximately 30 to 40% within the mouse cerebellum, cerebral cortex and hippocampus. Moore *et al.* (1993); Moore *et al.* (1993). 7-NI does not increase blood pressure, like other NOS inhibitors. Babbedge *et al.* (1993). Moreover, the similarity in [ $^3$ H]L-NA binding in eNOS mutant mice and wild-type mice further supports the use of eNOS mutant mice to screen compounds for use in the treatment or prevention of cerebral ischemia or stroke.

distribution of [<sup>3</sup>H]L-NA binding presumably reflects the density and distribution of nNOS, the predominant isoform in brain which comprises more than 95% of NOS activity in the brain.

While the density and distribution of binding was similar in the two wild-type strains, it was relatively higher in mouse than rat brain (Fig. 13). In particular, higher binding was detected in the hippocampus of the mouse which may correspond to the greater NADPH-diaphorase activity reported in mouse CA1 pyramidal cells. Wallace *et al.* (1992). Because activity of the inducible isoform, type 2 NOS (iNOS), is undetectable in normal mouse brain, Yoshida *et al.* (1995), it is unlikely to be a major source for [<sup>3</sup>H]L-NA binding in our studies. The values of [<sup>3</sup>H]L-NA binding in our rat study were higher than those of Kidd *et al.* (1995), although the rank order of binding activity in rat brain regions was similar in both studies. *Id.* These discrepancies may be due to strain differences or different concentrations of added [<sup>3</sup>H]L-NA.

[<sup>3</sup>H]L-NA binding in nNOS mutant mice was remarkably lower than wild-type or eNOS mutant mice and the L-NA displaceable [<sup>3</sup>H]L-NA binding was distributed diffusely throughout the brain (Table 4). Thus, it is presumed that the loss of [<sup>3</sup>H]L-NA binding reflected the absence of nNOS. The residual binding probably did not reflect the labeling of eNOS, since the binding in nNOS mutant brain was not stereoselective and could be displaced by both L- and D-NA.

D-NA displaceable binding, detectable in brain of both wild-type strains, may represent an additional binding site for L-arginine unrelated to NOS protein. The fact that both L-NA and D-NA were able to decrease [<sup>3</sup>H]L-NA binding to the gelatinized glass slide (see Fig. 14) suggests that the D-NA-displaceable component of [<sup>3</sup>H]L-NA binding is non-specific. Therefore, "specific" binding should not be equated with "displaceable" binding, especially when the displacer is the unlabelled tracer, or closely related to the tracer.

Michel *et al.* (1993) reported that L-NA and D-NA displaced [<sup>3</sup>H]L-NA binding with  $pl_{50}$  values, i.e., the logarithm of the concentration of competing compound causing 50% inhibition of [<sup>3</sup>H]L-NA binding, of 7.1 and 3.1 (log

by approximately 20 to 30% in SV-129 mice (Figs. 14A, 14B, Table 6). Both L-NA and D-NA decreased slightly the binding to the gelatinized slide itself (Fig. 14C, 14D). Binding in brain of the nNOS mutant mice was not significantly higher than background in any regions (Fig. 11D).

5      ***NOS catalytic activity (Table 7)***

10      The highest NOS catalytic activities in SV-129 mice were found in the cerebellum, thalamus/hypothalamus and cerebral cortex/amygdala. Moderate activities were observed in the brain stem, hippocampus, olfactory bulb and striatum. The activities in eNOS mutant mouse brain were similar to those found in SV-129. In nNOS mutant mice NOS activity was dramatically reduced in all regions investigated. Very low levels of residual NOS catalytic activity were measured in type 1 mutant mice (0-1.7% of SV-129) (Table 7).

***Discussion***

15      In this Example, the distribution and density of [<sup>3</sup>H]L-NA NOS binding sites in the brains of wild-type, eNOS mutant mice, and nNOS mutant mice was examined using quantitative *in vitro* autoradiography. Previous studies showed that [<sup>3</sup>H]L-NA binds specifically and stereospecifically to the nNOS isoform in the rat brain. Kidd *et al.* (1995); Michel *et al.* (1993). Specific binding of [<sup>3</sup>H]L-NA to the endothelium of placental blood vessels was recently established by  
20      Rutherford *et al.* (1996) using *in vitro* autoradiography. Using similar techniques, we recently observed specific [<sup>3</sup>H]L-NA binding to pig aortic endothelium, which is displaceable by unlabelled L-NA. Hence, this ligand can detect the presence of both eNOS and nNOS by *in vitro* autoradiography.

25      The highest density of [<sup>3</sup>H]L-NA binding was observed in the olfactory bulb, the amygdaloid complex, the islands of Calleja, and the cerebellum (Fig. 12). In general, these regions exhibit the highest NADPH-diaphorase activity and brain NOS positive immunostaining in the mouse, Huang *et al.* (1993), and in the rat, Schmidt *et al.* (1992); Vincent *et al.* (1992). Thus, the density and

transition. Also, the islands of Calleja, tenia tecta, rhinal fissure, hippocampal CA3 subfield, dentate gyrus, anterior cortical and basomedial amygdaloid nuclei, lateral mammillary nucleus, superficial grey layer of the superior colliculus and cerebellar molecular layer contained high densities of [<sup>3</sup>H]L-NA (50-90 fmol/mg tissue). Other area of prominent binding (30-50 fmol/mg tissue) were the plexiform layer of the olfactory bulb, cortical layers I-II, hippocampal CA1 subfield, dorsomedial and ventromedial hypothalamic nuclei, central amygdaloid nuclei and granule layer of cerebellum. The striatum and pontine reticular nucleus showed relatively poor binding (<20 fmol/mg tissue) (Figs 11A, 11B and 12, Table 4). Binding was not significantly different from background in cortical layers III-VI, posterior and ventral posteromedial thalamus nuclei and medial mammillary nucleus (Figs 11A, 11B and 12).

The density of [<sup>3</sup>H]L-NA binding in nNOS mutant mice was significantly decreased in all regions (Fig. 11D). [<sup>3</sup>H]L-NA in eNOS mutant mice was similar to wild-type mice (Fig. 11C, Table 4).

The distribution of [<sup>3</sup>H]L-NA binding was similar in mouse and rat brain as shown in Fig. 13. Although the binding was relatively higher in mouse brain.

***Effects of 7-NI on [<sup>3</sup>H]L-N<sup>G</sup>-nitro-arginine binding (Fig. 14 and Table 5)***

In the presence of 7-NI (100 μM), [<sup>3</sup>H]L-NA binding was significantly decreased in all regions measured in wild-type (Fig. 14) and eNOS mutant mice, but not in nNOS mutant mice. In the presence of 7-NI, the densities of [<sup>3</sup>H]L-NA binding did not show significant differences between wild-type, eNOS mutant and nNOS mutant mice (Table 5).

***Effects of L-NA and D-NA on [<sup>3</sup>H]L-N<sup>G</sup>-nitro-arginine binding (Figs. 11, 14 and Table 6)***

In the presence of L-NA (10 μM), the density of [<sup>3</sup>H]L-NA binding sites was very low in all brain regions of all mouse strains (Figs. 11D, 12H). In the presence of D-NA (10 μM), the density of [<sup>3</sup>H]L-NA binding sites was decreased

### *NOS catalytic activity*

NOS activity was measured by the conversion of [ $^3\text{H}$ ]arginine to [ $^3\text{H}$ ]citrulline according to the method described by Bredt *et al.* (1990b) with minor modifications. Samples were homogenized in 500  $\mu\text{l}$  cold 50 mM HEPES buffer (Research Organics Inc., OH, U.S.A.) containing 1 mM EDTA (pH 7.4, Sigma). Homogenates were centrifuged at 500  $\times g$  for 5 min. at 4°C and the supernatant used for assay. The incubation mixture contained 100  $\mu\text{l}$  HEPES (50 mM, pH 7.4), EDTA (1 mM), reduced  $\beta$ -nicotinamide adenine dinucleotide phosphate ( $\beta$ -NADPH, 1 mM, Sigma), dithiothreitol (1 mM, Sigma), calmodulin (10  $\mu\text{g}/\text{ml}$ , Calbiochem, CA, U.S.A.) and  $\text{CaCl}_2$  (1 mM) and 25  $\mu\text{l}$  of 100 mM L-[ $^3\text{H}$ ]arginine (1 mCi, Dupont NEN, MA, U.S.A.). The reaction was started by adding the supernatant (25  $\mu\text{l}$ ) and stopped after 20 min incubation at 37°C by adding HEPES buffer (20 mM, pH 5.5) containing EDTA (2 mM), pH 5.5. The mixture was then applied to cation-exchange columns containing Dowex AG50WX-8 ( $\text{Na}^+$  form; Bio-Rad, Richmond, VA, U.S.A.) and eluted with 2 ml of distilled water. [ $^3\text{H}$ ]Citrulline was measured within eluates by a scintillation spectrometry (Packbeta 1209, LKB, Gaithersburg, MD, U.S.A.).

### *Statistical analysis*

Data are presented as mean  $\pm$  SE. Statistical comparisons were made by one-way ANOVA and Tukey's multiple-range test or Student's *t*-test using the software super ANOVA (Abacus Concepts, Berkeley, CA, U.S.A.).

### *Results*

#### *Regional distribution of [ $^3\text{H}$ ]L-N $^G$ -nitro-arginine binding in the 4 mouse strains (Figs. 11-13, Table 4)*

[ $^3\text{H}$ ]L-NA binding was heterogeneously distributed in wild-type (SV-129 and C57Black/6) mouse brain, with highest densities ( $>90$  fmol/mg tissue) associated with the granular layer of the olfactory bulb, the medial amygdaloid nuclei, posteromedial cortical amygdaloid nuclei and amygdaloid piriform

*et al.*, (1995). Prior to experiments, sections were brought to -20°C and then to room temperature. Sections were preincubated for 15 min at room temperature in 50 mM Tris-HCl (pH 7.3) to remove the endogenous ligands and/or modulators, then incubated for 30 min at room temperature in 50 mM Tris-HCl buffer containing 10 µM CaCl<sub>2</sub> and 25 nM N<sup>G</sup>-nitro-L-[2,3,4,5-<sup>3</sup>H]arginine hydrochloride ([<sup>3</sup>H]L-NA, specific activity: 48-57 Ci/mmol, Amersham, Arlington Heights, IL, U.S.A.). Unlabelled L-N<sup>G</sup>-nitro-arginine (L-NA, Sigma, St. Louis, MO, U.S.A.), D-N<sup>G</sup>-nitro-arginine (D-NA, RBI, Natick, MA, U.S.A.) and 7-nitroindazole (7-NI, Cookson Chemicals Ltd., England) was added at concentrations of 10, 10, and 100 µM, respectively. The sections were then washed twice for 5 min in ice-cold buffer and rinsed for 10 sec in ice-cold distilled water to eliminate residual buffer. After drying with cold air, the slides were tightly apposed to <sup>3</sup>H-Hyperfilm (Amersham) together with tritiated polymer standards (Amersham) and exposed at -4°C for 6 weeks.

#### ***Densitometric analysis***

Films were developed in Kodak D-19 and fixed in Kodak Rapid Fixer, according to the manufacturer's instructions. The optical density of the regions of interest was measured by a computer-assisted image analysis (System M4, Imaging Research, St. Catharines, Ontario, Canada). The relationship between optical density and radioactivity was examined with reference to the tritium standards (Amersham, [<sup>3</sup>H]microscale) co-exposed with the tissue sections. The optical density of the brain regions measured in the present study was in a range in which the optical density and the radioactivity of the <sup>3</sup>H-microscale showed a near linear relationship. The densities of NOS binding sites are expressed in fmol bound [<sup>3</sup>H]L-NA/mg tissue using the [<sup>3</sup>H]L-NA concentration of 25 nM.

-47-

other hemodynamic mechanism. These results emphasize the importance of knockout mice to dissect the role of individual proteins in these pathophysiological events.

## ***Example 12***

### ***Brain Distribution of NOS in Wild-type and Mutant Mice***

#### ***Experimental Procedures***

##### ***Animals***

Adult male wild-type, SV-129 and C57black/6 (Taconic Farms, Germantown, NY, U.S.A.), and adult male and female nNOS mutant, Huang *et al.*, *Cell* 75:1273-1286 (1993), and eNOS mutant mice weighing 22 to 29 g and adult male Wistar rats (Charles River, MA, U.S.A.) weighing 250 to 300 g were allowed free access to food and water.

##### ***Tissue preparation***

Mice and rats were sacrificed by decapitation under 2% halothane anesthesia (30% O<sub>2</sub> + 70% N<sub>2</sub>O). The brains were rapidly removed, immediately frozen in powdered dry ice, and stored at -70°C. Twelve µm sagittal or coronal sections were cut in a cryostat-microtome at -18°C (Leitz 1720, Leica, Deerfield, IL, U.S.A.) and thaw-mounted onto gelatin-coated slides (1% gelatin and 0.1% KCr<sub>2</sub>O<sub>7</sub>). Adjacent sections were stained with cresyl violet and hematoxylin eosin, and stored at -70°C.

##### ***[<sup>3</sup>H]L-NG-Nitro-arginine autoradiographic binding assay***

The method for the autoradiographic visualization of NOS binding using [<sup>3</sup>H]L-NG-Nitro-arginine ([<sup>3</sup>H]L-NA) has been described previously. Rutherford

ischemia, Kano *et al.* (1991), and reduced cerebral perfusion during hemorrhagic hypotension. Koketsu *et al.* (1992). The above evidence coupled with our observation that arterial blood pressures are less stable in eNOS mutant animals, e.g., during hypercapnic challenge, shows the importance of eNOS regulation of vascular hemodynamics and its potential importance to stroke outcome.

eNOS mutant mice maybe more susceptible to ischemic injury because NO modulates the microcirculation. NO may also block leukocyte adhesion and decrease microvascular stasis often seen following MCA occlusion. Garcia *et al.* (1993). Kubes *et al.* (1991) reported that superfusing mesenteric vessels with NOS inhibitors increased leukocyte adhesion. Kurose *et al.* (1994) found that L-arginine attenuated ischemia-induced platelet-leukocyte aggregation, mast cell degranulation and albumin extravasation. We also found that rCBF was more severely reduced in homologous brain areas after MCA occlusion in eNOS but not nNOS mutant mice. Huang *et al.* (1994). These findings confirm that NO plays a role in the modulation of the microcirculation which may contribute to the outcome of ischemia.

eNOS inhibition may account for the increases in infarct size in some studies after nitro-L-arginine, particularly after large doses. Yamamoto *et al.* (1992); Zhang and Iadecola (1993); Morikawa *et al.* (1994b). By contrast, neuroprotection was reported after selective nNOS inhibition with 7-nitroindazole, Yoshida *et al.* (1994), or FPL17477, Zhang *et al.* (1995). Consistent with present findings, infarction size increased when nitro-L-arginine was administered to mutant mice expressing only the eNOS isoform (i.e., nNOS knockout mouse). Importantly, iNOS enzyme activity is not measurable in mouse (SV-129 strain) brain for at least 4 days after permanent MCA occlusion. Yoshida *et al.* (1995).

We conclude that NO possesses a dual role in focal cerebral ischemia. Depending upon its source, NO may be toxic or protective to brain under ischemic conditions. Parenchymal NO overproduction may lead to neurotoxicity whereas endothelial NO may protect brain tissue by increasing rCBF or some

Japan) and recorded using the MacLab data acquisition and analysis system. After baseline stabilization, nitro-L-arginine or nitro-D-arginine solution (1 mM) was superfused into the window and the diameter of pial arteriole measured continuously 40 min thereafter.

5 As depicted in Figure 10, unlike wild-type mice, nitro-L-arginine superfusion alone increased vessel diameter in eNOS mutant animals, reaching maximum at 30 min ( $p < 0.05$  vs wild-type). Similar changes in rCBF were recorded in preliminary experiments by laser Doppler flowmetry using the closed cranial window technique (data not shown). There was no change in MABP  
10 during nitro-L-arginine superfusion. No change was found in pial diameter after nitro-D-arginine superfusion in eNOS mutant mice (data not shown).

In the eNOS mutant, nitro-L-arginine superfusion inhibits nNOS within subjacent brain parenchyma, and there is published evidence for a contribution from parenchymally-derived NO to cerebrovascular tone. Iadecola *et al.*, 1994.  
15 This example provides evidence that nitro-L-arginine may directly decrease tone in resistance vessels or surrounding tissues of eNOS mutants by showing that nitro-L-arginine superfusion dilates pial arterioles in these mutants. However, the mechanism remains unknown.

NO is a potent vasodilator and it, or a closely related chemical, is proposed as EDRF or endothelium-derived relaxing factor. Ignarro *et al.* (1987);  
20 Palmer *et al.* (1988). This is evidence to support the hypothesis that endothelium-derived NO or reaction product may be beneficial to stroke by augmenting rCBF in ischemic territory. Infusion of L-arginine, a substrate for NOS, caused NO-dependent vasodilation and increased rCBF distal to MCA occlusion in rats.  
25 Morikawa *et al.* (1994a). Dynamic susceptibility contrast magnetic resonance imaging also suggests that L-arginine infusion cerebral blood flow and blood volume. Hamberg *et al.* (1993). Zhang *et al.* (1994) reported that NO donors improved rCBF in the ischemic area and reduced infarct size as well. In addition, sectioning of NOS-containing parasympathetic cerebrovascular fibers in  
30 sphenopalatine ganglia, Nozaki *et al.* (1993), increased infarct size after focal

-44-

in eNOS mutant mice, this decrease was likely caused by nNOS inhibition. However, the reductions after nitro-L-arginine treatment were not as large as expected (24% decrease) based on the observation in nNOS mutant, suggesting that either the degree of nNOS inhibition was small using the employed protocol or that undocumented factors such as systemic hypotension induced by nitro-L-arginine, may have attenuated an even greater reduction in infarct size.

### ***Example 11***

#### ***Increase in Blood Vessel Diameter after Nitro-L-arginine Superfusion in Wild-type and eNOS Mutant Mice***

The mouse head was fixed in a stereotaxic frame and the skull exposed by a longitudinal skin incision. A stainless steel cranial window ring (8.0 mm in inner diameter, 2.0 mm in height) containing three ports was imbedded into a loop of bone wax over the skull. Dental acrylic was then applied. A craniotomy (2 x 1.5 mm) was made in the left parietal bone within the ring of the window. After dura was opened and the brain surface superfused with artificial cerebrospinal fluid (aCSF), a cover glass was placed to close the window. The volume under the window was approximately 0.1 ml. The composition of aCSF was as follows (in mMol/L): Na<sup>+</sup> 156.5, K<sup>+</sup> 2.95, Ca<sup>++</sup> 1.25, Mg<sup>++</sup> 0.67, Cl<sup>-</sup> 138.7, HCO<sub>3</sub><sup>-</sup> 24.6, dextrose 3.7 and urea 0.67. The pH value of aCSF was kept at 7.35-7.45, and monitored continuously with a pH meter (Corning Inc., Corning, NY). The aCSF was superfused by an infusion pump (0.4 ml/min) via a PE-100 tubing connected to a window port. Intracranial pressure was maintained at 5-8 mm Hg. The temperature of aCSF within the windows was maintained at 36.5-37.0°C.

Pial vessels were visualized through a cranial window by an intravital microscope (Leitz, Germany) equipped with a video camera (C2400, Hamamatsu Photonics, Hamamatsu, Japan). The diameter of a single pial arteriole (20-30 µm) was continuously measured by a video width analyzer (C3161, Hamamatsu,

The core temperature was kept normothermic as above. The level of rCBF was monitored by laser Doppler flowmetry. Dalkara *et al.* (1995).

Following reflection of the skin and subcutaneous tissue, an rCBF probe tip was secured directly over the parietal skull with glue (Borden Inc, Columbus, OH), away from pial vessels. An initial rCBF recording was taken as 100% and subsequent flow changes were expressed relative to this value. After heparin (10 units, iv) administration, arterial blood pressure was lowered -10 mmHg every 5 min by withdrawing femoral artery blood (0.05-0.15 ml). Corresponding rCBF readings were averaged for each 10 mm Hg stepwise reduction. The duration of total experiment was approximately 2 - 2.5 hrs. The upper limit of autoregulation was not tested in these mice.

When arterial blood pressure was lowered step-wise by controlled hemorrhagic hypotension in wild-type mice, cerebral blood flow stayed relatively constant until <40 mmHg. However, as depicted in Figure 9, at low blood pressures, the autoregulation curve was shifted slightly to the right in eNOS mutant animals, suggesting higher cerebrovascular resistance than wild type at lower perfusion pressures.

The data in Examples 9-10 demonstrate that deletion of the mouse eNOS gene is associated with larger brain infarcts and more pronounced rCBF reductions in corresponding brain regions after MCA occlusion. *See* Figure 8. eNOS mutants also exhibit proportionally lower rCBFs at reduced perfusion pressures during controlled hemorrhagic hypotension. *See* Figure 9. While the reduction in rCBF at reduced perfusion pressure may be due to hypertension in the eNOS mutant animal, no hypertensive changes were noted in the vessel wall or heart on preliminary histopathological analyses. The contribution of high blood pressure to infarct enlargement in eNOS animals was probably minor since infarct size did not change in eNOS mutants made normotensive by hydralazine administration.

Nitro-L-arginine decreased infarct volumes in eNOS mutant mice but not in wild-type animals. Since nNOS is the only constitutively expressed isoform

- Morikawa *et al.* (1994a), *Stroke*. 25:429-435.  
Morikawa *et al.* (1994b), In: *The human brain circulation* (J Bevens, eds.), Harbor Basin Conference, Vermont. 373-387.  
Murphy *et al.* (1993), *Trends Neurosci.* 16:323-328.  
5 Nathan (1992), *FASEB J.* 6: 3051-3064.  
Nathan & Xie (1994), *Cell* 278:915-918.  
Nozaki *et al.* (1993), *J. Cereb. Blood Flow Metab.* 13: 70-79.  
O'Dell *et al.* (1991), *Proc. Nat'l Acad. Sci. (USA)* 88: 11285-11289.  
O'Dell *et al.* (1994), *Science*. 265:542-546.  
10 Palinski *et al.*, *Proc. Natl. Acad. Sci (USA)* 86:1372-1376 (1989).  
Palinski *et al.*, *Arterioscler. Thromb.* 14:605-616 (1994).  
Palmer *et al.* (1987), *Nature* 327: 524-526.  
Palmer *et al.* (1988), *Nature*. 333:664-666.  
Peng *et al.* (1995), *J. Biol. Chem.* 270: 14214-14219.  
15 Plump *et al.* (1992), *Cell* 71:343-353.  
Purcell-Huynh *et al.* (1995), *J. Clin. Invest.* 95: 2246-2257.  
Radomski *et al.* (1991), *Trends in Pharm. Sci.* 12:87-88.  
Radomski *et al.* (1995), *Atherosclerosis* 18: S69-80.  
Rajfer *et al.* (1992), *N. Engl. J. Med.* 326: 90-94.  
20 Ramagopal & Leighton (1989), *Eur. J. Pharmacol.* 174: 297-299.  
Ramdomsky *et al.* (1990), *Proc Natl Acad Sci USA.* 87:5193-5197.  
Rees *et al.* (1990), *Br J Pharmacol.* 101: 746-752.  
Remington's Pharmaceutical Sciences, Mack Publishing Co., Easton, PA (1990).  
Ross (1996), *Nature Medicine* 2:527-528.  
25 Ross (1995), *Ann. Rev. Physiol.* 57:791-804.  
Rutherford *et al.* (1995), *Br. J. Pharmacol.* 116:3099-3109.  
Schmidt & Walter (1994), *Cell* 78:919-925.  
Schmidt *et al.* (1992), *J. Histchem. Cytochem.* 40:1439-1456.  
Schultz *et al.* (1996), *J. Neurochem.* 67:430-433.  
30 Schulz *et al.* (1995a), *J. Neurochem.* 64:936-939.  
Schulz *et al.* (1995b), *J. Neurosci.* 15: 8419-8429.  
Schuman & Madison (1991), *Science* 254: 1503-1506.  
Schwartz *et al.* (1995), *Circulation Res.* 77: 445-465.  
Shibuki & Okada (1991), *Nature* 349: 326-328.  
35 Snyder *et al.* (1991), *Trends Pharmacol Sci.* 12:125-128.  
Snyder (1992), *Science* 257: 494-496.  
Snyder (1995), *Nature* 377:196-197.  
Sobey *et al.* (1995), *Circ. Res.* 77: 536-543.  
Toda & Okamura (1990), *Biochem. Biophys. Res. Comm.* 170: 308-313.  
40 Topors *et al.* (1995), *Circulation* 92:I-564.  
Tottrup *et al.* (1991), *Am. J. Physiol.* 260:G385-G387.  
Tybulewicz *et al.* (1991), *Cell* 65: 1153-1163.  
van den Maagdenberg *et al.* (1993), *J. Biol. Chem.* 268: 10540-10545.  
Vincent *et al.* (1992), *Neurosci* 46:755-784.  
45 Wallace *et al.* (1992), *NeuroReport* 3:953-956.

- Wilcox *et al.* (1994), *Circulation* 90 (supp I):I-298.  
Yamamoto *et al.* (1992), *J Cereb Blood Flow Metab.* 12:717-726.  
Yang *et al.* (1994), *Stroke* 25:165-170.  
Yla-Herttuala *et al.*, *J. Clin. Invest.* 84:1086-1095 (1989).  
5 Yoshida *et al.* (1994), *J Cereb Blood Flow Metab.* 14:924-929.  
Yoshida *et al.* (1995), *Neuroscience Letter.* 194:214-218.  
Zea-Longa *et al.* (1989), *Stroke.* 20:84-91.  
Zhang *et al.* (1992), *Science* 258:468-471.  
Zhang *et al.* (1993), *NeuroReport.* 4:559-562.  
10 Zhang *et al.* (1994), *J Cereb Blood Flow Metab.* 14:217-226.  
Zhang *et al.* (1995), *J Cereb Blood Flow Metab.* 15(Suppl.):S90.  
Zhang & Snyder (1992), *Proc. Nat'l Acad. Sci (USA)* 89: 9387-9385.

***What Is Claimed Is:***

1. A method of screening compounds for potential utility to treat cerebral ischemia or stroke, comprising:

5 (a) providing a transgenic non-human animal having a disrupted endothelial nitric oxide synthase gene;

(b) administering a compound to be tested to said transgenic animal;

(c) determining the effect of said compound on infarct size following induction of focal cerebral ischemia in the brain of said animal; and

10 (d) correlating the effect of said compound on infarct size with a potential therapeutic utility to treat cerebral ischemia or stroke;

wherein said compound is not a NOS inhibitor.

2. The method of screening compounds as claimed in claim 1, wherein said transgenic non-human animal is a mouse.

15 3. The method of screening compounds as claimed in claim 1, wherein the blood pressure of said transgenic non-human animal has been rendered normotensive.

4. The method of screening compounds as claimed in claim 2, wherein said compound induces nitric oxide synthesis in the endothelia.

-76-

5. The method of screening compounds as claimed in claim 4, wherein said compound does not induce neuronal nitric oxide overproduction.

6. The method of screening compounds as claimed in claim 4, wherein focal ischemia is induced by occluding the middle cerebral artery.

5 7. A method of screening compounds for potential utility to treat atherosclerosis, comprising:

(a) providing a transgenic non-human animal having a disrupted endothelial nitric oxide synthase gene;

(b) administering a compound to be tested to said transgenic animal;

10 (c) determining the effect of said compound on atherosclerosis in said animal; and

(d) correlating the effect of said compound on atherosclerosis in said animal with a potential utility to treat atherosclerosis;

wherein said compound is not a NOS inhibitor.

15 8. The method of screening compounds as claimed in claim 6, wherein determining the effect of said compound on atherosclerosis is determined by measuring neointima formation following vascular injury.

-77-

9. The method of screening compounds as claimed in claim 6, wherein determining the effect of said compound on atherosclerosis is determined by measuring the rate of endothelial regeneration following vascular injury.

10. The method of screening compounds as claimed in claim 6, wherein said transgenic non-human animal has a disrupted apoE gene.

11. A method of screening compounds for potential utility to treat a vascular endothelial disorder comprising:

(a) providing a transgenic non-human animal having a disrupted endothelial nitric oxide synthase gene;

(b) administering a compound to be tested to said transgenic animal;

(c) determining the effect of said compound on said vascular endothelial disorder in said animal; and

(d) correlating the effect of said compound on said vascular endothelial disorder in said animal with a potential utility to treat said vascular endothelial disorder;

wherein said compound is not a NOS inhibitor.

1/24

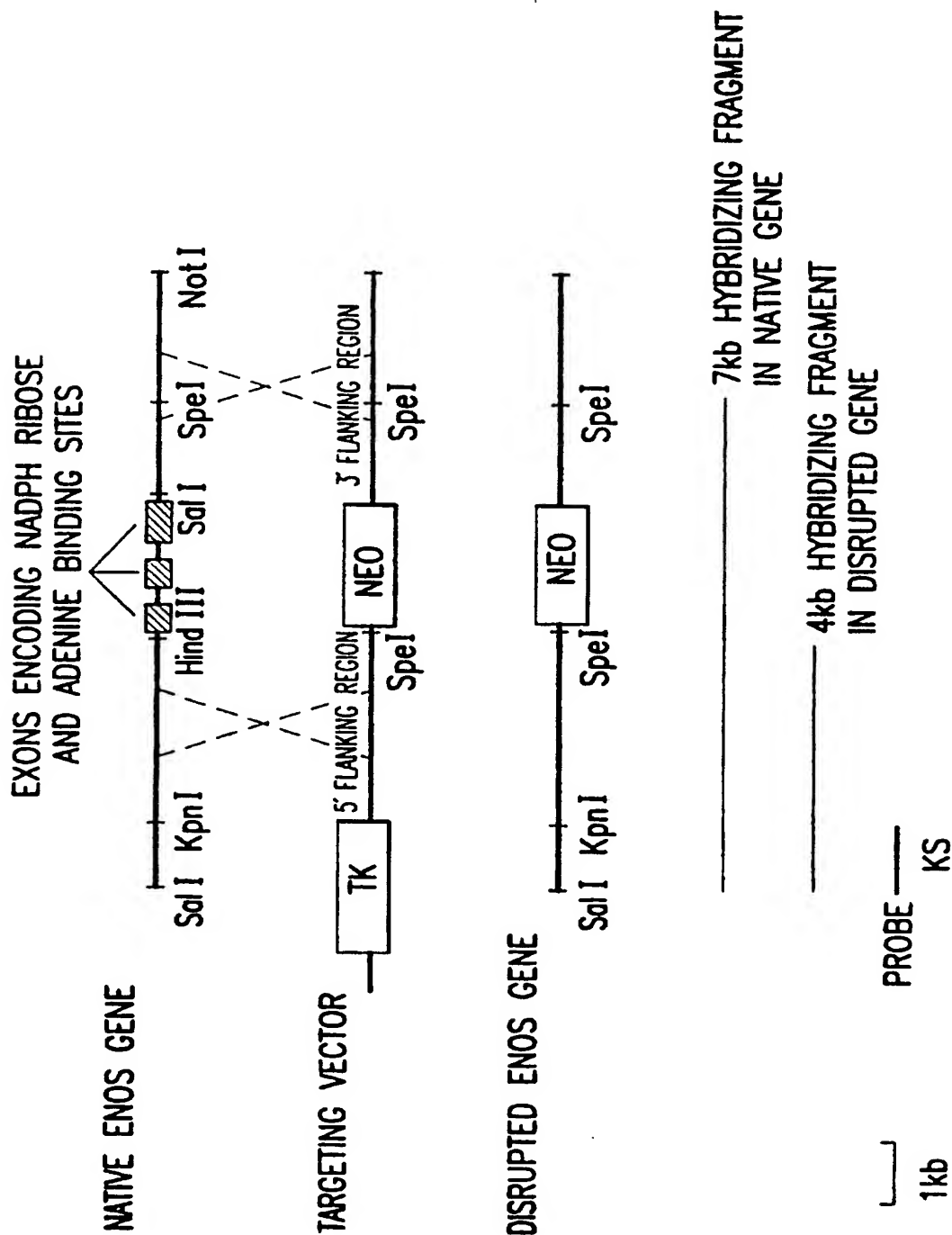


FIG.1

2/24

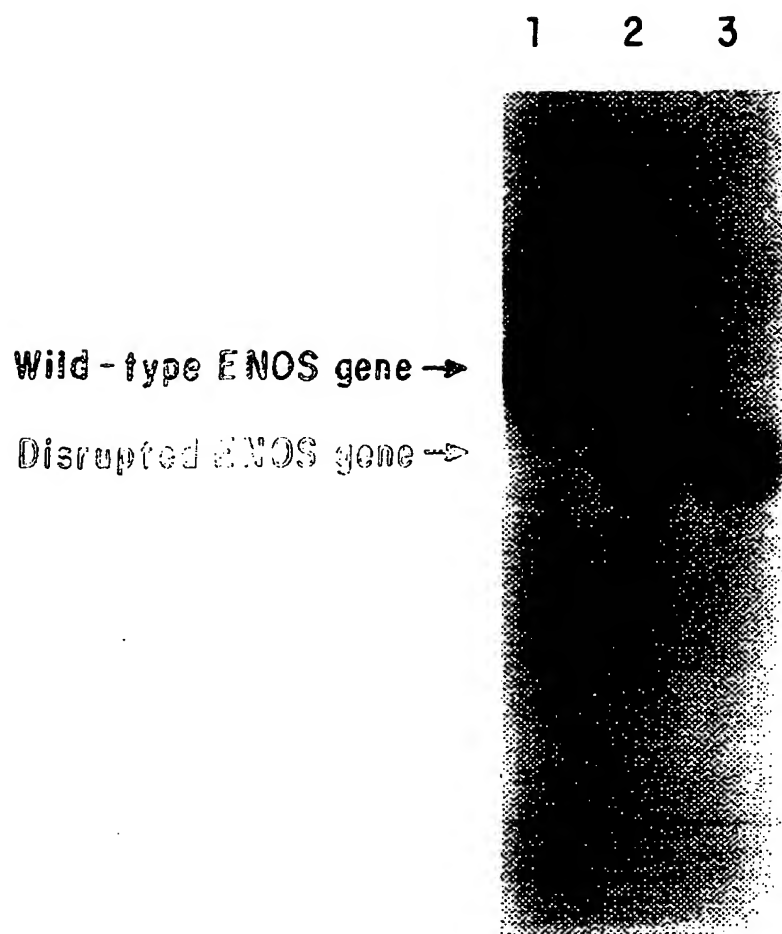


FIG. 2

SUBSTITUTE SHEET (RULE 26)

3/24

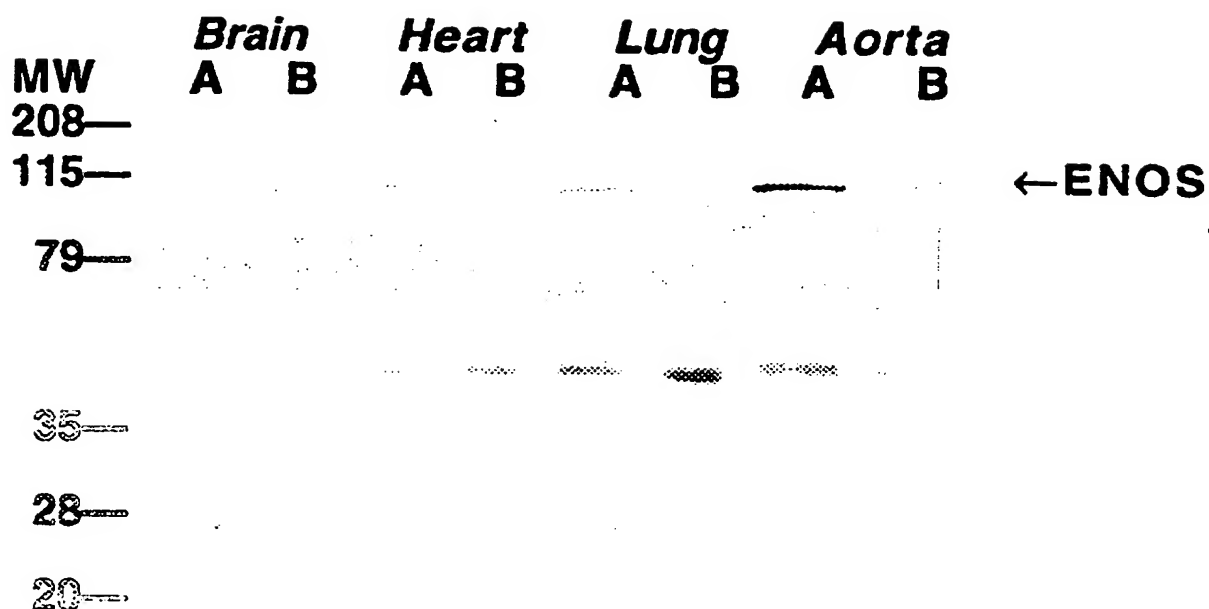


FIG. 3

SUBSTITUTE SHEET (RULE 26)

4/24

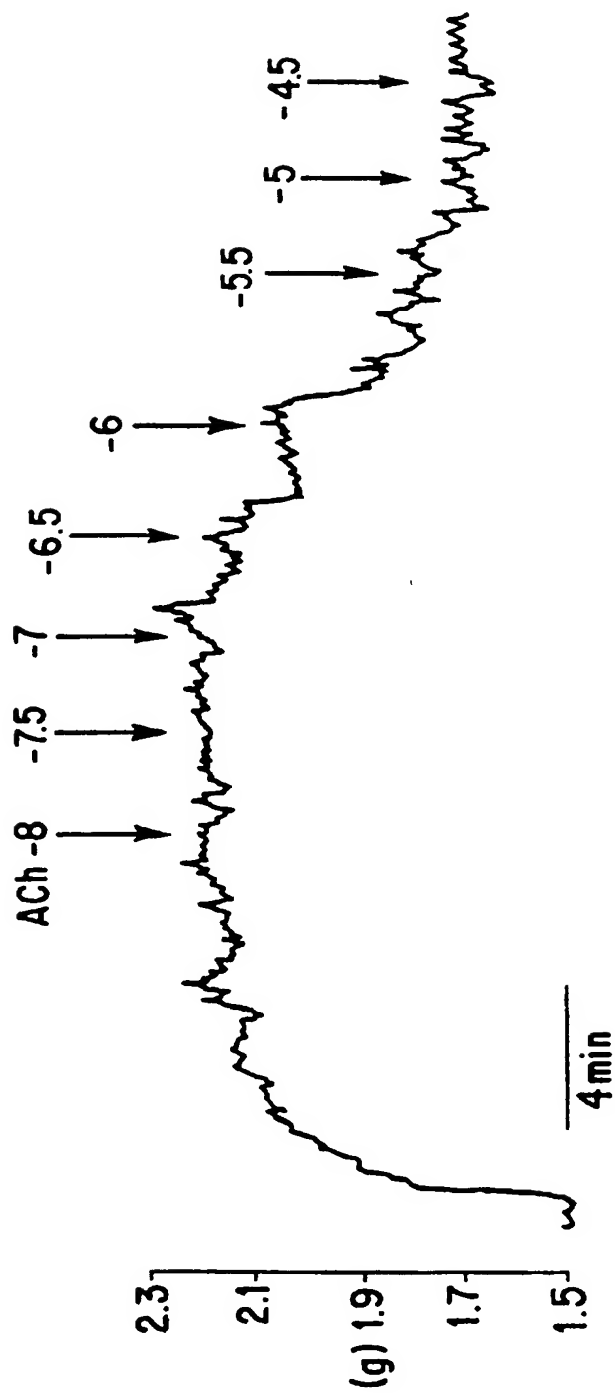


FIG. 4A

5/24

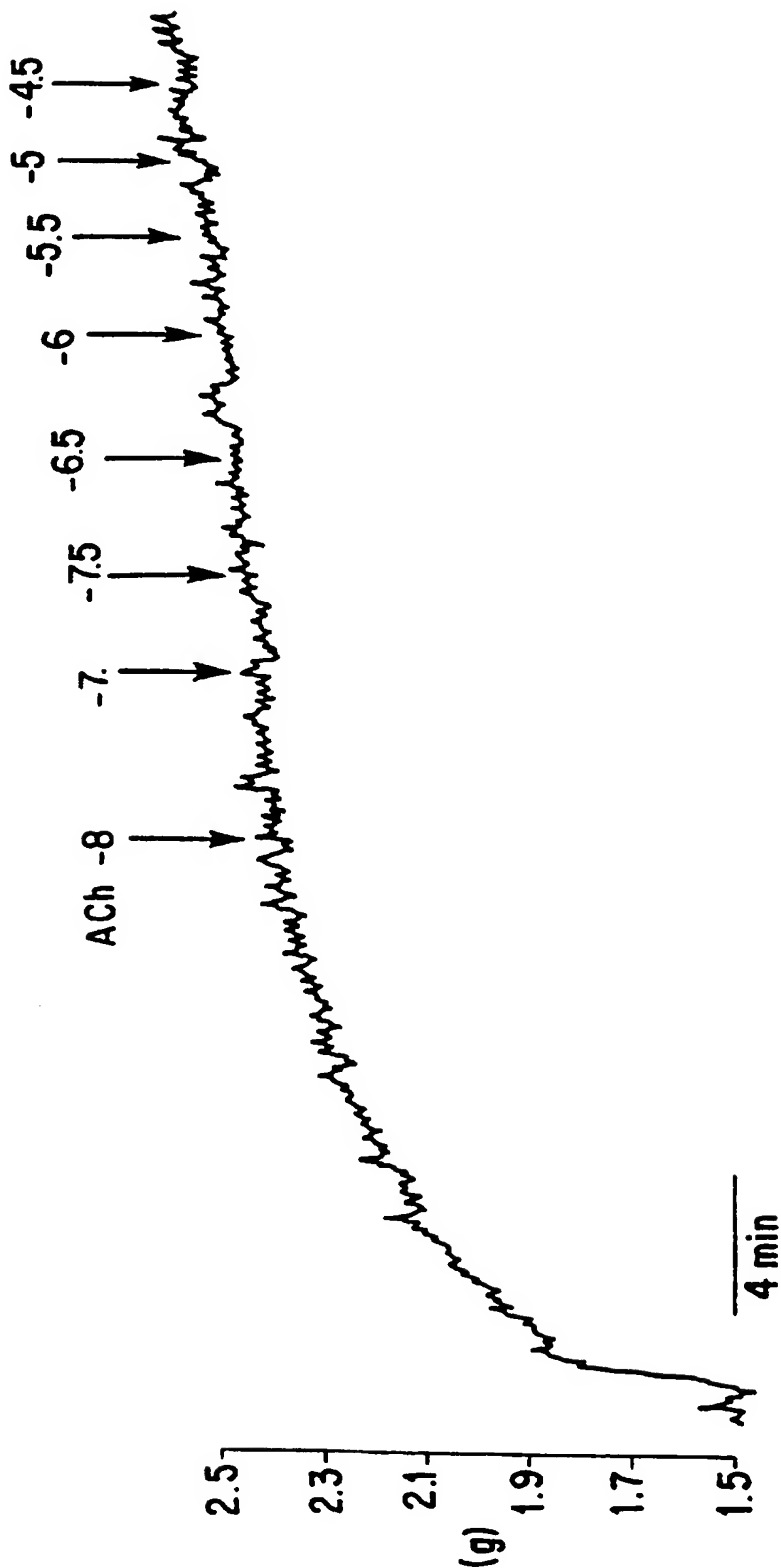


FIG. 4B

6/24

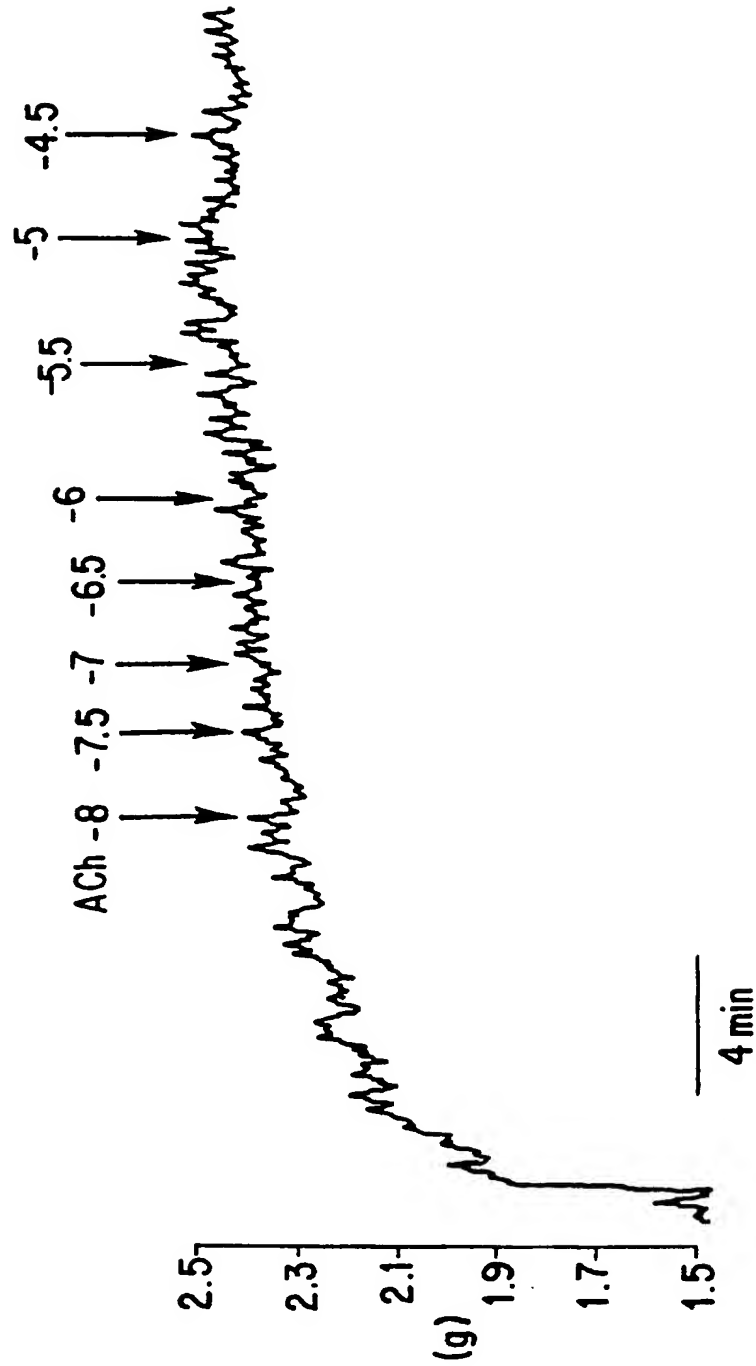


FIG. 4C

7/24

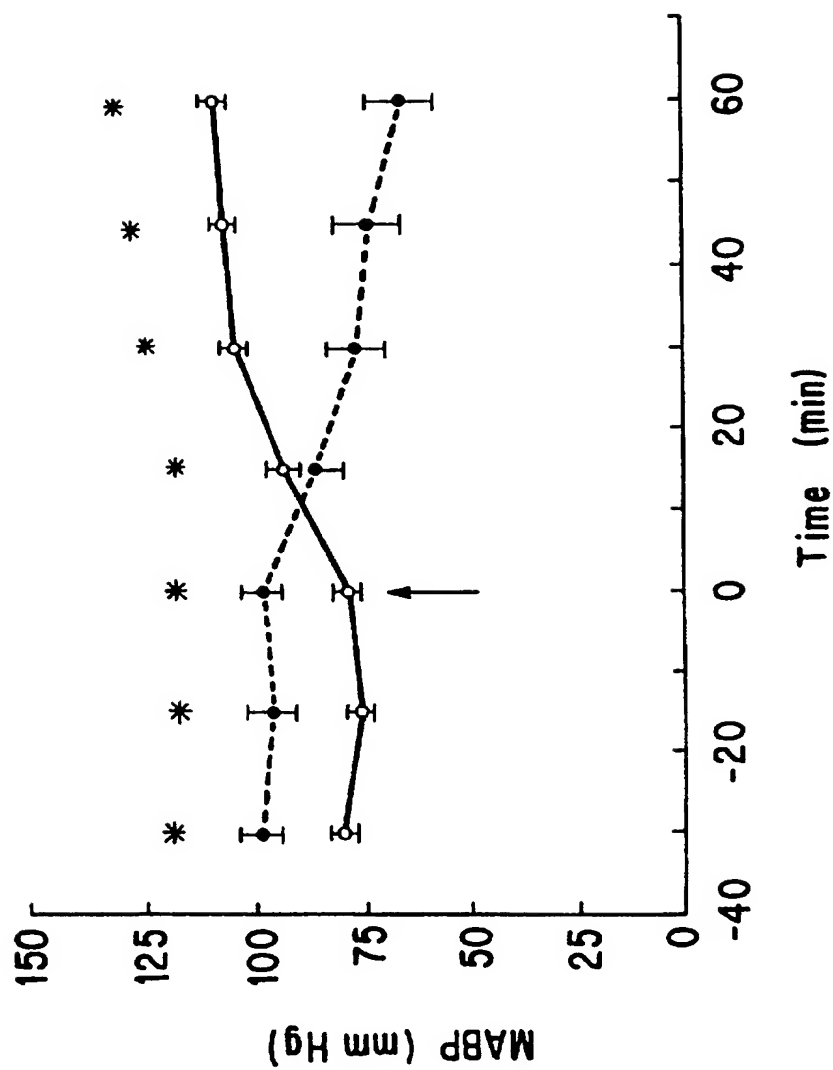


FIG. 5

8/24



FIG. 6A

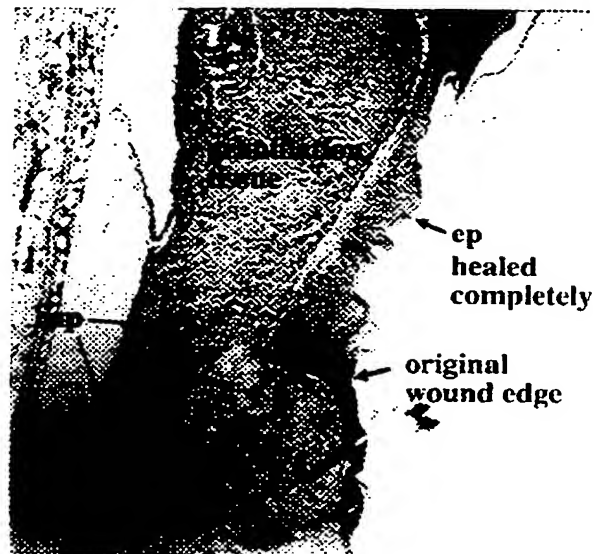


FIG. 6B

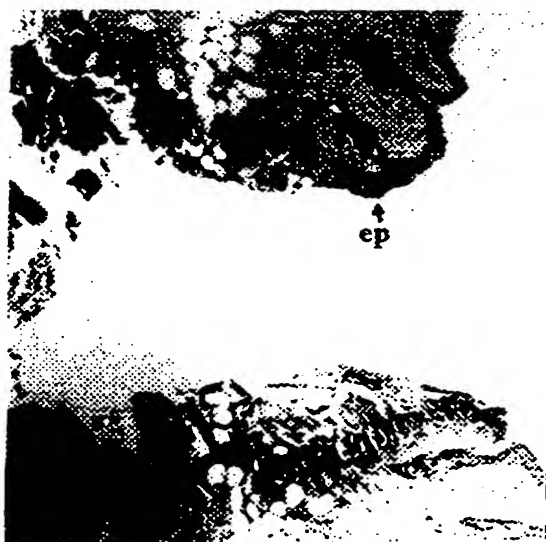


FIG. 6C

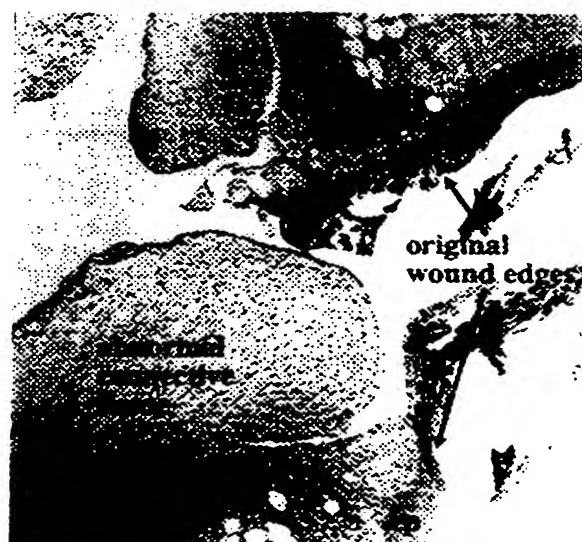


FIG. 6D

SUBSTITUTE SHEET (RULE 26)

9/24

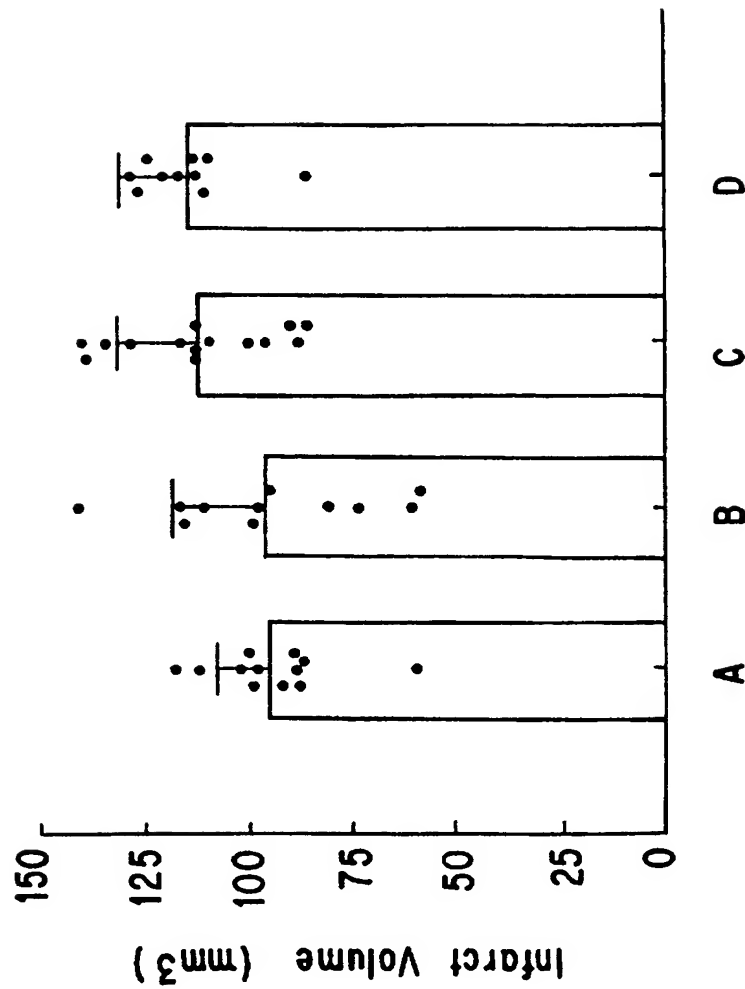


FIG. 7A

10/24

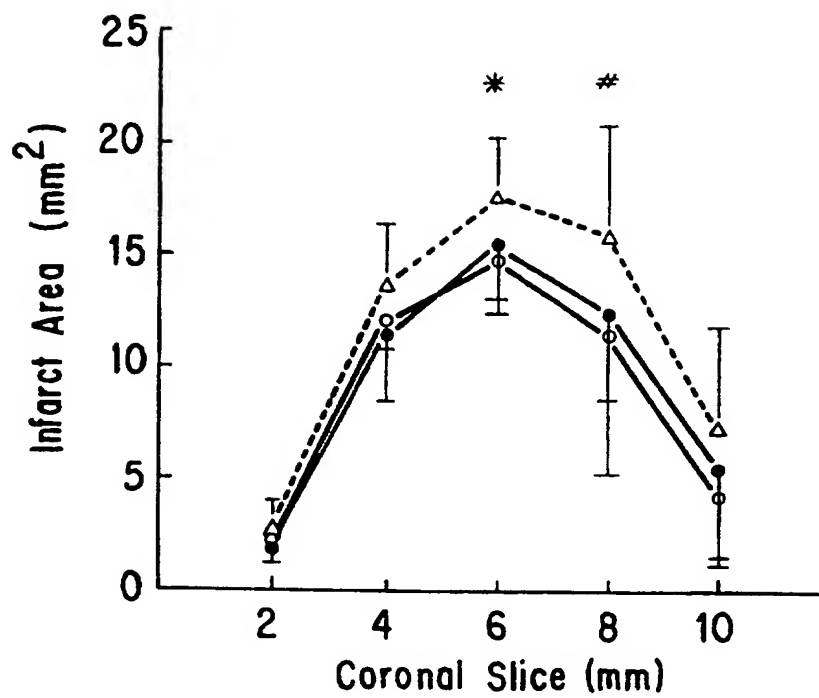


FIG. 7B

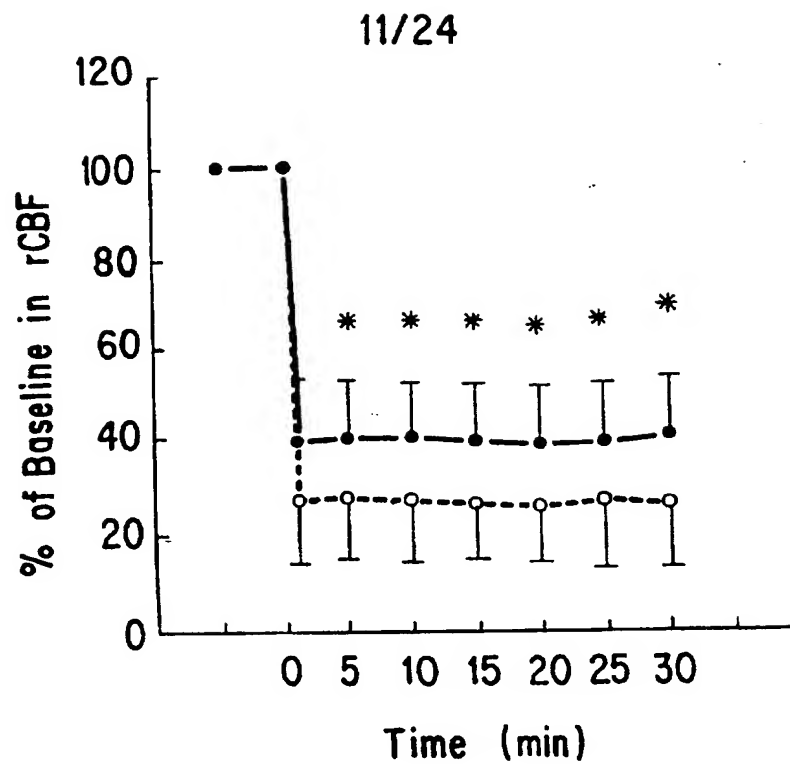


FIG. 8

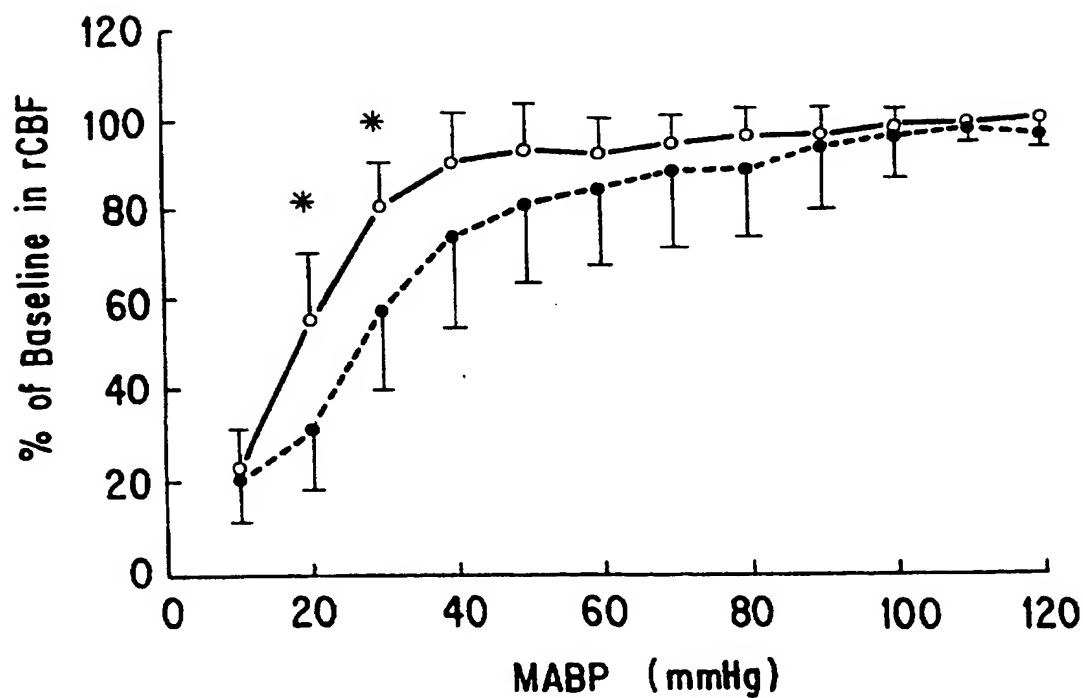


FIG. 9

12/24

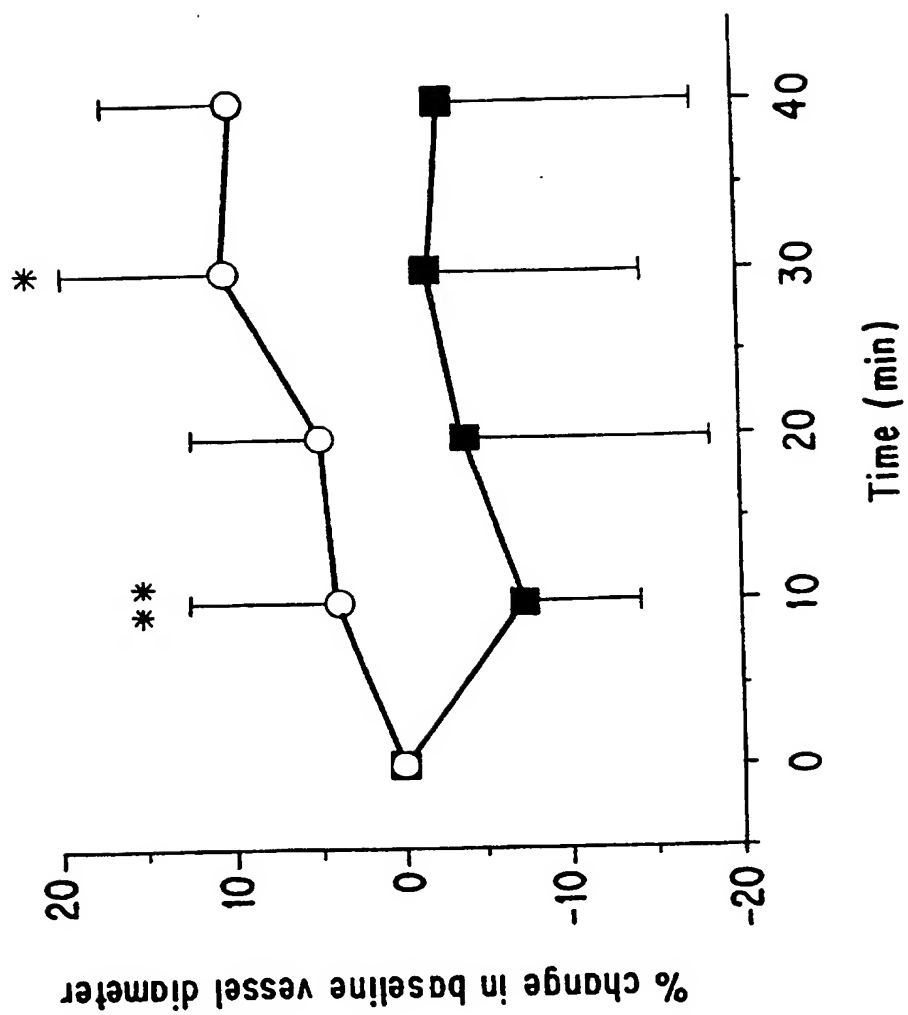


FIG. 10

13/24



FIG. 11B



FIG. 11D

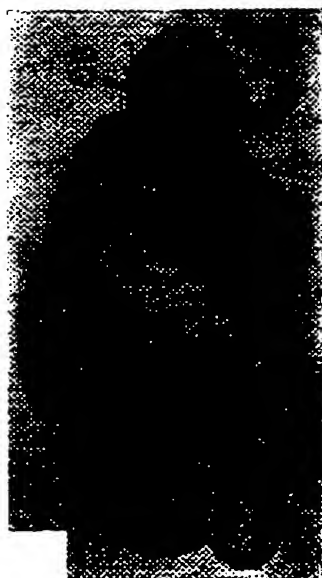


FIG. 11A



FIG. 11C

SUBSTITUTE SHEET (RULE 26)

14/24

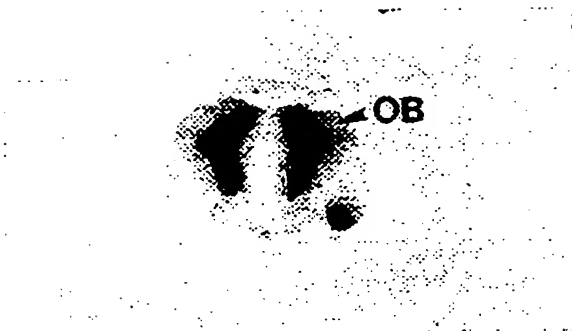


FIG.12A

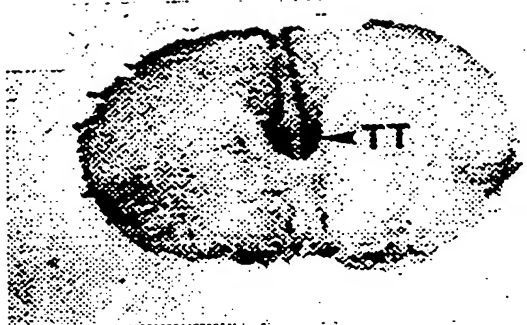


FIG.12B

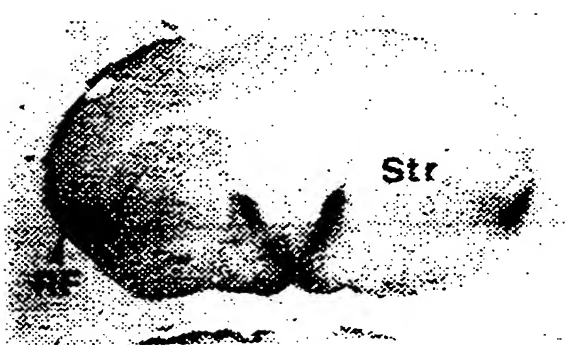


FIG.12C



FIG.12D

SUBSTITUTE SHEET (RULE 26)

15/24

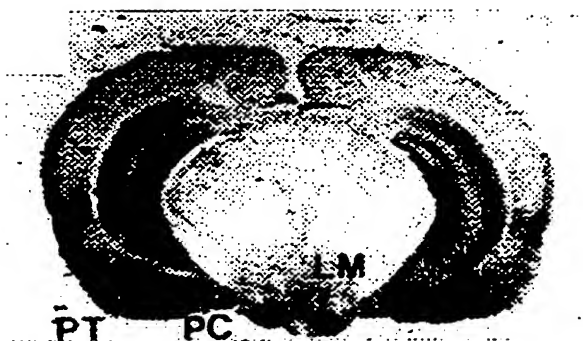


FIG. 12E

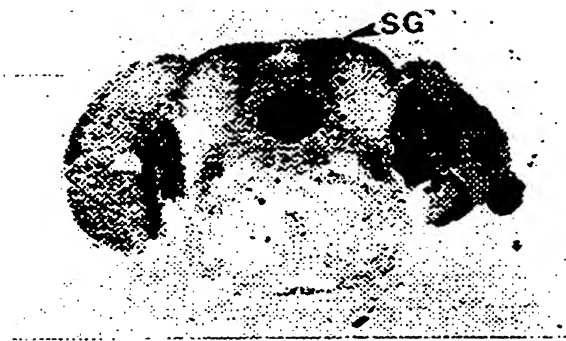


FIG. 12F



FIG. 12G

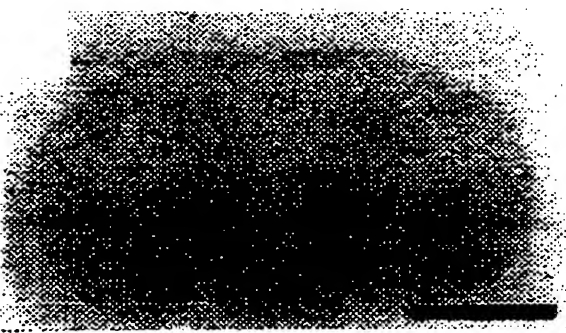


FIG. 12H

16/24

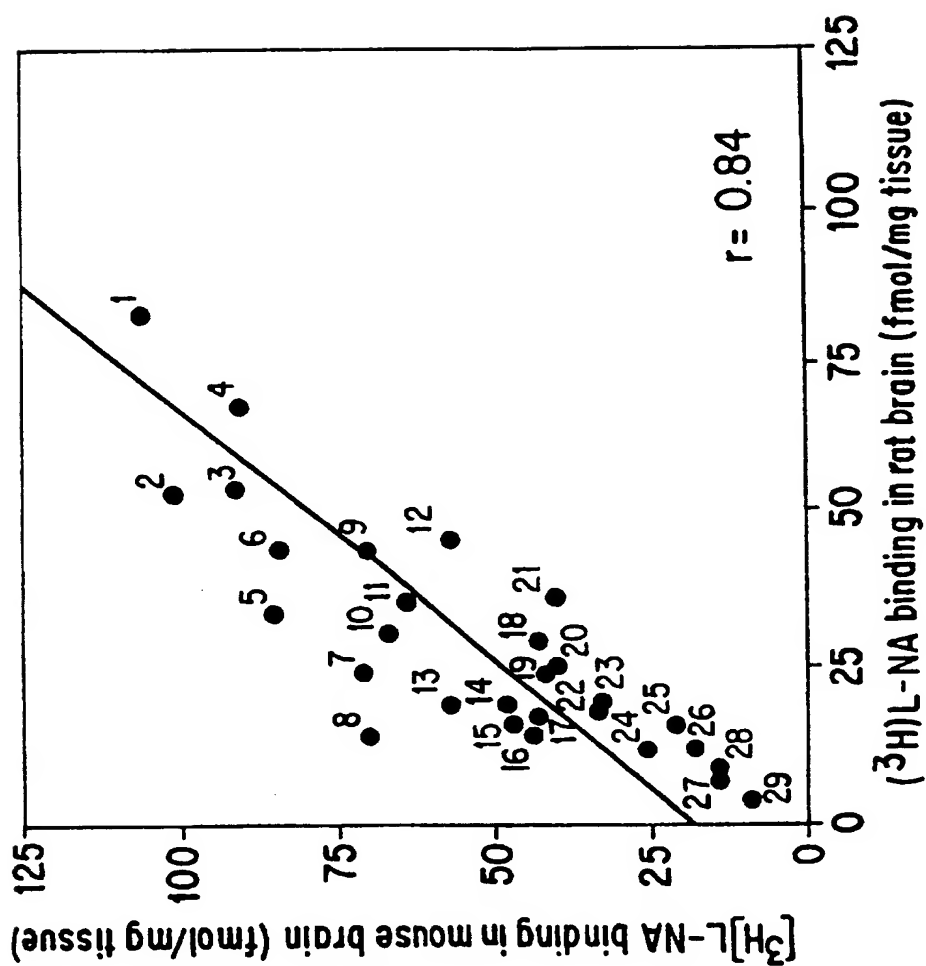


FIG. 13



FIG. 14B

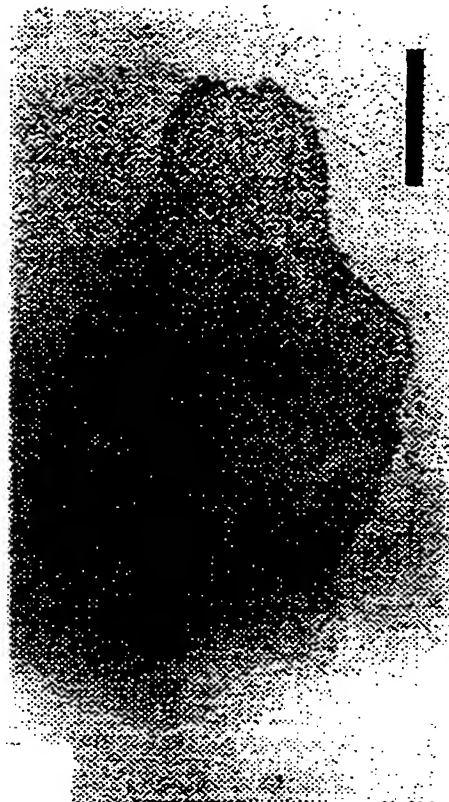


FIG. 14D



FIG. 14A

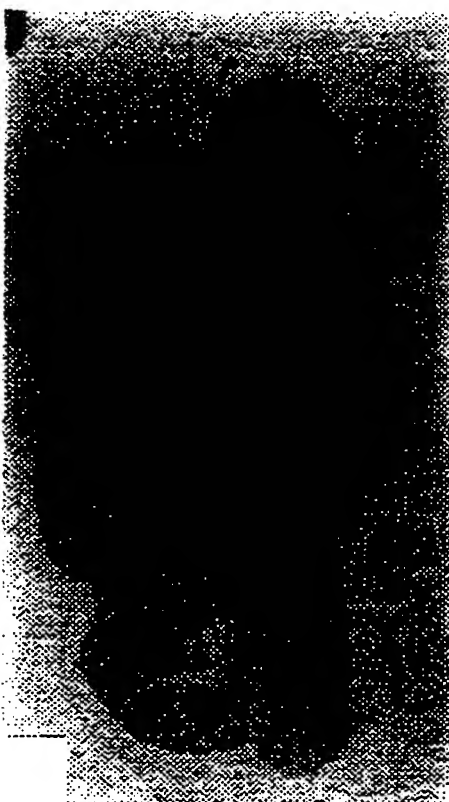


FIG. 14C

18/24

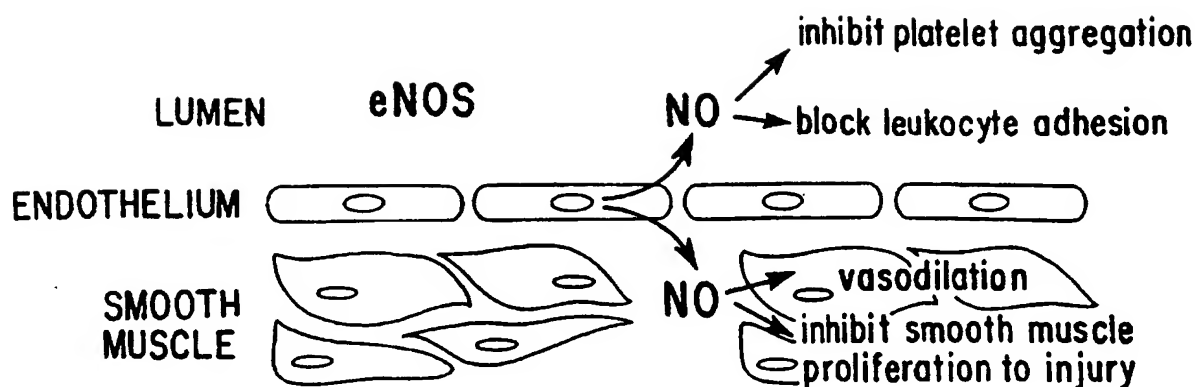


FIG. 15A

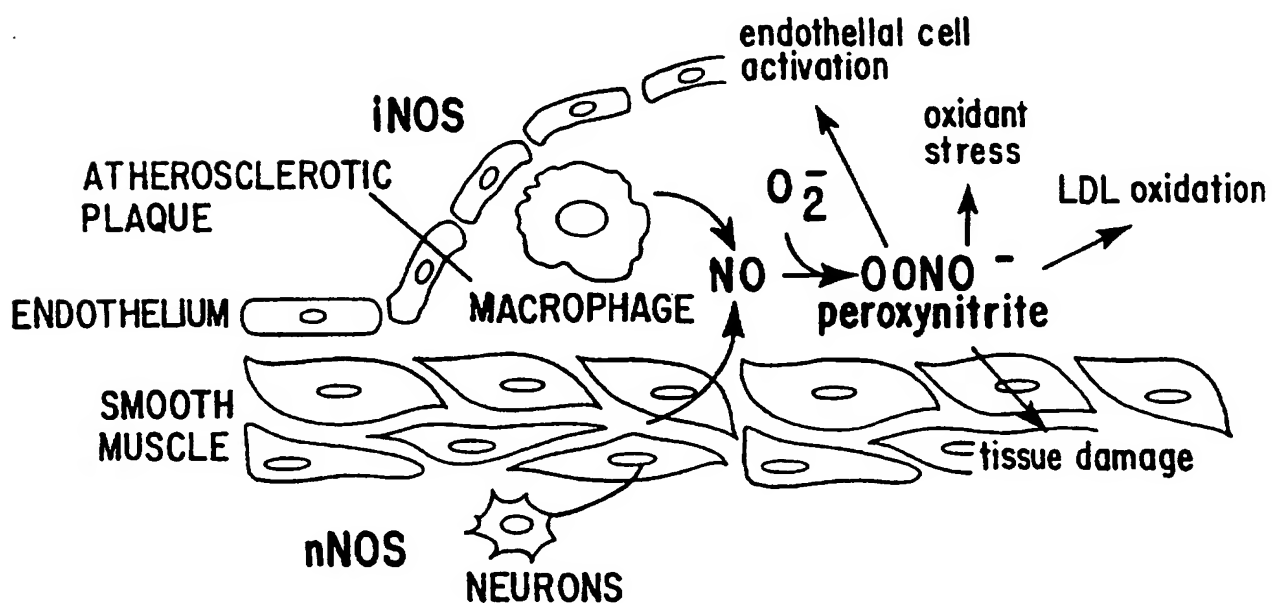


FIG. 15B

19/24

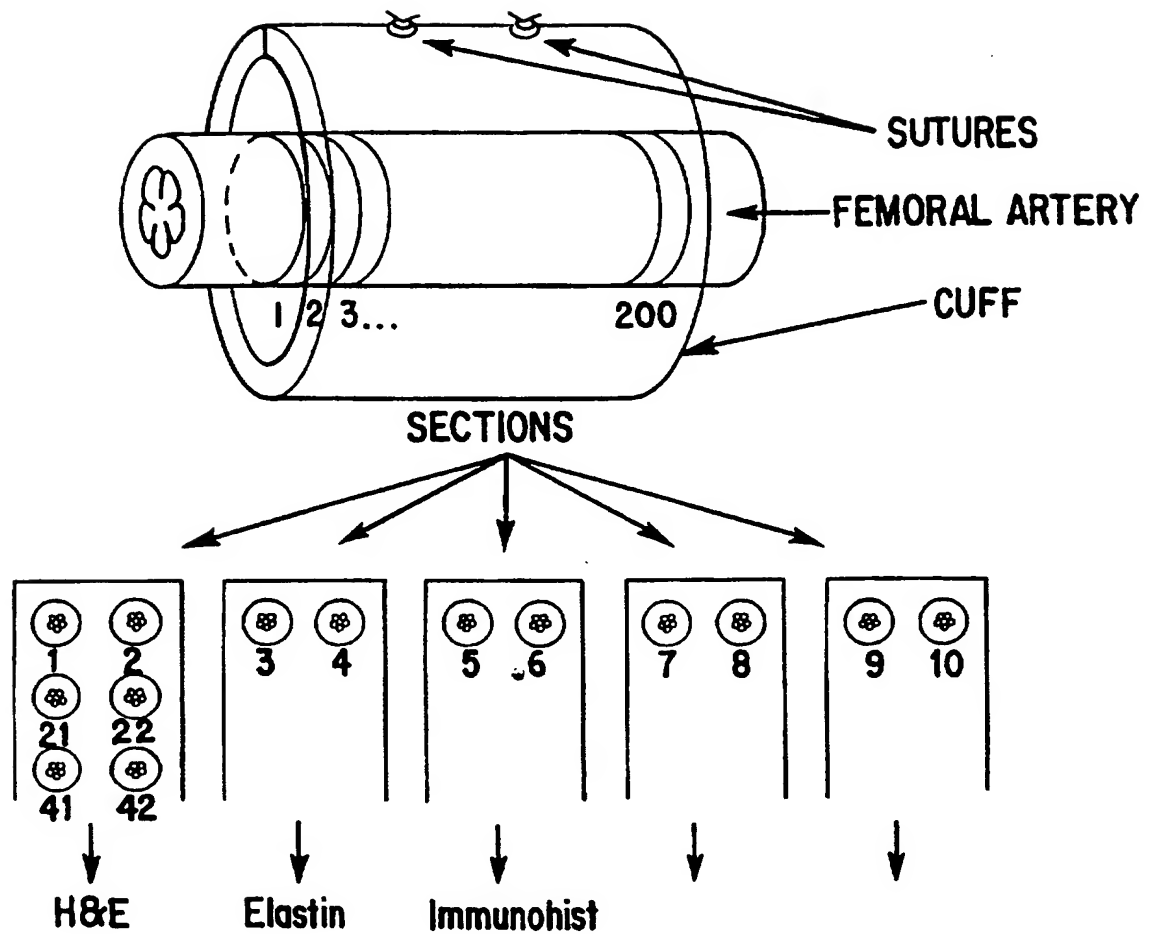


FIG. 16



FIG. 17A



FIG. 17B



FIG. 17C



FIG. 17D

SUBSTITUTE SHEET (RULE 26)

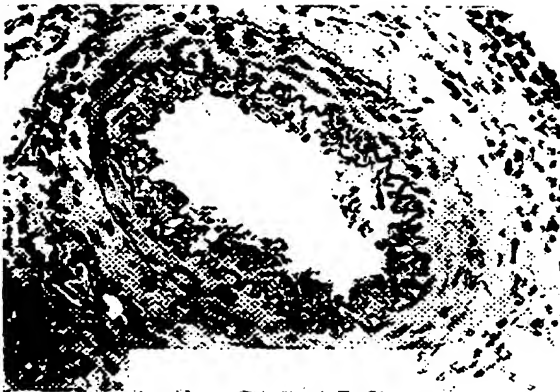


FIG. 18A

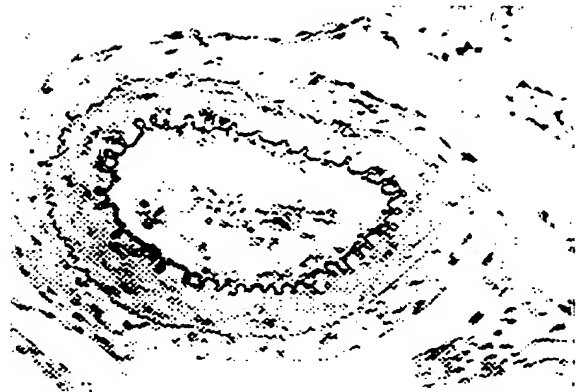


FIG. 18B



FIG. 18C

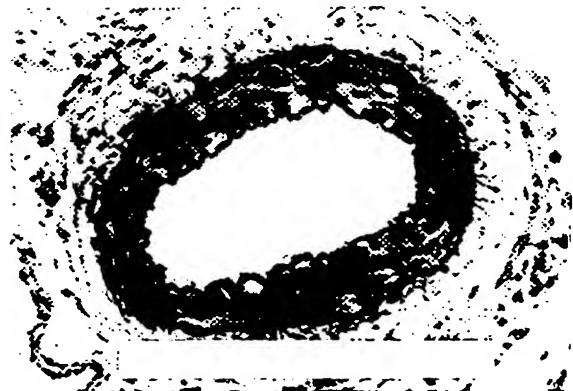


FIG. 18D

22/24

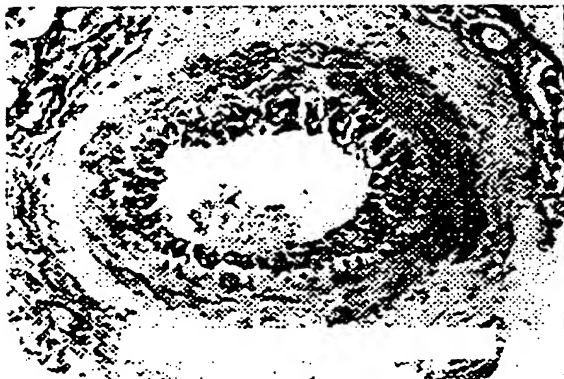


FIG. 18E

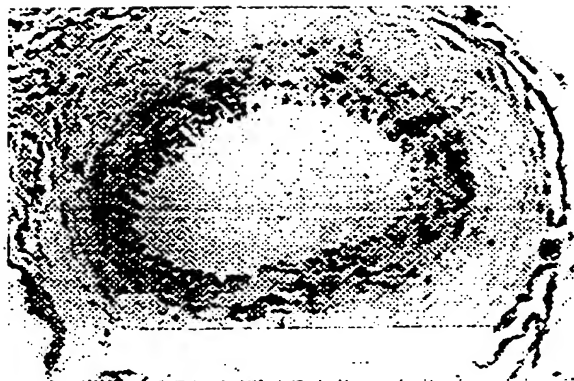


FIG. 18F

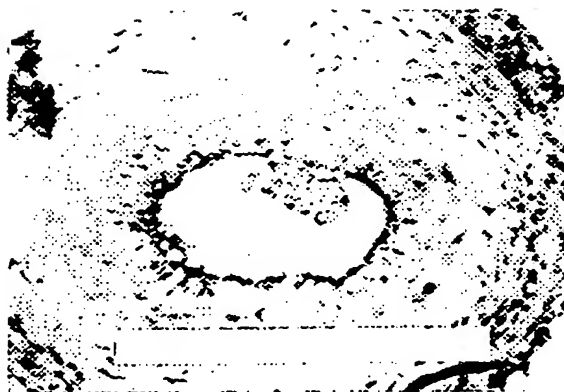


FIG. 18G

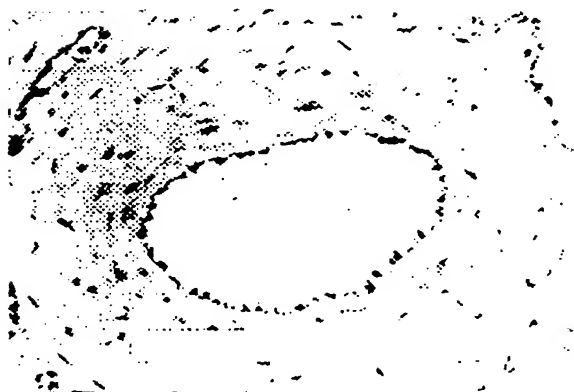


FIG. 18H

SUBSTITUTE SHEET (RULE 26)

23/24

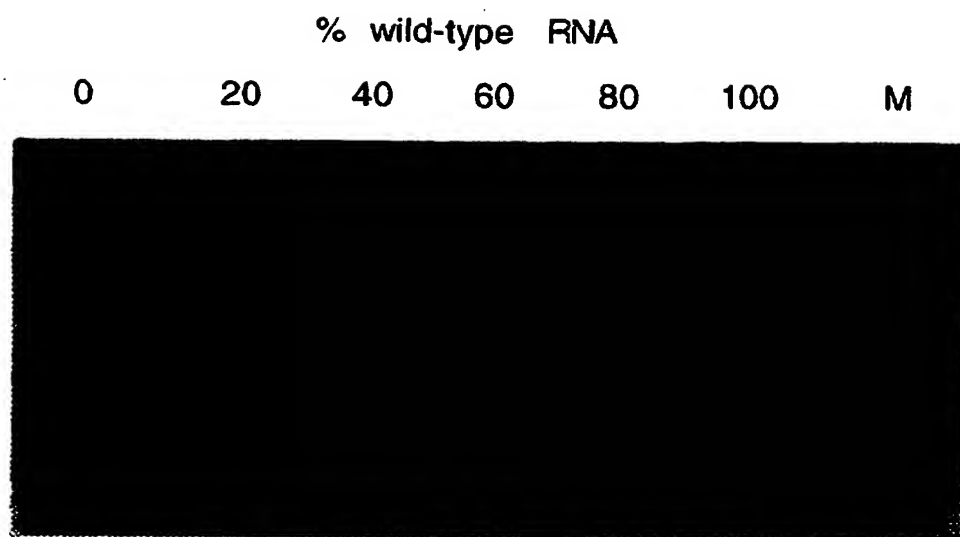


FIG. 19

SUBSTITUTE SHEET (RULE 26)

24/24



FIG. 20B



FIG. 20D



FIG. 20A



FIG. 20C

SUBSTITUTE SHEET (RULE 26)

# INTERNATIONAL SEARCH REPORT

International Application No  
PCT/US 97/04184

## A. CLASSIFICATION OF SUBJECT MATTER

IPC 6 C12N15/00 A01K67/027 C12N9/02 C12N15/53

According to International Patent Classification (IPC) or to both national classification and IPC

## B. FIELDS SEARCHED

Minimum documentation searched (classification system followed by classification symbols)

IPC 6 A01K C12N

Documentation searched other than minimum documentation to the extent that such documents are included in the fields searched

Electronic data base consulted during the international search (name of data base and, where practical, search terms used)

## C. DOCUMENTS CONSIDERED TO BE RELEVANT

Category *	Citation of document, with indication, where appropriate, of the relevant passages	Relevant to claim No.
X	STROKE, vol. 27, no. 1, 25 January 1996, page 173 XP000607805 HUANG Z ET AL: "FOCAL CEREBRAL ISCHEMIA IN MICE DEFICIENT IN EITHER ENDOTHELIAL (ENOS) OR NEURONAL NITRIC OXIDE (NNOS) SYNTHASE" see abstract	1-4,6,11
X	NATURE, vol. 377, 21 September 1995, pages 239-242, XP002021109 HUANG P L ET AL: "HYPERTENSION IN MICE LACKING THE GENE FOR ENDOTHELIAL NITRIC OXIDE SYNTHASE" see abstract see page 241, column 1, paragraph 2	7-9,11

☒ Further documents are listed in the continuation of box C.

☒ Patent family members are listed in annex.

### \* Special categories of cited documents:

- "A" document defining the general state of the art which is not considered to be of particular relevance
- "E" earlier document but published on or after the international filing date
- "L" document which may throw doubts on priority claim(s) or which is cited to establish the publication date of another citation or other special reason (as specified)
- "O" document referring to an oral disclosure, use, exhibition or other means
- "P" document published prior to the international filing date but later than the priority date claimed

- "T" later document published after the international filing date or priority date and not in conflict with the application but cited to understand the principle or theory underlying the invention
- "X" document of particular relevance; the claimed invention cannot be considered novel or cannot be considered to involve an inventive step when the document is taken alone
- "Y" document of particular relevance; the claimed invention cannot be considered to involve an inventive step when the document is combined with one or more other such documents, such combination being obvious to a person skilled in the art
- "&" document member of the same patent family

Date of the actual completion of the international search

26 June 1997

Date of mailing of the international search report

11.07.97.

Name and mailing address of the ISA

European Patent Office, P.B. 5818 Patentlaan 2  
NL - 2280 HV Rijswijk  
Tel. (+31-70) 340-2040, Tx. 31 651 epo nl,  
Fax (+31-70) 340-3016

Authorized officer

Chambonnet, F

# INTERNATIONAL SEARCH REPORT

International Application No

PCT/US 97/04184

## C.(Continuation) DOCUMENTS CONSIDERED TO BE RELEVANT

Category *	Citation of document, with indication, where appropriate, of the relevant passages	Relevant to claim No.
A	WO 93 19166 A (UNIV NORTH CAROLINA) 30 September 1993 see the whole document ---	10
P,X	CIRCULATION, vol. 94, no. 8 sup, 15 October 1996, page 1154 XP000676824 MOROI, M. ET AL.: "Mice mutant in endothelial Nitric Oxide synthase: vessel growth and response to injury" see abstract ---	8,9,11
P,X	AMERICAN JOURNAL OF PHYSIOLOGY, vol. 272, no. 3 pt 2, March 1997, page h1401 XP000676924 HUANG, Z. ET AL.: "bFGF ameliorates focal ischemic injury by blood flow-independent mechanisms in eNOS mutant mice" see the whole document ---	1
T	JOURNAL OF MOLECULAR MEDICINE, vol. 74, no. 8, 1996, pages 415-421, XP000610408 HUANG P L ET AL: "GENETIC ANALYSIS OF NITRIC OXIDE SYNTHASE ISOFORMS: TARGETED MUTATION IN MICE" see the whole document -----	1

# INTERNATIONAL SEARCH REPORT

information on patent family members

Internal Application No

PCT/US 97/04184

Patent document cited in search report	Publication date	Patent family member(s)	Publication date
WO 9319166 A	30-09-93	AU 3814393 A	21-10-93
-----			

## Interaction of Genetic Deficiency of Endothelial Nitric Oxide, Gender, and Pregnancy in Vascular Response to Injury in Mice

Masao Moroi,\* Lin Zhang,\* Tsunehiro Yasuda,\* Renu Virmani,\* Herman K. Gold,\* Mark C. Fishman,\* and Paul L. Huang\*  
\*Cardiovascular Research Center and Cardiac Unit, Massachusetts General Hospital-East, Charlestown, MA 02129; and \*Department of Cardiovascular Pathology, Armed Forces Institution of Pathology, Washington, DC 20306

### Abstract

To begin to dissect atherogenesis as a complex genetic disorder affected by genetic makeup and environment, we have (a) generated a reproducible mouse model of neointimal growth; (b) evaluated the effect of disruption of a single gene, endothelial nitric oxide synthase, believed to be central to intimal growth, and (c) examined the modifying effects of gender and pregnancy upon the vascular response. Cuff placement around the femoral artery causes reproducible intimal growth. We assessed the response to injury by quantitative morphometry, measuring the intimal to medial (I/M) volume ratio. In wild-type mice, cuff placement causes pronounced intimal proliferation without affecting the media, resulting in I/M ratios of 31% (SV129 males) and 27% (C57BL/6 males). eNOS mutant male mice have a much greater degree of intimal growth (I/M ratio of 70%). Female mice show less intimal response than do males, although eNOS mutant female mice still have more response than do wild-type females. Most dramatic, however, is the effect of pregnancy, which essentially abolishes the intimal response to injury, even overriding the effect of eNOS mutation. We conclude that eNOS deficiency is a genetic predisposition to intimal proliferation that is enhanced by male gender, and that may be overridden by pregnancy. (*J. Clin. Invest.* 1998, 101:1225-1232.) Key words: vascular endothelium • animal disease models • transgenic mice • tunica intima • atherosclerosis

### Introduction

Multiple genes interact with each other and with environmental factors to affect hereditary propensity to atherosclerosis. We are interested in studying the interaction of individual genes believed to function in vascular response to injury with modifiers, such as gender. Endothelial nitric oxide synthase (eNOS)<sup>1</sup> synthesizes nitric oxide (NO), which accounts for endothelium-derived relaxing factor activity. NO has physiologic effects that may normally serve to prevent atherosclerosis, in-

cluding suppression of smooth muscle proliferation (1), inhibition of platelet aggregation and adhesion (2), and inhibition of leukocyte adhesion (3, 4). A reduction in endothelial NO levels would be expected to diminish these normally protective effects, and predispose to atherogenesis. Endothelial dysfunction, characterized by diminished vasodilatory responses to cholinergic stimulation and by diminished endothelial NO levels, is observed in atherosclerosis (5, 6), hypertension (7), diabetes mellitus (8), and hypercholesterolemia (9). It is unclear whether diminished endothelial NO levels are merely associated with endothelial dysfunction, or whether they cause increased propensity to atherosclerosis. This distinction is important, because if the latter is true, then approaches to restore endothelial NO levels may retard atherosclerosis.

In this report, we use eNOS mutant mice to test the hypothesis that reduction in endothelial NO production leads to increased propensity to atherosclerosis. To do this, we need a model that mimics features of human atherosclerosis with a quantitative and reproducible endpoint. In addition, the model should be one in which the endothelium itself is not directly injured so that we can study the effect of eNOS deficiency in the setting of an otherwise preserved endothelium. We adapted an external vascular cuff model previously used in rabbits (10, 11) to mice. We describe here the characterization of this model, and results using this model in eNOS mutant mice. We have found that eNOS deficiency markedly enhances intimal growth in response to injury, but this effect is completely obviated during pregnancy.

### Methods

**Animals.** We have previously described the generation of eNOS mutant mice (12). These mice have a combined genetic background of both SV129 and C57BL/6 strains. Thus, both wild-type SV129 and C57BL/6 mice were used as controls to ensure that variation due to genetic background would not confound our results. Animals were divided into nine groups: SV129 males, SV129 females, SV129 pregnant females, C57BL/6 males, C57BL/6 females, C57BL/6 pregnant females, eNOS mutant males, eNOS mutant females, and eNOS mutant pregnant females. All animals were 7-8 wk old, and weighed 17-27 g. Pregnant mice were 6 or 7 d pregnant at the time of cuff placement (normal mouse gestation is 20-21 d).

**Femoral artery cuff placement.** Mice were anesthetized with an intraperitoneal injection of pentobarbital (50 mg/kg). The left femoral artery was isolated from surrounding tissues, loosely sheathed with a 2.0-mm polyethylene cuff made of PE-50 tubing (inner diameter, 0.56 mm; outer diameter, 0.965 mm; Becton Dickinson, Mountain

Address correspondence to Paul L. Huang, M.D., Ph.D., Massachusetts General Hospital East, 149 Thirteenth Street, Charlestown, MA 02129. Phone: 617-724-9849; FAX: 617-726-5806; E-mail: huangp@helix.mgh.harvard.edu

Received for publication 24 July 1997 and accepted in revised form 12 January 1998.

The Journal of Clinical Investigation  
Volume 101, Number 6, March 1998, 1225-1232  
<http://www.jci.org>

1. Abbreviations used in this paper: BrdU, bromodeoxyuridine; eNOS, endothelial nitric oxide synthase; I/M, intima-to-media ratio; iNOS, inducible nitric oxide synthase; NO, nitric oxide.

View, CA) and tied in place with an 8-0 suture. The cuff is larger than the vessel, and does not obstruct blood flow. The right femoral artery was dissected from surrounding tissues (sham-operated), but a cuff was not placed. The femoral arteries were replaced, and the wounds were sutured. After recovery from anesthesia, the animals were given standard diet and water ad libitum.

For determination of cellular proliferation, in additional animals a model 2002 Alzet pump containing a solution of bromodeoxyuridine (BrdU) was placed at the time of cuff placement for administering BrdU. The infusion rate was 0.5  $\mu$ l/h, corresponding to a total BrdU dose of 350 mg/kg body wt over a 14-d period.

**Tissue harvesting and histologic staining.** 2 wk after cuff placement, animals were anesthetized and killed. Vessels were fixed in situ by constant pressure fixation at 100 mmHg with 10% formalin through a 22-gauge butterfly angiocatheter placed in the left ventricle of the heart. Both right and left femoral arteries were harvested. Each artery was embedded in paraffin, and cross-sections (10  $\mu$ m) were continuously cut from one edge to the other edge of the cuffed portion, and in the corresponding segment of the contralateral control artery. Each section was mounted in order on five series of slides. Parallel sections were subjected to standard hematoxylin and eosin staining as well as to immunohistochemistry.

**Morphometry.** Morphometric analyses were performed on hematoxylin and eosin-stained tissue. For each animal, 10 cross-sections from the cuffed left femoral artery and the control right femoral artery were photographed, and the images were digitized using a Kodak RF 2035 Plus Film Scanner (Eastman Kodak Co., Rochester, NY). For each artery section, the thickness of the intima and media were measured. For area/vol calculations, four measurements were made using an image analysis computer program (NIH Image; National Institutes of Health, Bethesda, MD): luminal circumference, luminal area, area inside the inner elastic lamina, and area inside the outer elastic lamina. Mean vascular diameter was calculated as luminal circumference/ $\pi$ . The intima was defined as the area between the lumen and the internal elastic lamina. The media was defined as the area between the internal and external elastic laminae. The volumes of intima and media were calculated by integrating the areas over the length of the cuffed region. The observers of the sections were blinded to the gender or genotype of the mice. The intraassay variability, using independent observers or analyzing adjacent sections from the same vessel, was < 3%.

**Immunohistochemistry.** Immunohistochemical stains were performed using the following antisera and dilutions: anti-alpha smooth muscle actin (1:500 dilution, monoclonal mouse; Sigma Chemical Co., St. Louis, MO); anti-von Willebrand factor (1:2,200 dilution, polyclonal rabbit; DAKO Corp., Carpinteria, CA); anti-inducible NOS (iNOS; 1:1,000 dilution, polyclonal rabbit; Transduction Laboratories, Lexington, KY); anti-BrdU (1:100 dilution, monoclonal rat; Harlan Sera-Lab, Loughborough, England). The secondary antibodies (biotinylated anti-mouse, anti-rat, or anti-rabbit) were applied followed by avidin-peroxidase complexes (Peroxidase Vectastain Elite ABC kit, Vector Laboratories, Inc., Burlingame, CA). The reaction was visualized with 3,3'-diaminobenzidine.

**Statistical analysis.** All values were expressed as mean  $\pm$  SEM. Luminal diameter, intimal and medial thickness, and the ratios of intimal to medial volumes of the 9 groups of mice studied 14 d after cuff placement were first tested by ANOVA. When the ANOVA demonstrated significant differences, Bonferroni/Dunn's analysis was used posthoc to compare groups. Luminal diameters and medial thickness of two groups (cuffed arteries and contralateral control arteries) were compared using a paired Student's *t* test. For all statistical analyses, *P* < 0.05 was considered significant.

## Results

**Characterization of cuff model.** To characterize the cuff model, we studied both C57BL/6 and SV129 wild-type mice, since the

Table I. Response to Vessel Injury in Wild-type Mice

	C57BL/6 strain		SV129 strain	
	Male	Female	Male	Female
n	7	7	15	9
Weight (g)	24.5 $\pm$ 0.4	17.7 $\pm$ 0.4	24.9 $\pm$ 0.5	20.2 $\pm$ 0.1
Control intimal thickness ( $\mu$ m)	0	0	0	0
Control medial thickness ( $\mu$ m)	24.6 $\pm$ 1.5	30.0 $\pm$ 1.5	28.5 $\pm$ 1.6	30.2 $\pm$ 1.3
Cuffed intimal thickness ( $\mu$ m)	7.3 $\pm$ 1.8	5.3 $\pm$ 0.5	9.2 $\pm$ 0.9	7.0 $\pm$ 2.3
Cuffed medial thickness ( $\mu$ m)	21.8 $\pm$ 1.9	25.3 $\pm$ 2.0	26.1 $\pm$ 1.8	28.5 $\pm$ 2.0
Cuffed I/M volume ratio (%)	27.7 $\pm$ 5.2	18.2 $\pm$ 1.5	31.1 $\pm$ 3.0	17.2 $\pm$ 4.7

eNOS mutant mice have a genetic background derived from both these strains. No baseline intima was present in the femoral arteries of either wild-type strain. There was reproducible neointimal formation 2 wk after placement of the cuff. We used morphometric analysis to make two types of measurements. First, we measured the thickness of the intima and media. Second, we determined the area of the intima and the media in 10 equally spaced sections along the cuffed region, and calculated the volume of intima and media. The degree of intimal formation was expressed as intimal/media volume ratio.

Table I shows the results in wild-type mice. Male mice of both SV129 and C57BL/6 strains have more intima after cuff placement than do female mice. This result is apparent in terms of intimal thickness, as well as intimal to medial volume ratios. Male mice have intimal to medial (I/M) ratios of 27.7% (C57BL/6) and 31.1% (SV129), as compared with female mice with I/M ratios of 18.2% (C57BL/6) and 17.2% (SV129). There were no differences in luminal diameters or medial thickness among any of the groups. No intima developed on the sham-operated side in any of the mice.

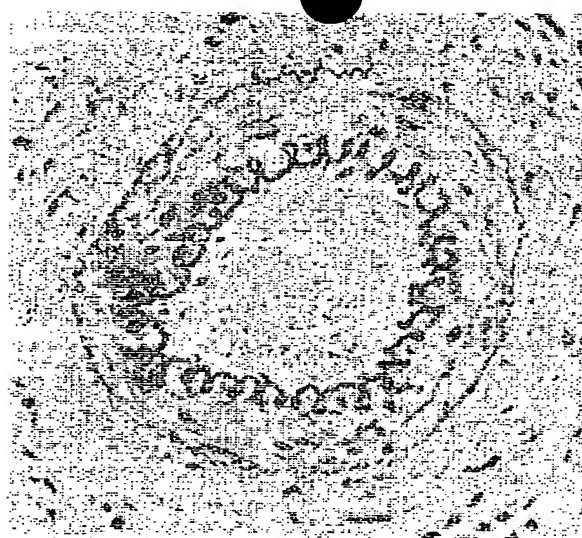
**Effect of eNOS gene deficiency.** Neointimal formation after cuff injury was greater in eNOS mutant male mice compared with male mice of either wild-type strain (*P* < 0.05, Table II). Male eNOS mutant mice had I/M volume ratios of 70.0%, as compared with wild-type values of 27.7% (C57BL/6) and 31.1% (SV129). Female eNOS mutant mice had less intimal proliferation (I/M volume ratio of 42.7%) than did male eNOS mutant mice, but had more than did wild-type female mice (I/M volume ratios of 18.2% for C57BL/6 and 17.2% for SV129). There were no significant differences in luminal diameters or medial thickness among the groups. As for wild-type mice, eNOS mutant mice did not have any visible intima at

Table II. Effect of eNOS Gene Disruption on Response to Vessel Injury

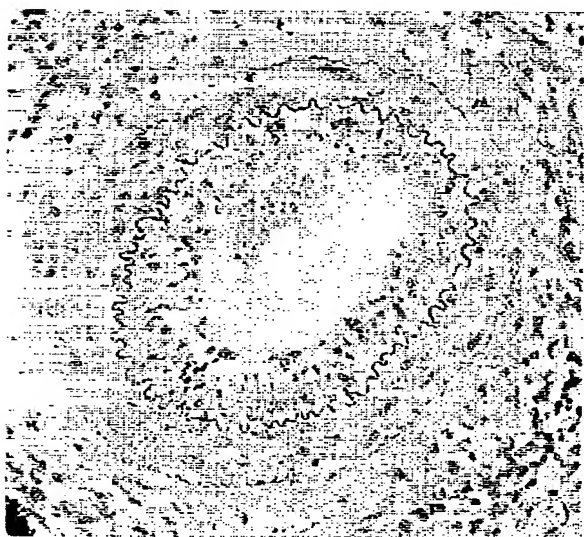
	eNOS mutant	
	Male	Female
n	9	9
Weight (g)	23.9 $\pm$ 0.9	24.6 $\pm$ 0.4
Control intimal thickness ( $\mu$ m)	0	0
Control medial thickness ( $\mu$ m)	30.2 $\pm$ 1.2	23.8 $\pm$ 3.0
Cuffed intimal thickness ( $\mu$ m)	20.3 $\pm$ 1.5	11.1 $\pm$ 1.8
Cuffed medial thickness ( $\mu$ m)	23.4 $\pm$ 0.8	20.7 $\pm$ 2.8
Cuffed I/M volume ratio (%)	70.0 $\pm$ 6.4	42.7 $\pm$ 1.8



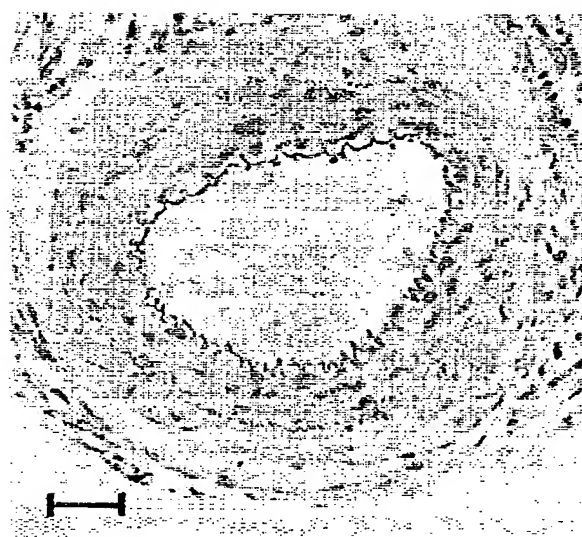
A



B



C



D

**Figure 1.** Response of wild-type and eNOS mutant mice to cuff injury. Hematoxylin and eosin-stained sections from male wild-type injured (A), sham-operated (B), and eNOS mutant injured (C) and sham-operated (D) vessels. The intima is seen within the internal elastic lamina. eNOS mutant mice show substantially more neointimal formation in response to cuff injury than wild-type mice. Bar, 30  $\mu$ m.

baseline, nor did sham-operated vessels show intimal proliferation. Fig. 1 shows representative sections of sham-operated and cuff-injured vessels.

**Histologic characterization of intimal response.** Fig. 2 shows sections of cuff-injured and sham-operated control arteries from an eNOS mutant male mouse. Smooth muscle cells in the media normally stain for alpha actin (Fig. 2 F). In the corresponding cuff-injured artery (Fig. 2 E), not only do cells in the media (inside the internal elastic lamina) stain, but so do the majority of cells in the neointima (outside the internal elastic

lamina). On the other hand, staining for von Willebrand factor occurs only in the endothelial layer in both cuff-injured and sham-operated vessels. In the cuff-injured vessel, the vWF staining is separated from the internal elastic lamina by the neointima (Fig. 2 G), whereas on the sham-operated side, the vWF-stained cells directly appose the internal elastic lamina because there is no intima (Fig. 2 H). The endothelial layer is intact in both the sham-operated and the cuff-injured vessels.

Fig. 3 shows a high-power magnification of a section from a wild-type cuff-injured vessel 7 d after cuff placement. The in-

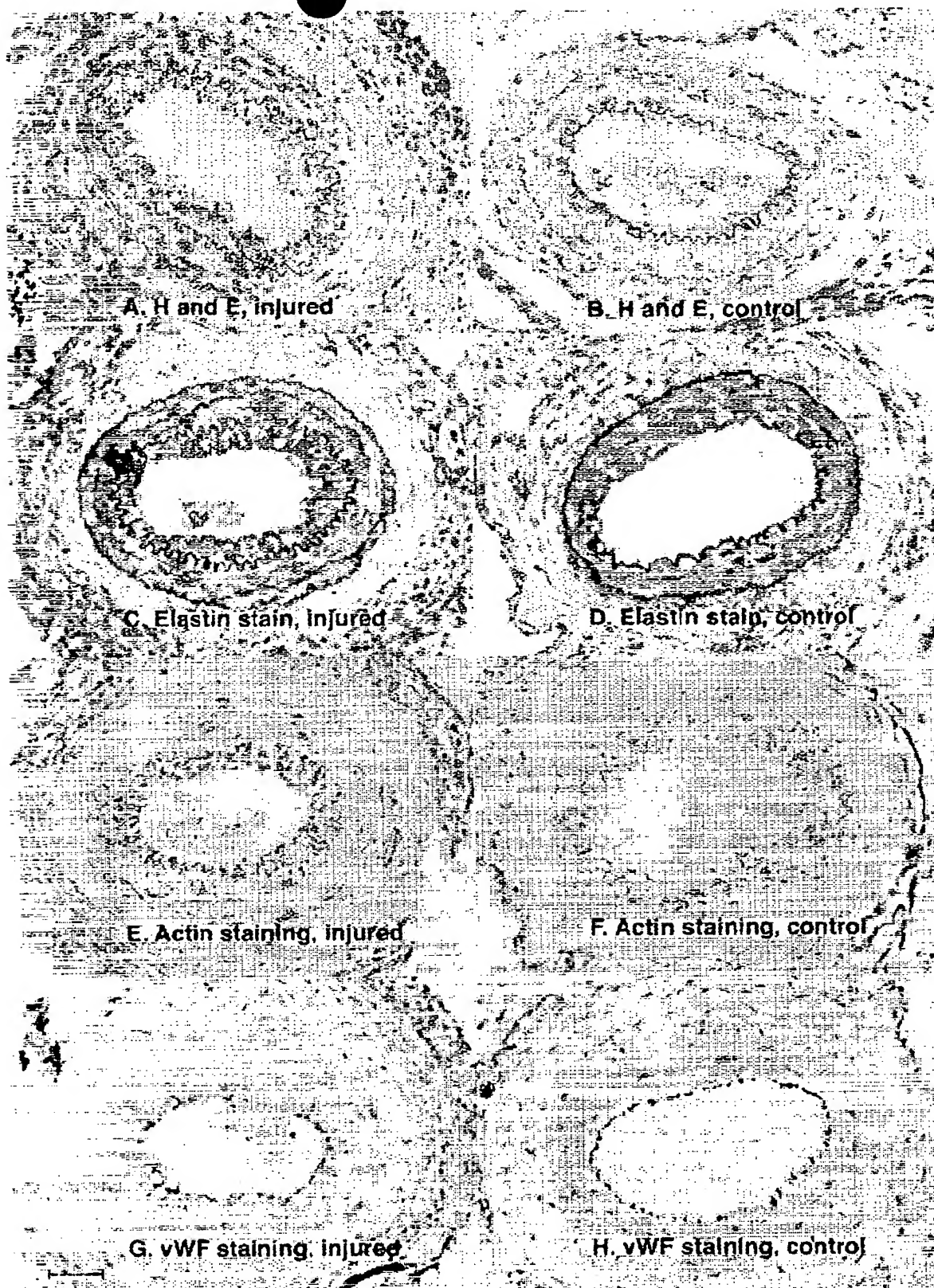


**Figure 2.** Histology and immunochemical staining of injured and control vessels. One injured (*left side*) and one sham-operated (*right side*) femoral artery was dissected from an eNOS mutant male mouse. The sections were adjacent sections processed for hematoxylin and eosin staining (A and B), elastin staining (C and D), immunohistochemical staining for alpha actin (E and F), and immunohistochemical staining for von Willebrand factor (G and H). Bar, 30  $\mu$ m.

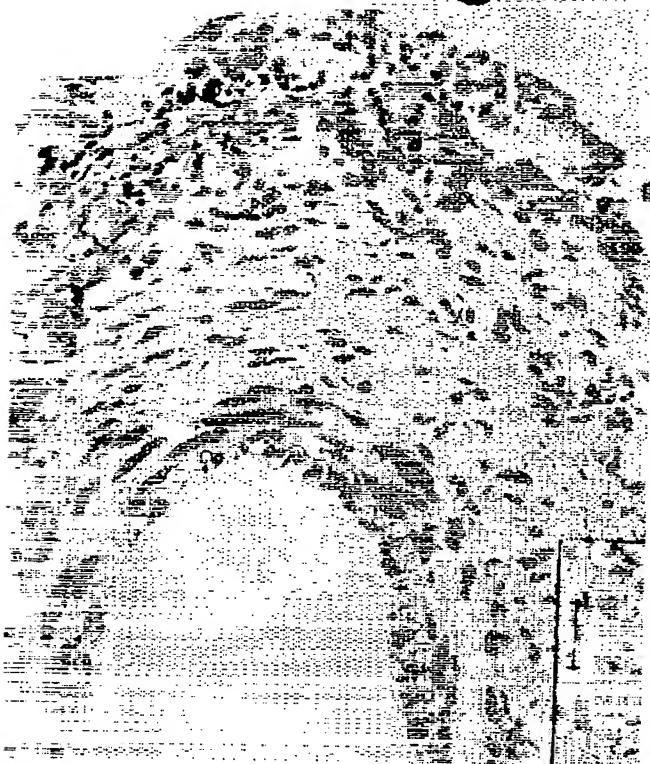


**Figure 3.** High-power magnification of cuffed femoral artery from wild-type mouse 7 d after cuff placement. This section was stained with hematoxylin and eosin. Inflammatory cells are seen in the adventitia. At 7 d, there is less intima present than at the 14-d endpoint. Bar, 30  $\mu$ m.

Intima is visible at 7 d of injury, although it is not as thick as it was 14 days after cuff placement. Inflammatory cells are visible in the adventitia of the vessel. To determine whether iNOS is expressed after cuff injury, and how this relates temporally to cellular proliferation, we performed a separate series of time-course experiments. Vessels were stained for iNOS immunohistochemistry and BrdU uptake at 3, 7, 10, and 14 d after injury. The results were the same in wild-type and eNOS mutant mice. There was no significant BrdU staining or iNOS staining in the sham-operated vessels. As seen in Fig. 4, iNOS expression is absent at 3 d, but is detectable in adventitial cells at 7 d

**Table III.** Effect of Vessel Injury in Pregnant Female Mice

	C57BL/6	SV129	eNOS mutant
n	8	7	7
Weight (g)	19.6 $\pm$ 0.5	22.3 $\pm$ 0.5	23.2 $\pm$ 1.0
Control intima ( $\mu$ m)	0	0	0
Control media ( $\mu$ m)	28.1 $\pm$ 1.2	24.7 $\pm$ 3.7	30.5 $\pm$ 2.0
Cuffed intima ( $\mu$ m)	0.3 $\pm$ 0.1	0.7 $\pm$ 0.2	2.0 $\pm$ 0.3
Cuffed media ( $\mu$ m)	26.3 $\pm$ 0.7	26.6 $\pm$ 2.2	26.9 $\pm$ 0.7
Cuffed I/M vol. ratio (%)	0.9 $\pm$ 0.4	2.1 $\pm$ 0.5	6.5 $\pm$ 1.2

and in neointimal and adventitial cells at 10 and 14 d. Staining for BrdU, on the other hand, is clearly present at 3 d. It occurs in the adventitia, media, and intimal layers, and increases with time. Thus, cellular proliferation occurs before iNOS expression.

**Effect of pregnancy.** Pregnant mice showed a striking lack of intimal proliferation after cuff placement. As seen in Table III, pregnant female wild-type mice had I/M ratios of 0.9% (C57BL/6) and 2.1% (SV129), as compared with pregnant eNOS mutant mice that had I/M ratios of 6.5%. These values are markedly lower than the I/M ratios of nonpregnant female mice of the same age (Tables I and II).

## Discussion

In this report, we describe and characterize a new mouse model of vessel injury that involves placing a nonocclusive cuff around the femoral artery. This model has been previously described in rabbits (10, 11). In our hands, it results in predictable formation of neointima in mice over a 14-d period. It differs from other rodent models such as the filament model (13) and the balloon model (14, 15) in several important ways. In the present cuff model, the endothelial cells are not directly manipulated or removed, allowing study of the effect of individual endothelial factors, including endothelium-derived NO. In contrast, the filament and balloon models involve removing the endothelial layer. In the cuff model, the primary endpoint is neointimal formation. In the filament model, intimal formation occurs to varying degrees, but the primary endpoint is an increase in medial thickness (13, 16).

We believe that the cuff model is complementary to the filament model, and that both may be useful animal models with which to examine vessel responses to injury that are relevant to atherosclerosis. The cuff model is reproducible, easily quantitated, and lends itself well to analysis of individual gene products that can be manipulated by transgenic approaches and targeted gene disruption. In our study, the C57BL/6 and the SV129 mouse strains, often used to generate transgenic and null-mutant mice, showed similar responses (Table I). Thus, these genetic backgrounds should not affect the quantitative analysis of vascular intimal formation in mice generated using SV129 embryonic stem cells and bred using C57BL/6 mice.

The mechanism of intimal formation after cuff injury is not known. Booth et al. propose that neointimal formation in the rabbit model of cuff injury may be mediated by obstruction of the adventitial vasa vasorum with the creation of a localized ischemic region (10). In addition, local hemodynamic changes may be involved (17). Kockx et al. report that the rabbit cuff model is characterized by smooth muscle cell replication in the media before neointimal formation (11). The temporal sequence suggests that medial proliferation is followed by migration of cells through the internal elastic lamina into the intima. The adventitia of the cuff-injured, but not sham-operated, vessels shows infiltration of inflammatory cells, in agreement with our observations in mice.

Our results indicate that absence of eNOS increases the neointimal proliferative response to vessel injury from cuff placement, consistent with protective roles for eNOS that normally serve to prevent vascular intimal formation in vivo. These results support the notion that the reduction in endothelial NO levels observed in hypertension, diabetes, and hypercholesterolemia is not only associated with atherosclerosis, but



**Figure 3.** High-power magnification of cuffed femoral artery from wild-type mouse 7 d after cuff placement. This section was stained with hematoxylin and eosin. Inflammatory cells are seen in the adventitia. At 7 d, there is less intima present than at the 14-d endpoint. Bar, 30  $\mu$ m.

tima is visible at 7 d of injury, although it is not as thick as it was 14 days after cuff placement. Inflammatory cells are visible in the adventitia of the vessel. To determine whether iNOS is expressed after cuff injury, and how this relates temporally to cellular proliferation, we performed a separate series of time-course experiments. Vessels were stained for iNOS immunohistochemistry and BrdU uptake at 3, 7, 10, and 14 d after injury. The results were the same in wild-type and eNOS mutant mice. There was no significant BrdU staining or iNOS staining in the sham-operated vessels. As seen in Fig. 4, iNOS expression is absent at 3 d, but is detectable in adventitial cells at 7 d

and in neointimal and adventitial cells at 10 and 14 d. Staining for BrdU, on the other hand, is clearly present at 3 d. It occurs in the adventitia, media, and intimal layers, and increases with time. Thus, cellular proliferation occurs before iNOS expression.

**Effect of pregnancy.** Pregnant mice showed a striking lack of intimal proliferation after cuff placement. As seen in Table III, pregnant female wild-type mice had I/M ratios of 0.9% (C57BL/6) and 2.1% (SV129), as compared with pregnant eNOS mutant mice that had I/M ratios of 6.5%. These values are markedly lower than the I/M ratios of nonpregnant female mice of the same age (Tables I and II).

## Discussion

In this report, we describe and characterize a new mouse model of vessel injury that involves placing a nonocclusive cuff around the femoral artery. This model has been previously described in rabbits (10, 11). In our hands, it results in predictable formation of neointima in mice over a 14-d period. It differs from other rodent models such as the filament model (13) and the balloon model (14, 15) in several important ways. In the present cuff model, the endothelial cells are not directly manipulated or removed, allowing study of the effect of individual endothelial factors, including endothelium-derived NO. In contrast, the filament and balloon models involve removing the endothelial layer. In the cuff model, the primary endpoint is neointimal formation. In the filament model, intimal formation occurs to varying degrees, but the primary endpoint is an increase in medial thickness (13, 16).

We believe that the cuff model is complementary to the filament model, and that both may be useful animal models with which to examine vessel responses to injury that are relevant to atherosclerosis. The cuff model is reproducible, easily quantitated, and lends itself well to analysis of individual gene products that can be manipulated by transgenic approaches and targeted gene disruption. In our study, the C57BL/6 and the SV129 mouse strains, often used to generate transgenic and null-mutant mice, showed similar responses (Table I). Thus, these genetic backgrounds should not affect the quantitative analysis of vascular intimal formation in mice generated using SV129 embryonic stem cells and bred using C57BL/6 mice.

The mechanism of intimal formation after cuff injury is not known. Booth et al. propose that neointimal formation in the rabbit model of cuff injury may be mediated by obstruction of the adventitial vasa vasorum with the creation of a localized ischemic region (10). In addition, local hemodynamic changes may be involved (17). Kockx et al. report that the rabbit cuff model is characterized by smooth muscle cell replication in the media before neointimal formation (11). The temporal sequence suggests that medial proliferation is followed by migration of cells through the internal elastic lamina into the intima. The adventitia of the cuff-injured, but not sham-operated, vessels shows infiltration of inflammatory cells, in agreement with our observations in mice.

Our results indicate that absence of eNOS increases the neointimal proliferative response to vessel injury from cuff placement, consistent with protective roles for eNOS that normally serve to prevent vascular intimal formation in vivo. These results support the notion that the reduction in endothelial NO levels observed in hypertension, diabetes, and hypercholesterolemia is not only associated with atherosclerosis, but

**Table III. Effect of Vessel Injury in Pregnant Female Mice**

	C57BL/6	SV129	eNOS mutant
n	8	7	7
Weight (g)	19.6 $\pm$ 0.5	22.3 $\pm$ 0.5	23.2 $\pm$ 1.0
Control intima ( $\mu$ m)	0	0	0
Control media ( $\mu$ m)	28.1 $\pm$ 1.2	24.7 $\pm$ 3.7	30.5 $\pm$ 2.0
Cuffed intima ( $\mu$ m)	0.3 $\pm$ 0.1	0.7 $\pm$ 0.2	2.0 $\pm$ 0.3
Cuffed media ( $\mu$ m)	26.3 $\pm$ 0.7	26.6 $\pm$ 2.2	26.9 $\pm$ 0.7
Cuffed I/M vol. ratio (%)	0.9 $\pm$ 0.4	2.1 $\pm$ 0.5	6.5 $\pm$ 1.2

may indeed be involved in its pathogenesis. There are several possible mechanisms for this involvement. First, NO suppresses smooth muscle cell proliferation. The effect of NO donors on smooth muscle proliferation and on neointimal formation has been demonstrated in a rat model of intimal injury (18). Second, NO inhibits platelet adhesion and aggregation (2). Third, NO suppresses leukocyte-endothelial interactions (3, 4). NO markedly attenuates leukocyte rolling along the endothelium and leukocyte adhesion in part by inhibiting expression of P-selectin on the vascular endothelium (19–21), and in part by inhibiting ICAM-1 and VCAM-1 (22). Each of these mechanisms would have the effect of suppressing responses to vessel injury. Reductions in endothelial NO levels would therefore cause increased responses to injury.

In addition to local tissue effects, eNOS deficiency has systemic hemodynamic effects. The eNOS mutant mice are hypertensive (12) compared with wild-type animals. In the current study, we have not demonstrated that systemic hypertension does not affect intimal formation in the cuff model. However, because hypertension itself is associated with endothelial dysfunction and reduced endothelial NO levels, it would be difficult to separate the hemodynamic effects of hypertension from its endothelial effects. The effect of hypertension in this model needs to be further evaluated by experiments involving local gene transfer of eNOS into vessels of eNOS mutant animals. This transfer would separate the local effects of eNOS expression on suppressing smooth muscle cell proliferation from systemic hypertension and its neurohumoral effects. In the current study, the animals studied were young adults (7–8 wk), and we did not note any histologic evidence of vascular abnormality or increased wall thickness secondary to hypertension.

To determine the time course of neointimal proliferation and the possible role of the iNOS isoform, we performed a separate series of experiments in mice in which Alzet pumps were placed for administration of BrdU. We examined vessels at 3, 7, 10, and 14 d after cuff placement for BrdU staining for cellular proliferation and iNOS staining by immunohistochemistry. Neither significant BrdU staining nor iNOS expression was noted in any of the sham-operated control vessels. BrdU-positive cells reflecting cellular proliferation were present in the cuffed vessels as early as day 3, and occurred in the intima, media, and adventitia. In contrast, iNOS staining was not detected at 3 d, but was present at later time points in both the intima and the adventitia. Thus, the proliferative response begins to occur in the cuffed vessels before iNOS expression.

These results are in agreement with a recent report on the cuff model, in which iNOS expression was found in cuffed arteries only after cellular proliferation and neointimal formation. In the rabbit model, as we find in the mouse model, iNOS is induced not only in the adventitia, but also in the intima. One unresolved question is why iNOS expression is not sufficient to overcome the absence of eNOS expression in the eNOS mutant mice. The first explanation is that iNOS expression clearly occurs after cellular proliferation has started, so it may not be expressed early enough to suppress the initial events in neointimal formation. A second possibility is that the manner in which eNOS generates NO in response to physiologic signals such as flow, shear stress, stretch, and circulating signals is important. Despite its ability to generate larger quantities of NO, iNOS may not generate it in a manner or location that triggers the same results as eNOS in suppressing smooth

muscle proliferation. Finally, while we have documented the presence of iNOS protein by immunohistochemistry, we have not shown whether it is active. It is possible that iNOS protein induced may remain as monomers or otherwise inactive forms, or that by virtue of its high turnover, the amount of L-arginine substrate may become limiting.

Our results show a clear gender difference in the response of wild-type mice to cuff injury, with I/M ratios of 28 and 31% in males and 17 and 18% in females. Gender differences have also been noted in the filament injury model, the rat balloon injury model (16), and the cuff model (24), paralleling the atheroprotective effects of estrogens observed in humans. Recent work suggests that these effects of estrogen persist in estrogen receptor alpha mutant mice, suggesting that they do not require the estrogen alpha receptor (25). The eNOS mutant mice still show a significant difference in neointimal formation between male and female mice, indicating that the effects of estrogen do not require eNOS expression.

Inhibition of vascular intimal formation by pregnancy was impressive. To our knowledge, there has been no report about vascular intimal formation during pregnancy. Coronary artery disease is rare among pregnant women, in part due to the younger age of pregnant women. In our initial studies, we noted a remarkable reduction in intimal formation in a mouse that was pregnant, so we systematically examined this reduction in all three mouse strains studied. We placed the cuff around the femoral artery on day 7 of pregnancy. Normal mouse gestation lasts 20 d, and the endpoint for the model is 14 d, so the mouse delivered pups within 1 d of vessel harvesting. Further studies will be necessary to define why pregnancy suppresses intimal proliferation in response to vessel injury, and whether this effect is due to circulating estrogens, chorionic gonadotropin, or other changes.

In summary, we have characterized a cuff model of vessel injury in mice that results in reproducible formation of neointima in 14 d. Male mice show more intimal formation than female mice, and the response of C57BL/6 and SV129 mouse strains are similar. Mice in which the eNOS gene is disrupted show substantially increased vascular neointimal formation in response to cuff injury, with more intima in male mice than female mice. Pregnancy suppresses the response to vessel injury in both wild-type and eNOS mutant mice.

## Acknowledgments

We thank Chris Simpson and Brigid Nulty for excellent technical assistance.

P.L. Huang is an Established Investigator of the American Heart Association and is supported by grant NS33335 from the National Institute of Neurologic Diseases and Stroke, National Institutes of Health.

## References

1. Mootadian, D.L., T.C. Hutsell, and L.K. Keefer. 1995. Nitric oxide (NO) donor molecules: effect of NO release rate on vascular smooth muscle cell proliferation in vitro. *J. Cardiovasc. Pharmacol.* 25:674–678.
2. Radomski, M.W., R.M. Palmer, and S. Moncada. 1991. Modulation of platelet aggregation by an L-arginine-nitric oxide pathway. *Trends Pharmacol. Sci.* 12:87–88.
3. Bath, P.M.W. 1993. The effect of nitric oxide donating vasodilators on monocyte chemotaxis and intracellular cGMP concentrations in vitro. *Eur. J. Clin. Pharmacol.* 45:53–58.
4. Lefer, A.M. and X. Ma. 1993. Decreased basal nitric oxide release in hypercholesterolemia increases neutrophil adherence to rabbit coronary artery endothelium. *Arterioscler. Thromb.* 13:771–776.

5. Flavahan, N.A. 1992. Atherosclerosis or lipoprotein induced endothelial dysfunction: potential mechanisms underlying reduction in EDRF/nitric oxide activity. *Circulation*. 85:1927-1938.
6. Freeman, R.C., G.C. Mitchell, D.D. Heistad, M.L. Armstrong, and D.G. Harrison. 1986. Atherosclerosis impairs endothelium-dependent vascular relaxation to acetylcholine and thrombin in primates. *Circ. Res.* 58:783-789.
7. Linder, L., W. Kiowski, F.R. Bühler, and T.F. Luscher. 1990. Indirect evidence for release of endothelium-derived relaxing factor in human forearm circulation in vivo: blunted response in essential hypertension. *Circulation*. 81:1762-1767.
8. King, G.L., T. Shiba, J. Oliver, T. Inoguchi, and S.E. Bursell. 1994. Cellular and molecular abnormalities in the vascular endothelium of diabetes mellitus. *Ann. Rev. Med.* 45:179-188.
9. Celermajer, D.S., K.E. Sorensen, V.M. Gooch, D.J. Spiegelhalter, O.I. Miller, I.D. Sullivan, J.K. Lloyd, and J.E. Deanfield. 1992. Non-invasive detection of endothelial dysfunction in children and adults at risk of atherosclerosis. *Lancet*. 340:1111-1115.
10. Booth, R.F.G., J.F. Martin, A.C. Honey, D.G. Hassall, J.E. Beegley, and S. Moncada. 1989. Rapid development of atherosclerotic lesions in the rabbit carotid artery induced by perivascular manipulation. *Atherosclerosis*. 76:257-268.
11. Kockx, M.M., G.R.Y. De Meyer, L.J. Andries, H. Bult, W.A. Jacob, and A.G. Herman. 1993. The endothelium during cuff-induced neointima formation in the rabbit carotid artery. *Arterioscler. Thromb.* 13:1874-1884.
12. Huang, P.L., Z. Huang, H. Mashimo, K.D. Bloch, M.A. Moskowitz, J.A. Bevan, and M.C. Fishman. 1995. Hypertension in mice lacking the gene for endothelial nitric oxide synthase. *Nature*. 377:239-242.
13. Lindner, V., J. Fingerle, and M.A. Reidy. 1993. Mouse model of arterial injury. *Circ. Res.* 73:792-796.
14. Hansson, G.K., Y.J. Geng, J. Holm, P. Hardhammar, A. Wennmalm, and E. Jennische. 1994. Arterial smooth muscle cells express nitric oxide synthase in response to endothelial injury. *J. Exp. Med.* 180:733-738.
15. Ferns, G.A.A., A.L. Stewart-Lee, and E.E. Anggard. 1992. Arterial response to mechanical injury: balloon catheter de-endothelialization. *Atherosclerosis*. 92:89-104.
16. Sullivan, T.R., R.H. Karas, M. Aronovitz, G. Faller, J. Smith, T. O'Donnell, and M.E. Mendelsohn. 1995. Estrogen inhibits the response to injury in a mouse carotid artery model. *J. Clin. Invest.* 96:2482-2488.
17. Yong, A.C., G. Townley, and G.W. Boyd. 1991. Hemodynamic changes in the Moncada model of atherosclerosis. *Clin. Exp. Pharmacol. Physiol.* 19:339-342.
18. Guo, J.P., M.M. Panday, P.M. Consigny, and A.M. Lefer. 1995. Mechanisms of vascular preservation by a novel NO donor following rat carotid artery intimal injury. *Am. J. Physiol.* 269:H1122-H1131.
19. Gauthier, T.W., R. Scalia, T. Murohara, J.P. Guo, and A.M. Lefer. 1995. Nitric oxide protects against leukocyte-endothelium interactions in the early stages of hypercholesterolemia. *Arterioscler. Thromb. Vasc. Biol.* 15:1652-1659.
20. Gauthier, T.W., K.L. Davenpeck, and A.M. Lefer. 1994. Nitric oxide attenuates leukocyte-endothelial interaction via P-selectin in splanchnic ischemia-reperfusion. *Am. J. Physiol.* 267:G562-G568.
21. Davenpeck, K.L., T.W. Gauthier, and A.M. Lefer. 1994. Inhibition of endothelial-derived nitric oxide promotes P-selectin expression and actions in the rat microcirculation. *Gastroenterology*. 107:1050-1058.
22. De Caterina, R., P. Libby, H.B. Peng, V.J. Thannickal, T.B. Rajavashisth, M.A. Gimbrone, Jr., W.S. Shin, and J.K. Liao. 1995. Nitric oxide decreases cytokine-induced endothelial activation. Nitric oxide selectively reduces endothelial expression of adhesion molecules and proinflammatory cytokines. *J. Clin. Invest.* 96:60-68.
23. Arthur, J.F., Z.L. Yin, H.M. Young, and G.J. Dusting. 1997. Induction of nitric oxide synthase in the neointima induced by a periaortic collar in rabbits. *Arterioscler. Thromb. Vasc. Biol.* 17:737-740.
24. Akishita, M., Y. Ouchi, H. Miyoshi, K. Kozaki, S. Inoue, M. Ishikawa, M. Eto, K. Toba, and H. Oritani. 1997. Estrogen inhibits cuff-induced intimal thickening of rat femoral artery: effects on migration and proliferation of vascular smooth muscle cells. *Atherosclerosis*. 130:1-10.
25. Iafrazi, M.D., R.H. Karas, M. Aronovitz, S. Kim, T.R. Sullivan, D.B. Lubahn, T.F. O'Donnell, K.S. Korach, and M.E. Mendelsohn. 1997. Estrogen inhibits the vascular injury response in estrogen receptor alpha deficient mice. *Nat. Med.* 3:545-548.